UNITED STATES DEPARTMENT OF THE INTERIOR
GEOLOGICAL SURVEY

RESULTS AND DATA FROM SEISMOLOGIC AND GEOLOGIC STUDIES FOLLOWING EARTHQUAKES OF DECEMBER 7, 1988, NEAR SPITAK, ARMENIA S.S.R.

---

edited by

Roger D. Borcherdt

Volume I

OPEN-FILE REPORT 89-163A

Menlo Park, California
1989

TABLE OF CONTENTS

VOLUME I

PREFACE

The earthquakes of December 7, 1988, near Spitak, Armenia SSR, serve as another grim reminder of the serious hazard that earthquakes pose throughout the world. We extend our heartfelt sympathies to the families of the earthquake victims and intend that our cooperative scientific endeavours will help reduce losses in future earthquakes. Only through a better understanding of earthquake hazards can earthquake losses be reduced for all peoples in seismically active regions of the world.

The tragic consequences of these earthquakes remind scientists and public officials alike of their urgent responsibilities to understand and mitigate the effects of earthquakes. On behalf of the U.S. Geological Survey, I would like to express appreciation to our Soviet colleagues for their kind invitation to participate in joint scientific and engineering studies. Without their cooperation and generous assistance, the conduct of these studies would not have been possible.

This report provides seismologic and geologic data collected during the time period December 21, 1988, through February 2, 1989. These data are presented in their entirety to expedite analysis of the data set for inferences regarding hazard mitigation actions, applicable not only in Armenia but other regions of the world exposed to high seismic risk.

Dallas L. Peck
Director, United States Geological Survey

FOREWORD

This volume represents one of a five-part set, which present preliminary results and data for the seismologic and geologic investigations conducted following the earthquakes of December 7, 1988, near Spitak, Armenia S.S.R. The first volume of this set describes the field experiments, instrumentation, the data set, formats for data dissemination, and preliminary conclusions permitted by data analyses completed as of this writing. Volumes II, III, IV, and V present the seismograms for the digital recordings of aftershocks obtained during the time periods indicated. Because of limited computer facilities and data format incompatibilities, the digital-event recordings are presented as analog seismograms. The seismograms are included to expedite analysis of the data for developing appropriate hazard mitigation measures for future potentially damaging earthquakes.

This data set is a testament to the generous cooperation and assistance provided by our colleagues in the Union of the Soviet Socialist Republics. Without their contributions this data set would not have been possible. For their contributions, we express our most sincere appreciation.

Roger D. Borcherdt
March 15, 1989

SUMMARY

R. Borcherdt

On December 7, 1988 a tragic earthquake (M_s6.9, M_b6.2) occurred near Spitak, Armenia S.S.R. This earthquake and an aftershock (M_b5.8) four minutes later resulted in the collapse of many structures with subsequent life loss exceeding 25,000. The earthquakes occurred in the lesser Caucasus highlands about 80 kilometers south of the main chain of the Caucasus Mountains. The region is one of considerable north–south crustal shortening (average about 5 cm/year) associated with collision of the Arabian and Eurasian plates (McKensie, 1972, Chapter 2). Teleseismic data yield estimates for moment and moment magnitude of 1.8×10^{26} dyne-cm and 6.8 (Kanamori and others, pers. commun., 12/88).

Surface faulting investigations by Soviet, French and American geologists (Chapter 4) indicate reverse-thrust and right-lateral movement along a rupture surface with a dip of 55° to the northeast and a strike of about N70° W roughly consistent with focal mechanism solutions. Surface rupture documented for 8 kilometers showed maximum slip of 2 meters with a 1.6-meter vertical component and a 0.5-meter right-lateral component. The previously unnamed fault strikes parallel to major tectonic features of the Caucasus mountain chain with little geomorphic expression compared to a more throughgoing feature apparent about 8 km farther northeast.

Seismologic investigations resulted in the deployment of 24 seismographs (12 analog and 12 digital) and a self-contained computer system (Chapters 5 and 6). Deployment of the instrumentation commenced December 21, 1988 with operation continuing through January 4, 1989. Seven digital instruments continue to be deployed as of this writing. Data sets retrieved as of February 2, 1989 are reported herein.

The instrumentation network yielded an extensive set of analog and digital data (about 1750 three-component digital recordings as of January 4, 1989). Preliminary locations of the aftershocks show aftershock activity extending over a northwest–southeast zone over 40 kilometers in length (Chapter 8). The zone extends from near Kirovakan in the southeast

to an area near Spitak then suggests a slight change in strike to a more east–west direction north of Leninakan (each of these cities experienced significant damage). The activity deepens to the west to depths of about 15 kilometers. The largest aftershocks recorded were assigned magnitudes of 4.7 and 5.2. The first of these occurred in a deeper cluster of activity in the western zone and the second in a region of shallower activity near the change in strike of the aftershock zone.

Investigations of damage statistics for the three largest cities most heavily damaged by the earthquake shows that 87 percent of the structures in Spitak collapsed or suffered heavy damage, 24 percent of those in Kirovakan and 52 percent in Leninakan (Chapter 9). The greater damage in Spitak can be attributed in part to its proximity to the surface rupture (1–9 km). The damage in Leninakan, which is about 32 km from the zone of surface rupture, was in general greater than that in Kirovakan at a distance of about 25 km. In particular, taller structures of precast frame-panel and composite stone-panel experienced greater damage.

Aftershock recordings obtained at a site in Leninakan show that ground displacements were 4–8 times larger at this site than those obtained at rock sites at a comparable distance. Spectral ratios computed for aftershock recordings show spectral amplifications for ground motions in the 0.6–3-second period band that peak at levels between about 20 and 35. The aftershock recordings obtained to date suggest that the amplification of the longer-period ground motions by the thick layers of soil and volcanic tuff underlying Leninakan could have been a major contributory factor to the increased damage levels experienced by Leninakan as compared to Kirovakan.

The digital recordings of the aftershocks through February 2, 1989 are presented herein as three-component analog seismograms. They also are available for dissemination on 9-track magnetic tape in ASCII and binary formats, on IBM Optical Disk cartridge, and on Floppy Disk in individual station and event formats. Formats for the various media are described.

CHAPTER 1

INVESTIGATIONS CONDUCTED BY THE U.S. TEAM FOLLOWING THE EARTHQUAKES OF DECEMBER 7, 1988, NEAR SPITAK, ARMENIA S.S.R.

J. Filson

This chapter describes the organization and itinerary for studies undertaken by a team of U.S. scientists, engineers and technicians in cooperation with colleagues of the U.S.S.R. to investigate the cause and effects of the disastrous earthquake which occurred on December 7, 1988, near Spitak, Armenia S.S.R. This chapter describes the activities undertaken by all members of the U.S. team. Results and data derived by Earth Science members of the team are presented in subsequent chapters of this report. Results derived by all members of the U.S. team are being published under separate cover under the auspicies of the Earthquake Engineering Research Institute.

Background. The first reports received from the national seismological reporting services indicated a moderate earthquake had occurred with a magnitude in the 6.5–7.0 range. There was no immediate indication that a disaster of enormous human and economic proportions had taken place. Within the next two days the scale of the disaster was reported in the western press and its seriousness was emphasized by the decision of General Secretary Gorbachev to cancel the remaining portion of a visit to the United States and return to the Soviet Union to lead the relief effort.

Post-earthquake investigations are an extremely important part of any earthquake hazards mitigation strategy. The public law that established the U.S. National Earthquake Hazards Reduction Program recognized this and states that the "research elements of the program shall include studies of foreign experience with all aspects of earthquakes." Damaging earthquakes are rare occurrences and each should be studied carefully to ensure that the relevant lessons are incorporated into earthquake hazard mitigation actions.

Various private and governmental groups within the United States have participated in or provided support for post-earthquake investigations in the past. The groups include

the National Academy of Sciences (NAS), the National Science Foundation (NSF), the Earthquake Engineering Research Institute (EERI), the Office of U.S. Foreign Disaster Assistance (OFDA), the U.S. Geological Survey (USGS), the Federal Emergency Management Agency (FEMA), and others. Because these groups have differing missions and interests, such as engineering and social response, seismological and geological effects, and disaster response and relief organization; they usually act independently in the response to a foreign, and even domestic, earthquake. For example, the response to the Mexico City disaster of 1985 chiefly involved the engineering community while the response to the Borah Peak earthquake in Idaho in 1983 was led by seismologists and geologists. The former event affected one of the world's largest population centers, the latter was in a sparsely populated area.

Organization. Independent responses by individual agencies, private groups, and persons were not appropriate in the case of the Armenian earthquake. It was clear that any post-earthquake investigations would have to be conducted with the approval and support of the governments of the two countries involved. Fortunately the NAS, NSF, and USGS had in place cooperative programs for the joint study of earthquakes and earthquake engineering with counterpart governmental groups in the Union of Soviet Socialist Republics (U.S.S.R.).

The NAS and USGS programs were with the U.S.S.R. Academy of Sciences, and as it turned out, the President of that body, Academician G. I. Marchuk began a long-planned visit to the United States on December 8, 1988, as a guest of the NAS. Soon after his arrival offers of technical and scientific assistance were made to him by Dr. Frank Press, President of the NAS, and Dr. Dallas Peck, Director of the USGS. President Marchuk had to return to the U.S.S.R. within a few days to deal with issues related to the earthquake, but before doing so he verbally accepted the offers of assistance. In order to facilitate planning, coordination, and logistics, the U.S. agencies involved decided to send one team comprised of engineers, seismologists, geologists, a social scientist, technicians, and an executive officer.

The formal charge to the team was as follows:

1. To provide technical expertise and assistance to the authorities of the Union of Soviet Socialist Republics regarding the use of geological, seismological, and engineering data with respect to immediate post-earthquake relief efforts including: establish a temporary array of seismographs in the epicentral region to record and locate aftershocks; provide rapid reporting of regional earthquakes; provide engineering assessments in such areas as soil and structural performance, architectural issues, ground failures, performance of lifeline systems and industrial facilities, and seismic risk, and provide support to geological field surveys.

2. To gather data and information needed to assess the factors that contributed to the catastrophic nature of the earthquake, identifying knowledge gaps where focused research efforts can contribute to mitigating future earthquake devastation in the United States, the Soviet Union, and other earthquake-prone regions of the world.

The week of December 11 was one of intense preparation and planning for all of those involved. The anticipated team membership of around thirty was forced to be cut in half. Living and weather conditions in Armenia were uncertain and there was great concern that support required for the team in Armenia may detract from the relief effort. At first, it was assumed that the team would have to provide its own food, water, and shelter during the entire study, but these requirements were relaxed as reports came back from Armenia. The seismological equipment needed for studies of aftershocks and site response caused additional logistical problems. Despite these uncertainties and difficulties, the team met at the USGS headquarters in Reston, Virginia, on Sunday evening, December 18, to begin its journey and its work.

The team members were:

Mihran S. Agbabian	University of Southern California
Roger D. Borcherdt	U.S. Geological Survey
Edward Cranswick	U.S. Geological Survey
Armen Der Kiureghian	University of California, Berkeley
Christopher M. Dietel	U.S. Geological Survey
John R. Filson	U.S. Geological Survey

Fredrick Krimgold	Virginia Polytechnic Institute
Charley J. Langer	U.S. Geological Survey
H. S. Lew	National Institute for Standards and Technology
Dennis Mileti	Colorado State University
Thomas O'Rourke	Cornell University
Anshell Schiff	Stanford University
Eugene D. Sembera	U.S. Geological Survey
Robert V. Sharp	U.S. Geological Survey
David W. Simpson	Lamont–Doherty Geological Observatory
Andre Varchaver	National Academy of Sciences
Loring A. Wyllie, Jr.	H. J. Degenkolb Associates
Peter Yanev	EQE Incorporated

The principal Soviet counterpart team members were:

N. P. Laverov	Vice–President, U.S.S.R. Academy of Sciences
V. I. Keilis–Borok	Institute of Physics of the Earth, Moscow
S. Kh. Negmatullaev	President, Tadjik Academy of Sciences
I. L. Nersesov	Institute of Physics of the Earth, Moscow
N. B. Shebalin	Institute of Physics of the Earth, Moscow
A. V. Nikolaev	Institute of Physics of the Earth, Moscow
S. V. Grigorian	Director, Institute of Geology, Armenian Academy of Sciences, Yerevan
V. K. Karapetian	Yerevan Polytechnic Institute
S. G. Shaginian	Director, Armenia Scientific Research Institute of Civil Engineering and Architecture
S. S. Tsigankov	Seismological Council, U.S.S.R. Academy of Sciences
E. Kh. Geodakian	Institute of Geology, Yerevan
L. A. Akhverdian	Institute of Geology, Yerevan
F. O. Arakelian	Director, Yerevan Branch of the ATOMENERGOPROJECT, U.S.S.R. Ministry of Atomic Energy

After a briefing and last-minute organizational meeting at the USGS the team left for Andrews Air Force Base where it departed on an Aeroflot cargo plane loaded with Red Cross supplies at 0240 on the morning of December 19 (all times are local, 24–hour clock). After two refueling stops the plane landed in Moscow at 0230 on Tuesday, December 20. The team was met and briefed at the airport in Moscow by representatives of the U.S.S.R.

Academy of Sciences and the Institute of Physics of the Earth. Some members of these organizations then joined the team in boarding the plane which departed Moscow at 0552 for Yerevan where it arrived at 0930.

Chronology. What follows is a brief chronology of the team's activities taken from my field notes.

Tuesday, December 20. Arrive Yerevan. Unload plane and transfer equipment and supplies to Geological Institute. Check into Hotel Armenia. Held team meeting that evening, met and briefed on situation by V. I. Keilis–Borok.

Wednesday, December 21. Morning briefing and organizational meeting at Geological Institute. In the afternoon some of the engineering members visited an institute specializing in lift-slab construction and met with the Mayor of Yerevan. Seismological stations were installed at Garni and the nuclear power plant west of Yerevan.

Thursday, December 22. Team left Yerevan for the disaster area in a small caravan with Japanese team, some members of the Soviet counterpart team, and the seismological equipment. At Spitak the team divided with the engineering group going on to Leninakan and the seismological group proceeding to Kirovakan to establish a forward base of operations. The engineering group returned to Yerevan that night while the seismological group stayed east of Kirovakan.

Friday, December 23. Two 3–man parties from the engineering group returned to the disaster area for further investigations. These teams stayed overnight in Leninakan. Seismological group moved their base to just outside Kirovakan and deployed portable equipment at 10 sites using three teams. Throughout the rest of the investigation the seismological group operated out of this base near Kirovakan. It was primarily concerned with the installation and maintenance of the portable stations and the retrieval of data, and preliminary analysis of event locations.

Saturday, December 24. Engineering parties return to Yerevan. Planning meetings with representatives of the Geological Institute. Michan Agbabian ap-

peared on Soviet television with members of the Soviet counterpart team. Continued seismic recording and geological field investigations for Kirovakan.

Sunday, December 25. Engineering group met for several hours with officials of the Armenian Scientific Research Institute of Civil Engineering and Architecture and with the Chief of the Laboratory of Earthquake Engineering. Continued seismic recording and geological field investigations from Kirovakan.

Monday, December 26. One party from the engineering group returned to the disaster area for further surveys. The rest of the engineering group visited the Yerevan nuclear power plant. Officials of this plant hosted an evening meal for members of the team in Yerevan. Continued seismic recording and geological field investigations from Kirovakan.

Tuesday, December 27. One party of the engineering group returned to Leninakan to investigate earthquake effects to specific structures. Arrangements made for return of most of team members to the United States. Continued seismic recording from Kirovakan.

Wednesday, December 28. Party of six team members left Yerevan at 0615 and a second party of four left at 1300 for return to the United States via Moscow. Seven team members remained in Armenia. Another team member had returned earlier. Seismic recording continued from Kirovakan.

December 29–January 3. Continued seismic recording from Kirovakan.

January 4–5. Retrieve a portion of portable seismic equipment from the field.

January 6. Seismological group returns to Yerevan.

January 7. Seismological group conducts briefing on results at Geological Institute in Yerevan, completes deployment of seven digital stations in a regional network to be left temporarily in Armenia, packs remaining equipment for return to United States.

January 8. Seismological group leaves Yerevan for return via Moscow.

Upon return to the United States various members of the team participated in numerous briefings in order to pass initial results and impressions on to colleagues in the interested professional communities here. This report and the EERI reconnaissance report are the first publications of team activities and results.

Acknowledgments. Letters of appreciation of the team's efforts have been received by Frank Press from President Marchuk of the U.S.S.R. Academy of Sciences and from His Excellency Jack F. Matlock, Jr. the United States Ambassador in Moscow. These letters are reproduced in the EERI reconnaissance report.

Many organizations and people helped the team carry out its investigations. Major organizational responsibilities fell upon the NAS, the USGS, and EERI, with the USGS bearing most of the logistical burdens. At the NAS the efforts of Dr. Riley Chung were essential to the success of the investigation. He was assisted there by Dana Caines, Lynne Cramer, Norma Giron, Marla Lacayo–Emery, Virginia Lyman, Susan McCutchen, and Stephen Rattien. Walt Hays was the chief planner at the USGS. Also at the USGS Rob Wesson, Mary Ellen Williams, Carolyn Hearn, Darrell Herd, Paul Hearn, Jerry Wieczorek, Bill Greenwood, Joyce Costello, and many others worked long and intense days to get the team launched. Susan Tubbesing of EERI played a key role in the organization of the group. Fred Cole of OFDA was a voice of information, reason, and advice on what to expect in Yerevan. Sidney Smith of the Environmental Protection Agency provided valuable diplomatic guidance.

From the United States the investigations of the team were supported by the National Science Foundation, the National Academy of Sciences, the U.S. Geological Survey, the Earthquake Engineering Research Institute, the National Center for Earthquake Engineering Research, the American Society of Civil Engineers, the Office of U.S. Foreign Disaster Assistance, the Federal Emergency Management Agency, the Nuclear Regulatory Commission, the Federal Highway Administration, and the Electric Power Research Institute. The trip was carried out under existing agreements between the NAS and the U.S.S.R. Academy of Sciences and under Area IX (Earthquake Prediction) of the U.S.–U.S.S.R. Joint Committee for Cooperation in the Field of Environmental Protection.

Dr. Frank Press of the U.S. Academy of Sciences, Dr. Dallas Peck of the U.S. Geo-

logical Survey, and Academician G. I. Marchuk of the U.S.S.R. Academy of Sciences were personally involved in the initiation, planning, and guidance of this investigation. Without their early evolvement and sustained support it would not have happened.

Mr. Victor V. Slaviantsev, Third Secretary (Science and Technology) of the Embassy of the U.S.S.R. in Washington, D.C., was of immense help in dealing with problems of visas and general coordination with Soviet authorities.

In the Soviet Union primary support for the team came from the Institute of Physics of the Earth, both in Moscow and Yerevan, and the Geological Institute in Yerevan. Without reservation it may be stated that the people from these institutes made every effort possible, under extremely trying conditions, to provide the support requested and to make the investigation a success. In particular the efforts of V. I. Keilis–Borok, I. L. Nersesov, N. B. Shabalin, and A. V. Nikolaev from the Institute of Physics of the Earth are deeply appreciated. At the Geological Institute in Yerevan we are indebted to Professor S. V. Grigorian, E. Geodakian, A. E. Karpathian, M. Satian, L. Hakhverdian, and G. Khachatrian for hospitality, support, and infinite patience. There are hundreds of other people that welcomed us and helped us in Armenia.

These acknowledgments are made to some of those who helped us as a team. Individual team members may add to them in the chapters that follow. It is impossible here to generalize or summarize the impressions and observations of each team member. However, I believe it is safe to say that each of us was awed and overwhelmed by the tragic effects of this earthquake, each of us greatly appreciated the efforts made in our behalf in the Soviet Union, each of us was deeply moved by the kindness and spirit of the Armenian people, and, because of these experiences, none of us will ever be the same.

CHAPTER 2

INTRODUCTION FOR SEISMOLOGIC AND GEOLOGIC STUDIES CONDUCTED FOLLOWING THE EARTHQUAKE OF DECEMBER 7, 1988, NEAR SPITAK, ARMENIA S.S.R.

R. Borcherdt, R. Sharp, D. Simpson, and C. Langer

The main shock occurred on December 7, 1988 at 11:41 AM local time near Spitak, Armenia S.S.R. This earthquake and subsequent aftershocks caused extensive damage over an area of about 1800 square kilometers with damage and loss of life reported up to 80 km from the epicenter in the Kars region of Turkey. Official death estimates for the earthquake exceed 25,000. This tragic loss of life from an earthquake sequence is exceeded this century only by the loss of life which occurred from the 1976 Tengshan earthquake in China. Most of the life loss occurred as a result of the collapse of buildings on their occupants. Because many of the damaged buildings were of modern design, the earthquake was a dramatic reminder of the importance of proper seismic design and construction in seismically prone regions of the world.

The largest cities to have been most severely damaged are Leninakan (Armenia's second largest city, pop. 290,000) and Spitak (pop. ~30,000). Major damage also occurred in Kirovakan (pop. 150,000) and more than 24 villages in the region. Based on data collected as of January 24, 1989 and reported by A. Der Kiureghian (pers. commun., 3/89) a total of 314 buildings collapsed, 641 are to be demolished, 1,264 buildings need repair or strengthening, and 712 in the region of damage remained habitable. All structures except one precast panel structure in Spitak either collapsed or were badly damaged (A. Der Kiureghian, pers. commun., 3/89). Spitak was closer to the zone of surface rupture (~9 km) than either of the other two larger cities. The amount of damage reported for Leninakan at a distance of about 32 km from the surface rupture was significantly greater than in Kirovakan at a closer distance of about 25 km. Fifty-two percent of the structures in Leninakan collapsed or had to be demolished while only twenty-four percent of those in Kirovakan were in these categories (A. Der Kiureghian, 3/89). Preliminary data suggest

that the geologic setting may have been a major contributory factor to the increased amounts of damage in Leninakan.

The team, sent by the United States, consisted of a geologist, seismologists, structural and geotechnical engineers, a search and recovery expert, a sociologist, and seismic instrumentation specialists. This report describes the results of the geologic and seismologic investigations conducted by the team. Investigations undertaken by all team members are described in Chapter 1 of this volume. Results as derived by all team members are being prepared for publication under separate cover by the Earthquake Engineering Research Institute.

Geologic studies were conducted in cooperation with Soviet and French geologic teams. Results of these studies are described in Chapter 3 of this volume. Seismologic studies were conducted using 12 digital and 12 analog seismic recorders in cooperation with Soviet colleagues. Descriptions of the seismologic investigations are presented in Chapter 5 of this volume. Instrument descriptions, data summaries, and preliminary conclusions concerning effects of site conditions in Leninakan are presented in Chapters 5 through 9. Seismograms for the digital data recorded through February 3, 1989 are presented in Volumes II, III, IV, and V of this report. A complete set of seismograms, derived from the digital recordings, is provided to aid in analysis of the data set by Institutions with limited computer compatibilities. The digital data is also being disseminated via 9-track 1600 bpi magnetic tape, optical disc, and limited portions on floppy disc. Data formats for these media are presented in Chapters 10, 11, and 12 of this volume.

CHAPTER 3

TECTONIC AND SEISMIC SETTING FOR THE MAIN SHOCK OF DECEMBER 7, 1988

J. Filson

The Armenian earthquake occurred in the Lesser Caucasus highlands, about 80 km south of the spine of the main range of the Caucasus Mountains. The tectonic setting is complex, but, in general, is governed by compression and shortening of the crust due to the convergence of the Arabian and Eurasian plates as depicted in Figure 3.1. The primary evidence of this shortening is represented by the Caucasus Mountains themselves, part of a broad mountainous belt that stretches across southern Europe and Asia from the Alps to the Himalayas. This belt contains areas of moderate to high seismicity; the latter found in and around the Aegean Sea, in southern Iran, and in western Afghanistan and Tadjikistan. Compared to these regions the seismicity of Armenia is moderate in terms of both rate and maximum size of earthquake experienced.

The tectonic and geological trends in the Lesser Caucasus fall parallel to the northwest–southeast trend of the main Caucasus chain. The trend in northern Armenia is marked by northwest–southeast striking thrust faults, fold axes, and parallel zones of exposure of igneous and sedimentary rocks. These zones consist of basaltic, andesitic, rhyolitic extrusives, as well as ophiolitic rocks and marine sedimentary rocks. The epicenter of the Armenian earthquake lies 45 km north of Mt. Aragats, a 4000-m-high volcano of Quaternary age and a source of pyroclastic rocks, lava flows, and volcanic sedimentary rocks that overlie much of the region.

Despite the general picture of north–south compression, the geologically recent volcanism may be evidence of extensional zones within the compressional regime. Despite this complexity, first-motion and moment-tensor analyses of recent earthquakes indicate that the current active tectonics is restricted to either thrust or strike-slip faulting (McKensie, 1972).

The earthquake catalogue in the vicinity of Armenia begins in 139 AD. Historical accounts indicate that Yerevan and Leninakan have been heavily damaged by earthquakes in the past. In 1899 and 1940 damaging earthquakes occurred within 100 km of the recent epicenter; these events were near magnitude 6 (see Figure 3.1). Figure 3.2 shows the historical seismicity as represented by earthquakes of about magnitude 5 or greater in the Caucasus region between the Black and Caspian Seas. There are no clear patterns or alignments in these locations. As pointed out above, although the region has a long history of earthquakes, its seismicity is not as high as that found in nearby western Turkey.

Figure 3.3 shows earthquake epicenters based on instrumental recordings during the period 1962–1987 of events greater than magnitude 2.8. There is a tight cluster of events just northwest of the recent epicenter and several other clusters to the south in Turkey and to the north in the main Caucasus chain. There is some hint of a northwest–southeast trend in these locations but no strong patterns are evident.

The Armenian earthquake was recorded by seismographs worldwide. The standard event parameters as reported by the National Earthquake Information Center (NEIC) of the U.S. Geological Survey are:

Origin time:	December 7, 1988 07h 41m 24.96s UTC
Latitude (deg):	40.996N $\pm$ 2.9 km
Longitude (deg):	44.197E $\pm$ 1.8 km
Depth:	10 km (held fixed)
Magnitudes	M_b 6.3 average based on 87 observations M_s 6.8 average based on 17 observations of the vertical component M_s 7.0 Berkeley

The preliminary event parameters reported by the Institute of Physics of the Earth (IPE) of the U.S.S.R. are:

Origin time:	December 7, 1988 07h 41m 24.96s UTC
Latitude (deg):	40.92N

Longitude (deg):	44.20E
Depth:	10 km
Magnitude:	7.0

A preliminary fault plane solution by the NEIC based on first-motion observations at XX stations is given in Figure 3.4. The parameters of this solution are:

	Azimuth	Plunge	
Compression (P) axis:	154.6°	14.6°	
Tension (T) axis:	253.7°	31.2°	
Null (B) axis:	43.0°	54.8°	
	Strike	Dip	Rake
Fault plane 1	290.0°	57.0°	167.0°
Fault plane 2	27.2°	79.1°	33.7°

Preliminary information on the faulting mechanism also exists from the inversion of body and surface-wave data from this event. Charles Esterbrook of Lamont–Doherty Geological Observatory had done a preliminary inversion of the body-wave data recorded at Harvard, MA and Pasadena, CA yielding the following parameters:

	Strike	Dip	Rake
Fault plane 1:	295°	72°	167°
Fault plane 2:	?	?	?
Moment:	1.0 10^{26} dyne-cm		
Moment magnitude (M_w):	6.6		
Depth:	7.5 km		

An inversion of the long-period surface waves from the same two stations by Hiroo Kanamori, Kenji Satake, and Hitoshi Kawakatsu of the California Institute of Technology Seismological Laboratory gives the following results:

	Strike	Dip	Rake
Fault plane 1:	282°	70°	117°
Fault plane 2:	46°	33°	39°
Moment:	1.7 10^{26} dyne-cm		
Moment magnitude (M_w):	6.8		

This earthquake sequence consisted of a foreshock, the main shock, a major aftershock, and hundreds of additional aftershocks, many of which were near magnitude 5. A listing of the larger events located by NEIC is given in Table 3.1. Hundreds of the aftershocks were recorded by a network of portable seismographs installed in the epicentral area and the results of this study will be discussed below. Based on this preliminary table several observations can be made. First, there was an isolated and well-recorded foreshock. In a discussion with personnel at the Yerevan Seismological Observatory they pointed out that earthquakes of this size occur several times a year in what became the epicentral region. It is possible that the occurrence of such earthquakes alone could have been used as the basis for a warning; but, if so, the false alarm rate would have been high. Secondly, there was a strong aftershock within five minutes of the main shock. This aftershock was only .4 of a body-wave magnitude unit smaller than the main shock. (The surface-wave magnitude of this aftershock is not easily measured because its surface waves are mixed with those of the main shock.) It is reported that this aftershock caused extensive additional damage in structures already weakened or damaged by the main shock. Many persons in the process of evacuating buildings damaged, but still standing, were trapped by collapses caused by this aftershock. Finally, it should be noted that this was a very vigorous aftershock sequence. There were at least 13 aftershocks greater than magnitude 4.5 and these were still occurring a month after the main shock.

REFERENCES – CHAPTER 3

Borcherdt, R. D., J. B. Fletcher, E. G. Jensen, G. L. Maxwell, J. R. Van Schaack, R. E. Warrick, E. Cranswick, M. J. S. Johnston, and R. McLearn (1985). A General Earthquake Observation System (GEOS), Bull. Seis. Soc. Am. 75, 1783–1825.

Earthquakes in the USSR (1962–1987). Annual reports, "Nauka," Moscow.

Kondorskaya, N. V., and N. V. Shebalin (1977). New Catalogue of Strong Earthquakes of the Territory of the USSR, "Nauka," Moscow.

McKensie, D. (1972). Active tectonics of the Mediterranean region, Geophys. J. R. astro. Soc. 30, 109–185.

Medvedev, S. V. (ed.) (1968), *Seismic Zoning of the USSR*, "Nauka," Moscow.

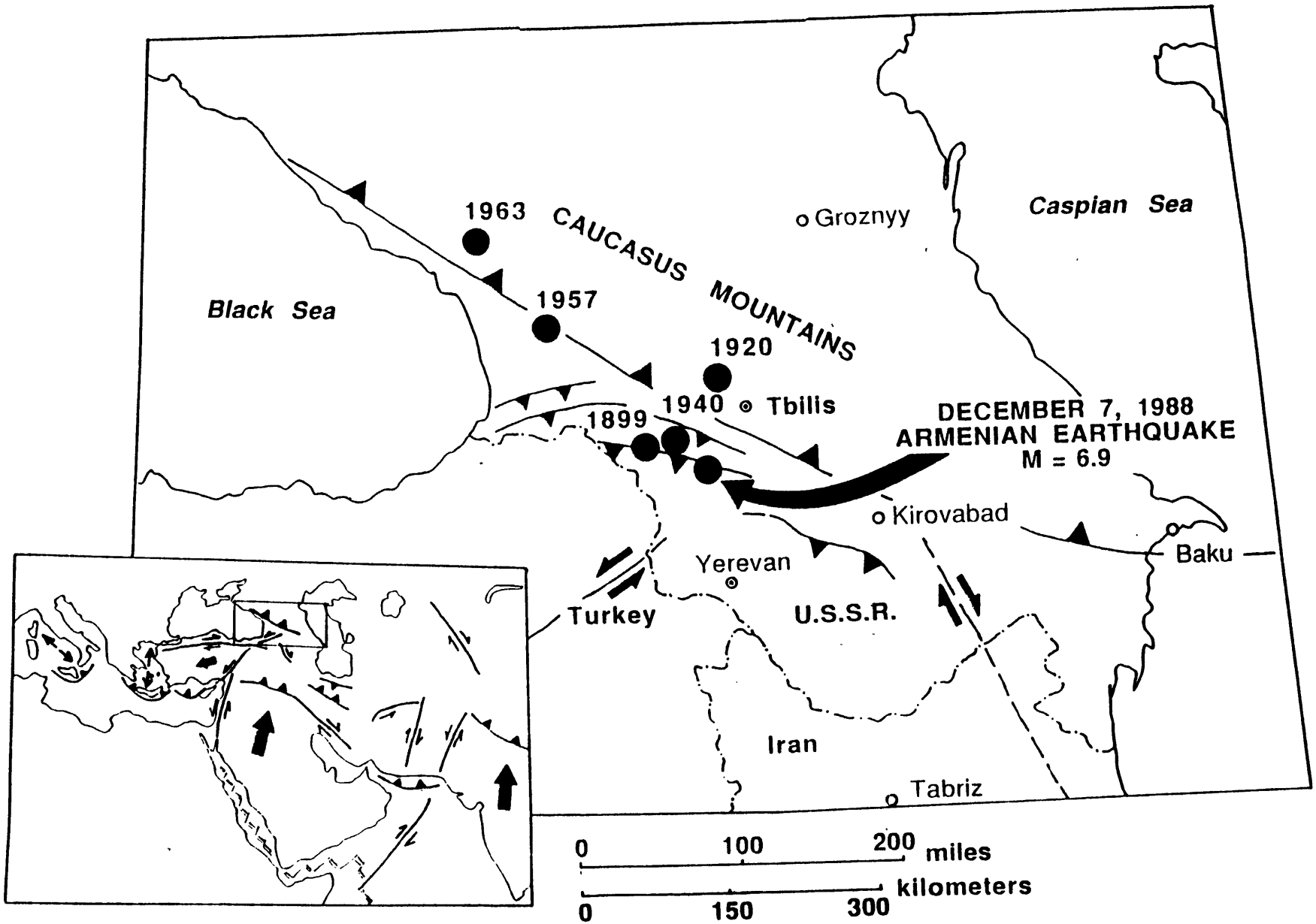

FIGURE 3.1. Large historic events and tectonic boundaries for the region surrounding the Armenian earthquake of December 7, 1989 (Simpson, pers. commun.).

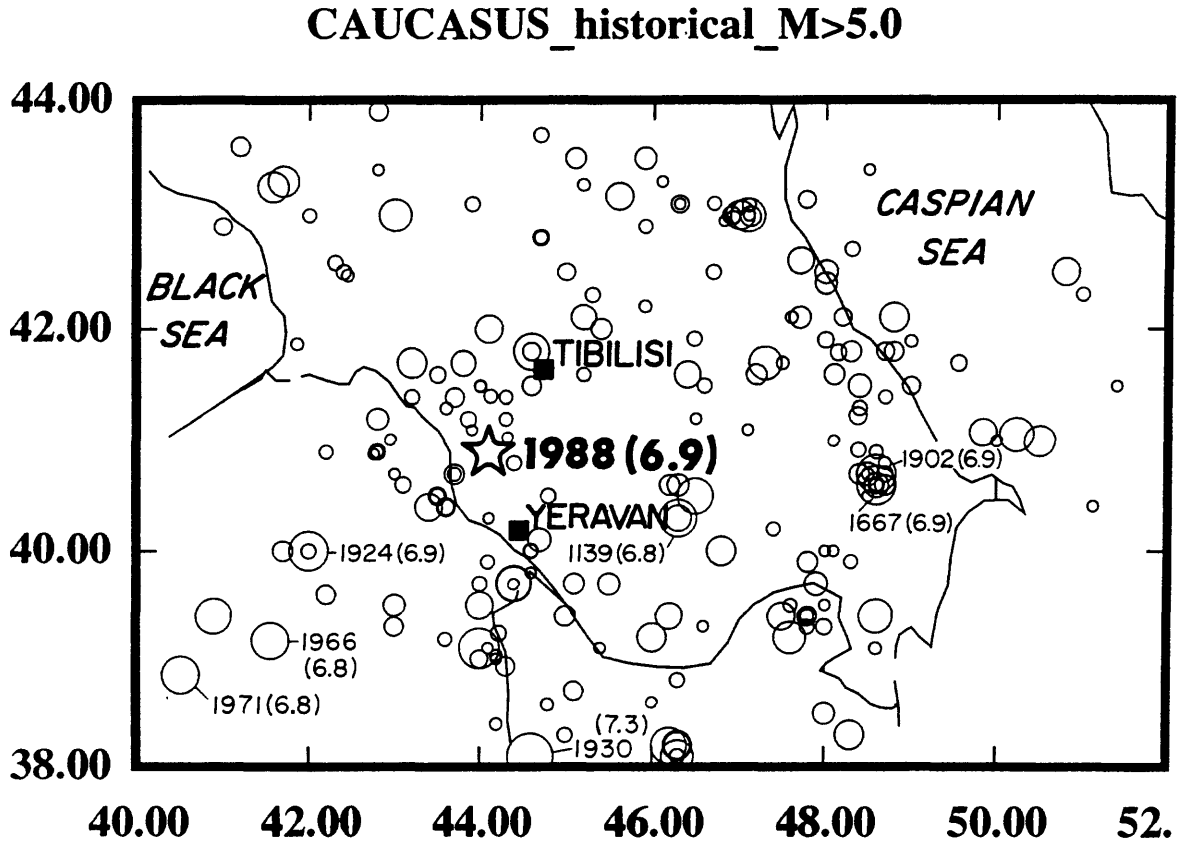

FIGURE 3.2. Historical seismicity for events larger than magnitude 5 in region of Armenian earthquake of December 7, 1988 (Simpson *et al.*, pers. commun.).

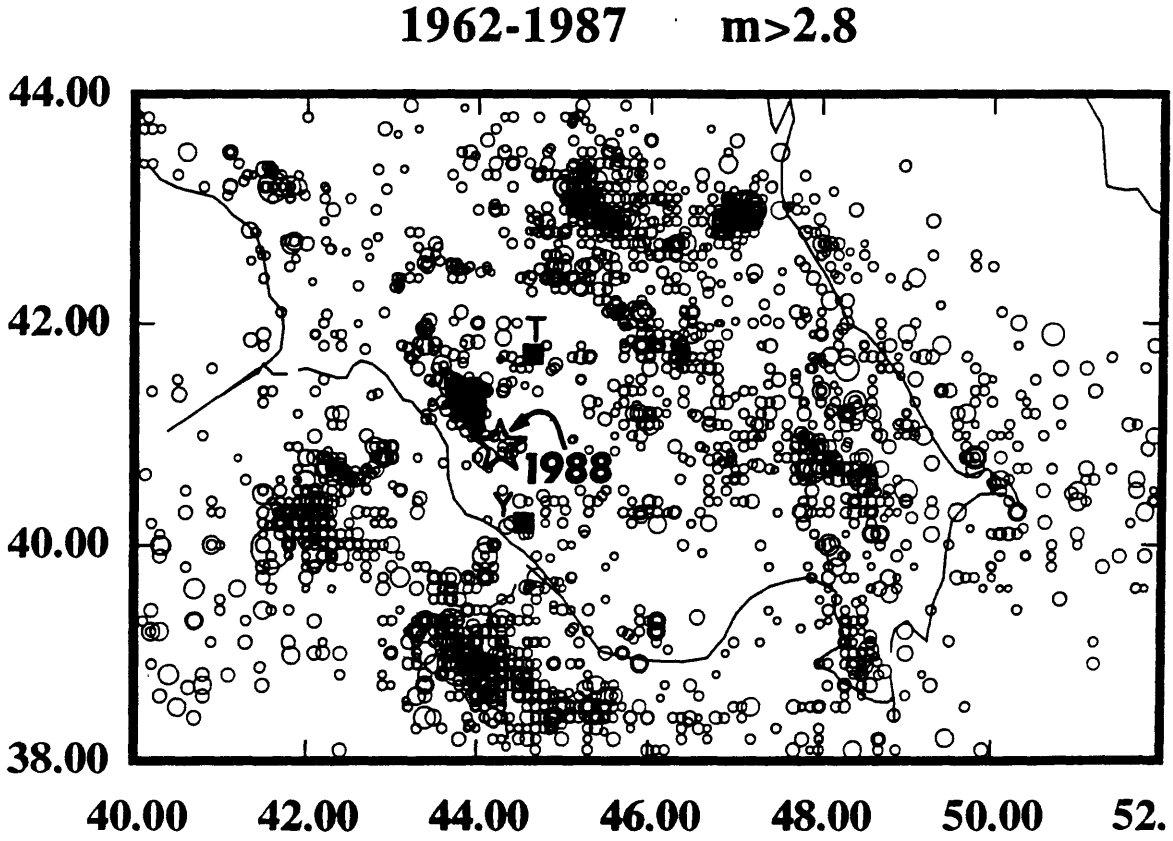

FIGURE 3.3. Instrumental seismicity for events larger than magnitude 2.8 in region of December 7, 1988 earthquake near Spitak, Armenia S.S.R.

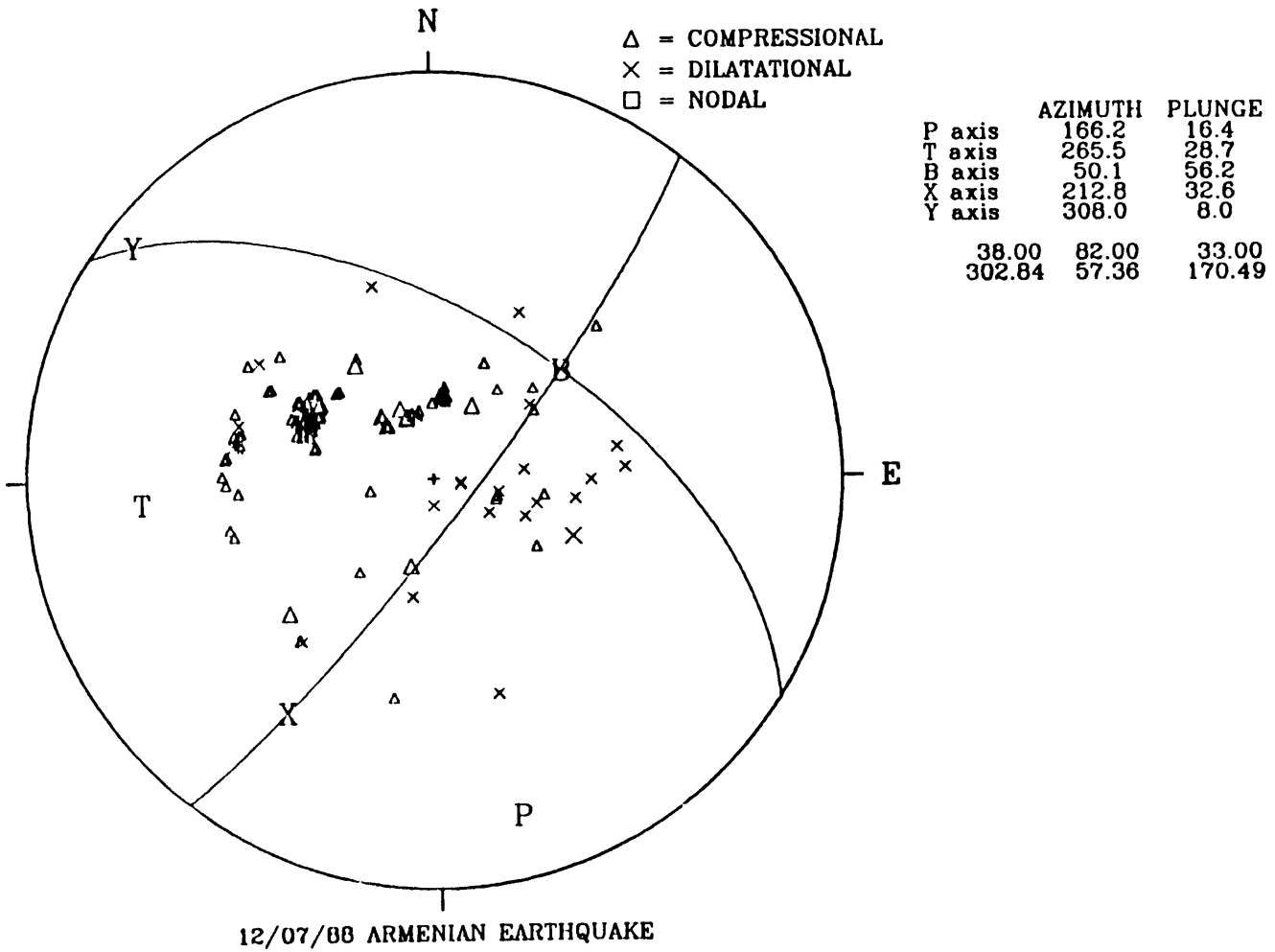

FIGURE 3.4. Fault plane solution for Armenia earthquake of December 7, 1988 derived by NEIC.

Table 3.1. Preliminary list of significant events in the Armenian earthquakes sequence

		Origin Time			Magnitude	Source
Month	Date	Hr	Min	Sec	(m_b)	
Dec.88	06	15	27	06.9	3.0	USSR/IPE
Dec.88	07	07	41	25.0	6.3	NEIC
Dec.88	07	07	45	46.0	5.9	NEIC
Dec.88	07	08	06	28.2	4.7	NEIC
Dec.88	07	09	34	33.9	5.0	NEIC
Dec.88	07	18	05	42.3	4.6	NEIC
Dec.88	07	20	07	30.6	4.6	NEIC
Dec.88	08	01	15	55.7	4.8	NEIC
Dec.88	08	01	49	41.4	4.1	NEIC
Dec.88	08	04	09	37.2	4.7	NEIC
Dec.88	08	05	36	29.8	5.0	NEIC
Dec.88	08	07	46	00.0	4.6	NEIC
Dec.88	08	20	32	06.2	4.7	NEIC
Dec.88	10	19	13	59.1	4.4	NEIC
Dec.88	12	15	36	15.1	4.6	NEIC
Dec.88	31	04	07	10.6	4.7	NEIC
Jan.89	04	07	29	40.8	5.0	NEIC

CHAPTER 4

SURFACE FAULTING ASSOCIATED WITH THE 7 DECEMBER 1988 ARMENIAN S.S.R. EARTHQUAKE: A PRELIMINARY VIEW

Robert V. Sharp

INTRODUCTION AND ACKNOWLEDGMENTS

This description of surface faulting near Spitak, Armenian S.S.R. is based on a field inspection made on 22–26 December 1988. Although these observations were made after post-earthquake snow had obscured parts of the trace and made high elevations in the mountainous epicentral region inaccessible by vehicle and foot, Soviet and French geologists had mapped part of this surface rupture before the snow fell. These geologists include B. A. Borissov, A. I. Gorshkov, I. V. Palamodov, and E. A. Rogozhin of the Institute of Physics of the Earth, Moscow, and J. Bousquet and H. Philip of the Languedoc University of Science and Technology, Montpellier. Although much of the information presented here is based on their work, jointly made observations near the ends of the surface rupture confirm their reports of features in the central part that I did not see. I express my gratitude to them for their generously offered descriptions of the surface faulting and for their assistance and camaraderie.

These observations should be considered preliminary and a minimum assessment of the surface faulting for this event. Because of snow cover, areas that were considered important to check in the epicentral region could not be traversed, and additional breaks along the checked trace of surface rupture could easily have been overlooked. The most pronounced photolineaments that may indicate active fault traces on pre-earthquake Landsat images in fact were located in inaccessible places in the mountains north of Spitak, and because of snow these were not investigated. Finally, Soviet geologists (and perhaps others) plan to make a more complete inspection of the region when it is snow-free. To aid the completeness of this second investigation, I discuss the need for field checking of photolineaments near Spitak.

SURFACE RUPTURE WEST OF SPITAK

Surface faulting, mostly crossing exposed bedrock, broke along at least 8 km of an unnamed fault that extends from near Spitak west–northwestward to near the town of Nalband (Figure 4.1). The strike of this rupture parallels the nearby ranges of the Lesser Caucasus and to the tectonic grain and topography of the Caucasus Mountains farther north. On average the fault dips toward the north–northeast, and the hanging wall moved upward and due southward with respect to the footwall. The surface breaks lie southwest of the main shock and early aftershock epicenters, and thus mutual agreement exists between all of these elements.

In detail, the surface rupture shown in map view in Figure 4.2 is locally discontinuous, and although the average strike is west–northwestward, there are significant departures, including one short segment that trends northeastward. Near the east end of rupture, branch breaks extend southeastward across an alluviated surface. Here, however, the fault motion on the branch was principally right-lateral, and vertical components varied in both sense and amount.

A possible tectonic rupture, nearly 5 km west of the principal mapped surface break (Figure 4.2), showed right-lateral offset associated with a vertical component that was primarily up on the northeast but changed in sense along strike. The fact that this fracture was apparently confined to a steep southward slope allows that it may be an earthquake-triggered slope failure with movement driven primarily by gravity. Scarps representing the head of a landslide mass were not found upslope of this feature, however.

Depending on location, the surface displacement was either concentrated or distributed. Where concentrated at a single narrow break, the inclination of the fault surface, on average about 55 degrees toward the north–northeast, was easily observed in some places on the face of the overhanging headwall. More commonly, however, displacement was distributed across multiple fractures in a zone of 10 m or greater width (Figure 4.3). Vertical profiles of the latter type of break were rounded and irregular at the leading edge of the hanging wall (Figure 4.4).

DISPLACEMENT

In bedrock, displacement of the ground surface associated with the earthquake was at most places of right-reverse type. The azimuth of the displacement was southward directed in these sites, regardless of the local strike of the fault. Where the fault locally trends northeastward, for example, southward displacement resolves into left-lateral and reverse components. The fact that the displacement direction was so consistent, despite local complications in the fault trace, suggests that the bedrock outside of the shear zone behaved as a rigid block with no significant deformation distributed internally.

The vertical component of slip along the principal 8-km segment of the surface rupture reached a maximum of 1.6 m near the southeast end, but it averaged about 1 m over most of the rupture length. The 1.6 m maximum vertical component, combined with the average orientation of the fault and azimuth of the movement, yields a composite description of the maximum fault movement at the ground surface. This composite, shown in Figure 4.5, was constructed from the following four quantities measured in the field: (1) the average strike of the approximately continuous surface rupture as determined by mapping was about 292°(using displacement conventions of Aki and Richards (1980)); (2) the average fault inclination along the rupture, 55° toward the northeast, was determined principally from dips measured at sites where the leading edge of the hanging wall had not collapsed; (3) azimuths of the fault displacement were measured directly at several bedrock sites and found to be nearly constant and due southward, thus forming an angle with respect to the average fault strike of 112°; (4) the estimate of the vertical component of slip at the point of its maximum development, 1.6 m, was measured by visually projecting the ground surface of the hanging wall across the rupture zone to the footwall. These four elements define the net slip and allow computation of its other components illustrated in Figure 4.5: the strike-slip and contractional components (SS and C, respectively), the net maximum slip (**S**), the plunge angle of slip (P) in the vertical plane containing the slip vector, and rake angle of slip (R) in the fault plane. The values of these quantities are given in the caption of Figure 4.5. The average fault plane for the surface rupture may be combined with the auxiliary plane that is normal to the slip vector (**S**) to obtain a faulting mechanism based solely on the characteristics of the surface breaks. This mechanism,

	Strike	Dip
Fault plane:	292°	55°
Auxiliary plane:	90°	37°

can be compared to the similar but somewhat different main shock focal mechanisms that were obtained with teleseismic techniques and summarized by Filson and others (1989).

In alluvium near the southeast end of surface rupture, the displacement differed in both direction and type from the bedrock sites. The azimuth of movement there was southeastward, parallel, or nearly so, to the traces of the fault breaks. Although vertical deformation was also apparent across a relatively broad zone along some parts of these breaks in alluvium, at one site (Figure 4.6) the displacement vector closely approximated the inclination of the ground surface in the direction of the fault trace. The fact that no scarp was produced by the nearly 1-meter right-lateral component of slip means that the southwest side of the fault was slightly elevated at that site. Nearby but a few hundred meters farther downslope, the vertical component of movement was clearly opposite to, and much larger than at the site of Figure 4.6. Vertical component reversals along fault displacements that are dominantly strike-slip in character are not uncommon, however (see, for example, Sharp and others, 1989).

No evidence of post-seismic growth of displacement has been reported for this surface rupture. I personally observed only one feature that bears on this phenomenon. On the alluvial fractures near Spitak, an unpaved temporary road crossing the trace was in use after the coseismic fault movement, as indicated by the fact that wheel tracks obliterated the fault fractures. After the post-earthquake accumulation of snow, use of the roadway ceased, indicated in late December by a residual layer of undisturbed snow covering the road at a point near the fault trace. The pre-snow wheel tracks were not obviously offset laterally where they crossed the fault trace which had shifted horizontally earlier. Although not a sensitive test for the absence of afterslip, these observations suggest that no large post-seismic movements took place during about two weeks, at least at that location.

PRE-EARTHQUAKE SURFACE EXPRESSION OF THE FAULT

The most apparent topographic expression of the newly ruptured fault trace is degradational in character. That the trace crosses three mountain passes and in some segments follows major canyons demonstrates long-term erosional etching of fractured rocks along the fault. Where the fault crosses smoother slopes, however, the pre-earthquake ground surface showed little, if any, evidence of local relief due to earlier Holocene movement. However, in some places, such as that shown in Figure 4.7, slopes steeper than typical appeared to coincide with the rupture trace. These scarp-like features may have resulted from differential erosion localized near gullies crossing the fault, despite the fact that bedrock was apparently the same on both sides of the fault there. If the fault ever was expressed in alluvium near the ends of the rupture, near Spitak and Nalband, the features have been obscured by agricultural activity or other cultural modifications.

One of the most surprising aspects of this surface rupture is that, at the location of maximum displacement near the site of Figure 4.7, no clearly defined zone or concentration of intensely sheared rocks was evident. On the one hand, this implies that the amount of displacement since the accumulation of the Neogene rocks that are cut by this fault has not been large. On the other, past displacements, like the present one, might have been so broadly distributed that intensely sheared rocks failed to form. In any case, I observed no clear evidence there in the nature of the shear zone exposed in bedrock that this surface rupture occurred along a preexisting fault with large displacement.

PHOTOLINEAMENTS IN LANDSAT IMAGES

Although the expression of the fault trace activated at the time of this earthquake is not prominent in the Landsat image shown in Figure 4.2, thrust and reverse faults generally have a poor reputation in this regard. In this image, however, two prominent linear features are visible, and each may have tectonic significance. The more extensive of the two, apparently marked by a series of aligned stream meanders and linear gullies, passes (probably coincidentally) through the epicentral dot near the top of the image and continues beyond this view to the southeast. The character of these topographic features suggest a steeply inclined structural boundary. Its parallelism to the trend of the Caucasus,

as well as to the mountain range in which it occurs and to the already recognized surface faulting, all hint at a tectonic origin of the feature. For these reasons a field check of this feature should be made when the region is snow-free.

The second lineament, the nearly straight stream course extending northwestward from Nalband, may represent tectonic controlled drainage along an extension of the fault that ruptured. The possible tectonic significance of this feature has already been recognized by other geologists working on this fault rupture, and the possibility that faulting may not be exposed along the water course renders it a marginal prospect for gaining tectonic insight.

SURFACE FAULTING COMPARED TO AFTERSHOCKS

Detailed comparison of the surface faulting to the aftershocks is not yet possible. Preliminary data of Simpson and others (1989), however, show that the overall distribution of aftershocks north–northeast of the surface rupture permits a moderate fault dip in that direction. Three independent teleseismic focal mechanisms for the main shock also suggest a moderate to steep dip. Eventually, focal mechanisms of aftershocks may reveal whether faults of other orientations have been active and which might have dominated. In cross section normal to the surface fault strike, projected foci of aftershocks do not clearly mark a zone of activity that is inclined in that direction (Simpson and others, 1989). If anything they suggest a steeply inclined fault that would intersect the ground surface near the centerline of epicenters located in the mountains north of Spitak. Because of the coincidence of this centerline with the pronounced Landsat photolineament described earlier, there appears to be even more reason to field check the lineament for surface rupture.

Aftershocks beyond the eastern limit of the mapped 1988 surface rupture appear to curve southeastward in their distribution, and this change in orientation may be reflected in the similar changes in strike of the surface faulting where it leaves bedrock and enters alluvium near the southern part of Spitak.

CONCLUSIONS AND SPECULATIONS

The 2 m of maximum surface displacement fits well within the range of reliably mea-

sured maximum surface offsets for historic reverse and oblique reverse faulting events throughout the world as indicated by Bonilla and others (1984). At $M_s = 6.8$ to 7.0, the range of displacement for these historic events is about 0.8 to 3.6 m. By contrast, the presently known length of surface rupture near Spitak, 8 to possibly 13 km, is shorter than any other reverse or oblique reverse event of magnitude greater than 6.0 that are deemed to be well-determined by Bonilla and others (1984). Although the focus of the main shock may have been deep enough to account for the short length, few aftershocks extend below about 14 km, only approximately fixed because of uncertain velocity structure (Simpson and others, 1989). Because the deepest aftershocks seem to be consistent with a shallow focus, the enigma of the possibly short length of surface rupture remains. This anomaly may be another reason to suppose that additional surface rupture might remain unmapped.

The right-reverse surface faulting near Spitak makes interesting contrast to the mostly left-reverse displacements associated with the San Fernando, California, earthquake in 1971. Although the surface-wave magnitude at San Fernando was only 6.5, the maximum surface displacement there was larger, about 2.5 m, and the 15-km rupture was longer (Sharp, 1975). In a fortuitous similarity, at San Fernando the left-reverse slip changed westward to oblique left-lateral slip, a mirror image of the relations near the east end of surface faulting near Spitak.

Several segments of the San Andreas fault in California are bounded on one side by thrust or reverse faults sharing the same strike but dipping inward toward the San Andreas fault. These are especially common northeast of the San Andreas in the western Mojave Desert. The width of the rising blocks between the two structures is commonly about 2 to 5 km. Although no historic surface faulting is known for these thrust faults in California, the interesting possibility of displacement on both master break and bordering reverse fault in association with a single major earthquake deserves consideration. If the major photolineament near Spitak discussed earlier does represent a fault trace that displaced in this event, although this possibility is only a speculation now, the pair of simultaneous surface ruptures would be of special interest and applicability to seismotectonic studies in North America, as well as many other regions of the world.

REFERENCES – CHAPTER 4

Aki, K., and P. G. Richards (1980). Quantitative Seismology—Theory and Methods, v. 1, Freeman and Co., San Francisco, 557 p.

Bonilla, M. G., R. K. Mark, and J. J. Lienkaemper (1984). Statistical relation among earthquake magnitude, surface rupture length, and surface fault displacement, Bull. Seism. Soc. Am. 74, 2379–2411.

Filson, J. and others (1989). Tectonic setting and seismic setting for the main shock of December 7, 1988, this volume.

Sharp, R. V. (1975). Displacement on tectonic ruptures, *in* the San Fernando, California, earthquake of 9 February 1971, Calif. Div. Mines and Geol., Bull. 196, Chap. 15, 187–194.

Sharp R. V., K. E. Budding, J. Boatwright, M. J. Ader, M. G. Bonilla, M. M. Clark, T. E. Fumal, K. K. Harms, J. J. Lienkaemper, D. M. Morton, B. J. O'Neill, C. L. Ostergren, D. J. Ponti, M. J. Rymer, J. L. Saxton, and J. D. Sims (1989). Surface faulting in the Superstition Hills fault zone and nearby faults associated with the earthquakes of 24 November 1987, Bull. Seism. Soc. Am. 79, in press.

Simpson, D. W., M. Andrews, E. Cranswick, and G. Glassmoyer (1989). Preliminary aftershock locations (December 21–January 30, 1989), this volume.

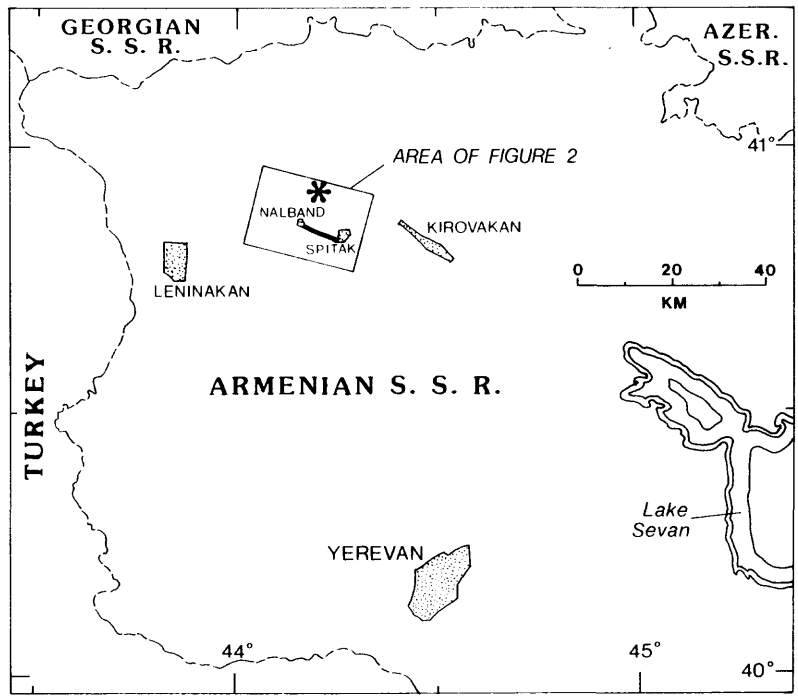

FIGURE 4.1. Index map of part of Armenian S.S.R. showing locations of surface faulting (heavy line) and the epicenter of the main shock (asterisk).

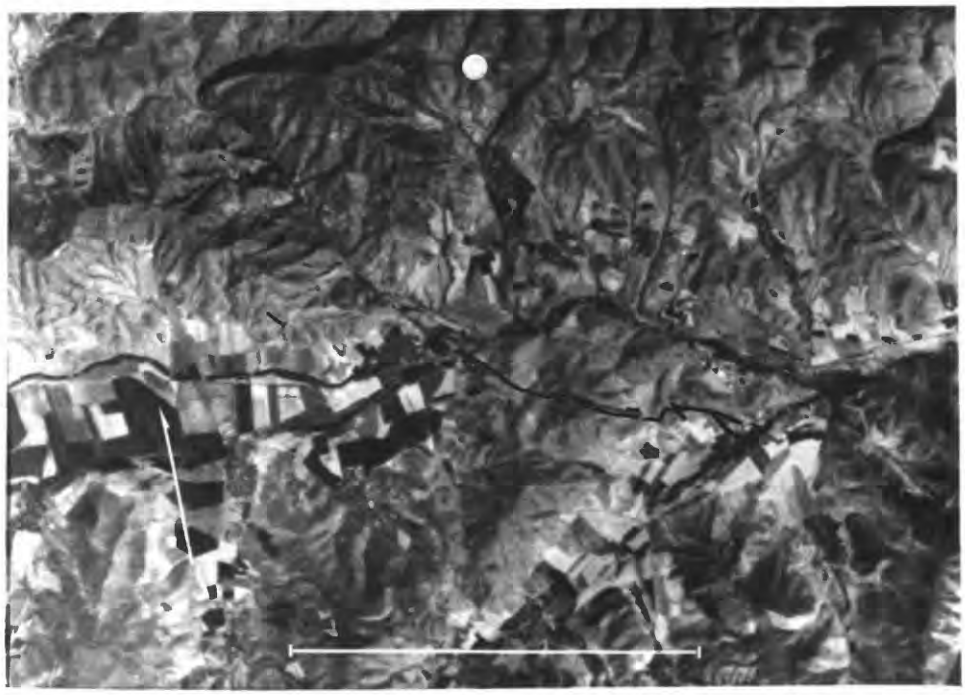

FIGURE 4.2. Trace of surface faulting near Spitak drawn on a pre-earthquake Landsat image. North is indicated by the arrow, and the bar near the bottom indicates 10 km. Surface ruptures are indicated by the black lines, and the epicenter of the main shock from Soviet seismic data is indicated by a white dot.

FIGURE 4.3. Trace of the surface rupture near Spitak. View is toward west–northwest. The surface breaks are visible near the upper edge of the snowy area on the lower left. Crest of small ridge where man faces fault (right of center) trends N–S and was not offset laterally.

FIGURE 4.4. Profile view of deformation of the ground surface along the fault trace. Location and direction of view is the same as in Figure 3. The breadth of the rupture and the rounded profile of the leading edge of the hanging wall (right side) is easily seen at the skyline.

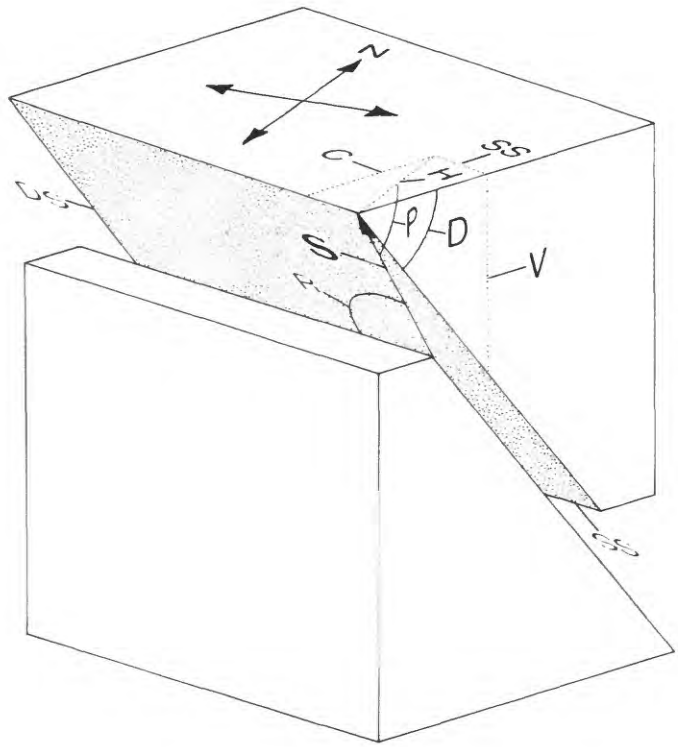

FIGURE 4.5. Maximum surface slip vector, by projection of the vertical component onto the average orientation of the fault plane in bedrock. The pre-earthquake (undisplaced) cube has 3-m edges and vertical faces parallel and normal to fault strike. The arrow in the fault plane (stippled) is the slip vector. The labeled dimensions, angles and directions are: N = north; azimuth of fault strike (not labeled) = 292°; dip of fault (D) = 55°; slip (S) = 2.0 m; vertical component (V) = 1.6 m; strike-slip component (SS) = 0.5 m (right-lateral); contractional component (C) = 1.1 m; horizontal component (H) = 1.2 m; dip-slip component (DS) = 1.9 m; plunge of slip (P) = 53°; rake of slip (R) = 109°.

FIGURE 4.6. Right-lateral offset of plow furrows in alluvium near Spitak. The more deeply-cut furrow on the right indicates the horizontal slip here to be about 1 m. View northeastward.

FIGURE 4.7. Bedrock fractures and earlier shearing along the fault trace near Spitak. Bedrock on both sides and within shear zone consists of Neogene volcanic rocks, but Cretaceous limestone crops out nearby.

CHAPTER 5

SEISMOLOGICAL INVESTIGATIONS (OBJECTIVES AND FIELD EXPERIMENTS)

R. Borcherdt, D. Simpson, C. Langer, G. Sembera, C. Dietel, E. Cranswick, C. Mueller, T. Noce, M. Andrews, and G. Glassmoyer

Soviet capabilities to monitor regional seismicity including aftershocks were severely restricted. The center for analysis of seismic observations, prior to the main shock, was located in Leninakan. Many of the center's facilities suffered damage. The tragic upheaval of the city, including initial lack of power and communications, and the emphasis on rescue efforts severely limited local efforts to maintain a regional seismic monitoring capability. Developing such a capability was of special concern, because of the need to assess the seismic hazard for the cities of Kirovakan, near a south-east projection of the fault trace and Yerevan, the capitol city with a population of 1.2 million, both cities with construction similar to that destroyed in Leninakan. Learning of these concerns upon our arrival, it was clear that an important objective of the seismological investigations was to deploy the seismic stations so as both to provide accurate locations for the seismicity occurring in the epicentral region as well as a capability to monitor low levels of seismicity as they might be occurring near Yerevan.

Another subject of considerable concern was the seismic safety of the Armenian Nuclear Power Plant, comprised of three reactors, two with seismic design provisions and one built prior to provision development. The plant, about 70 km from the epicentral region, had experienced about 1.8 percent g at ground level during the main shock. As safe-shutdown level for the plant was indicated to be 2.5 percent g, the plant continued to operate during and after the main shock; with the exception of a 48-hour period used for safety inspections. As a result of public concern for safety of the plant, Soviet colleagues encouraged the monitoring of ground motions at the site. Stations were installed in the epicentral region for purposes of event location, focal-mechanism determination, source parameter analysis, strong-motion observation, and effects of local geologic deposits. As

these experiments were nearing completion, concern for seismic safety of Yerevan resulted in encouragement to establish a regional network to monitor seismicity throughout the region encompassing the epicenter for the main shock and the city of Yerevan. Towards this objective a seven-station network was established near the end of our initial stay in Armenia S.S.R. This network is in operation as of this writing.

Equipment transported by the U.S. seismological team for installation included; 12 analog seismographs (MEQ; see Chapter 6.3), 12 digital seismographs (GEOS; see Chapters 6.1 and 6.2), and necessary support equipment; including, Omega time receivers, master clocks, and a self-contained computer system with independent power supply. To meet export restrictions and achieve compatibility with Soviet computer systems, an 11/73 computer system was utilized (see Chapter 6.2). Logistic considerations resulted in the computer center for playback and analysis being established in Yerevan at the Yerevan seismic station. Field headquarters for instrument deployment was established near the epicentral region in Kirovakan, about 100 km from Yerevan or 3–6 hours by motor vehicle depending on traffic conditions. Difficult logistics including temperatures often below 0°C restricted site availability and capabilities to conduct short-term experiments of 2–3 day duration.

Locations occupied by the digital seismic recorders are shown in Figures 5.1 and 5.3. Locations occupied by the analog seismographs are shown in Figure 5.2. Coordinates for the sites and station identifications are given in Table 5.1. Deployment time intervals for each of the stations are given in Table 5.2. Descriptions of the sites used for the digital sites are provided in Appendix A, Volume I. Digital recorders were selected for the southern sites required for location of seismicity near Yerevan, in order to permit longer periods of unattended operation. The three southern stations installed for purposes of locating seismicity near Yerevan and the Armenian Nuclear Power Plant were installed December 22, 1988. Upon establishment of a field headquarters in Kirovakan, ten stations were established in the epicentral region on December 23, 1988 using three deployment teams. Station deployment intervals are described in detail in Chapter 7.

Five of the station locations in the epicentral region were chosen to colocate both analog and digital recorders in order to provide redundancy for event locations and focal mechanism determinations (compare Figures 5.1 and 5.2). The remaining locations

were chosen to improve event location and focal mechanism capabilities, for near-source strong-motion observation, for source parameter determination and for investigation of the influence of site conditions in Leninakan on damage. Data from the analog stations were used to provide preliminary event locations at the field headquarters in Kirovakan. The digital recordings were examined at the field headquarters with a portable playback unit to evaluate instrument performance and transported to the computer center in Yerevan for playback and analysis.

Sites were selected for regional monitoring of the seismicity, because of the concern for public safety (Figure 5.3). Plans to establish this array were developed on December 27, 1988. Establishment of the array required that the digital recorders be utilized and that the systems be reprogrammed to permit 3–6 weeks of unattended operation. To increase the number of events that could be recorded fourfold, digitization rates were decreased from 200 sps to 100 sps and the systems reprogrammed to record 3 input channels as opposed to 6. Both auto batteries and local power were used to provide power. The data sets recorded on the systems are described in Chapter 7 and displayed in subsequent volumes.

Table 5.1. Station coordinates for digital and analog recorders.

GEOS	MEQ	Latitude		Longitude		Elev.	Site
	ALI	40	46.00N	44	23.10E	1620	Alavar
APP		40	15. N	44	16. E	980	Armenian nuclear power plant
	ARE	40	52.55N	44	16.40E	1800	Arevashok
ART	ART	40	50.20N	44	2.60E	1760	Artagyukh
	BAZ	40	52.30N	44	26.50E	1600	Bzovdal
BYR		40	19.08N	44	16.29E	1400	Byurakan
DZH	DZH	40	47.25N	44	11.20E	1690	Dzhrashen
GIB	GIB	40	44. N	44	41. E	1800	Geologic Institute Base
GOG		40	53.82N	44	11.94E	1870	Gogaran
GSS		40	8.16N	44	43.44E	1460	Garni seismic station
	KAT	41	2.28N	44	13.14E	1600	Katnakhpyur
KET	KET	40	52.70N	43	50.85E	1740	Nizhnyaya Keti
KIR	KIR	40	47.20N	44	29.55E	1500	Kirovakan site 1
KI2		40	47.20N	44	29.55E	1500	Kirovakan site 2
LEN		40	48.79N	43	50.80E	1560	Leninakan
MOO	MOS	40	59.55N	43	56.40E	2090	Moosailanski site 1 (school)
MO2	MO2	40	59.45N	43	56.30E	2090	Moosailanski site 2 (house)
NAB		40	50.95N	44	9.50E	1670	Nalband
	PIN	40	56.35N	44	28.90E	1400	Pushkinskiy
SCH		40	47.2 N	44	9.5 E	1800	Lernavan school
SEV		40	35.0 N	44	57.5 E	2000	Sevan
	SIP	40	43.48N	44	16.25E	2150	Sipovar
SPT		40	49.90N	44	16.20E	1540	Spitak
SSS		41	0. N	44	23. E	1400	Stepanavan seismic station
STE	ARM	41	1.20N	44	19.50E	1500	Armanis
YSS		40	10.98N	44	30.00E	1000	Yerevan seismic station

Station locations are given in degrees, minutes, and fractions of minutes—accurate to no better than 0.05 minutes. Blank spaces in the fractional minutes columns indicate that the coordinates of those stations were not measured as accurately. In addition, locations of GIB, SCH and SEV are particularly suspect. The GIB and SCH station locations were not determined in the field. Their coordinates were measured after the field party returned to the U.S. by guessing at their location on a 1:250,000 scale map. These locations may be in error by as much as 2 minutes. The SCH station may actually be in Dzhrashen with coordinates similar to DZH. The SEV coordinates indicate a location that is inconsistent with map locations of the town, lake, and roads (possible alternate location: 40 33.6N, 44 57.5E). The YSS coordinates may also be inconsistent with map locations of the city and roads (possible alternate location: 40 11.8N, 44 28.4E).

Elevations are in meters—accurate to approximately 50 meters.

Table 5.2. Deployment time intervals for digital and analog recorders.

GEOS	MEQ	Deployment	Intervals
APP		356 14:17	– 365 07:50
	ALI	359	– 005
	ARE	359	– 005
ART		359 12:40	– 004 08:16
	ART	359	– 004
	BAZ	358	– 004
BYR		365 14:00	– current
DZH		360 14:18	– 004 09:54
	DZH	360	– 005
GIB		357 15:58	– 358 03:50
	GIB	357	– 358
GOG		365 12:00	– 004 11:03
GSS		356 13:54	– current
	KAT	366	– 004
KET		358 14:06	– current
	KET	358	– 004
KIR		358 19:48	– 001 09:12
	KIR	358	– 005
KI2		001 11:23	– current
LEN		358 15:37	– 366 11:38
MOO		358 11:41	– 364 10:36
	MOS	358	– 364
MO2		364 13:12	– 004 10:33
	MO2	364	– 004
NAB		358 14:52	– 363 07:37
	PIN	358	– 004
SCH		358 13:09	– 359
SEV		002 12:45	– current
	SIP	359	– 005
SPT		358 11:25	– 360 13:00
SSS		003 11:18	– current
STE		358 10:27	– 003 08:30
	ARM	358	– 004
YSS		357 05:44	– 362 07:53
YSS		007 15:12	– current (re-occupied)

Current implies instrument was still deployed as of 7 February 1989 (038).

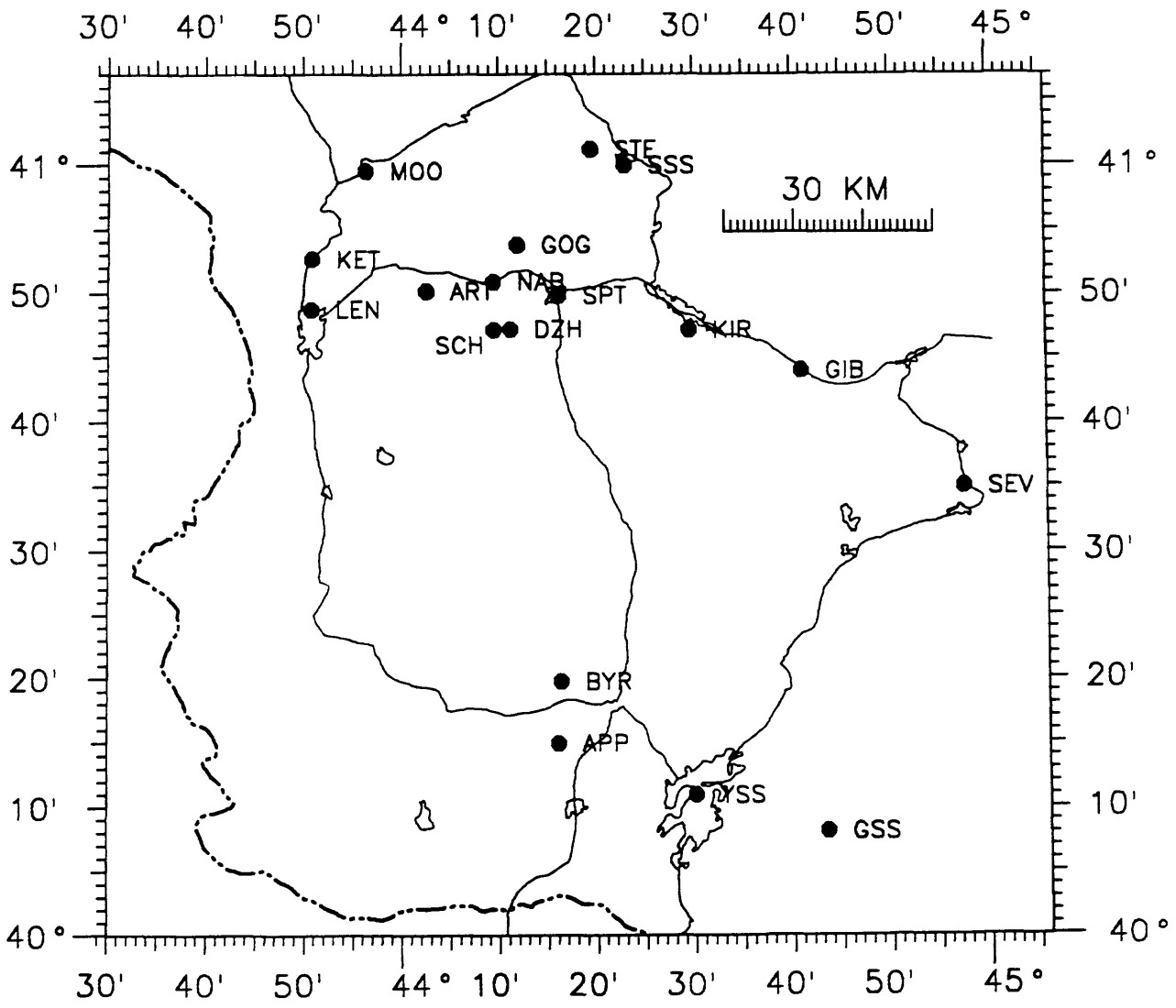

FIGURE 5.1. Location map for deployment sites of digital recorders (GEOS) used during the time period of December 21, 1988 through about March 1, 1989. Cities, roads, Armenia S.S.R.–Turkey border, and three-letter station identification codes are indicated on the map.

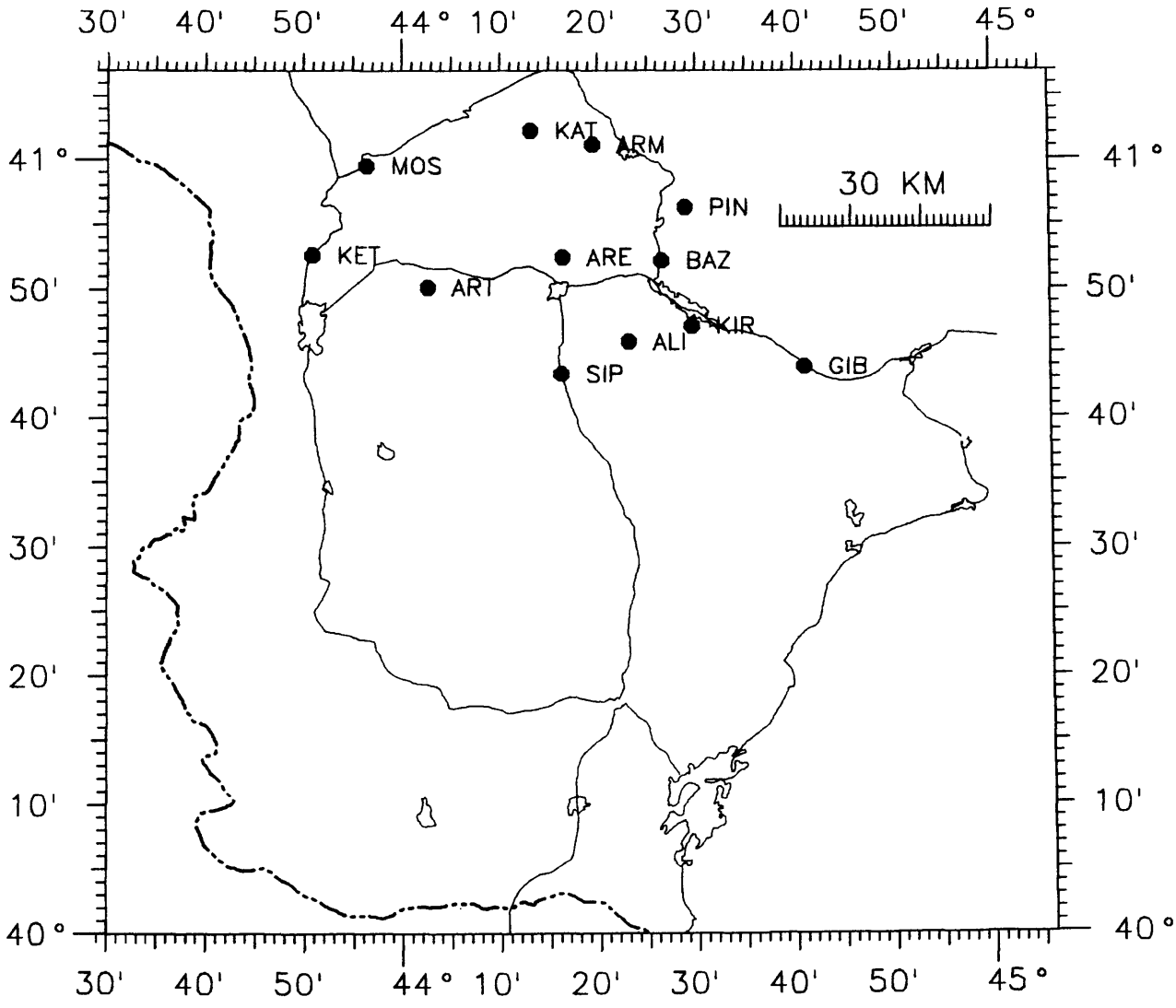

FIGURE 5.2. **Location map for deployment sites of analog recorders (MEQ) used during the time period of December 22, 1988 through January 4, 1989. Cities, roads, Armenia S.S.R.–Turkey border, and three-letter station identification codes are indicated on the map.**

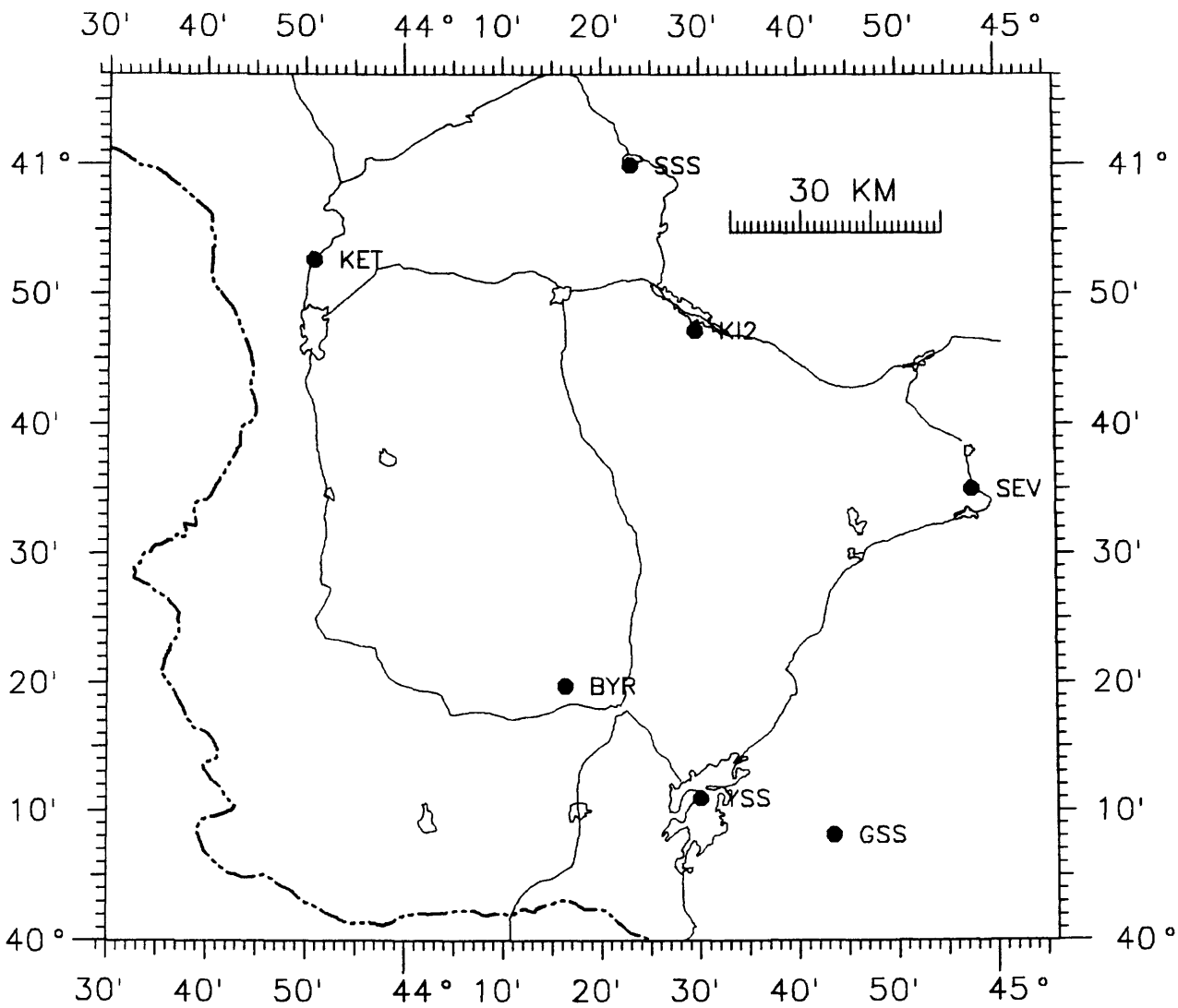

FIGURE 5.3. Location map for deployment sites of digital recorders (GEOS) used during the second longer-term deployment of GEOS to monitor seismicity in the epicentral region.

CHAPTER 6

INSTRUMENTATION USED FOR SEISMOLOGICAL INVESTIGATIONS

Twelve digital and twelve analog recording systems were transported to the Soviet Unon together with appropriate support equipment for deployment, timing and data playback. Characteristics of this equipment pertinent to the studies described herein are presented in subsequent sections.

6.1 Digital Recording Systems

R. Borcherdt, G. Maxwell, J. Sena, M. Kennedy, G. Jensen, and J. Van Schaack

The digital recording systems used for the seismological investigations were developed by the U.S. Geological Survey for use in a wide variety of active and passive seismic experiments (GEOS; Borcherdt *et al.*, 1985). Broad-bandwidth (0–600 Hz), high signal resolution (16-bit; 96 dB), wide effective dynamic range (180 dB), and microprocessor selectable operation parameters are features of the systems which permit flexibility in utilization of the systems for a wide variety of experiments; including structural response, soil structure interaction, post main shock ground motion, seismicity, near-source high frequencies, seismic refraction, large array tomography, teleseismic earth structure, earth tidal strains and free oscillations.

Versatility in application of the systems to a wide variety of experiments was achieved by isolating major functions required of digital seismic data acquisition systems on hardware modules which in turn are under control of a central microcomputer via computer bus. Major system modules are those for signal conditioning of analog outputs, digital conversion of analog signals, temporary solid-state data storage for data preprocessing, and dissemination, data storage, retrieval and transmission, time reference, system calibration and operator interface. General segmented software was developed to control modules, perform on-line system functions and system debugging. Segmented software facilitates module replacement for repair and system modification for a variety of experiments as

well as technology upgrades of components (see Borcherdt *et al.*, 1985, for a detailed description of the system). The General Earthquake Observation System (GEOS) together with the two sets of these component sensors (force-balance accelerometers and velocity transducers) as deployed in Armenia is shown in Figure 6.1.1.

For use in Armenia, each of the six input channels of the signal conditioning modules were utilized. Three of the channels were used to record analog signals from L–22, 2 Hz velocity transducers and three to record the signals from accelerometers (FBA–13, 100 Hz). This sensor configuration allows the system to obtain on-scale recordings ranging in amplitude from a few nanometers of seismic background noise at 10 Hz to 2 g in acceleration at 10 Hz for ground motions near large earthquakes. The analog-to-digital conversion module, equipped with a 16-bit CMOS analog-to-digital converter, affords 96 dB of linear dynamic range, which with 60 dB of gain in 6 dB steps, affords an effective total system dynamic range of about 180 dB near 10 Hz. Gain settings for the velocity transducers varied from 36 dB at the noisier sites to 60 dB at the quietest site near Garni (GSS). Gain settings for the force-balance accelerometers were set between 0 and 18 dB depending on distance from anticipated sources of strong shaking. Sampling rates were chosen at 200 sps per channel for all sites except those occupied for long-term monitoring purposes (see Figure 5.3). Sampling rates were chosen at 100 sps for these sites. Seven-pole Butterworth anti-aliasing filters with corners at 50 and 33 Hz were chosen for the two sampling rates.

Microprocessor control of a time-standard provides the capability to synchronize the internal clock via internal receivers (WWVB), external master clock, or conventional digital clocks. Microprocessor control of internal receivers permits systems on command to determine time corrections with respect to an external standard. This capability permits especially accurate corrections for the conventional drift of internal clocks. Timing for the Armenian experiments was achieved using an Omega receiver to establish a time standard. Portable master clocks were then used to obtain clock connections between the internal clocks of the recorders and the time standard provided by the Omega receiver.

Accurate *in situ* calibration of system components improves data accuracy and permits on-site evaluation of potential system performance malfunctions. The calibration module currently implemented in the GEOS permits calibration of three types of sensors

and the signal-conditioning module under software control of the CPU. Calibration capabilities for sensors include velocity transducers with and without calibration coils and force-balance accelerometers. In the case of the velocity transducers, a DC voltage, derived under CPU control for appropriate gain setting from the D/A converter, is applied to either the main or calibration coil of the transducer for a software-selectable time interval. Voltage termination corresponds to an applied step function in acceleration to the sensor mass with the resultant signal determining relative calibration. In the case of force-balance accelerometers ± 12 volts are applied to the damped and undamped control lines. The signal-conditioning module is calibrated using an impulse of one sample duration and an alternating DC voltage derived and applied under software control to the amplifiers while the sensors are disconnected via appropriate relays. For the Armenian deployments, operators were instructed to obtain a recording system calibration with the replacement of each tape cartridge. These calibration data are available upon request, but for brevity are not included in this report. Response curves for the recording system equipped with FBAs and L–4 (1 Hz) velocity transducers are given in Figure 6.1.2

The 32-character alphanumeric display under control of the microcomputer allowed the GEOS to be readily reprogrammed in the field with parameters most appropriate for the site selected and experiment being conducted. The English language prompts of the system have been shown to reduce operator errors and facilitate system reprogramming. (We learned an obvious lesson on this trip, however, when it came time to train observers to change tapes on the systems during the longer-term deployment phase. English language prompts were not especially helpful to those that don't read English. The help of interpreters turned out to be essential for the success of the experiment.)

For data retrieval 1600 bpi tapes with a capacity of about 1.25 Mbytes were used. Recording parameters, station identifications, and timing information are recorded on the tape together with the digital event data in ANSI standard format. This format is used to facilitate access to the data via mini-computer systems. (GEOS under construction utilize higher density cartridges, 6400 bpi, with a capacity of about 16 Mbytes and an expanded data buffer, 1 Mbyte, in order that the recorders can serve as solid state or dual media recorders. The expanded data buffer facilitates data transmission via telecommunications

and use of the systems in cold environments.) Each of the tape cartridges retrieved were examined using a portable playback system which includes many of the same modules in the GEOS field recorder, with the exception of the analog-to-digital module which is replaced with a digital-to-analog module. Once the data were evaluated for instrument performance the cartridge tapes were transported to Yerevan for playback and analysis on the computer system set up at the Yerevan seismic station (YSS). Configuration of the computer system is described in the next section.

Due to temperature specifications of the magnetic tape and the low temperatures encountered during the deployment periods, sites for deployment of the recorders were selected so as to provide some shelter from direct wind. Most shelters were unheated. A detailed description of the sites selected is presented in Appendix 1. Considering the adverse weather conditions, the instrumentation performed remarkably well. One unit showed high clock drift rates at one of the sites (KET). Difficulties in magnetic tape recording, attributed to especially low temperatures, were encountered at two sites (ART, SCH).

6.2 Field Computer for Playback of Digital Data in Armenia S.S.R.

G. Maxwell and M. Kennedy

A field computer was configured and transported to the region to provide copies of the digital data and to conduct preliminary analyses. The computer system was used to process the cartridge tapes produced by the GEOS recorders, catalogue the recorded time series, interactively determine P- and S-wave arrivals for event location, and to make copies of the data.

The computer system was composed of a Digital Equipment Corp. LSI–11/73 microcomputer, 1 megabyte of MOS parity memory, an Emulex 110 megabyte disk drive, a DSD–890 30 megabyte disk drive, a Cipher Products 9-track 1600 bpi tape drive, an Apple LaserWriter II printer, two Tandberg TDC–3000 cartridge tape drives, and a Digital Engineering VT640 Retrographics terminal. Most of the system components were housed in a ruggedized, shock-resistant shipping container. The RSX–11M–Plus operating system, version 4.1, and a standard suite of Fortran programs utilized by the USGS for earthquake processing comprised the software for the computer system. This set of computer hard-

ware was chosen for compatibility with known host-country hardware and to comply with export restrictions. The hardware and software were configured for shipping within seven days prior to the team's departure.

Because of the need to operate the computer system in a self-sufficient environment, electrical power to operate the computer system was supplied by a Onan 6.5 kilowatt gasoline-powered generator, with the generator output conditioned by a Deltec 5 KVA power conditioner. The generator was tested and adjusted by the vendor prior to shipment to supply the correct voltage and frequency (120 VAC, 60 Hz) for the intended power rating of the computer system. It was intended to also utilize an uninterruptable power supply (UPS) to further condition the power and provide emergency power, but shipping problems prevented the UPS from being included with the shipment of equipment.

The computer system was installed and set up at the Yerevan Seismic Station on December 25, 1988. As recorded GEOS tapes were brought back from the field, they were read back into the computer system for visual display, analysis, and copying in digital and analog formats. Intermittent problems with the 110 Mbyte disk drive prevented collation of the entire data set and completion of the analyses intended. The intermittent problems with the disk drive were eventually traced, with the assistance of Soviet colleagues and hardware, to the power supplied by the generator at 57 Hz, which was below the 60 ± 1 Hz requirement of the disk drive. Fine adjustments of the governor for the generator were required to achieve desired frequency output so as not to exceed power input requirements of power conditioner.

6.3 Analog Recording Systems

C. Langer and D. Simpson

Twelve smoked-paper recording seismographs (Sprengnether Instrument Company MEQ–800s (see Figure 6.3.1), provided the core instrumentation for gathering data to locate aftershock hypocenters. The single-component MEQ–800 portable recorders, weighing about 11 kg, without batteries, were designed specifically to operate under severe field conditions such as snow and cold weather enountered during the Armenia study. Each system includes a high-gain amplifier (60 to 120 dB in six dB steps) with low-cut and

high-cut filters, a temperature compensated crystal controlled timing system (long-term stability of $\pm 5 \times 10^{-8}$ per month), precision drum drive and pen-motor translation mechanisms synchronized to the clock, and a vertical component (1 Hz natural period) velocity sensing transducer for detecting the microearthquake signals. System power is delivered by an external battery pack, consisting of two twelve-volt (6.5 amp/hour) gel-cell batteries, which is changed and recharged at two-day intervals.

In Armenia, the seismographs were adjusted to record at drum rotation speeds of 60 mm/min with a trace separation of 1 mm/revolution, allowing 48 hours of continuous operation between record changes (Figure 6.3.2 shows example seismogram). During record changes, precise time corrections were determined with an oscilloscope by comparing the recorder clock drift against the output from a master clock set to Omega time. After a one- or two-day stabilization period for adapting to ambient temperature conditions, the recorder clocks generally did not drift more than about 50 ms/day. Those recorders subject to large temperature swings (*e.g.*, approximately -25 to $+5$°C at SIP and ALI) experienced clock drifts as large as 200 ms/day.

Seismograph magnifications ranged between about 85,000 and 350,000 at 10 Hz. Amplifier gains were limited by the background noise at recording sites, many of which were located close to cultural noise sources and on unconsolidated soils. To minimize noise (mainly from wind) filter settings of 5–10 Hz or a peaked response at 10 Hz (filter setting of 10–10 Hz) were used. At several stations where intense aftershock activity was occurring, peak-to-peak deflections of recorder styli were electronically restricted at 20 mm to prevent "over writing" of recorded aftershock data. Special care was taken in the field to maintain the integrity of first-motion polarities for each seismograph system, that is, seismometers, cables, and recorders were not intermixed. Upon return to the Golden, Colorado laboratory facility, polarities were verified in addition to checking amplitude and phase responses.

To provide a continuous monitor of the seismicity in the aftershock area, 12 MEQ–800 recorders were installed at the sites shown in Figure 5.2 Site locations and dates of operation are shown in Tables 5.1 and 5.2.

Site Locations. The main purpose of the analog recorders was to provide dense,

uniform coverage for hypocentral locations. The selection of sites was made based on the available knowledge of the epicentral distribution from felt reports, preliminary Soviet and French data and geological information. An effort was made to surround the epicentral area with station spacing on the order of 10 km. Except for the north-central region, where access was limited because the only road was closed due to snow in the high elevations, the distribution of stations provides good azimuthal and distance coverage. For security reasons and because of the cold weather, most instruments were installed in enclosed buildings, usually in small sheds, root cellars beneath or near abandoned houses, or in the basements of public buildings. A description of the sites used is given in Appendix A. Noise conditions were not ideal Because of weather conditions and the limited number of roads, it was difficult to find sites far removed from cultural noise. In spite of this, the relatively high level of activity meant that a reasonable number of events were recorded. Stations ALI and ARE, located almost directly on top of the fault zone, recorded extremely high numbers of small events. At ALI, small events were often both heard and felt during record changing.

6.4 Automated Computer Processing of the Armenian Data Set Recorded by GEOS Portable Autonomous Digital Seismographs (PADS)

E. Cranswick

Introduction

A field computer was established at the Yerevan Seismic Station (Chapter 6.2) to process the tape cartridges recorded by GEOS (Borcherdt *et al.*, 1985). Over the last nine years, I have developed a software package for use on field or office computers to efficiently process data sets collected on Portable Autonomous Digital Seismographs (PADS). The software is designed for flexibility in terms of speed and disk-space requirements. The software is designed to produce scientific analyses and results for PADS data sets within a short period of time after it is recorded: within hours or days depending on the amount of data and the complexity of the analysis. In Armenia, all the field computer's functions which had been specified as part of the field program goals were performed: 1) tape cartridge playback, 2) file management/data organization; 3) time series display; 4) spectral analysis; 5) interactive graphical phase picking; 6) earthquake location (using a modified version of HYPOINVERSE, Klein, 1978); 7) epicenter maps; 8) hardcopy of graphical output; and, 9) transfer of digital data to our Soviet counterpart personnel via ASCII time-series files on 9-track tapes.

Due to power supply problems related to the gasoline-powered electric generator used as a power source, the total uptime of the field computer was approximately only 20% of the two weeks it was operated; and therefore, the goal of complete playback, event picking and locating, and data transfer was not achieved during the field program. The large volume of data collected required the full-time efforts of three people, two computers, and two laser printers for about a month to process and analyze the data to the extent described here. Field computer processing essential for several critical "near real-time" applications during the field program; including, tape cartridge playback to identify hardware malfunctions. The field computer and autonomous power supply were established within one day after

returning from the field. Establishment of the system and installation of the PADS software permitted my identification of the Leninakan site response (see Chapter 9), allowed plots of time-series and spectra for several of the larger aftershocks, the location of a limited number of events, and transfer of some data to digital magnetic tape for our hosts.

The data set described herein provides examples of the processing capabilities of the PADS software. Records of events as recorded by six or more stations are presented in Chapter 7.2. Seismograms as processed from the digital seismograms are provided in Volumes II, III, IV, and V. P and S arrival times determined using PADS software were used in conjunction with manually determined times to provide the aftershock locations presented in Chapter 8. The software was used to prepare the data set for dissemination via IBM optical disk cartridge (see Chapter 12), floppy disk (Chapters 11 and 12), and magnetic tape (Chapter 10).

The PADS software was initially designed for operation on small-scale ruggedized minicomputer systems with limited memory for deployment in the field. The software has recently been modified and expanded to operate not only under RSX and VMS operating systems but also to operate under MS–DOS for use on IBM–PC-compatible systems (Cranswick *et al.*, 1989). This software and a selected subset of the data reported herein are provided on IBM–PC-compatile floppy diskettes to expedite analysis of this important data set (Cranswick *et al.*, 1989). The MS–DOS version of the software, entitled PC–VECTOR, provides time and frequency domain analyses capabilities for essentially any digital data set acquired on portable autonomous digital seismographs.

The Logical Structure of PADS Data

As discussed by Cranswick (1983), the computer is clearly essential for the scientific analysis of the digital waveform data recorded on PADS—but it is also necessary for the efficient file management of the potentially thousands of data files produced by a field program during which ten or more GEOSs are deployed for periods of a week or more (*e.g.,* the Armenian data set). Digitally-recorded telemetered seismograph networks have an advantage with respect to seismograph networks made up of PADS stations in that the seismic signals of the former are recorded with reference to the same time base as a result

of either real-time multiplexing along the transmission path or real-time synchronized digitization and recording at the central recording site. Furthermore, since the real-time digital signals are recorded together on the same storage volume under control of the same central processor, the time series of seismic events, from the moment they enter the computer system, are contained within an organized file structure. By contrast, PADS stations each record their own seismic signals with reference to their own independent time base on their own individual storage volumes (tape cartridges). After the PADS have made their recordings, a computer is required to operate in a post-real-time mode to appropriately merge the data sets recorded on individual seismographs into a logical file structure comparable to that produced in real-time by a telemetry network. The four basic tasks of a PADS processing system are:

Playback. The procedure by which the data recorded in the field is entered into the computer system. The term data refers to two categories of information: 1) the digital-waveform integer-time series as recorded on the original storage media (tapes, cassettes, cartridges, solid-state memory, etc.); 2) the accessory Station/Instrument Parameters (SIP) which define and scale the integer time series such as amplifier gains, transducer characteristics and orientation, station location, etc. The reading/uploading of the original media usually requires special hardware (*e.g.,* tape drives) and/or software which are specific to the original digital recording device. The SIP information is of a more general nature (though different PADSs themselves record different aspects of this information), but it requires a standardized procedure for inputting handwritten data from field notebooks and cassette labels into a human-computer-readable form: these parameters are stored in some form of ASCII computer file. Figure 6.4.1 is a cartoon representation of the flow of information through the PADS hardware and processing system: from the Earth to the eye of the analyst. The various components of the PADS which control/modify the information content of the record of the seismic signal and whose parameters must be entered into a SIP file are designated by the following three-letter codes:

JUG— ground-motion sensor: acceleration, velocity, displacement, strain; damping; transducer constant (volts/[unit of ground motion]).

PAM— pre-amplifier: gain/magnification

AMP— ampiflifier: gain/magnification

FIL— filter: type; low- or high-frequency; corner frequency; roll-off

ADC— analog/digital converter: input full-scale voltage; output number of resolution bits; gain-step number, gain, and threshold

TRG— trigger algorithm: type; absolute threshold level; short-term average (STA); long-term average (LTA); STA/LTA ratio

TIM— time of internal PADS clock: year; day; hour; minute; second; millisecond; microsecond

CKC— clock correction/error: time difference of PADS with respect to standard time

BAT— battery: voltage

Management. Refers to the bulk manipulation and control of the system's data mass without reference necessarily to the information contained within the individual time series *per se*. File management is a basic concern for as long as the data is part of the PADS processing system. The primary tasks of management are creating a file structure that permits accessing data from the different stations by event and establishing a common time-base for all the records of each event. This involves the association of individual waveform files (signal) that are co-incident in time and the identification of false-trigger files (noise) which can be deleted from the system. The step of winnowing out the noise files from the datamass can lead to a dramatic reduction in the size of the latter. The resulting data structure is then used in further processing of the data

Analysis. The process of applying various algorithms to the data to determine the characteristics of the signal: generally for the purpose of inferring the properties of seismic sources and earth structure.

Archival. The transfer of the data set to a permanent storage medium in such a form as to permit its rapid restoration (retrieval) to its functional internal form within the PADS processing system: this ensures that any data that have been entered into (processed by) the system are readily accessible thereafter. Efficient and reliable archival is critical to PADS data acquisition because PADS data are used by legislative bodies and regulatory agencies to establish government regulations and public policy based on objective information contained within the data set.

A Summary of Procedures for Processing GEOS Data

The program RDGEOS developed by G. Maxwell reads the data (individual trigger files containing waveform time series and SIP information recorded by the GEOS) from the separate tape cartridges using the Tandberg tape drive. It reformats the data from each trigger file into a standard waveform data-file format called "GEOS Format" and writes the resulting files to disk. "GEOS Format" files are blocked binary and consist of two blocks of header information containing those associated parameters (*i.e.,* , SIP) necessary to describe the waveform data followed by blocks which contain the waveform time series itself. Each trigger file is named with reference to the time of the first sample of the waveform time series or Initial Sample Time (IST). An example of an arrival file name is given below:

2801401J1.G10

where the first 8 characters express the IST: '280' is the Julian day; '1401' is the hour and minute; and 'J' is 10th of the 20 three-second intervals 'A'-'T' into which 60 seconds are divided, and 'J' corresponds to the time of 27–29 seconds. Since a properly functioning GEOS can trigger no more than once during any three-second interval, the time specification makes the filename unique for any given recorder. The character '1' just to the left of the '.' is the GEOS channel number of the time series. The three characters to the right of the '.' constitute the station/instrument code (STI) for the provenance of the data. This code does not merely refer to station, *i.e.,* , location in space, since it is possible in an experiment to have more than one instrument (seismograph) at the same station.

Once the GEOS tape cartridges have been loaded on disk, the primary method of organizing the arrival files from the several STIs is to arrange them chronologically by their respective ISTs. In order to make this significant to the network as a whole, it should contain all the ISTs from all STIs for a given time period. In the most general case of field study, the continuous monitoring of seismic activity for a period of several days at stations whose tapes are changed either regularly or intermittently, there must be sufficient disk space to store at least two tapes from each STI so as to allow for the overlap of tape-on/tape-off between any two STIs. The program ORDARR extracts the ISTs

from the arrival file headers and constructs an ordered-arrival list containing the arrival file specifications (paths—the respective resident directories—and filenames) arranged in order of ISTs "Julian second": Julian day time expressed in seconds (*i.e.*, , midnight of the New Year is Julian second = 86,400).

Since the purpose of a network, an array, or a geophone spread is to record the arrivals of seismic phases emanating from the same source and therefore arriving approximately at the same time, in the absence of other information, simultaneity of trigger (either self-triggered or pre-set) is generally the most effective criterion for categorizing the scientific value of an individual arrival file. The analysis programs (VECTOR, PC-VECTOR, RECSEC) determine the presence of earthquake records by using an ordered-arrival list to identify ISTs which occur within a moving-time window with a duration equal to the seismic-wave travel time across the seismograph network. Alternatively, trigger files corresponding to seismic events may be distinguished by correlating ISTs with a list of event times obtained *a priori* to any information contained in the internal structure of the ordered-arrival list. Three possible sources of this external information are: 1) observations of events on visible recorders such as smoked-paper seismographs (*e.g.*, MEQ800); 2) summary-card origin times from telemetered network locations such as that provided by the Calnet RTP; or, 3) a list of times from felt reports.

REFERENCES – CHAPTER 6

Borcherdt, R., J. B. Fletcher, E. G. Jensen, G. L. Maxwell, J. R. Van Schaack, R. E. Warrick, E. Cranswick, M. J. S. Johnston, and R. McClearn (1985). A general earthquake observation system (GEOS), Bull. Seism. Soc. Am. 75, 1783–1825.

Converse, A. (1984) AGRAM: a series of computer programs for processing digitized strong-motion accelerograms, Version 2.0; USGS Open–File Report 84–525.

Cranswick, E. (1983). Automated file management and automated signal processing of portable digital seismograph data, Proceedings of the CCSS Workshop on Portable Digital Seismograph Development, p. 65.

Cranswick, E., K. King, and R. Banfill (1989). PC–VECTOR, a program to perform time and frequency domain analysis of vector (three component) time series recorded by Portable Autonomous Digital Seismographs (PADS), U.S. Geol. Survey Open–File Report 89–, in press.

Klein, (1978). HYPOINVERSE, USGS Open–File Report No. 78–694.

*Dietel, C. and E. Cranswick (1986). DSDMAP: Digital Seismic Data Management/Analysis Package; USGS Open–File Report 86-_____

*Tarr, A., and E. Cranswick (1985). SDAP: Seismic Data Analysis Package, USGS Open–File Report 85-_____

*These manuscripts exist in essentially complete form, and are being used as internal USGS reports as user manuals, but they have never been formally published.

FIGURE 6.1.1. Side and front panel view of General Earthquake Observation System (GEOS), together with a WWVB antenna and two sets of three-component sensors commonly used to provide an effective dynamic range for the system of 180 dB.

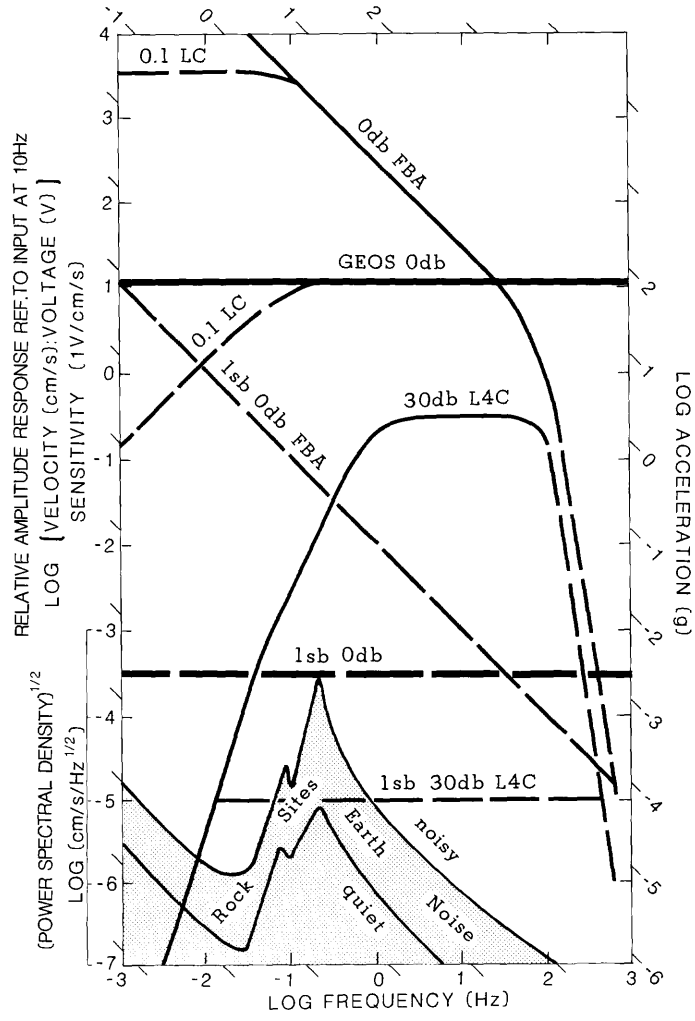

FIGURE 6.1.2. Unit-impulse response for the GEOS recorder, spectra for Earth noise (Aki and Richards, 1980), and recorder-sensor response for force-balance accelerometer at 0 dB gain and for L4–C velocity transducer (1 Hz) at 30 dB gain.

FIGURE 6.3.1. MEQ–800 seismograph (Sprengnether Instrument Company), portable oscilloscope and master clock as deployed at station ALI.

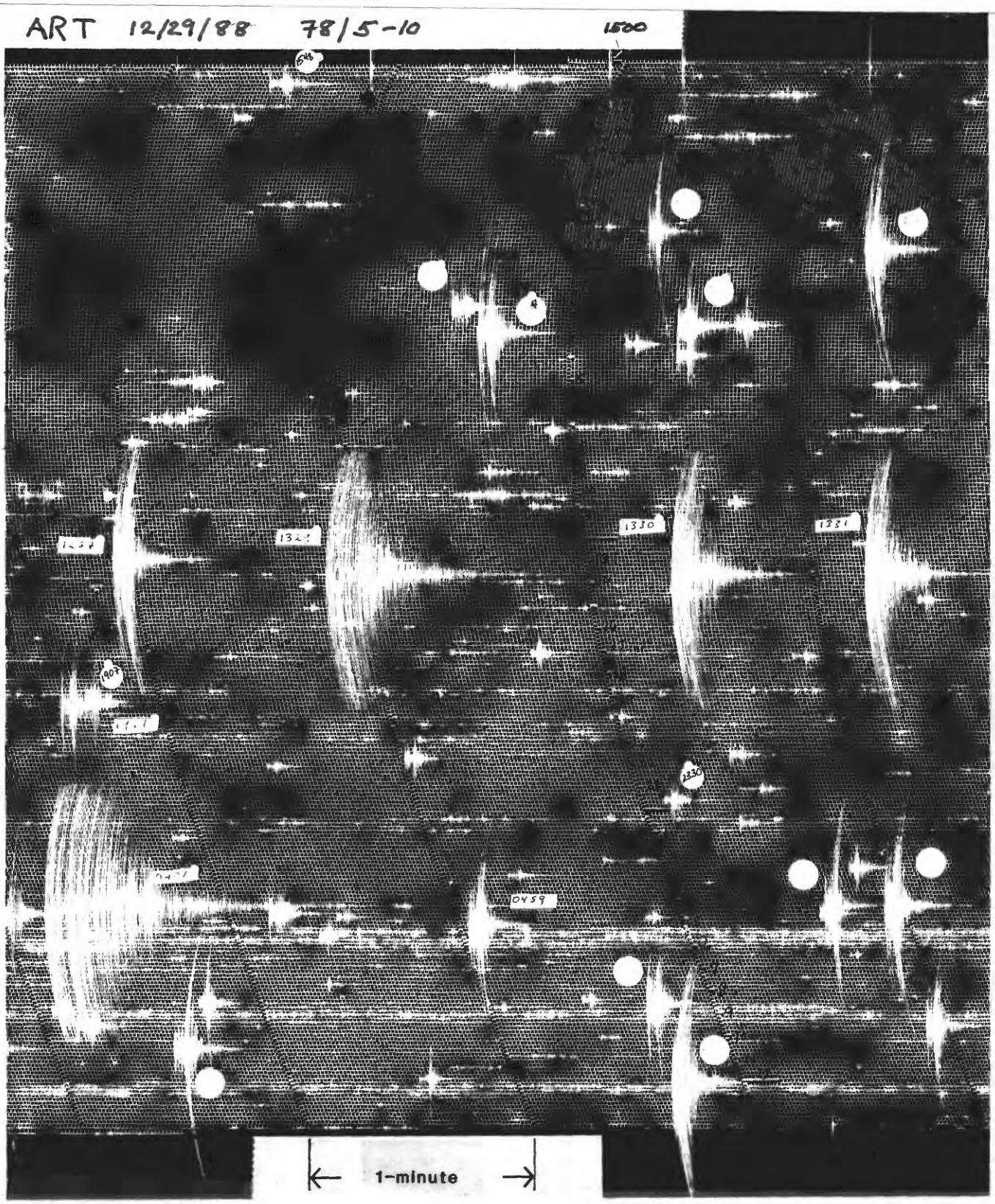

FIGURE 6.3.2. Seismograms recorded at station ART for a 48-hour time interval commencing on December 29, 1988.

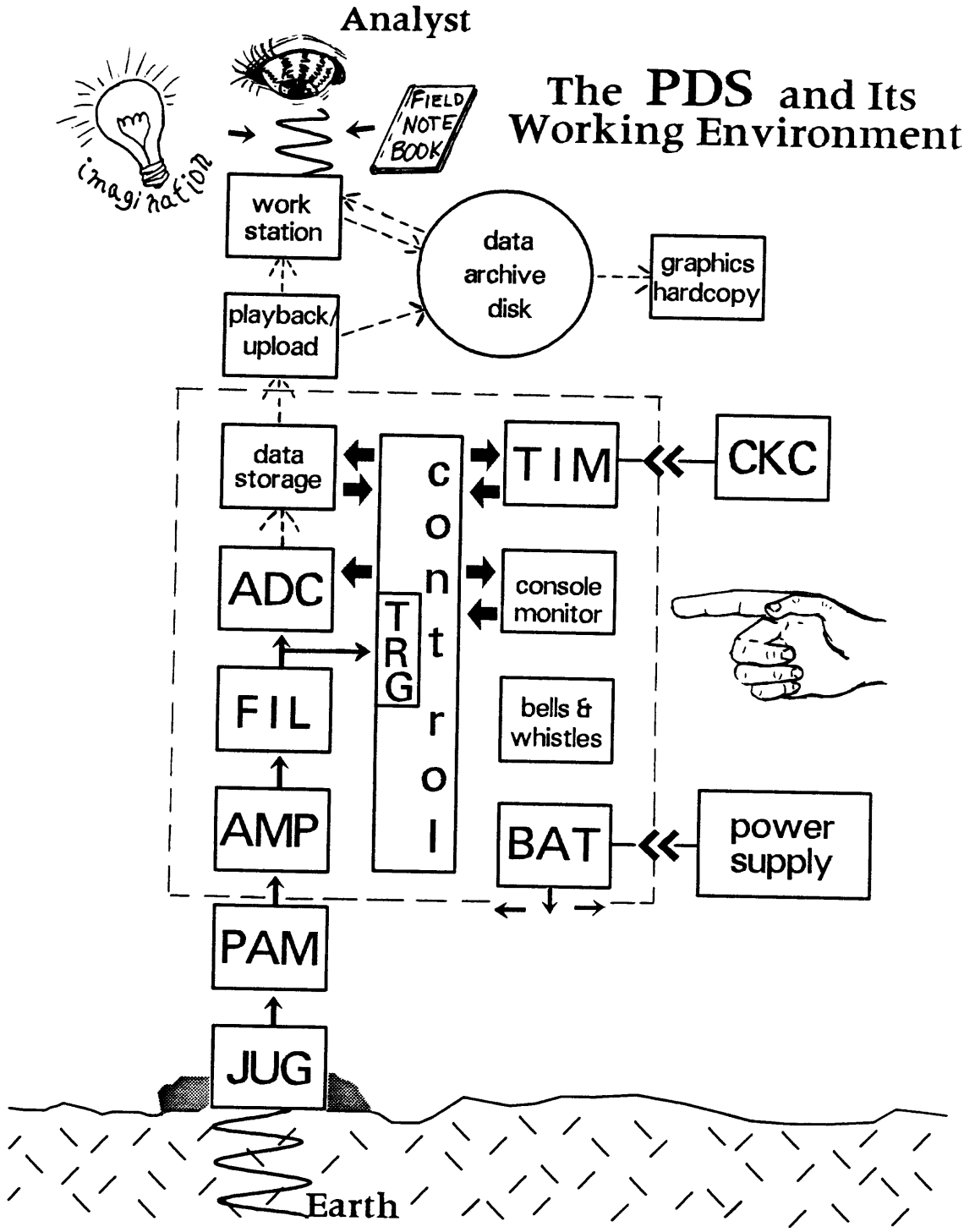

FIGURE 6.4.1. Cartoon representation of information flow through Portable Autonomous digital Seismographs (PADS) hardware (see text for abbreviations).

CHAPTER 7
SUMMARY FOR DIGITAL SEISMOGRAMS

This chapter includes descriptions of the procedures used to playback and process the data (7.1). The chapter also includes a description of waveforms and record sections for events recorded on six or more GEOS recorders (7.2, Appendix C).

7.1 Processing of Digital Seismograms Recorded During the Time Period 21 December 1988 through 7 Feburary 1989

G. Glassmoyer and G. Maxwell

Introduction

As of this writing 68 GEOS tape cartridges, representing the time period 21 December 1988 through 7 February 1989, have been played back into the Digital Electronic Corporation (DEC) PDP–11/70 computer of the National Strong Motion Data Center. The recordings obtained include 2053 three-component velocity records as listed in Appendix B. For 1728 of these (through about 4 January 1989) there are also corresponding three-component acceleration records.

Format

The format used for the digital data is a blocked-binary file consisting initially of two blocks (512 bytes each), one 2-byte integer, one 4-byte real, of header information. Integer and real values are stored in the format used by DEC PDP and VAX computers. (2-byte integer values are stored as low-byte first, high-byte second signed integers in two's complement form. 4-byte real values are stored as high-word (low-byte, high-byte) first, low-word (low-byte, high-byte) second). The information included in these headers is detailed in Table 7.1.1 (integer) and Table 7.1.2 (real). These can be followed by optional headers if so indicated in the initial header blocks. The data blocks follow.

During data playback and processing, seismograms are identified in the computer by a 13-character filename (constructed from the start-of-record time, uncorrected for clock drift, component, and station name): characters 1–3 = Julian day (001–366), characters 4–5

= hour (00–23), characters 6–7 = minute (00–59), character 8 = second code (A–T, where A = 0.000–2.999, B = 3.000–5.999, ..., T = 57.000–59.999), character 9 = component code (1–3 for acceleration, 4–6 for velocity), character 10 = ".", and characters 11–13 = station name. The seismogram data set listing in Table B.1 is based on this filenaming scheme. In the table, each line summarizes one event, which is identified by a computer algorithm that counts triggers in a sliding time window (22 seconds long, this report). Events are specified in the left column by the filename time of the earliest recording (rather than the actual event origin time, which is generally unknown at early stages of data processing), and recordings are specified in the station columns by the filename second-code character. For example, an aftershock at Julian day 359, hour 14, minute 14 was recorded at stations ART, KIR, MOO, NAB (with start-of-record time in second-bin Q = 48.000–50.999), and KET (with start-of-record time in second-bin R = 51.000–53.999). This aftershock is identified in Table B.1 as 3591414Q.

The playback procedure involves demultiplexing of the data on tape cartridge using the computer program RDGEOS which writes to disk separate files for each channel recorded on GEOS plus a time-file that contains the time-stamps of when each block of data recorded on the GEOS began.

Corrections

The GEOS instruments currently do not recognize leap-years. Therefore the first correction that had to be applied to the data files was to account for this on files recorded up until the GEOS internal clock was reset which was done on or about 4 January 1989. This represents a clock changes for data recorded on or after 31 December 1988. Clock changes are made using the computer program CHGCLOCK.

Normally the GEOS can be relied upon to write to tape cartridge the complete recording sufficiently well to be read and accurately interpreted by the RDGEOS program. It has been a recognized phenomenon that under cold weather conditions some of the GEOS instruments may fail in part or whole to write an accurate tape. These types of failures occurred in several forms for this study. In the case of data that can be read by the program RDGEOS, these failures can be grouped into two types, bit-errors and block-errors.

An exact correction can usually be made for bit-errors. These are what are often referred to as "glitches." The symptom is an occasional data value that is a large power of two different from the preceding and subsequent data values. The cause typically is memory board failures, but can also be in the analog-to-digital conversion circuit. This was a common phenomenon on the KET GEOS where bit-errors had a value of ± 64. The computer program BITFIX has been used to find and correct these bit-errors whenever the bit-errors were sufficiently large compared to the true rate of change between data values. Almost all of the bit-errors recognized for the KET GEOS occurred during the two-second pre-event where they were easily corrected. It is possible however, that some of the KET recordings may still contain 64-count bit-errors in the velocity recordings of the larger aftershocks. Recordings that did not appear to be aftershocks were not examined for bit-errors.

Block-errors usually cannot be fully corrected. These are instances where the data block to be written to GEOS tape cartridge either is not written or that which is written is corrupt. During playback the program RDGEOS attempts to identify where data blocks are missing from tape by examining the data block time-stamps. When these are identified, the null data value (integer header offset 3 of Table 7.1.1) is written to the data file in place of the missing data. The KIR recordings have several instances where there are these data gaps.

If the first data block of an event is corrupt, then the file created for that event will initially be given a name that does not indicate the time of that event. These files may also contain meaningless data in the beginning of their records. Files of this type were most common at ART and NAB. These files were easily recognized by the program CHKTIME which compares the time-stamps written to the time-files of each recorded data block to an expected time value. Not so easily achieved was correcting these files to their true time, but this was nevertheless done for all files with corrupt first data blocks using the program CHGTIME. The meaningless data at the beginning of some of the files was "cut" from the record using the program DR1SEG to provide the current release.

In addition to allowing files to be given the correct start times, the program CHK-TIME, reading the time-files, also verifies the integrity of the internal timing in the record-

ings. By this means several recordings have been found to have faulty internal timing. Provisions for fixing these failures is incomplete. Those recordings that have not been fixed are identified in Table 7.1.3. The cause of these failings is not always certain, but often is the result of reading a corrupt data block in the midst of an event.

Corrections for clock-drift are included in the files. These have been determined by using field measurements of variations of the GEOS internal clocks relative to two master clocks and by field measurements of variations of the master clocks relative to Omega Time from satellite. The clock correction values have been written to the real header (offset 60, Table 7.1.2) using the computer program VECHED.

Difficulties have been encountered in identifying clock-corrections for stations KET, SEV, and YSS. For the SEV and YSS stations, the clock-drift rate cannot be determined since the relation to master clocks was determined at only one time for each station. Estimated drift rates indicate that the clock errors at both SEV and YSS may reach as large as 1 to 2 seconds. The early (prior to 363 10:32) clock-corrections at KET cannot be relied upon. Early recordings at KET have shown timing residuals when used for aftershock locations of greater than two seconds. At the time of these early recordings measurements of clock-drift rate were variable and extremely large.

7.2 Waveform Characteristics of Digital Seismograms Recorded in the Period 21 December 1988 to 4 January 1989

E. Cranswick

Introduction

The digital waveforms recorded by the GEOS (see Chapter 6 for description of instrumentation) Portable Autonomous Digital Seismographs (PADS), deployed by the USGS aftershock team during the 1988 Armenian Earthquake field program constitute one of the largest and richest digital data sets ever produced by an aftershock chase. Roughly 2000 records were recorded at 18 stations distributed over an area that encompasses both the epicentral region and a southern region which includes the Station GSS (near Yerevan, Armenia) at roughly 100 km range. The S-minus-P times of the recorded events as a whole range from fractions of a second to about twenty seconds, and most of the stations in the epicentral region display S-minus-P times of 1–8 seconds because of the 50-km length of the source volume.

Sites in the epicentral region have elevations of 1000–2000 m and exhibit a diversity of geological setting which ranges from thrust-block ridges of crystalline rock overlain by thin layers of surficial material to alluvium-filled valleys containing on the order of a kilometer of low-velocity sediments (Station GSS is sited within a 100-m-long tunnel). In addition to the appearance of many converted phases—S-to-P and P-to-S—in the seismograms which suggest that the fault itself may act as a channel waveguide, many waveforms display high-frequency complexities—obvious resonances and phase delays between different components—which imply a corresponding complexity of near-surface structure.

Before any reliable interpretations of high-frequency source and propagation phenomena can be made, it is essential to place some bounds on the high-frequency transfer function of each recording site. Repeated experience has demonstrated that site/source reciprocity inevitably produces some degree of site/source ambiguity—and all too often, the unsuspecting researcher "migrates" some hardware idiosynchrasy back to the source... and then writes a paper about a source anomaly. Because of cold weather con-

ditions, all the GEOS PADS were deployed within some protective building/structure, and at several stations, significant soil/structure interactions and the presence of local noise sources are suspected to be responsible for some peculiarities observed in the seismograms. Detailed analyses of the waveforms performed in conjunction with information about source locations, focal mechanisms, etc., can also constrain uncertainties regarding Station/Instrument Parameters (SIP) such as Directions-of-Positive-Motions (DPM) of the sensor orientations. Furthermore, both the P- and S-waves of many seismograms are frequently difficult to "pick," and an understanding of some of the features of the propagation/site response would greatly aid the correct identification of these phases and lead to improved hypocenter solutions of the events.

Record Sections for Selected Events

Based on their source locations, the aftershocks can be divided into two categories: 1) larger events spatially associated with faults that ruptured during the main shock and major aftershocks; 2) smaller events distributed throughout the epicentral region which represent the relaxation of the source volume as a whole in response to the strain relieved by slip on the large faults. The strain-relaxation events are comparable to the "crackle" which contributes to high-frequency ambient seismic noise and which is thought to be related to the loading/unloading cycle of tidal strains (URI, 1988, oral communication). These sources are generated within bodies of competent rock, and because of their high corner frequencies (> 20 Hz), they are only recorded at stations separated from hard rock by thin layers (< 100 m) of low-velocity, low-Q surficial materials.

Three-component record sections, derived with PADS software, are provided in Appendix C. The events recorded on six or more digital stations are shown. An example is provided in Figure 7.2.1. The record sections are plotted for the time histories recorded from the three-component velocity transducers. On-scale component accelerometer recordings also exist for each of the corresponding stations and are provided on magnetic tape (Chapter 10) and optical disk cartridge (Chapter 12). The data included in Appendix C are provided on IBM-floppy diskette. Magnitudes and hypocenter locations derived from the events using PAD-affiliated software are presented in Chapter 8.

The record sections provide a useful one-page summary of the data for a variety of analyses and data-quality evaluations. The record sections permit rapid evaluations of phase correlation and relative amplitudes as well as identification of off-scale time histories and timing errors. Gaps in the seismograms for the KIR station indicate data missing as of this writing. These missing data currently are attributed to tape cartridge malfunction probably associated with cold temperatures at the KIR site. However, playback of these data in the field did not reveal any problems, so it may be possible to recover these data from the field tapes with additional processing in the future.

Table 7.1.1 Definition of GEOS header offsets for first header record.

First Header Record: 256 16–Bit Integers	
(1)	Number of optional integer header records in use
(2)	Number of optional ASCII header records in use
(3)	"Undefined value" used to flag unused offsets; also used to mark 16-bit integer data values that are unknown.
(4)	Data type flag: if positive, data are in floating point format; if negative, data are in integer format. The absolute value of this offset specified the number of bytes per data point. Special cases: if 1, then 32-bit floating point format; if "undefined," then 16-bit integer format.
(10)	Year of the event
(11)	Julian day
(12)	Hours
(13)	Minutes
(14)	Seconds
(15)	Milliseconds
(16)	Microseconds
(17)	Sample number of first tick mark
(18)	Detection amplitude of tick mark
(19)	Number of tick marks detected
(20)	Serial number of recording unit
(21)	Event sequence number
(27)	Number of first active channel recorded by unit
(28)	Recorder channel number used for this component
(29)	Number of active channels recorded by unit
(30)	Number of components recorded under this component's station name
(31)	Number of data records (excluding headers)
(32)	Index of the last sample in the last data record
(33)	Number of bytes per data record
(34)	Playback program identification code
(35)	Playback program major version number
(36)	Playback program minor version number
(37)	Recording unit type identification code
(38)	Major version number of recording unit software
(39)	Minor version number of recording unit software
(40)	Sensor serial number
(41)	Vertical orientation (degrees)
(42)	Horizontal orientation (degrees)
(43–49)	Sensor model ID (14 ASCII characters)
(50)	Station location number

Table 7.1.1 Definition of GEOS header offsets for first header record (Continued).

First Header Record: 256 16–Bit Integers (Continued)

(51)	Experiment or tape number
(52)	Trigger algorithm identification code
(53)	Trigger short-term average (STA) interval (tenths of seconds)
(54)	Trigger long-term average (LTA) interval (seconds)
(55)	Trigger STA/LTA ratio (2 raised to this power)
(56)	Trigger channel number
(57)	Pre-event memory size (tenths of seconds)
(58)	Post-trigger record duration (seconds)
(101–200)	Processing history (200 ASCII characters)
(208)	Data file directory I.D.
(209)	Data file sub-directory I.D.
(210–216)	Original filename (14 ASCII characters)
(217–219)	Study name (6 ASCII characters)
(252)	Clock type: 0 = none, 1 = WWVB, 2 = external, 3 = manual
(253)	Event type: 0 = continuous, 1 = trigger, 2 = preset, 3 = calibration, 4 = amplifier calibration, 5 = sensor calibration
(254)	Motion type: 1 = acceleration, 2 = velocity, 3 = displacement
(255)	Component number
(256)	Number of samples in event

Notes:

Header descriptions are version 1.2 dated 27 February 1987 of the National Strong Motion Data Center (NSMDC) binary data format.
The GEOS does not record tick marks.
Header record 1, offset 41: vertical orientation is expressed as a number from 0 to 180, with 0 representing true vertical and 90 representing true horizontal.
Header record 1, offset 42: horizontal orientation is expressed as a number from 0 to 359, with 0 representing true north, and 90 representing true east. Header record 1, offset 256: should only be used when header record 1, offsets 31 and 32 are not defined.

Table 7.1.2. Definition of GEOS header offsets for second header record.

Second Header Record: 128 32–Bit Floating Point Values	
(1)	Number of optional real header blocks in use
(2)	"Undefined value" to flag unused offsets
(5)	Component sampling rate, in samples per second
(6)	Component sample lag, in seconds
(39)	Transducer type (4 ASCII characters)
(40)	Sensor latitude (decimal degrees, positive North)
(41)	Sensor local x-coordinate (meters)
(42)	Sensor longitude (decimal degrees, positive East)
(43)	Sensor local y-coordinate (meters)
(44)	Sensor elevation (meters)
(45)	Sensor local z-coordinate (meters)
(46)	Digitizing constant, digital counts per volt
(47)	Anti-alias corner frequency (Hertz)
(48)	Poles of anti-alias filter
(49)	Sensor natural frequency (Hertz)
(50)	Sensor damping coefficient
(51)	Sensor motion constant (volts per motion-unit)
(52)	Amplifier gain
(60)	Clock correction (seconds)
(61)	Time since last clock correction (seconds)
(62)	Instrument battery voltage
(63)	Desired trigger algorithm STA/LTA ratio
(64)	Actual STA value at trigger moment
(65)	Actual LTA value at trigger moment
(66)	Maximum value of STA/LTA ratio during event

Notes:

Header descriptions are version 1.2 dated 27 February 1987 of the National Strong Motion Data Center (NSMDC) binary data format.

Header record 2, offset 48: filter roll-off equals 6 dB per pole indicated.
Header record 2, offset 52: gain expressed in dB if Header record 1, offset 5 is equal to one (1); otherwise, gain expressed as an algebraic factor.
Header record 2, offset 60: the clock correction is subtracted from the time specified in Header record 1 to generate the corrected time.

Table 7.1.3 File-groups identified by program CHKTIME as having internal timing problems.

3591448FG.ART
3631501FG.ART
3651535OG.ART
0012350RG.ART

3640803TG.DZH
0010917PG.DZH
0021539OG.DZH

3571559MG.GIB
3571937PG.GIB

3651200AG.GOG
3651200QG.GOG

3571224MG.GSS
3571813HG.GSS
3630346HG.GSS
0051152JG.GSS

3582218PG.KET
3592309EG.KET
3660811QG.KET

3592057MG.KIR
3592346LG.KIR
3600357BG.KIR
3630602AG.KIR
3630848DG.KIR
3630848HG.KIR
3630907DG.KIR
3631257FG.KIR
3631307PG.KIR
3631326HG.KIR
3631337BG.KIR
3631436EG.KIR
3631924HG.KIR
3631955TG.KIR
3640023EG.KIR
3640042MG.KIR
3640243QG.KIR
3640249IG.KIR
3640703OG.KIR
3641440MG.KIR
3641459GG.KIR
3641548IG.KIR
3650502MG.KIR
3650649DG.KIR
3651247SG.KIR
3651330IG.KIR
3651331FG.KIR
3652035TG.KIR
3652322JG.KIR

3660221PG.KIR
3660407FG.KIR
3660426SG.KIR
3660427AG.KIR
3660702NG.KIR
3660702QG.KIR

0171206QV.KI2

3581538CG.LEN
3621230FG.LEN
3651330HG.LEN

3581142DG.MOO
3581801LG.MOO
3582056TG.MOO
3590836AG.MOO
3591856HG.MOO
3612002PG.MOO
3632311QG.MOO

3641313KG.MO2
0021951NG.MO2

3612350HG.NAB

0350958CV.SSS

3581300PG.STE
3640257RG.STE

3602229FG.YSS
3602233QG.YSS

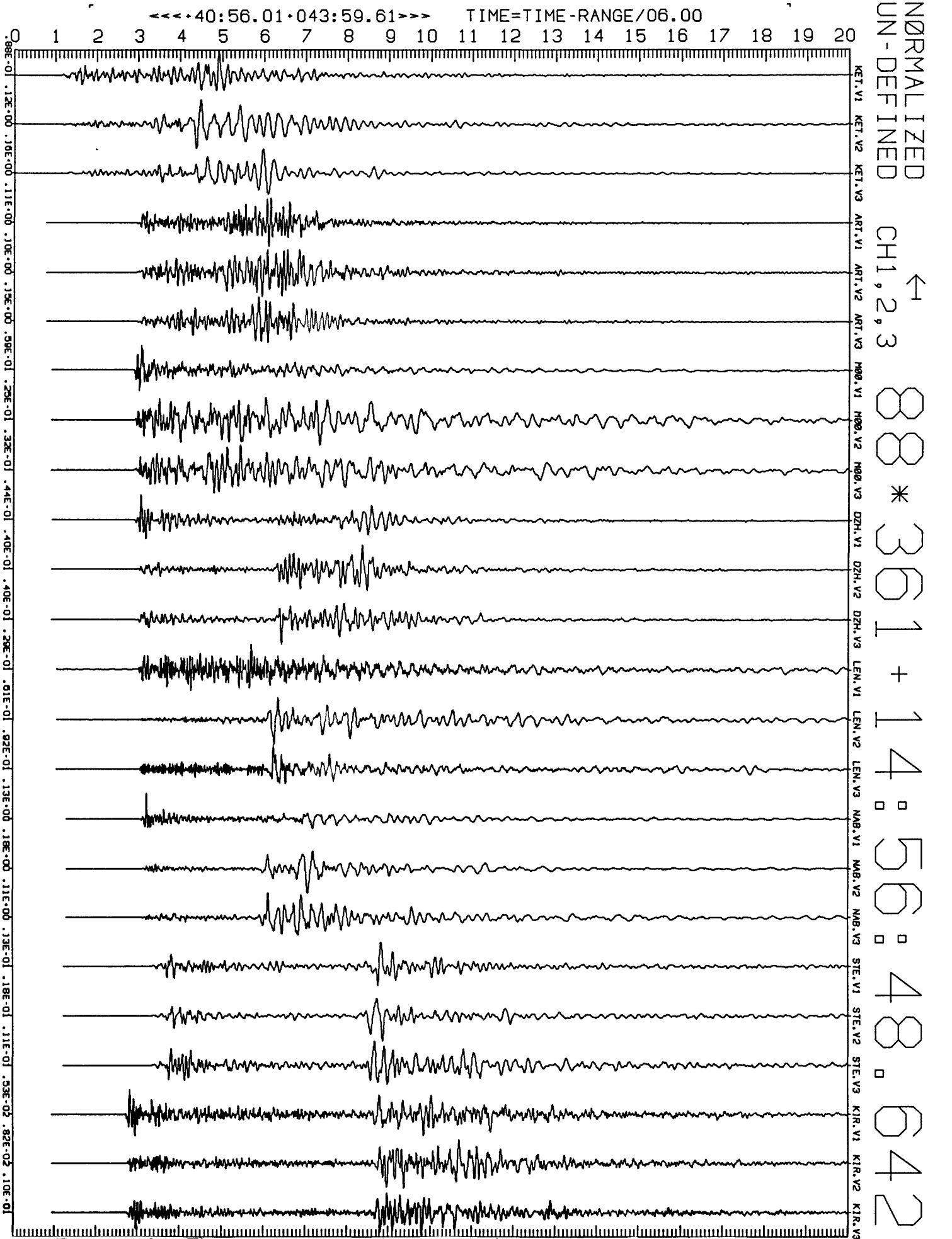

FIGURE 7.2.1. Three-component record section of velocity transducer recordings obtained with GEOS for an aftershock which occurred at Julian time 361 14:56.

CHAPTER 8

PRELIMINARY AFTERSHOCK LOCATIONS (DECEMBER 21, 1988–JANUARY 4, 1989)

D. Simpson, E. Cranswick, M. Andrews, and G. Glassmoyer

This section presents a preliminary analysis of the hypocentral data based on a combination of the MEQ and GEOS data. As this report is being written, the analysis of the MEQ records is continuing. The location of additional events and a significant improvement in the accuracy of hypocentral locations is expected as more data become available.

While in Armenia, times were read from a subset of 5 of the MEQ stations for 42 events during the time period December 23 to 29. These events were located (Figure 8.1) on a PC using W. Lee's version of the program HYPO–71–PC. Figure 8.1 shows the preliminary location of 150 events located after returning to the U.S. using additional times from the MEQ–800 and GEOS stations.

For these preliminary locations, the following simple P-wave velocity model was used and a P/S velocity ratio of 1.8:

Velocity	Depth
5.8	0
6.2	10
8.1	35

For most stations where GEOS and MEQ instruments were colocated, arrival times (especially for S-waves) and direction of motion could be picked more accurately on the GEOS records. In these cases, the GEOS times were used when both types of instruments recorded the same event. In general, the times from the GEOS and MEQ agreed to better than 0.1 sec. In those few cases where there were problems with the GEOS clocks, MEQ times were used to determine corrections to the GEOS times.

Magnitudes and hypocentral coordinates for the events are given in Table 8.1. The magnitudes were determined using measurements of peak amplitude from the GEOS recordings. The peak measurements were made from the integrated velocity transducer recordings, unless these recordings were clipped in which case they were derived from the

doubly integrated, high-pass filtered accelerometer recordings. The accelerometer recordings were filtered with 0.8-second high-pass filters to correspond to a Wood–Anderson seismometer response. The magnitudes were computed using

$$A_0 + \log_{10} (2800. \text{ peak displacement}) ,$$

where A_0 is as defined by Richter (1958).

A subset of 120 of the located events using only those of HYPO quality a–c are shown in Figure 8.2. For the better-located of these events, 10 to 15 arrival times (P and/or S) were used. RMS residuals were usually less than 0.25 sec and formal errors in location less than 0.8 km (horizontal) and 1.5 km (vertical). Arrival time data from additional stations are expected to significantly improve these locations. A subset of 50 events were assigned HYPO quality a–b (Figure 8.3). In general, these are the larger events with better station coverage. The locations of these events are not expected to change substantially with subsequent record reading. These events identify two well-defined trends in the seismicity.

Figure 8.4 shows all of the events plotted with symbols scaled according to source radius. Source radius for the events were calculated assuming a constant stress drop of one bar and Brune's source model (Brune, 1970). This schematic representation provides an indication of where events with the larger rupture surfaces occurred. These are located near the change in trend of the seismic activity near Spitak and in the western region.

While it is stressed that at this stage the analysis of the hypocentral data is very preliminary, a number of significant features can be identified from the existing data. The aftershock activity extends over a zone approximately 40 km long with a general NW–SE elongation. There appear to be two distinctly different sections to the aftershock activity. In the SE, the activity is shallow (0–8 km) and forms a narrow zone with strike of N125E. The strike of this segment and the depths are in general agreement with an extrapolation of the fault break observed at the surface immediately south of Spitak (see Chapter 4). A preliminary first-motion focal mechanism for a composite of events in this zone agreed with this interpretation. West of 44.2°E the shallow activity may continue along a trend that bends slightly more east-west, but the main activity in this segment lies south of a linear extension of the SE zone and is at greater depths (up to 15 km). There is an

obvious complexity in this area that will require more detailed analysis. This segment of the aftershock zone, and its role in the main shock rupture, is especially important since it lies closest to the city of Leninakan, where extensive damage occurred and where the GEOS data indicate there was strong amplification of ground motions from aftershocks located in this segment of the fault.

Preliminary analysis of teleseismic data for the December 7 event by C. Estabrook and J. Pacheco at Lamont–Doherty suggests that the main shock consisted of three significant sub-events. The two largest of these would agree with: 1) a shallow event in the SE with a strong thrust component along the strike observed in the aftershocks and 2) a deeper event in the west with a more EW strike.

The two largest events recorded by the network were of magnitude (NEIC) 4.7 on December 31 and magnitude 5.0 on January 4. These are identified by special symbols in Figure 8.2 and 8.3. The first of these was in the deeper cluster in the western portion; the second in the shallower segment to the southeast. Both of these events appear to be associated with clusters of activity including a significant number of small aftershocks and some foreshocks.

REFERENCES – CHAPTER 8

Richter, C. F. (1958). *Elementary Seismology*, W. H. Freeman and Co., San Francisco, 768 pp.

Brune, J. (1970). Tectonic stress and the spectra of seismic shear waves from earthquakes, J. Geophys. Res. 75, 4997–5009.

Table 8.1 EARTHQUAKE LOCATIONS

Preliminary hypocenters for Spitak earthquakes
December 23, 1988 to January 4, 1989
Hypocenters determined using combined data from MEQ and GEOS instruments.
Magnitudes determined as Richter ML magnitude based on scaling of GEOS data to equivalent Wood Anderson response.

YRMODA	HRMN	SEC	LATITUDE		LONGITUDE		DEPTH	MAG
			DEG	MIN	DEG	MIN	KM	ML
881223	1452	59.54	41N	07.60	43E	50.79	09.36	2.30
881223	1616	29.07	40N	57.33	43E	57.99	14.33	1.85
881223	1643	36.89	40N	53.73	44E	00.84	09.74	3.17
881223	1657	55.69	40N	54.51	44E	08.87	04.26	2.73
881223	1737	25.87	41N	07.59	43E	50.78	08.65	1.71
881223	1747	38.86	41N	07.35	43E	50.53	08.73	2.40
881223	1958	28.82	40N	55.92	43E	57.55	08.26	2.60
881223	2246	08.79	40N	55.94	44E	04.89	09.03	2.75
881223	2341	10.75	40N	46.39	44E	23.12	02.05	1.96
881224	0138	41.95	40N	56.28	43E	59.35	05.12	3.01
881224	0526	59.86	40N	46.63	44E	22.61	02.28	3.32
881224	0548	32.56	40N	51.38	44E	16.65	06.71	3.50
881224	0550	27.50	40N	53.47	44E	05.85	07.50	2.53
881224	1142	16.13	40N	50.73	44E	18.75	07.16	3.17
881224	1411	23.36	41N	01.47	43E	59.16	01.78	2.90
881224	1414	46.71	40N	54.28	44E	11.63	09.43	3.32
881224	1429	32.78	41N	07.34	43E	53.53	11.79	2.48
881224	1602	52.02	40N	54.29	44E	09.65	05.48	2.86
881224	1647	09.42	41N	00.12	44E	02.11	01.32	2.99
881224	1708	34.30	40N	49.67	44E	18.93	04.81	3.04
881224	2110	23.60	41N	00.68	44E	05.60	00.76	2.34
881224	2355	49.35	41N	01.35	44E	02.81	00.66	2.45
881225	0118	58.35	40N	54.64	44E	14.75	02.86	2.71
881225	0648	06.43	40N	54.39	44E	00.19	08.41	3.31
881225	1114	00.60	40N	58.31	43E	55.15	10.73	2.01
881225	1249	57.65	40N	59.71	43E	56.01	10.35	2.47
881225	1323	13.50	41N	00.36	43E	58.33	08.45	2.10
881225	1947	18.51	41N	06.22	43E	58.90	04.39	2.12
881225	2057	58.50	40N	51.96	44E	15.60	06.89	2.67
881225	2122	51.27	40N	46.16	44E	22.97	01.91	2.03
881225	2204	42.66	40N	53.19	44E	20.15	05.33	2.36
881226	0334	59.01	40N	47.01	44E	21.98	01.48	1.68
881226	0827	37.40	40N	46.54	44E	21.97	00.91	2.15
881226	1030	44.53	41N	00.91	44E	28.01	04.91	3.44
881226	1035	26.33	40N	56.71	44E	02.75	03.58	1.64
881226	1205	09.42	40N	51.89	44E	05.52	01.11	2.49
881226	1311	03.20	40N	53.30	44E	12.29	07.30	2.43
881226	1412	44.19	40N	56.07	44E	09.41	01.22	2.44
881226	1443	03.81	40N	51.98	44E	15.78	00.10	2.51
881226	1451	26.19	40N	52.27	44E	17.04	05.55	1.67
881226	1456	51.18	40N	56.01	43E	59.61	08.72	3.41
881226	1543	37.82	40N	52.08	44E	14.45	00.14	2.20
881226	1614	10.22	40N	53.18	44E	16.80	02.88	2.33
881226	1756	05.92	40N	52.43	44E	14.61	08.27	1.79
881226	1830	07.35	40N	53.10	44E	12.33	06.81	2.38

Table 8.1 EARTHQUAKE LOCATIONS (continued)

YRMODA	HRMN	SEC	LATITUDE		LONGITUDE		DEPTH	MAG
			DEG	MIN	DEG	MIN	KM	ML
881226	1841	16.79	40N	55.26	43E	56.95	07.18	2.52
881226	1856	58.62	40N	53.22	44E	15.21	04.70	2.43
881227	0015	03.86	40N	51.07	44E	18.52	04.83	1.98
881227	0057	23.40	40N	54.86	43E	59.00	19.41	2.26
881227	0504	14.54	40N	57.78	44E	02.89	09.08	2.64
881227	0745	15.75	40N	55.30	44E	05.11	09.93	3.76
881227	1115	26.40	40N	55.95	43E	59.68	07.95	3.14
881227	1117	21.21	40N	55.70	43E	59.90	04.10	3.25
881227	1129	56.89	40N	55.73	43E	58.86	06.51	2.56
881227	1230	14.28	40N	56.31	43E	59.40	07.86	3.54
881227	1317	01.98	40N	51.53	44E	19.02	05.14	1.95
881227	1649	12.44	40N	55.23	43E	58.60	07.85	2.65
881227	1802	45.76	40N	56.12	44E	09.18	08.59	3.41
881227	2031	35.10	40N	55.06	43E	57.19	09.80	2.41
881227	2044	41.72	40N	55.85	43E	54.12	06.32	3.19
881227	2310	01.50	40N	59.88	44E	01.18	06.94	2.21
881228	0346	04.91	40N	56.73	43E	59.27	4.49	3.84
881228	0624	10.78	40N	54.56	43E	52.60	05.43	2.68
881228	1307	46.36	40N	46.42	44E	23.12	00.87	1.37
881228	1542	21.43	40N	52.09	44E	14.16	03.69	2.27
881228	1558	48.90	40N	46.39	44E	22.17	00.58	2.60
881228	1926	23.23	41N	03.52	43E	55.21	02.23	1.93
881228	2246	58.47	40N	58.17	44E	02.32	00.71	2.80
881228	2249	37.20	40N	57.99	44E	00.70	06.58	2.73
881228	2309	27.86	40N	47.56	44E	22.87	02.54	2.06
881229	0000	52.90	40N	57.28	43E	55.81	4.48	2.39
881229	0023	13.79	40N	45.97	44E	21.65	05.63	2.30
881229	0045	35.99	40N	58.21	44E	02.55	05.69	2.49
881229	0257	51.24	40N	50.02	44E	19.22	07.83	2.17
881229	1008	43.41	40N	53.24	44E	16.86	02.84	3.50
881229	1402	05.70	40N	54.95	43E	58.04	06.51	1.99
881229	1432	11.16	40N	54.18	44E	12.08	04.64	2.56
881229	1448	42.53	40N	52.97	44E	14.08	07.35	2.60
881229	1548	23.65	40N	48.47	44E	22.40	02.23	2.28
881229	1843	50.09	40N	57.45	43E	57.51	09.05	3.64
881229	2311	14.17	40N	55.95	43E	54.67	13.20	2.83
881230	0022	09.19	40N	57.20	44E	06.32	12.04	2.23
881230	0139	25.33	41N	02.33	44E	00.36	10.33	2.09
881230	0230	26.20	40N	51.76	44E	12.59	07.71	1.95
881230	0249	32.88	40N	59.56	44E	02.51	09.49	2.69
881230	0502	36.09	40N	48.71	44E	19.05	04.06	2.88
881230	1151	49.75	40N	52.57	43E	56.89	07.35	2.94
881230	1247	52.24	40N	54.94	44E	11.95	06.66	2.83
881230	1328	48.59	40N	55.28	43E	58.97	10.39	4.17
881230	1404	03.32	40N	57.35	43E	59.90	04.72	3.04
881230	1907	37.31	40N	55.49	44E	11.50	07.32	2.53
881230	1917	30.78	40N	53.39	44E	14.22	05.25	2.45
881230	2330	03.93	40N	57.03	44E	10.63	04.98	2.05
881231	0407	09.53	40N	56.74	43E	59.16	14.26	4.69
881231	0651	37.06	40N	56.82	44E	11.30	06.15	2.91
881231	0811	49.13	40N	55.13	43E	56.33	05.06	2.44
881231	1234	39.12	40N	54.72	43E	55.30	06.34	3.07

Table 8.1 EARTHQUAKE LOCATIONS (continued)

YRMODA	HRMN	SEC	LATITUDE		LONGITUDE		DEPTH	MAG
			DEG	MIN	DEG	MIN	KM	ML
881231	1432	52.18	40N	54.98	43E	58.34	08.88	2.91
881231	1535	19.86	40N	52.96	44E	19.23	02.69	3.57
881231	1554	34.64	40N	52.09	44E	16.64	00.65	3.88
881231	1633	19.43	40N	52.92	44E	17.55	02.27	3.32
881231	1710	54.11	40N	52.27	44E	15.71	00.23	3.09
881231	1722	39.18	40N	51.85	44E	16.47	00.36	3.34
881231	1924	00.74	40N	56.87	43E	59.30	09.49	2.46
881231	2144	47.19	40N	55.65	43E	56.25	07.51	2.35
881231	2223	56.66	41N	00.62	44E	08.03	12.35	2.15
890101	0010	23.69	40N	46.48	44E	23.21	03.89	2.17
890101	0158	17.58	41N	03.52	43E	54.99	02.27	2.54
890101	0500	55.63	40N	51.56	44E	15.86	05.57	2.41
890101	0912	28.47	40N	49.95	44E	21.11	08.41	1.98
890101	1302	11.64	40N	50.63	44E	19.20	05.76	1.78
890101	1707	07.02	40N	53.91	44E	10.39	06.93	1.99
890101	1728	38.08	40N	54.50	44E	02.70	07.37	1.99
890101	2259	38.42	40N	46.63	44E	23.17	05.54	3.85
890101	2331	04.35	40N	46.69	44E	22.95	02.18	2.42
890102	0024	23.98	40N	52.60	44E	05.07	14.84	1.40
890102	0042	12.53	40N	58.07	44E	01.31	04.05	2.51
890102	0304	06.75	40N	55.20	44E	06.03	06.39	2.10
890102	1459	26.50	40N	57.30	44E	04.55	11.06	3.14
890102	1811	08.80	40N	55.91	44E	07.58	07.62	1.97
890102	1813	34.16	40N	55.09	44E	01.22	12.12	3.23
890102	2309	18.97	40N	56.49	43E	57.67	09.91	3.08
890103	0531	38.07	40N	55.26	44E	01.94	11.59	2.70
890103	0720	28.23	40N	47.21	44E	12.12	10.74	2.69
890103	0819	54.91	40N	52.46	44E	14.16	05.19	4.15
890103	0927	03.31	40N	54.61	44E	01.56	04.59	2.50
890103	1328	18.25	40N	50.38	44E	18.10	00.47	3.12
890103	1335	05.95	41N	13.48	43E	52.13	08.65	3.62
890103	1348	47.29	40N	52.08	44E	13.12	04.65	3.60
890103	1445	09.11	40N	54.21	44E	12.48	05.52	2.25
890103	2000	11.78	40N	54.77	44E	00.97	12.79	3.58
890104	0247	02.80	40N	47.41	44E	21.33	04.00	2.52
890104	0729	40.47	40N	53.76	44E	17.08	00.29	5.22
890104	0738	28.28	40N	53.61	44E	16.42	01.81	3.69
890104	0740	47.78	40N	54.15	44E	17.40	00.38	4.04

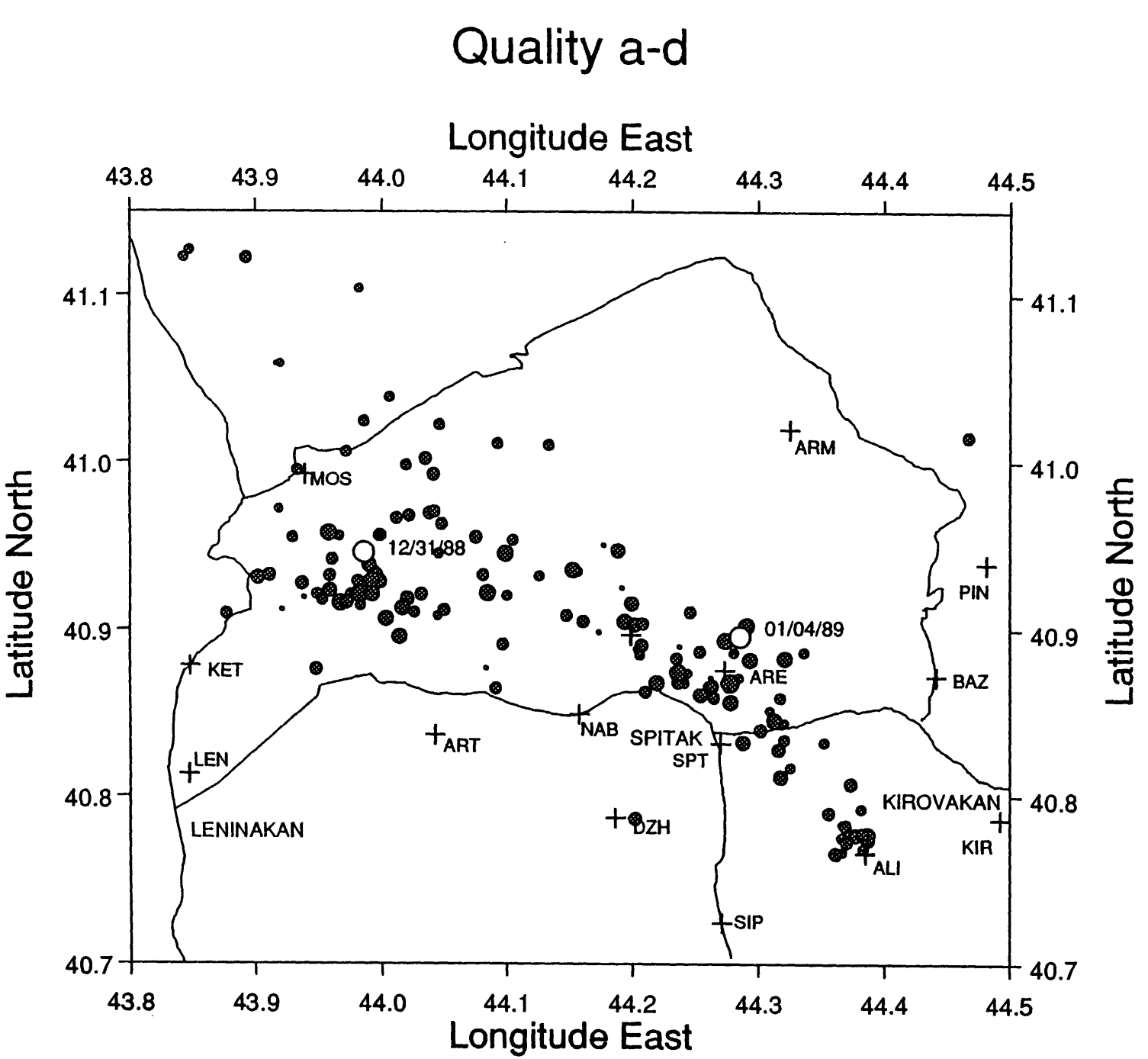

FIGURE 8.1. Epicenter locations for events with HYPO quality and ratings using times compiled as of March 19, 1989 from MEQ–800 and GEOS recordings of aftershocks of the earthquakes of December 7, 1988 near Spitak, Armenia S.S.R. These events occurred during the time period December 22, 1988 through January 4, 1989. They are assigned HYPO quality ratings a–d.

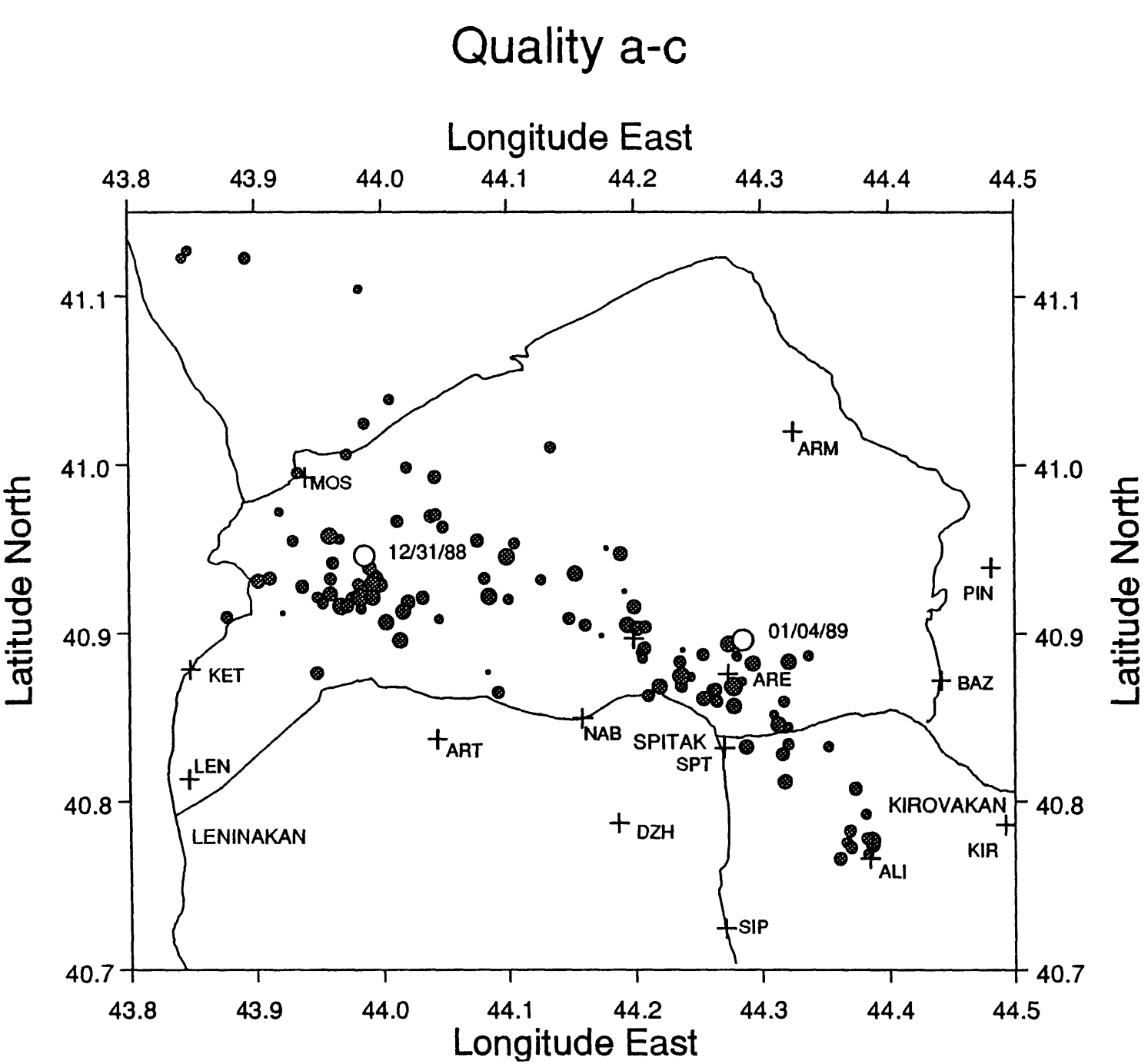

FIGURE 8.2. Epicenter locations for events with HYPO quality ratings a–c using times compiled from MEQ–800 and GEOS recordings as of March 19, 1989 for aftershocks of the earthquakes of December 7, 1988 near Spitak, Armenia S.S.R. The events occurred during the time period December 22, 1988 through January 4, 1988.

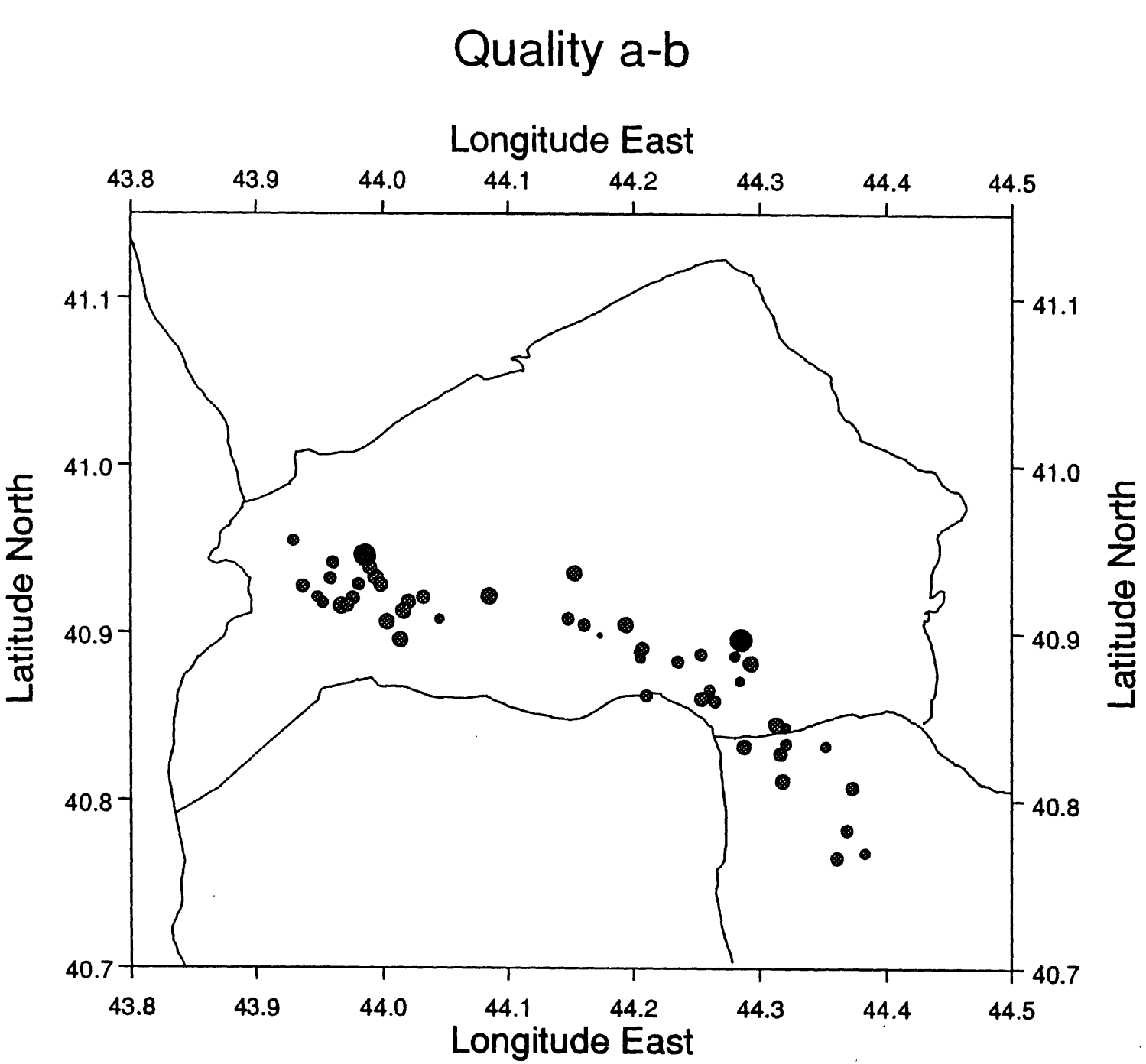

FIGURE 8.3. Epicenter locations for events with HYPO quality ratings a–b using times compiled from MEQ–800 and GEOS recordings as of March 19, 1989 for aftershocks of the earthquakes of December 7, 1988 near Spitak, Armenia S.S.R. The events occurred during the time period December 22, 1988 through January 4, 1988.

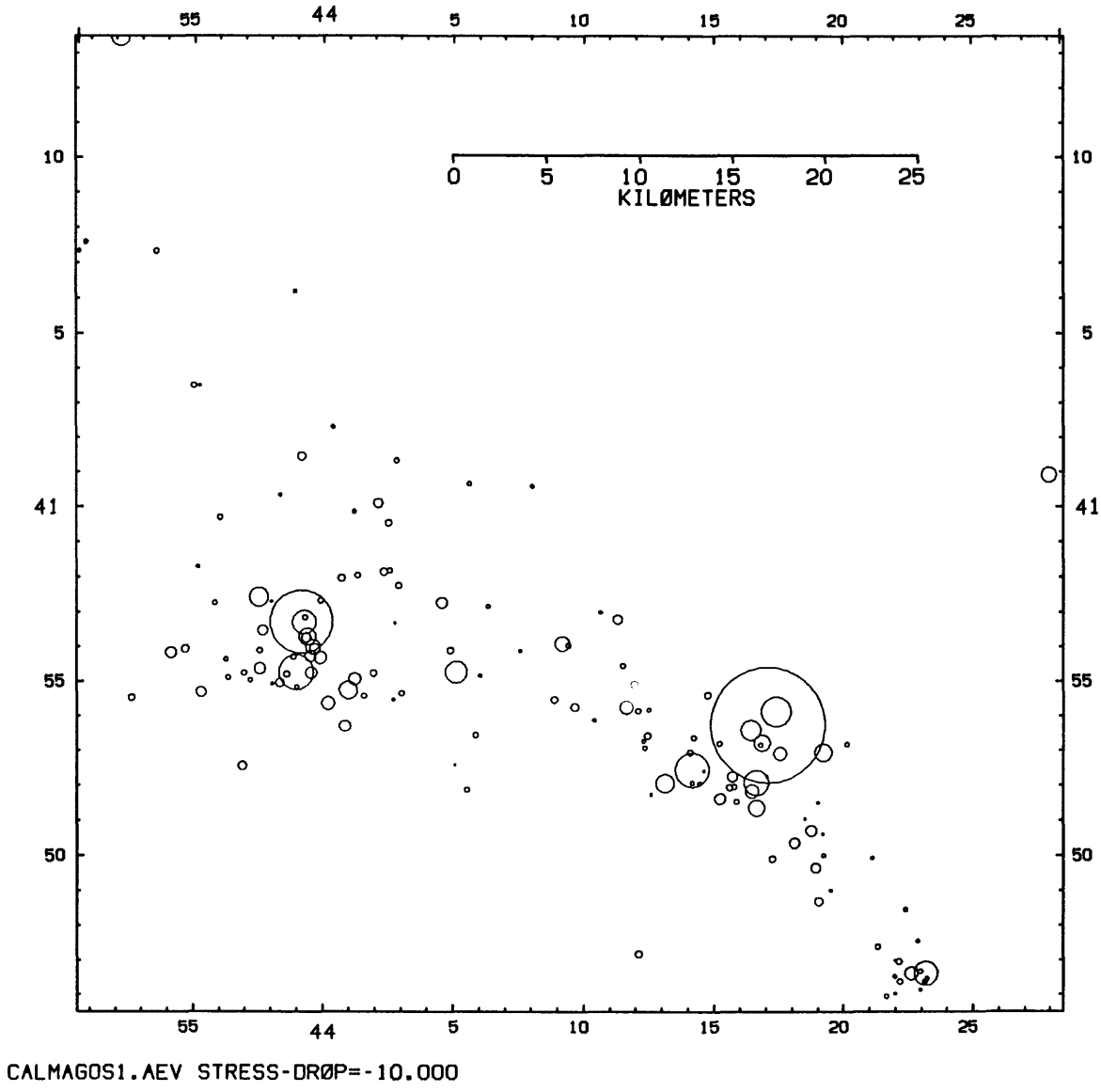

FIGURE 8.4. Epicenter locations for events with HYPO-quality ratings a–d plotted with symbols scaled according to source radius (see text).

CHAPTER 9

EFFECT OF SITE CONDITIONS ON GROUND MOTIONS IN LENINAKAN, ARMENIA S.S.R.

R. Borcherdt, G. Glassmoyer, A. Der Kiureghian, and E. Cranswick

Damage patterns and aftershock recordings suggest that the local geologic setting may have been a significant contributory factor to damage in Leninakan. The amplification of certain frequencies of ground shaking, especially, horizontal motions, by unconsolidated soils and alluvial deposits is a well-known phenomena. Its occurrence and contributory effects to damage is well documented in the literature (*e.g.,* Medvedev, 1965; Rosenbleuth, 1960; Gutenberg, 1957; Borcherdt, 1968) with the most recent illusration being the damage in Mexico City during the 1985 earthquake (Seed *et al.*, 1989; Singh *et al.*, 1989). Analysis of damage information and aftershock recordings suggests that this phenomena occurred in the city of Leninakan during the main shock and subsequent aftershocks. Evidence accrued to date is discussed.

9.1 DAMAGE DISTRIBUTION

Statistics on the damage to multi-story residential buildings in the affected area are presented in Table 9.1. These statistics, as reported by one of the authors (A. Der Kiureghian) and compiled as of January 24, 1989 by Soviet colleagues, provide an important data base to compare the relative amounts of damage experienced by cities and villages in the affected area.

The three largest cities that experienced heavy damage during the earthquake and its aftershocks, in order of increasing distance from the rupture zone, are Spitak (1–9 km), Kirovakan (25 km), and Leninakan (32 km). Of the total number of multi-story residential buildings in each of the largest cities (Table 9.1), 87 percent of the structures in Spitak collapsed or suffered heavy damage and are to be demolished. Twenty-four percent of the structures in Kirovakan and fifty-two percent of the structures in Leninakan are in these categories. The greater amount of damage in Spitak can be explained by the proximity of the city to the rupture zone. An important observation is that the amount of damage in Leninakan is greater than that in Kirovakan, which is closer to the zone of surface rupture. Factors that could contribute to greater damage in Leninakan are differences in structural

types, structural integrity, geologic setting, and levels of ground motion radiation that vary with azimuth. Without further data it is not possible to draw any conclusions with respect to possible differences in integrity of structures in the two cities, but we know of no information indicating that the structures in Leninakan were of poorer construction than structures of the same type in Kirovakan. Table 9.1 permits several conclusions regarding the performance of various types of structures.

1) Precast panel buildings performed well in all locations, including Spitak.

2) Precast frame-panel buildings performed poorly with those in Leninakan suffering significantly greater damage than those in Kirovakan. Of the total number of these buildings in Leninakan (133) 95 percent collapsed or have to be demolished. Of the total number in Kirovakan (108), none collapsed or have to be demolished. Although we don't have an accurate count, visits to the two cities indicate that the majority of structures of this type in Kirovakan did not exceed 4–5 stories, while in Leninakan a number of these structures were 9–12 stories. As the resonant periods for the taller structures are longer than those for the shorter structures, the structures in Leninakan would be expected to be more vulnerable to high levels of long-period motion than those in Kirovakan.

3) The composite frame-stone buildings are generally 4–5 stories. They consist of exterior stone shear walls, and a framing system cast within the walls as well as the interior of the building. Eighty-eight percent of these structures collapsed or had to be demolished in Spitak, 23 percent in Kirovakan and 62 percent in Leninakan. Clearly this type of structure was more vulnerable to damage in Leninakan than in Kirovakan. Of the total number of buildings of this type in each city, 62 percent of those in Leninakan and 23 percent of those in Kirovakan either collapsed or required demolishing. We suspect that these buildings would be more flexible than stone buildings and houses, more susceptible to long-period ground motions.

4) The stone buildings, with both interior and exterior stone walls, typically do not exceed 4 stories and are of older construction. These buildings suffered heavy damage in each of the three cities. Eighty-eight percent of these buildings collapsed or required demolishing in Spitak, forty-one percent in Kirovakan and thirty-eight percent in Leninakan. These structures are expected to be stiffer than those in the

previous categories, and hence more susceptible to shorter-period ground motions. The slightly higher percentage of damage to this type of structure, assuming other factors are the same, would be consistent with ground motions richer in higher frequencies in Kirovakan than in Leninakan.

A general conclusion that emerges from comparison of the damage statistics in the three cities is that the amounts of damage to the types of structures likely to have the longer fundamental periods (in particular, precast frame-panel structures) were significantly greater in Leninakan than in Kirovakan. The damage statistics are consistent with levels of long-period ground motion being greater in Leninakan than in Kirovakan. They are also consistent with levels of short-period motion being greater in Kirovakan than in Leninakan, as might be expected based on differences in the distances of the two cities from the zone of surface rupture.

9.2 GEOLOGIC SETTING

The three largest cities affected most severely by the earthquakes are located in the lesser Caucasus highlands, about 80 km south of the main Caucasus mountain chain. The region is one underlain primarily by igneous rocks in the form of basalts, andesites, rhyolites, tuffs, and some ophiolites (see Chapters 3 and 4). Mt. Aragats, about 40 km south of Spitak, is a 4000-meter volcano that has been active in Quaternary time. It is the source of many of the volcanic rocks in the region.

Spitak and Kirovakan are located along rivers in regions of mountainous terrain. The topography near Spitak is not as steep as that in Kirovakan. Much of both cities appears to be located on either old river deposits up to a thickness of 10 meters, on thin soil layers or on rock comprising the surrounding hills. A larger proportion of the structures in Kirovakan are probably underlain by rock.

Leninakan is located on a broad alluvial plain. Translation of a book describing the history of Leninakan by one of the authors (A. Der Kiureghian) indicates that the city is located in an old lake bed resulting from rivers being dammed by volcanic deposits more than 100,000 years ago. Geologic cross sections indicate that Leninakan is located in a broad sedimentary basin extending to depths of 3–4 km.

Geotechnical logs are consistent with this information. Shallow borehole logs as collected by T. O'Rourke for seven sites are shown in Appendix B. They show thin layers of

clays, sands, and volcanic tuffs. The logs suggest a lake environment with volcanic activity resulting in intermittent layers of volcanic tuff overlying and overlain by lake deposits. Recent information acquired by one of the authors (A. Der Kiureghian) indicates that the water table at many locations in Leninakan is at or near the surface.

As of this writing we have no information on seismic measurements in the area. However, because of proximity of the logs to rivers (see site map in Appendix D), it is reasonable to assume rather rapid sedimentation rates and that the sedimentary deposits are probably Holocene in age. With this assumption, estimates of the shear velocity have been made by T. Fumal (pers. commun., 3/89) based on an extensive set of shear velocity measurements derived from boreholes in the San Francisco Bay and Los Angeles Basin regions of California (Refs.). Estimates for shear velocity for the various layers range from about 200 m/s for clay, 230 m/s for sands, 300 m/s for gravels, to about 500–600 m/s for those comprised of volcanic tuffs. These estimates can be used to provide reasonable constraints on the total thickness required for the deposit to amplify various periods of earthquake ground motion. Effort is currently underway to obtain additional borehole information on thickness of the deposits and their seismic characteristics.

9.3 GROUND MOTION AMPLIFICATION IN LENINAKAN

Local geological conditions have been shown to substantially alter the characteristics of seismic waves (Borcherdt, 1968; Borcherdt and Gibbs, 1976). In particular, it has been shown that for unconsolidated water-saturated deposits, resonant phenomena often develop. For sites on these deposits levels of ground motion over certain period bands may be several times larger in amplitude and duration than levels at sites located on rock. It has also been shown, that for such deposits, it is often possible to characterize the first-order characteristics of the seismic response of such sites to damaging levels of ground motion using smaller ground motions as can be observed during aftershock sequences (Borcherdt, 1968; Borcherdt and Gibbs, 1976; Rogers *et al.*, 1984; Singh *et al.*, 1989). Consequently, it is of interest to compare the aftershock recordings obtained in Leninakan with those obtained at other sites underlain by rock or thin layers of soil overlying rock.

The aftershock recordings obtained in Leninakan during this initial study were obtained at the site of the Geophysical Institute, which is located about 100–150 meters west of the earthquake engineering laboratory and test facility. The accelerometers and

seismometers at this site were placed on a concrete pier along with several other seismic sensors belonging to the Leninakan seismic station. The concrete pier is located in the basement of a two-story masonry structure (see description of site LEN in Appendix A). Both the two-story structure and the earthquake engineering laboratory suffered significant damage during the earthquakes of December 7, 1988; however, neither structure collapsed. The structure housing the seismic instrumentation was habitable and continued to function as the headquarters for seismic observations in Leninakan.

Analog Amplifications in Leninakan

The aftershocks and corresponding seismograms recorded in Leninakan are presented in volumes II, III, and IV of this report. The largest aftershock recorded in Leninakan was a magnitude 4.7 event that occurred on December 31, 04:07 UTC. On-scale recordings of this aftershock were obtained from the accelerometers at seven stations. The largest peak accelerations recorded for this event were 5.7 and 3.1 percent of gravity, observed on the transverse components at stations in Keti (KET) and Leninakan (LEN), respectively. Equiscaled plots of the vertical, radial, and transverse components of recorded acceleration are shown in Figure 9.1. Corresponding plots of ground velocity and ground displacement are shown in Figures 9.2 and 9.3. The ground velocity time histories were derived by integration of the recorded acceleration time history filtered with a four-pole low-cut causal filter with a corner at 5 seconds. The displacement time histories were derived by double integration of the acceleration time history filtered with a 6-pole low-cut filter with a corner at 5 seconds. Hypocentral distance for each set of three-component recordings is indicated. Comparison of the recordings obtained in Leninakan with those obtained at the other sites shows that the character of the ground motions observed in Leninakan is significantly different from that observed at the other sites.

The equiscaled plots show that both the amplitude and duration of horizontal ground motion at periods of 0.6–3 seconds are significantly larger in Leninakan than at the other sites. The dramatic increase in duration of shaking at these periods is more apparent on the plots of ground velocity (Figure 9.2) than on those for acceleration (Figure 9.1) and most apparent on those for ground displacement (Figure 9.3). Because time histories of ground acceleration tend to emphasize the higher frequency components of motion, ground velocity the intermediate frequencies and ground displacement the lower frequencies, the

amplification characteristics of the soil deposits beneath the Leninakan site are most apparent on the displacement time histories.

A summary of the peak vertical, radial and transverse amplitudes for acceleration, velocity, and displacement for each of the seismograms, shown in Figures 9.1, 9.2 and 9.3, is given in Table 9.2, together with the hypocentral distances for each of the stations. Ratios of the peak amplitudes observed for Leninakan to those at each of the three other sites are given in Table 9.3. Each of the ratios have been multiplied by the corresponding ratio of hypocentral distance for each site in order to account for differences in hypocentral distance of the stations from the source. This correction assumes that the amplitudes decrease inversely with increasing distance. The ratios serve to summarize several interesting features of the data set.

The ratios computed with respect to stations GOG and DZH show remarkable agreement for each component of motion. The ratios computed with respect to site KET are consistently about a factor of two smaller. This reduction indicates peak ground motion levels were about a factor of two larger at site KET than at sites GOG and DZH. The KET site is underlain by a layer of soil probably 1–2 meters thick, while this is not the case at the other normalization sites. Another possible contributory factor is that such variations could easily be attributed to variations in near-source crustal structure or to the radiation pattern of the source. Nevertheless the agreement in the ratios as computed with respect to each of the three rock sites, provides strong evidence that the larger motions in Leninakan are due to local site conditions in Leninakan.

The means of the ratios show that the largest amplifications in Leninakan occur for the horizontal components of ground displacement. They indicate that the radial components of ground displacement were about 8 times larger in Leninakan than that which occurred on rock sites at comparable distances. They indicate the transverse components were about 5 times larger; however, the vertical components of displacement were amplified only by a factor of about 1.5. They show that neither vertical components of ground acceleration nor velocity in Leninakan differ significantly from those at rock sites at a corresponding distance. They show that the transverse components of acceleration are about 1.5 times larger and that both horizontal components of velocity were about 1.7–1.8 times larger in Leninakan than at corresponding rock sites. In general, the ratios show that the local

site conditions beneath Leninakan served to modify the peak acceleration amplitudes the least, the peak horizontal velocity amplitudes more significantly, and the peak horizontal displacement amplitudes by a large amount.

Spectral amplifications in Leninakan

To better characterize the amplitude response of the site conditions in Leninakan Fourier amplitude spectra, computed from the recordings of three different aftershocks, were normalized by the corresponding Fourier amplitude spectra computed for the three rock sites (KET, GOG, DZH).

Elementary linear system considerations suggest that the seismic amplitude response characteristics of unconsolidated deposits can be estimated by considering the ratio of the modulus of the Fourier transform of a seismogram recorded on a soil site to that recorded on a nearby rock site (Borcherdt, 1968). For vertical wave propagation in a horizontal layered elastic structure, the approximation can be shown to be exact. From a practical point of view the approximation is generally most representative of the response characeristics at sites with thick sections of soft soil. Such sites are often characterized by a steep velocity gradient near the surface causing much of the seismic energy arriving at the surface to be propagating at or near vertical. Since the effects of such soil layers are often a dominant feature of the seismograms, spectral ratios have been shown to provide a good first-order approximation to the site's amplitude response (Borcherdt, 1968; Borcherdt and Gibbs, 1976; Rogers *et al.*, 1984; Singh *et al.*, 1989).

Fourier spectra for each corresponding pair of recordings were computed for the time interval corresponding to the record of shortest length. (Experience has shown that the most stable estimate of the site response is generally provided by spectra computed from the entire seismogram as opposed to some portion.) Prior to computing ratios, the Fourier spectra were corrected for leakage using a 10 percent cosine taper on each end of the time series. The Fourier spectra were smoothed with a triangular Hanning window of half-width 0.1 Hz prior to computation of the ratios.

The spectral ratios corresponding to the vertical components of motion are shown in Figures 9.4 and 9.5. Those for the radial components of motion are shown in Figures 9.6 and 9.7 and those for the transverse components in 9.8 and 9.9. The ratios for Leninakan to each of the other sites are computed for three different aftershocks. The ratios for each

event are arranged in columns in order of increasing distance. The ratios of the hypocentral distances for the corresponding sites are provided on the ordinates. A dominant feature of the spectral ratios is the evidence for ground motion amplification in the period band 0.7–2.4 seconds (Figures 9.4–9.9). The fact that these amplifications are apparent, essentially independent of the station used for normalization, provides strong evidence that the local site conditions beneath Leninakan are responsible for large amplifications of ground motion (especially horizontal motion) in the period band of 0.7–2.5 seconds (0.4–1.5 Hz). The size of the horizontal amplifications and spectral ratios that have been computed of the P and S portions of the seismograms (not shown) suggest that resonance of the soil layers is the principal mechanism by which the large amplifications are developing. Comparison of the ratios provides several more detailed insights regarding the nature of ground motions in Leninakan.

The largest horizontal and vertical amplifications between 1 and 2.5 seconds are apparent for the largest aftershock; namely, the 366 04:07, M 4.7 event (compare column 1 and 2 on Figures 9.4, 9.6, and 9.8). This does not necessarily mean that the actual soil amplifications in this period band are dependent on magnitude or on the level of ground motions in Leninakan. Instead, it also can be an indication of the extent to which the seismic signals as recorded were resolved above sensor sensitivity levels and earth background noise levels. The magnitude 4.7 event generated ground motions sufficiently strong so as to provide strong signals recorded with good resolution by the accelerometers at all of the sites. Consequently, since the FBA response is flat in the range of 1–2.5 seconds, the spectra of the accelerometer signals in this period band are not contaminated by earth noise or instrument noise and provide the best estimate of the relative ground response. However, the signals recorded for the smaller events from the FBAs were not recorded at high gain and so were not recorded at resolutions as high as those for the larger event. As a result their spectra at the longer periods are more likely contaminated by noise over a larger bandwidth. The signals from the velocity transducers are recorded at high resolution for the smaller events, but not necessarily for periods as long as 2.5 seconds. Since the transducers have a 2 Hz natural frequency, their response falls off at about 12 dB per octave for frequencies below 2 Hz. Consequently, the signals at 0.4 Hz or 2.5 seconds are substantially reduced by the instrument response from those at 2 Hz. Since the signals

from the smaller events also generally contain less long-period energy than do larger events, the signals recorded from the velocity transducers at the longer periods (2.5 seconds) at the rock sites can be contaminated by noise. The spectral ratios for events 365 13:28 and 361 14:56 (Figures 9.4–9.9) are computed from recorded velocity transducer signals.

The decrease in the levels of spectral amplification at each of the sites with decreasing magnitudes is probably due in part to the fact that noise contamination near 2.5 seconds (0.4 Hz) increases at the rock sites with decreasing magnitude as discussed above. Additional evidence that this is the case is the consistent reduction in the longer-period spectral amplifications for all of the sites that recorded the 365 13:28 event (M 4.2) when compared to amplifications computed for the same sites for the 366 04:07 event (M 4.7). Also, the fact that the high-frequency spectral amplifications in the band 2–10 Hz do not show a similar overall decrease with decreasing magnitudes argues that the long-period decrease is due to noise contamination of these periods at the rock sites.

Several conclusions can be drawn from the spectral ratios shown in Figures 9.4–9.9:

1. Because of resolution at which the various events were recorded, the spectral ratios for the largest event are considered most representative of site response at the periods near 2 seconds.
2. The ground motions in the period band 0.6 to 3 seconds are significantly larger at the LEN site underlain by thick sections of soil and tuff layers than at three other sites (KET, GOG, DZH) underlain by thin soil or rock.
3. The horizontal (radial and transverse) components of ground motion show evidence of well defined "predominant ground periods" near 2.5 seconds and between 1.5 and 2 seconds.
4. The peak horizontal spectral amplifications (after scaling with the distance ratio) are between 22 and 36 for the site LEN normalized by the sites KET, GOG, and DZH.
5. The spectral ratios for the radial component, corresponding to P, SV and Rayleigh-wave energy, suggest two predominant ground periods, each with amplifications nearly equal in magnitude near 2.5 and 1 seconds. The transverse components corresponding to P, SH, and Love wave energy suggest that the predominant amplification in the transverse direction occurs for periods near 2.5 seconds .

6. The spectral amplifications for horizontal motion in the 0.6–2.5 second band (22–36) are larger than those for the vertical motion (10–25).

7. In addition to amplifications of horizontal shaking near 2.5 and 1 second, the spectral ratios suggest smaller amounts of amplification over the bands of 1–6 seconds (1–1.5 Hz) and 0.16–0.25 seconds (4–6 Hz).

The conclusions concerning the nature of ground response at site LEN in Leninakan are quite consistent with those implied by the damage statistics (see Section 9.1 and Table 9.1). The large amplifications of the longer-period ground motions are consistent with larger amounts of damage to longer-period structures in Leninakan, namely precast frame-panel and composite panel-stone buildings.

Present information indicates the natural period of the precast frame-panel buildings of 9–12 stories may be as short as 0.6 seconds. The spectral ratios suggest an amplification peak near 0.7 seconds. If such amplification occurred during the main shock, it could have intensified the initiation of damage to their longer-period structures. With the initiation of damage the fundamental resonant period of the structures would be expected to lengthen towards those periods for which the large spectral amplifications are occurring. Consequently, it appears that the ground response as observed at the site LEN in Leninakan could have been a major contributory factor to the damage experienced by the longer-period structures.

Without further measurements, it is difficult to address how the observed ground response might vary throughout the city. Previous experience suggests one would expect the dominant periods of amplification and the resulting peak levels to vary depending on relative thicknesses of the various soil and volcanic tuff layers. The characteristics of the ground response also are expected to vary with water table depth and overall thickness of the soil layers. Further study is necessary to define the variations likely to exist throughout the city.

The large amplifications observed in Leninakan are reminiscent of those observed in the San Francisco Bay region (Borcherdt *et al.*, 1968; Borcherdt and Gibbs, 1976; Rosenbleuth, 1960; Seed *et al.*, 1989). In both regions water-saturated clay and sand deposits with thicknesses up to and exceeding 35 meters have been shown to yield high levels of increased ground motion over certain period bands. In the San Francisco Bay region the

largest amplifications are observed for periods near 0.8–1.2 seconds. In Mexico City large amplifications near 2 seconds have been observed.

The well-defined predominant ground periods measured by Borcherdt (1968) for sites underlain by younger bay mud deposits and artificial fill have been shown to correlate well with areas of increased damage during the great earthquake (M 8.2) of April 18, 1906. The first-order characteristics of the ground response measured from distant seismic events also was shown to correlate well with those observed on strong-motion instruments for the nearby 1957 earthquake (M 5.7).

Evidence for large ground motion amplifications as recently recorded during the Michoacàn earthquake in Mexico City show significant levels of amplification near 2 seconds for the SCT site. These amplifications of ground motions in Mexico City also were found to correlate with structural damage (Seed *et al.*, 1989).

REFERENCES – CHAPTER 9

Borcherdt, R. D. (1970). Effects of local geology on ground motion near San Francisco Bay, Seism. Soc. Am. Bull. 60, 29–61.

Borcherdt, R. D., and J. F. Gibbs (1976). Effects of local geological conditions in the San Francisco Bay region on ground motions and the inensities of the 1906 earthquake, Seism. Soc. Am. Bull. 66, 467–500.

Gutenberg, B. (1957). Effects of ground on earthquake motion, Seism. Soc. Am. Bull. 32, 163–191.

Medvedev, S. V. (ed.) (1968). Seismic zoning of the USSR, "Nauka," Moscow.

Rosenbleuth, E. (1960). The earthquake of 28 July 1957 in Mexico City, Proc. Second World Conf. Eq. Eng., Tokyo and Kyoto, Japan, 359–379.

Seed, H. B., M. P. Romo, J. I. Sun, A. Jaime, and J. Lysmer, 1989, The Mexico earthquake of September 19, 1985—Relationships between soil conditions and earthquake ground motions, Earthq. Spectra, 687–729.

Singh, S. K., J. Lermo, T. Dominguez, M. Ordaz, J. M. Espinosa, E. Mena, and R. Quaas, 1989, The Mexico earthquake of September 19, 1985—A study of amplification of seismic waves in the valley of Mexico with respect to a hill zone site, Earthq. Spectra, 653–673.

Rogers, A. M., R. D. Borcherdt, A. M. Covington, and D. M. Perkins (1984). A comparative ground response study near Los Angeles using recordings of Nevada Nuclear Tests and the 1971 San Fernando earthquake, Seism. Soc. Am. Bull. 74, 1925–1950.

Table 9.1 Statistics of Multi-Story Residential Buildings in the Affected Area as of January 24, 1989

City or Town (Epicentral Distance, km)	Precast Panel				Precast Frame-Panel				Composite Frame-Stone				Stone			
	A	B	C	D	A	B	C	D	A	B	C	D	A	B	C	D
Spitak (9)	-	-	-	1	-	-	-	-	43	9	7	-	20	2	3	-
Stepanavan (23)	-	-	-	-	-	-	-	-	8	13	33	2	10	-	9	16
Kirovakan (25)	-	-	-	4	-	-	88	20	41	89	414	27	46	53	145	-
Akhourian (27)	-	-	-	-	-	-	-	-	18	4	17	2	1	2	5	3
Dzaghgahovid (30)	-	-	-	-	-	-	-	-	-	-	8	1	-	10	9	-
Kalinino (30)	-	-	-	-	-	2	11	5	-	-	4	-	-	3	-	-
Leninakan (32)	-	-	-	16	72	55	6	-	27	115	67	20	24	160	154	150
Aparan (33)	-	-	2	-	-	-	3	-	-	4	5	-	-	14	6	2
Artik (33)	-	-	-	-	-	-	-	-	-	2	47	25	-	14	2	-
Ghoukasian (34)	-	-	-	-	-	-	-	-	-	4	4	1	-	5	2	4
Amasia (37)	-	-	-	-	-	-	-	-	-	4	1	1	-	1	2	4
Pemzashen (38)	-	-	-	-	-	-	-	-	-	3	-	3	-	12	4	4
Maralik (44)	-	-	-	-	-	-	-	-	-	-	17	2	-	-	5	1
Alaverdi (47)	-	-	5	15	-	-	4	18	-	-	11	43	-	16	21	48
Dilijan (59)	-	-	-	-	-	-	3	5	-	19	8	47	-	7	5	2
Charentsavan (60)	-	-	6	21	-	-	8	7	-	-	19	79	-	-	-	-
Talin (62)	-	-	-	-	-	-	-	-	-	-	6	1	-	2	3	2
Razdan (63)	-	-	-	3	-	-	-	-	-	-	25	50	-	7	-	-
Ashtarak (65)	-	-	-	-	-	-	-	1	-	-	3	-	-	-	-	-
Sevan (73)	-	-	-	1	-	-	-	-	-	-	-	-	-	-	-	-
Noyemberian (74)	-	-	-	-	-	-	-	-	-	-	-	-	-	-	-	4
Abovian (78)	-	-	-	2	-	-	-	16	-	-	-	-	-	-	-	6
Idjevan (79)	-	-	-	2	-	-	7	5	-	-	23	3	-	-	9	13
Bert (100)	-	-	-	-	-	-	-	-	-	-	-	-	-	6	1	-
Krasnaselsk (102)	-	-	-	-	-	-	-	-	-	-	-	-	-	-	5	-
Googark (??)	-	-	-	-	-	-	-	-	-	-	-	-	3	2	9	1
Baghramian (??)	-	-	-	-	-	-	-	-	-	-	-	-	-	1	3	3
Total	-	-	13	65	72	57	130	77	137	266*	719*	307	104	317	402*	263*
Percent in Each Category																
Spitak	-	-	-	100	-	-	-	-	73	15	12	-	80	8	12	-
Stepanavan	-	-	-	-	-	-	-	-	14	23	59	4	29	-	26	46
Kirovakan	-	-	-	100	-	-	81	19	7	16	72	5	19	22	59	-
Leninakan	-	-	-	100	54	41	5	-	12	50	29	9	5	33	31	31
All Cities	-	-	17	83	21	17	39	23	10	19	50	21	10	29	37	24

A = Collapsed
B = Heavyly damaged; to be demolished
C = Damaged; to be repaired or strengthened
D = No significant damage; usable
* = Total not consistent with original Russian document
? = Epicentral distance could not be determined

Note: In addition to the above, there were two lift-slab residential buildings in Leninakan. One was a 10-story building that collapsed (state A) and the other was a 16-story building that was badly damaged (state B) and was torn down in February.

Table 9.2. Peak ground motion amplitudes for the magnitude 4.7 earthquake which occurred on 366 04:07 (UTC).

Station	Hypocentral Distance (km)	Peak Amplitude A (cm/s^2) Z	R	T	V (cm/s) Z	R	T	d (cm) Z	R	T
KET	19.9	42	38	57	1.6	1.4	1.9	.08	.07	.07
GOG	23.5	12	18	16	0.4	0.5	0.5	.028	.024	.037
LEN	23.6	17	15	31	0.4	1.1	1.0	.05	.25	.22
DZH	28.2	12	13	16	0.3	0.4	6.8	.025	.022	.042

Table 9.3. Ratios of peak ground motion from event 366 04:07 (UTC) at site LEN (ratios have been normalized by corresponding ratio of hypocentral distances to sites).

Station	Distance Ratio	Ratios of Peak Amplitude Acceleration Z	R	T	Velocity Z	R	T	Displacement Z	R	T
LEN/KET	1.19	0.5	0.5	0.6	0.3	0.9	2.2	0.7	4.2	3.7
LEN/GOG	1.00	1.4	0.8	1.9	1.0	2.2	2.0	1.8	10.4	5.9
LEN/DZH	0.84	1.2	1.0	1.6	1.1	2.3	1.0	1.7	9.5	4.4
Mean		1.0	0.8	1.4	0.8	1.8	1.7	1.4	8.0	4.7

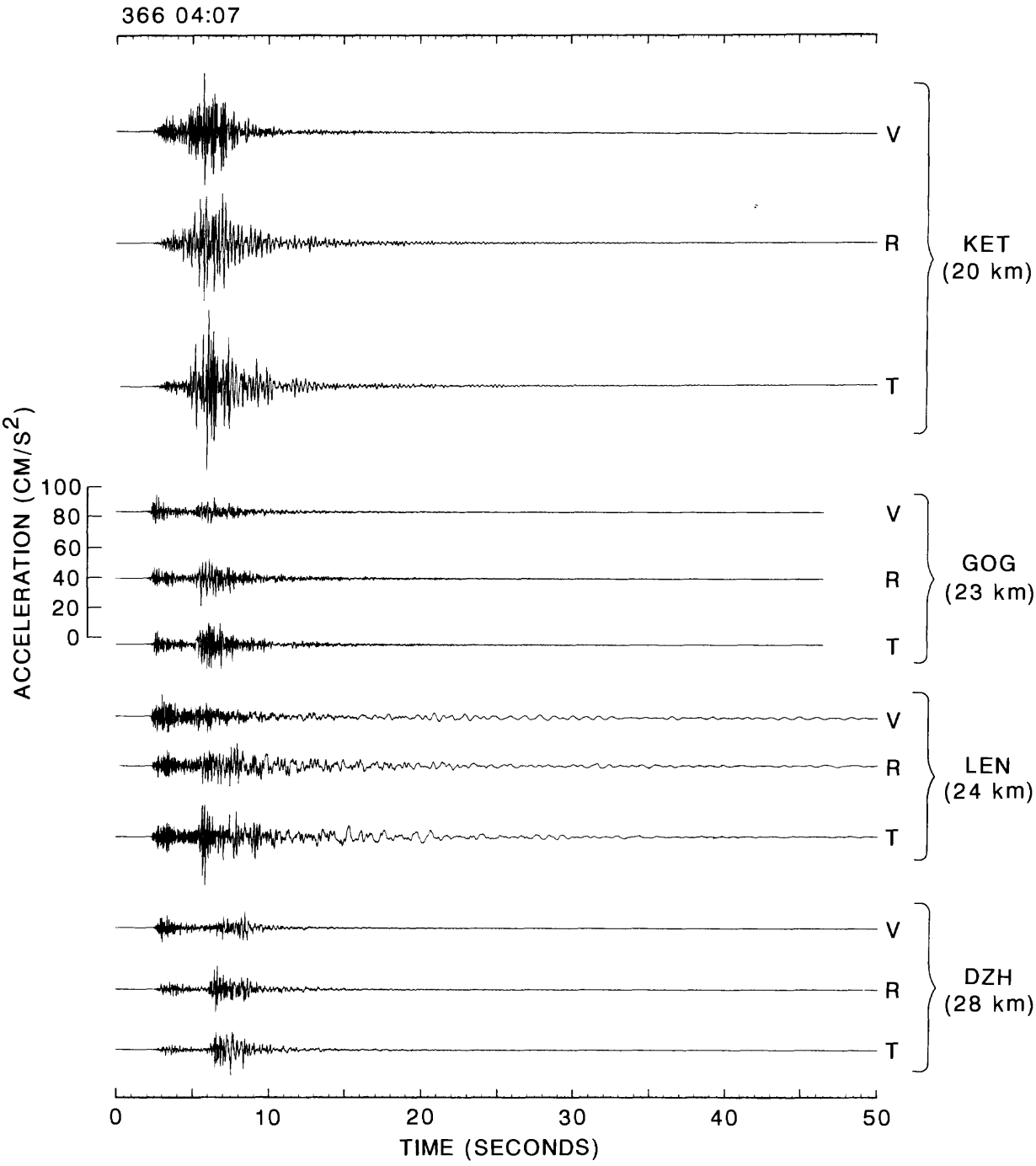

FIGURE 9.1. Equiscaled plots of the vertical, radial and transverse components of ground acceleration for aftershock 366 04:07 (see Figure 8.2) as recorded at site LEN underlain by layers of soil and volcanic tuff and at sites KET, GOG, and DZH underlain by rock or thin layers of soil (see Figure 6.1).

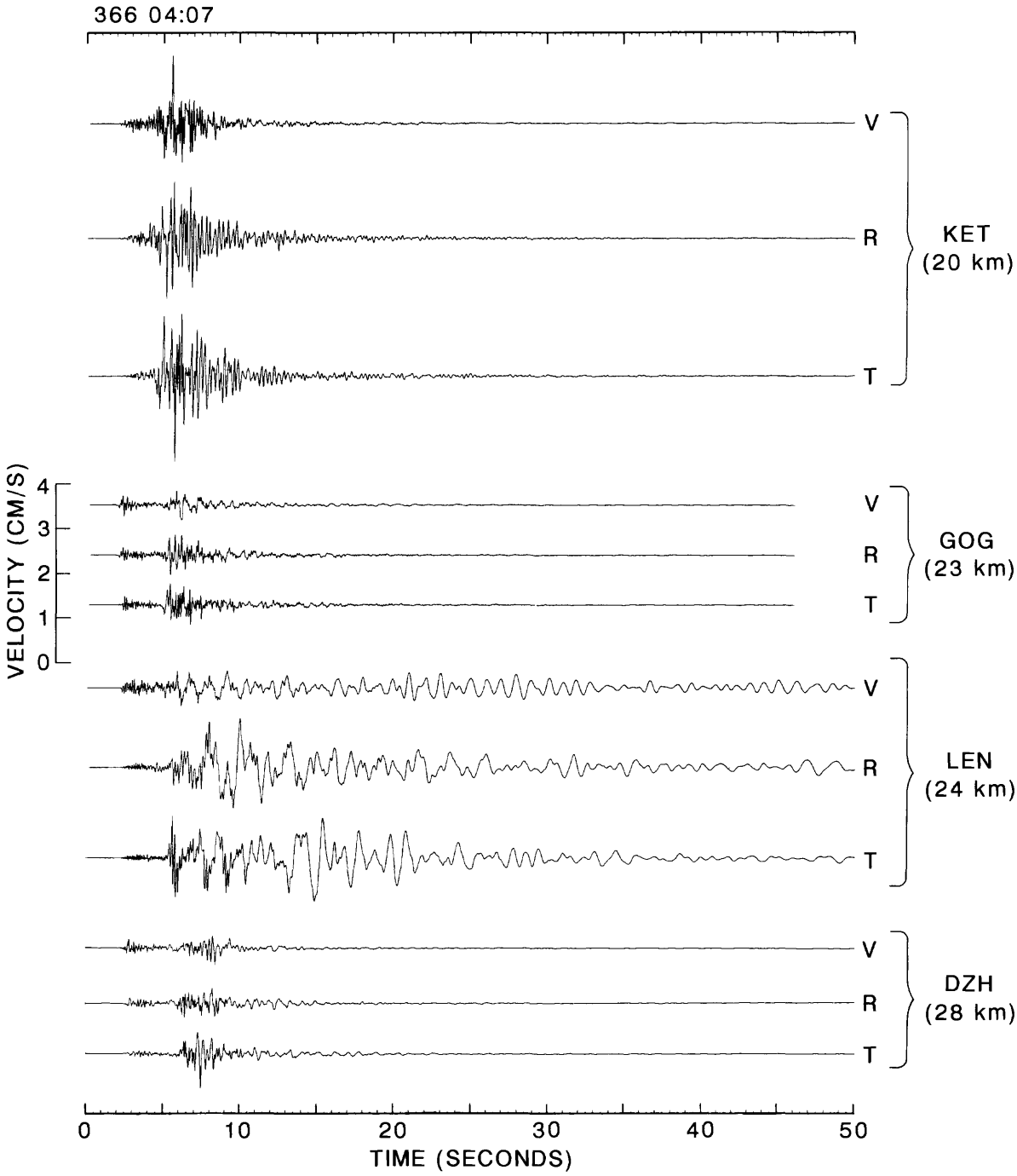

FIGURE 9.2. Equiscaled plots of the vertical, radial and transverse components of ground velocityinferred from the acceleration recordings of aftershock 366 04:07 (see Figure 8.2) at site LEN underlain by layers of soil and volcanic tuff and at sites KET, GOG, and DZH underlain by rock or a thin layer of soil (see Figure 6.1).

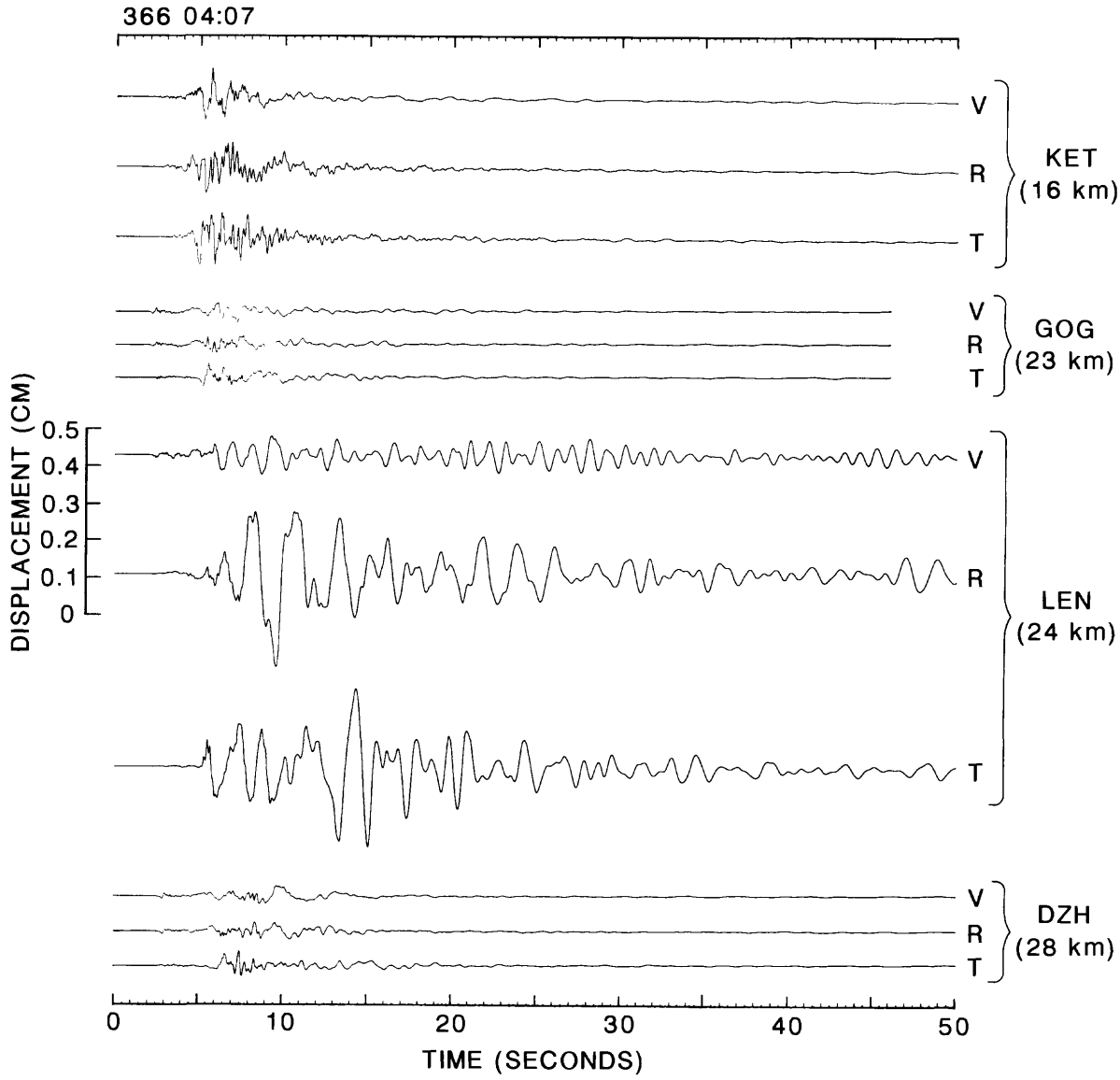

FIGURE 9.3. Equiscaled plots of the vertical, radial and transverse components of ground displacement inferred for aftershock 366 04:07 (see Figure 8.2) as recorded at site LEN underlain by layers of soil and volcanic tuff and at sites KET, GOG, and DZH underlain by rock or thin layers of soil (see Figure 6.1).

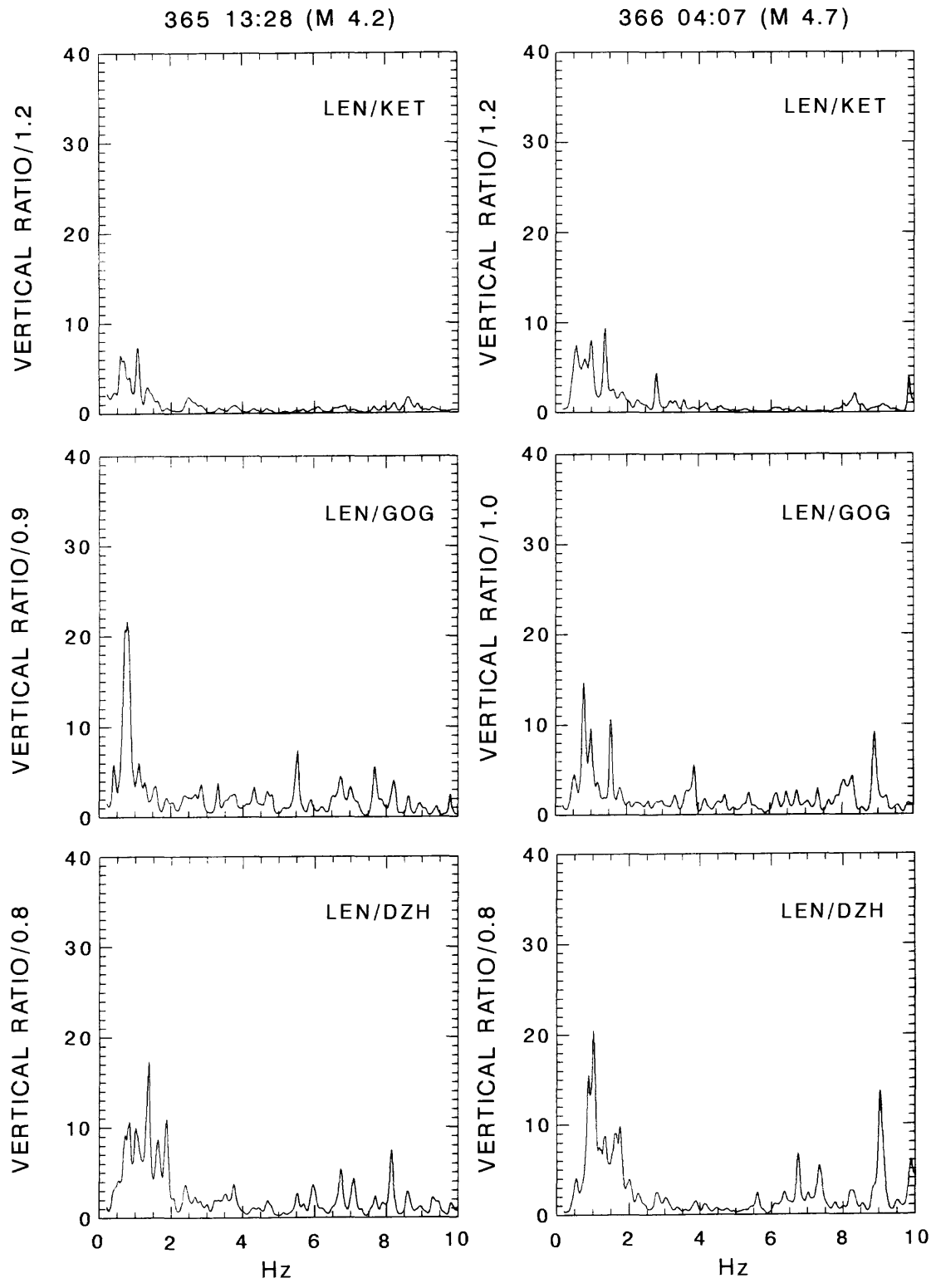

FIGURE 9.4. Spectral ratios for the vertical components of motion at staion LEN with respect to stations indicated for events shown. Ratios of hypocentral distances are shown on ordinates.

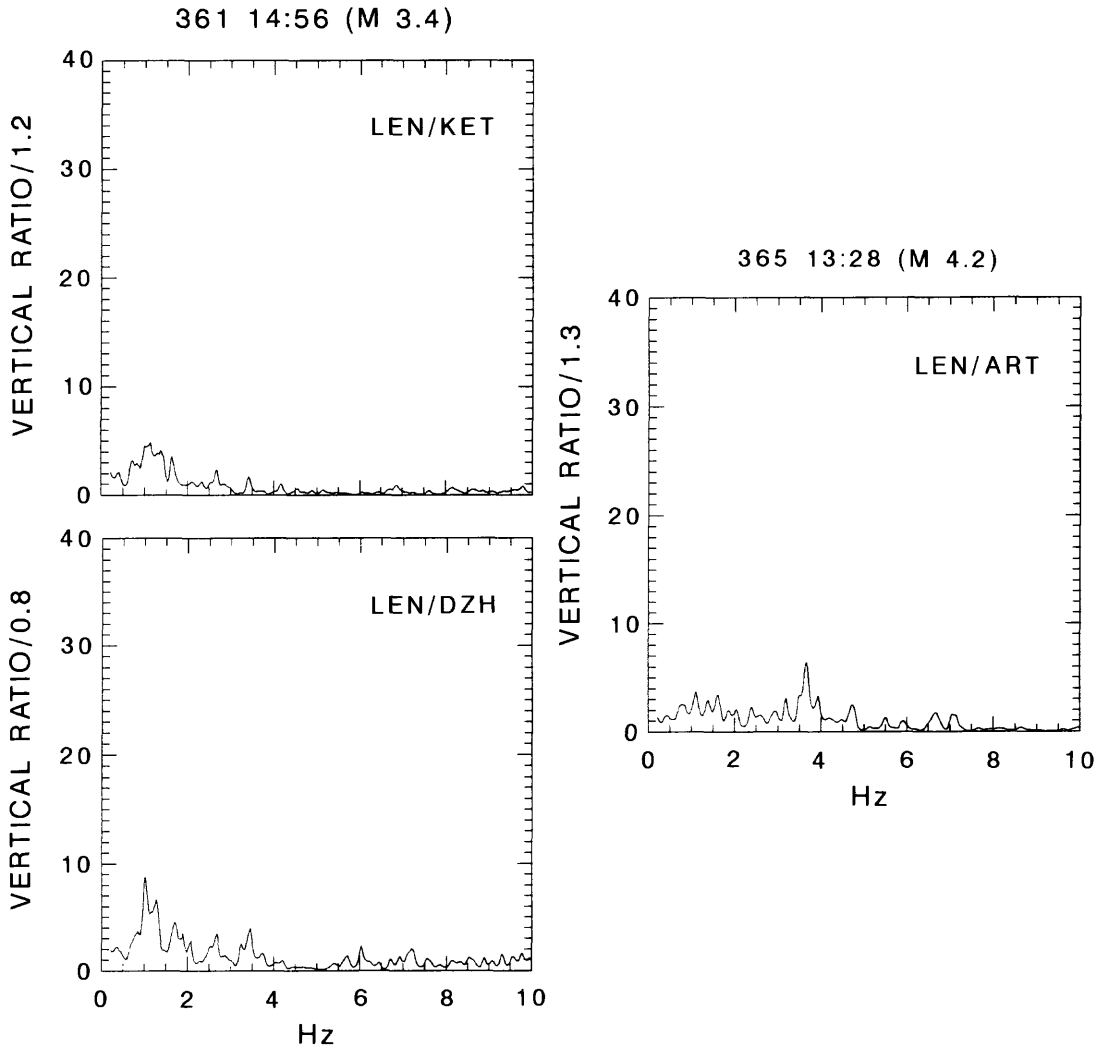

FIGURE 9.5. Spectral ratios for the vertical components of motion at staion LEN with respect to stations indicated for events shown. Ratios of hypocentral distances are shown on ordinates.

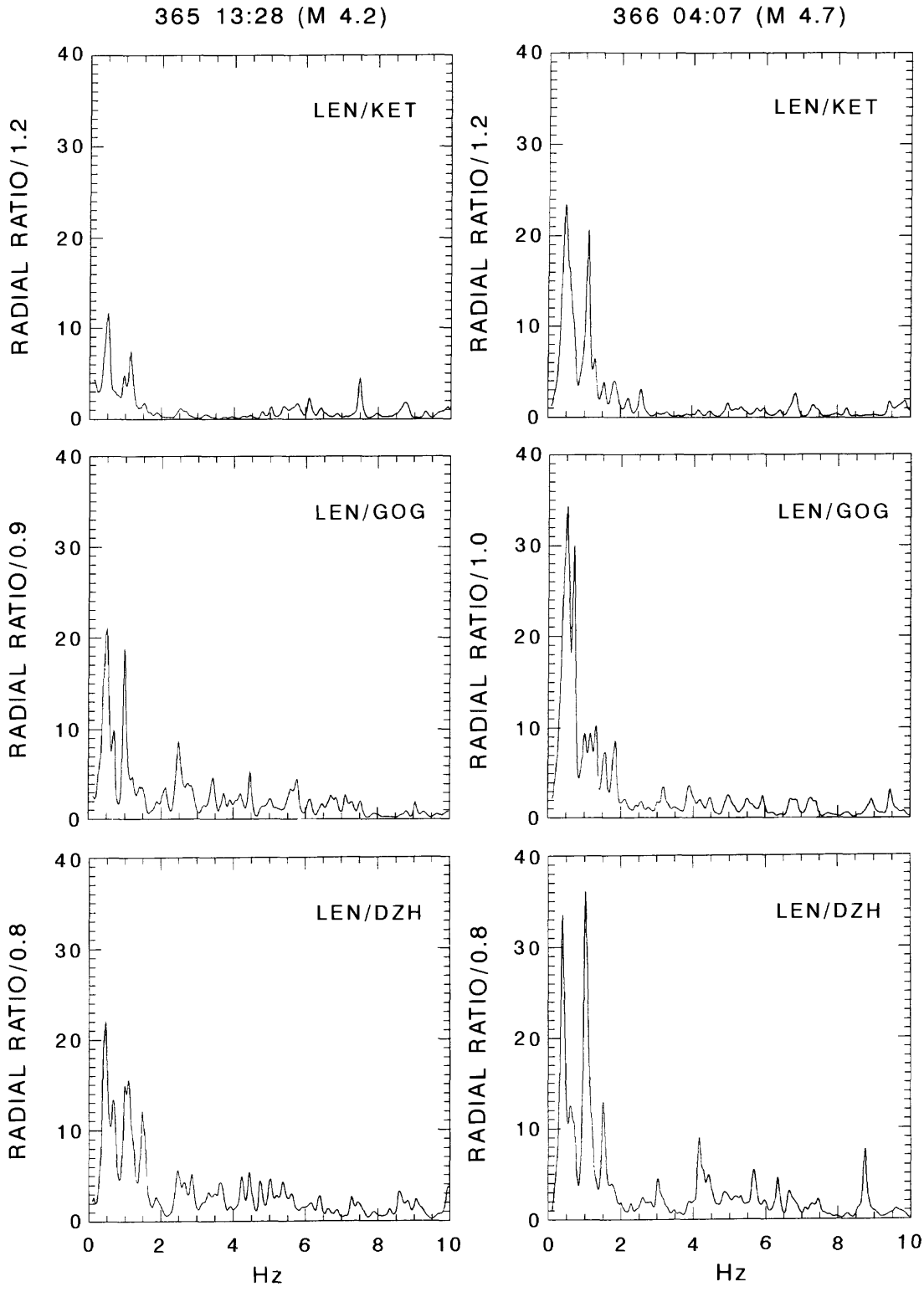

FIGURE 9.6. Spectral ratios for the radial components of motion at staion LEN with respect to stations indicated for events shown. Ratios of hypocentral distances are shown on ordinates.

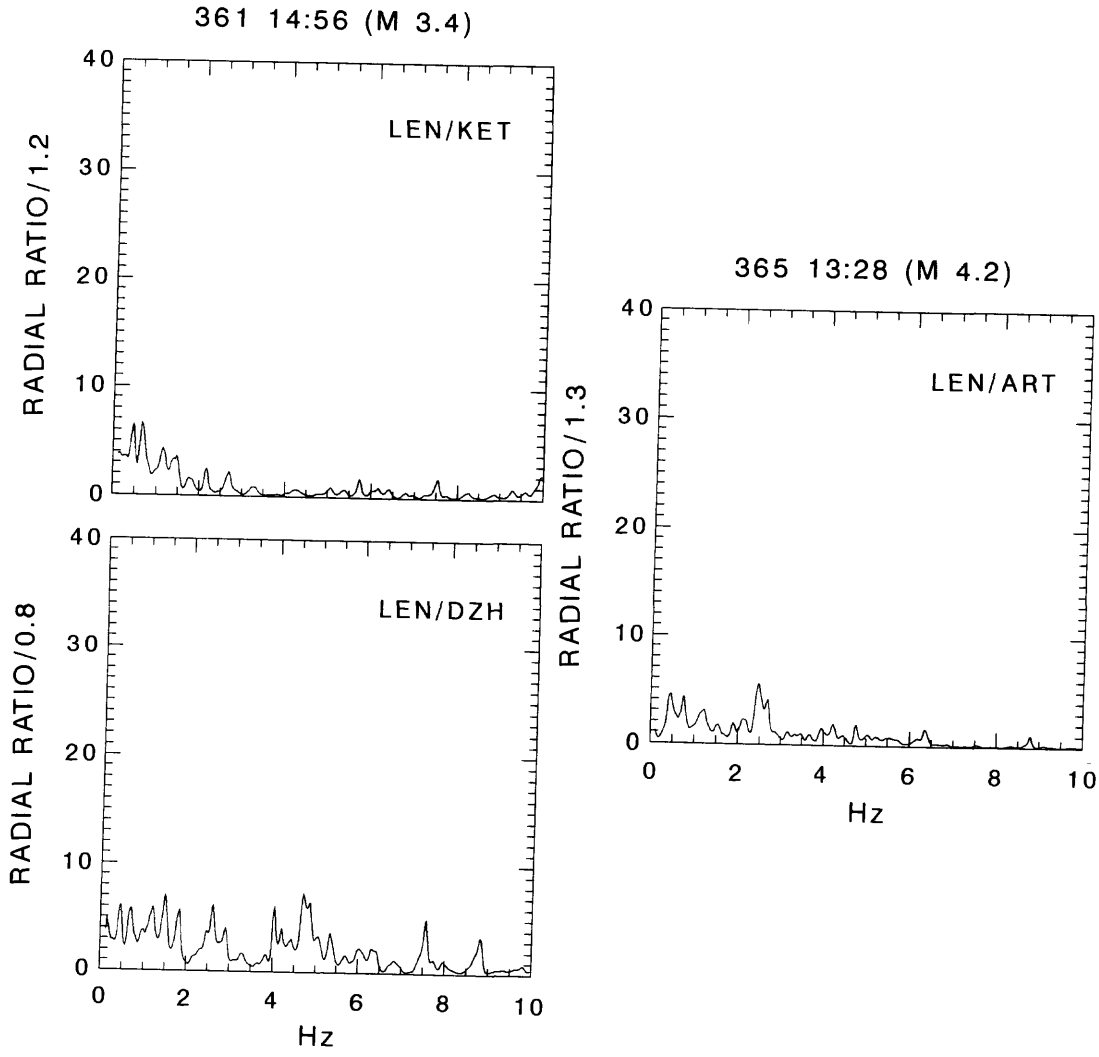

FIGURE 9.7. **Spectral ratios for the radial components of motion at staion LEN** with respect to stations indicated for events shown. Ratios of hypocentral distances are shown on ordinates.

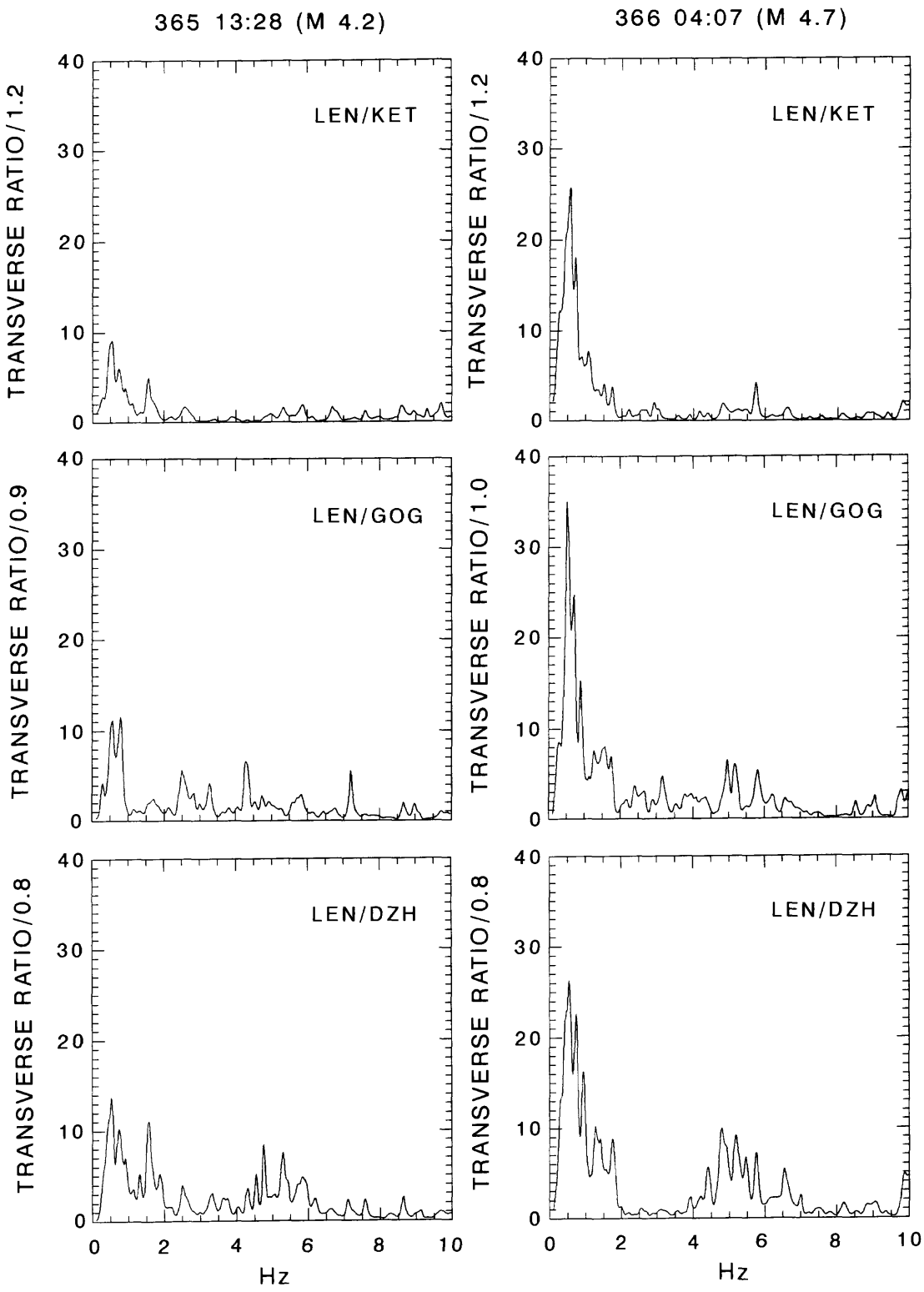

FIGURE 9.8. Spectral ratios for the transverse components of motion at staion LEN with respect to stations indicated for events shown. Ratios of hypocentral distances are shown on ordinates.

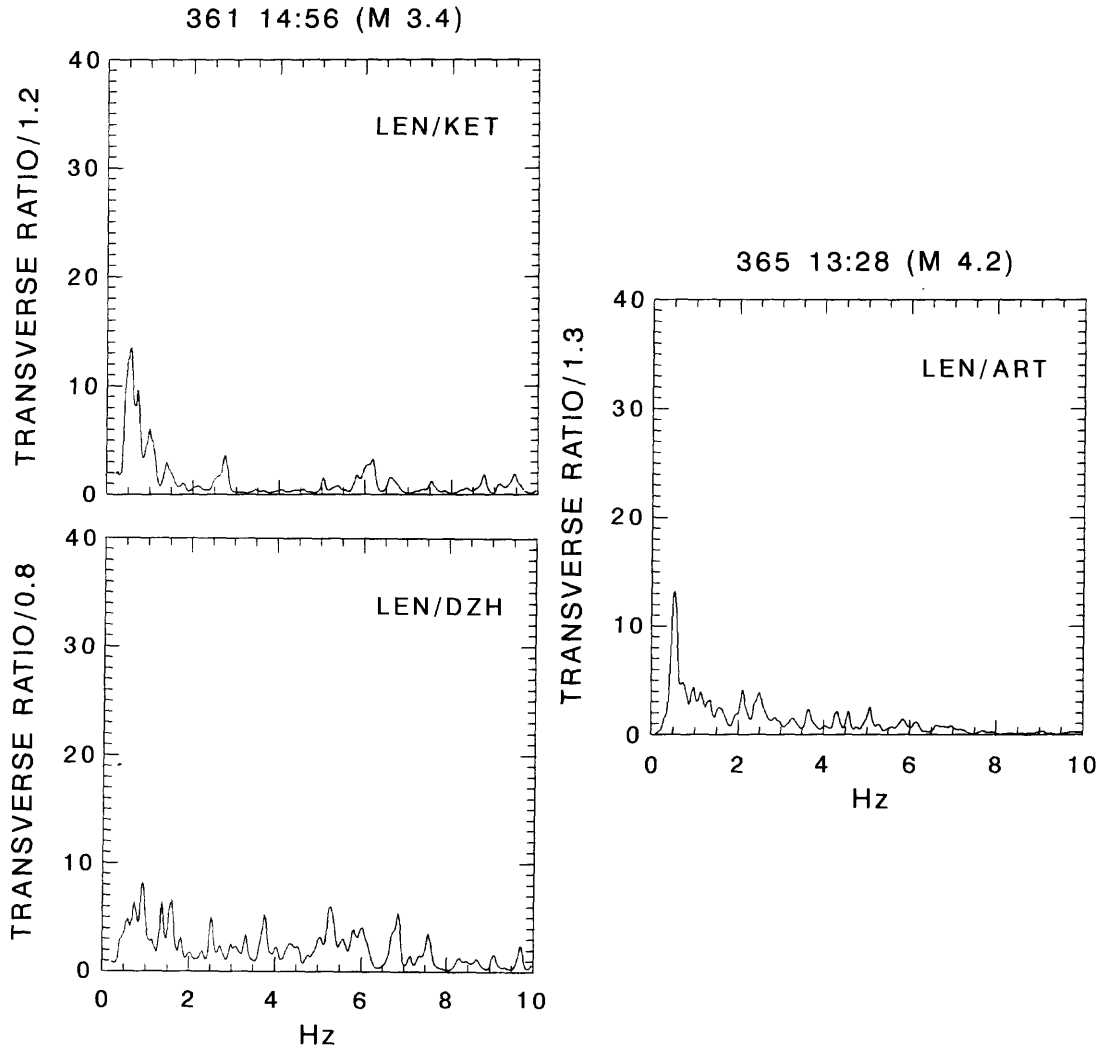

FIGURE 9.9. Spectral ratios for the transverse components of motion at staion LEN with respect to stations indicated for events shown. Ratios of hypocentral distances are shown on ordinates.

CHAPTER 10

DIGITAL TIME SERIES FOR AFTERSHOCKS OF DECEMBER 7, 1988 EARTHQUAKES ON DIGITAL MAGNETIC TAPE

G. Glassmoyer

Ten 1600-bit-per-inch (bpi) ANSI labeled 9-track tapes have been written that contain all 2053 of the velocity recordings from the GEOS collected as of 7 February 1989. Files on these tapes are in DR1EXP format (Table 10.1) In addition, one ANSI labeled 9-track tape has been written in DR1EXP format containing the acceleration recordings for 23 of the larger aftershocks. The list of included velocity recordings is the same as in Table B.1. The acceleration recordings are included when either one or more stations have velocity recordings that exceeded full-scale or when magnitude is greater than about 3.0. The list of included acceleration recordings is in Table 10.2.

The DR1EXP format consists of ASCII characters with record size of 80 characters. These files are derived from the National Strong Motion Data Center binary data using the computer program DR1EXP. The data content of the resulting ASCII files can differ from the binary data in at least two respects. First, in each file several values stored in the headers of the binary files (Tables 7.1.1 and 7.1.2) are not reproduced in the ASCII versions. Second, the ASCII versions are limited to the first 10752 samples per component or 99.999 seconds duration, whichever is less.

The first six records in the DR1EXP format are the header for a three-component recording. Refer to Table 10.1 for the position within a record for each of the following values. Record 1 contains the identification for the recording derived in the manner described in Chapter 7, however, these three-component files use either a 'V' for velocity or an 'A' for acceleration as the component code. Record 2 contains the station name; year, Julian day, hour, minute, second, and milliseconds of the start-of-record time, uncorrected for clock drift; duration of record in seconds; sampling rate in samples per second; event sequence number on source tape; and recording unit serial number. Record 3 contains the station latitude and longitude in degrees, minutes, and fractions of a minute; elevation

in meters; and sensor orientations for the first, second, and third components, each using two angles measured in degrees: first, from vertical and second, clockwise from North. Record 4 contains the transducer type, VEL (velocity) or FBA (acceleration); the coil constant (sensitivity) of the sensor in Volts per motion-unit (motion-unit for velocity is centimeters per second, motion-unit for acceleration is centimeters per second per second); natural frequency of sensor in Hertz; amplifier gains for each of the three components in decibels; and the digitization constant in digital counts per volt. Record 5 contains the frequency of the anti-aliasing filter in Hertz; the roll-off of the anti-aliasing filter in decibels per octave; and the clock-correction in seconds which should be subtracted from start-of-record time given in Record 2 to get the clock-drift corrected time. Record 6 contains the number of components (3); the number of samples per component; and the number of lines used to sequentially write each component's digital data.

The digital data records follow with 13 samples in each record with the possible exception of the last record for each component. For the example used in in Table 10.1 each component's data ends on a line (Record 6 plus 271 times 1, 2, and 3) that contains only 10 data values since the number of samples per component (3520) is not divisible by 13. There is no other indication within the data records of a change of component. A short line cannot, however, be relied upon to indicate the end of a component—a program used to read the data must use the information provided in Record 6 and count lines or samples in order to distinguish components.

Table 10.1 Example of DR1EXP output (ASCII format digital data). For brevity, shown here with ellipses (...) each used in place of 267 lines of data.

```
RSX "DR100" FILENAME: '3662343BV.MO2'
STATION=MO2  TIME=88*366+23:43:03.148  DUR=17.600  S/S=0200.00  E#00013,S#=00020
LAT.=+40:59.55, LON.=+043:56.40, ELV.=2090   ORIENTATION=000/000,090/000,090/090
TRNDUC=VEL  COIL=0.5000  NAT.FREQ.=02.00  GAIN=042,042,042  DIGIT.CON.=.3277E+04
ANTI-ALIASING-FILTER:CORNER=050.,ROLL-OFF=042DB/OCTAVE  CLOCK-CORRECTION=00.1715
NO.COMPONENTS=3  NO.SAMPLES/COMPONENT=03520  NO.LINES/COMPONENT=0271
     0     0     0     1     0     0     0     1     1     0     1     0     1
     1     0     1     2     1     1     1     1     1     0     1     1     0
...
     0     1     1     1     1     3     1     0     3     2     1     1     0
     0     0    -1    -1    -1    -2    -1    -2    -2    -1
     0     0     1     1     1     1     1     2     2     1     2     2     0
     1     1     0     1     1     1     1     1     1     1     1     1     1
...
     3     3     3     3     3     3     3     1     0     0     0    -1    -2
    -1    -1    -2    -2    -1    -1    -1    -1     0     0
     1     1     0     1     1     0     0     0     1     1     0     0     0
     0     0     0     1     0     0     1     1     1     1     1     1     0
...
    -4    -3    -4    -4    -3    -3    -2    -2    -1    -1     0     0     1
     1     1     2     1     3     3     4     5     6     6
```

Table 10.2 Listing of digital acceleration seismograms available in DR1EXP-ASCII format.

	APP	ART	BYR	DZH	GIB	GOG	GSS	KET	KIR	KI2	LEN	MOO	MO2	NAB	SCH	SEV	SPT	SSS	STE	YSS
3572123S					S		B													
3611456R		R		S				R	T		S	R		S					S	
3620745F				G				F	H		G	G		F						
3621115I				J			O	I			J	J		J						
3621230E				F				E	H		F	F		F						
3621802P				Q			A	P	Q		Q	Q		P						
3622044N				P			A	N			O	O		P						
3630346A				C			H	A	E		C	B								
3641843Q				R			C	Q	S		R		Q						S	
3651328Q		Q		Q		Q	C	Q	S		Q									
3651330G		H		H		H		G	I		H									
3651331E		E		E		E		E	F		E									
3660407D			G	D		D	J	D	F		D									
3661535G		H		G		G		I											G	
3661554L		M		L		L		M											L	
3661633G		H		G		G		H											G	
0012259M		O		N		N		O		M			O						N	
0030819S				S		S		T					T							
0031348P		Q		P		P		Q					Q							
0040729N			Q	N		N		O					O							
0040738J			M	J		J		K												
0040740P				Q		P		R												
0050815E			H																	

CHAPTER 11

DIGITAL TIME SERIES ON OPTICAL DISK CARTRIDGE AND CORRESPONDING PC ANALYSES SOFTWARE FOR AFTERSHOCKS OF DECEMBER 7, 1988 EARTHQUAKES NEAR SPITAK, ARMENIA S.S.R.

C. Valdes

Advances in microcomputer technology have made it possible to store the digital data recorded on GEOS (Borcherdt *et al.*, 1985) on one IBM 3363 optical disk cartridge. The data set consists of 378 seismic events recorded by two or more stations, and 957 events recorded by only one seismic station.

An IBM AT-type compatible microcomputer with an IBM 3363 optical drive is needed to read the seismic data. The GEOS format described in Dietel and Borcherdt, 1987, consists of a file-per-channel/station/trigger. This format has been converted to a one-file format that includes all channels and stations that recorded a particular seismic event.

The files have been named after the event's date of occurrence; for example, 88122614.A56, where 88, 12, 26, 14, and 56 are year, month, day, hour, and minute, respectively. The letter is to differentiate names in the case of several events in the same minute. The program PCEQ (Valdes, 1989) is an interactive program that allows the user to display a seismic trace at the time, enlarge a section of the trace, filter it, or obtain the spectra of a selected window. P- and S-wave arrival times can be read with PCEQ, as well as the amplitude level at low frequencies, the corner frequency and the slope of the high-frequency rolloff from the displacement spectra.

A description of the program PCEQ follows.

INTRODUCTION TO PCEQ

The estimation of earthquake parameters such as hypocentral location, magnitude, spectral characteristics, etc. has been restricted to large and usually expensive computers. Personal computers have grown in calculation power and have shrunk in price and in size. Thus making PCs ideal machines for earthquake processing.

The program PCEQ allows the user to interactively analyze seismograms on an IBM PC-type computer (clone or compatible). The principal features are are: a) selection P- and S-wave arrivals; b) filter the seismogram for better P- and S-wave selections; and c) calculation of the spectra of a selected section of the seismogram.

PCEQ program uses the output files generated by the PC based on a seismic data aquisition system developed by Lee *et al.* (1989). The seismic data file is written in binary. Digital seismograms in other formats can be converted into the PCEQ format. Appendix I describes such a format.

Two output files are created by PCEQ. One contains the arrival times for P- and S-waves written in the format used by the HYPO71PC earthquake locator program (this volume). The other file contains spectral parameters such as the amplitude of the low-frequency spectra, the corner frequency, and the slope of the high-frequency decay.

I. Hardware Requirements and Installation

In order to install and run PCEQ you need:

a) at least 512 kbytes of RAM memory,

b) a floppy disk drive (5 1/4 inch for an IBM PC/AT, or a 1.44 MB 3 1/2 inch for an IBM PS/2),

c) a hard disk,

d) a math coprocessor,

e) a color/graphics (EGA), or a Monochrome (Hercules) display,

f) a mouse.

To install the program you should place the diskette on the disk drive (let's assume A), and type (note: <CR> means pressing the enter key):

A: <CR> the computer will answer,

A: \ > then type,

INSTALL <CR>

The INSTALL program creates a directory named PCEQdemo, and copies eight files to that directory. The created directory C:\PCEQdemo (if it was installed in a hard disk named C:), has the following files:

INSTALL.BAT	Installation program.
PCEQ.EXE	Program to filter seismograms, to select *P*- and *S*-wave arrivals, to calculate and display the displacement spectra from a selected section of the seismogram.
EQ.WVM	Example input file of an earthquake in the Coalinga area, California, recorded by nearby stations.
INSTRU.FIL	Example of the file containing the instrument response curve. The file is optional. The program detects if it is present or not, but without the instrument response correction the spectra is meaningless.
SYSTEM16.FNT	
SYSTEM24.FNT	Font files. This file should be present in the directory where you are running the programs. Without it, no labels (fonts) will be written. SYSTEM16 and SYSTEM24 correspond to EGA and HERCULES graphics systems respectively.
PRTSCRN.EXE	Program to allow the Print Screen command to dump the screen into a dot matrix printer.
PCEQMAN.PRT	This manual.

II. Program PCEQ Description

PURPOSE: This program displays one seismic trace at a time. It allows the user to select a portion of the seismogram and to enlarge it to the length of the screen. The whole trace or portions of it can be filtered in order to enhance wave arrivals. Once a window containing a phase is chosen, the arrivals can be selected as well as their description and weights. The descriptions and weights are the ones specified by the earthquake locator program HYPO71 (Lee, 1971; Lee and Valdes, 1986).

This program also allows the user to calculate the spectra (displacement, velocity, or acceleration) of a selected portion of the seismogram or of the whole seismogram (provided it is less than 40 seconds long). The program is specifically intended for calculating the spectral displacement of shear waves in order to use Brune's (1970) dislocation model. You can select the flat part of the spectra and the corner frequency to calculate the seismic moment, stress drop and the source radius. For an example of the aplication of this method see the article by Archuleta *et al.* (1982). The previous processes are accomplished by using the mouse to interact with the program. If your input file is on a diskette, we recomend copying it to the hard disk. This will minimize considerably the amount of time spent reading the file.

INPUT:

The program uses the output file generated by the data acquisition system developed by Willie Lee *et al.* (1988). The file is written in binary representation. A sample file EQ.WVM is included. Digital seismograms can be converted into the format used by PCEQ, Appendix A describes the format.

OUTPUT:

a) This program creates an output file. The P- and S-wave arrival times are written to this file using the HYPO71 phase format. The program requests the name of the file, or uses a defult name: PHASE.OUT

b) The program creates an output file that contains the spectral amplitude, the corner frequency, and the slope of the high-frequency decay. The default name is: SPEC.OUT

RUNNING THE PROGRAM:

This program requires a mouse and it should be installed and enabled before running the program, otherwise PCEQ will lock the screen with a plot and you might have to reboot the computer to get out of this mode. If you want to make a hard copy of the plot on the screen, you should execute the program PRTSCRN before you run PCEQ. Note that PRTSCRN should be run only once at the very beginning of the session, this will set the printer for the rest of the working day (or until you turn the machine off).

To run the program type:

PCEQ <CR>

Now the program will ask you for an input file, type the name of the file (specify the whole path if the file is in another directory or drive), enter the name *i.e.,*

88122614.A56 <CR>

The program asks you for an output file name for the phases *i.e.,*

PHASE.OUT <CR>

One more <CR> is required to acknowledge the graphics routines. After this the program displays the first seismic trace. Figure 1 shows an example of this screen. At this point if the mouse is connected and enabled, by moving it, the cursor on the screen will move too. The screen shows the seismogram, and at the left is the name of the station and a number which is the maximum amplitude in counts. At the bottom is the time scale in seconds, and the line under it has the time of the first sample, and the name that you selected for the output file. To the right of this line you see "REPLOT EVENT." Moving the cursor to this area and pressing a button will cause the program to redisplay the original seismogram. The top line has the different functions. They can be executed by moving the cursor to that area and pressing a button. The explanation of each one of them follows:

WINDOW: When this function is enabled the word WINDOW changes color. Move the mouse to move the cursor. Pressing the left button will draw a left square bracket, which will indicate the beginning of the window. Pressing the right button will draw a right bracket and will mark the end of the window. You can mark as many brackets as you want but only the last left and right will be used. Figure 2 shows an example of this function. To plot the enlarged window, move to the WINDOW box and press any button. The program will display the enlarged window.

PICK: When this function is enabled the word PICK changes color. The seismic trace is the same as before, but the labels

are different. See Figure 3 for an example. Use the left button to "pick" the P-wave arrival. This will draw a cross and a P in the place selected. Again the last selection is the one that counts. Once you have selected the arrival you can use the boxes to describe the arrival (this is according to HYPO71 format):

EMERG	for an emergent arrival
IMPULS	for an impulsive arrival
UP	for upward first motion
DOWN	for downward first motion
+	for positive first motion
−	for negative first motion
?	for questionable first motion
0	for full weight
1	for semifull weight
2	for medium weight
3	for almost no weight
4	for no weight
5	for other type of weight

As you touch these boxes and press the button you will see the line above them changing as you select them. The time for the selected pick will be displayed. The S-wave is similar to the selection of for the P-wave. They can be done in the same window, or you can enlarge the area of the P arrival, do the "pick," and then enlarge the area for the S arrival. Moving to the MENU box and touching any button will send you back to the main menu. This can also be done by touching the area of REPLOT EVENT in the lower-right corner. The coda value shown in the top line represents the coda length. If you have not selected the coda before, it will be zero. The coda selection is described later.

NEXT: This selection will get the next seismogram and will display the main menu. The order the stations show up in is the order in which they were written to the file.

SELECT: This option will display the names of the stations available. Moving the cursor to one of the names and pressing

either buttom will display that seismic trace. Top part of Figure 1 shows this option.

CODA: This selection is similar to WINDOW, it uses the brackets to select the beginning and the end of the seismic event. The duration time is used by HYPO71 to calculate the event's magnitude. If you calculate the duration time before the PICK selection, the selected length will show up in the top line of the PICK menu.

FILTER: This selection will ask for the low and high frequencies to bandpass the seismogram. For example if you type:
5.0,10.0
The program will filter out waves with frequencies smaller than 5 and higher than 10. The filtered seismogram has only waves with frequencies between 5 and 10 Hz. By filtering the right frequencies you may clarify obscure wave arrivals. This option has to be used THOUGHTFULLY, poor seismograms will be POOR even if you filter them many times. Figure 4 shows the seismogram from Figure 2, filtered with a 10–20 bandpass. Note that it writes the band (the integer part only) below the filter box.

FFT: This selection will use the windowed section of the seismogram, or the whole seismogram, which should be less than 80 seconds long. Then it applies a Fast Fourier Transform to the data, removes the instrument correction (if the file INSTRU.FIL was provided, see Appendix B) and multiplies or divides it by frequency to obtain the displacement spectra. Figure 5 shows an example of the plot. The menus to the right of the spectra are described as follows:

OMEGA + Fc
With this option on, you can use the cursor to choose a point that will represent the level of the spectra (omega) at low frequencies (Y-axis), and at the same time the corner frequency (X-axis). Once you press the button, a line will extend from that point to frequency one. If you do not like the selection, try again, the last selection is the one saved. Touch the OMEGA + Fc box to leave the option.

GAMMA

With this option on you can choose a point on the section where the high frequency decays rapidly. The point will be connected with a line to the place where the corner frequency Fc was selected. The slope of the high-frequency decay is calculated with these two points.

MENU

Will take you back to the main MENU.

EXIT

This selection will exit the program.

VI. APPENDIX

a) INPUT FORMAT

The file is in binary and the record length is 512 words. Each record is described as follows:

RECORD 1

IBLANK	(INT*2)	empty variable
IBLANK	(INT*2)	empty variable
DATE(1)	(INT*2)	year (*i.e.*, 1989)
DATE(2)	(INT*2)	month (*i.e.*, 3)
DATE(3)	(INT*2)	day (*i.e.*, 14)
DATE(4)	(INT*2)	hour (*i.e.*, 15)
DATE(5)	(INT*2)	minute (*i.e.*, 35)
DATE(6)	(INT*2)	second (*i.e.*, 9)
DATE(7)	(INT*2)	millisec (*i.e.*, 189)
RATE	(INT*2)	digitizing rate in samples per second (*i.e.*, 100)
MAXTRA	(INT*2)	number of samples in the longest trace (*i.e.*, 6000)
NUMSTA	(INT*2)	number of seismic stations (*i.e.*, 16)
EVELAT	(REAL)	Event latitude (optional) (*i.e.*, 35.5000)
EVELON	(REAL)	Event longitude (optional) (*i.e.*, 120.4500)
DEPTH	(REAL)	Event depth in km (optional) (*i.e.*, 12.45)

RECORD 2

empty for further use

RECORD 3

empty for further use

RECORD 4

empty for further use

RECORD 5

empty for further use

RECORD 6

header for channel 1

IBLANK	(INT*2)	empty variable
IBLANK	(INT*2)	empty variable
STAT	(CHAR*4)	station name (*i.e.*, PARM)
GAIN	(INT*2)	station gain (optional)

Next 7 variables correspond to time of first sample in the trace.

DATE(1)	(INT*2)	year (*i.e.*, 1989)
DATE(2)	(INT*2)	month (*i.e.*, 3)
DATE(3)	(INT*2)	day (*i.e.*, 14)
DATE(4)	(INT*2)	hour (*i.e.*, 15)
DATE(5)	(INT*2)	minute (*i.e.*, 35)
DATE(6)	(INT*2)	second (*i.e.*, 9)
DATE(7)	(INT*2)	millisec (*i.e.*, 189)
BLOCK	(INT*2)	number of data blocks that have the seismic trace stored. BLOCK = points in trace/256. We use 256 because each point uses two words to be stored. (*i.e.*, 6000/256 = 23.43 = 24 blocks) One extra block to store the .43 part.

RECORD 7 data block for channel 1

DATA(L, L=1,256) first 256 samples for channel 1

RECORD 8 data block for channel 1

DATA(L, L=1,256) second 256 samples for channel 1

⋮

RECORD N (Where N=BLOCK) data block for channel 1

DATA(L, L=1,256) last samples for channel 1

RECORD N + 1 header for channel 2
same as header 1

RECORD N + 2 data block for channel 2

⋮

⋮ sequence repeat for every channel

⋮

RECORD M last data block for last channel

b) INSTRUMENT CORRECTION FILE

You can write comment lines before the data starts, by placing a letter C in the first column of the line.

LINE 1–10 Comment line. Start with a C in column one of each line.

LINE 11

ICURVE		(format I5)
	=1	do not multiply or divide the spectra by the frequency
	=2	divide the spectra by the frequency
	=3	multiply the spectra by the frequency

LINE 12

IPOINT	(format I5) number of points that define the instrument response curve (*i.e.*, 61)

LINE 13

AMP	(format 8f10.0) Logarithm of the amplitudes that describe the instrument response curve. There will be IPOINT values written 8 per line.

LINE 13 + IPOINT/8

FREQ	(format 8f10.0) frequencies corresponding to the amplitudes given before.

VII. TROUBLESHOOTING

THE CURSOR DOES NOT MOVE WHEN MOVING THE MOUSE. Probably the mouse is not installed properly. Try testing the mouse with programs provided with it.

THE CURSOR WAS MOVING BUT NOW YOU DO NOT SEE IT AT ALL. Probably the cursor got out of the screen. In some modes the cursor is very sensitive to small movements of the mouse. If you abruptly moved the mouse, the cursor is probably meters away from the physical area of the screen. It will be very hard to get back to the screen so better reboot the system and start again.

THE PLOT IS ON THE SCREEN BUT THERE ARE NO LABELS. The file SYSTEM16.FNT is not present in the same directory with the program.

AFTER YOU LOOKED FOR THE NEXT SEISMOGRAM THE SCREEN BECAME ILEGIBLE AND FUZZY. You reached the end of the file abruptly (sometimes it happens), type MODE CO80 (if you have an EGA system). You will not see the letters when you type them but after a <CR> the screen will be OK again.

WHEN YOU START THE PROGRAM THE COMPUTER ANSWERS: OUT OF ENVIRONMENT SPACE. Your computer does not have 640 kb of RAM memory, or you have run programs that left something in the memory. Check your autoexec.bat file, you may be loading in memory programs that take a lot of memory space . You can create a simple version of autoexec.bat; this will allow you to run the DEMO program.

ONLY THE UPPER HALF OF THE PLOT IS DISPLAYED. The program cannot recognize the graphics card installed in your system. To solve this problem you should type: PCEQ /E:4 if your graphics card is VGA (PS2 systems); PCEQ /H if your graphics card is a Hercules type. Note: a CGA graphics system will not work, because it has a small number of pixels to display the data.

VIII. PROGRAM PLOTPCEQ

The program PLOTPCEQ displays the seismic traces stored that are stored in the same format for PCEQ. The program asks how many traces you want to display at one page. The traces are scaled according to the number of traces per page. The more traces, the smaller their amplitude will be. If you want to make hard copies of what is displayed on the screen, you need to execute the program PRTSCRN before using PLOTPCEQ to enable the print screen command. Once the plot is on the screen and you have executed the PRTSCRN program, press in the Print screen key to send the plot to a printer. Figure 6 shows an example of this program.

REFERENCES – CHAPTER 11

Aki, K., and B. Chouet (1975). Origin of coda waves: source, attenuation and scattering effect, J. Geophys. Res. 80, 3322–3342.

Archuleta, R. P., E. Cranswick, C. Mueller, and P. Spudich (1982). Source parameters of the 1980 Mammoth Lakes, California, earthquake sequence, J. Geophys. Res. 87, 4595–4607.

Borcherdt, R. D., J. B. Fletcher, E. G. Jensen, G., Maxwell, J. R. Van Schaack, R. E. Warrick, E. Cranswick, M. J. S. Johnston, and McClearn, R., A general earthquake observation system (GEOS), Bull. Seismol. Soc. Am., 75, 1783–1823.

Dietel, C. and R. D. Borcherdt, eds., GEOS Data Summary for Active and Passive Seismic Experiments Conducted in Support of Northern Nevada Lithospheric Experiments, U.S. Geol. Survey Open–File Report 87–326, 320 pp.

Brune, J. (1971). Tectonic stress and the spectra of seismic shear waves from earthquakes, J. Geophys. Res. 75, 4997–5009 (correction, J. Geophys. Res. 76, 5002, 1972).

Lee, H. W. K, and C. Valdes (1985), HYPO71PC: a personal computer version of the HYPO71 earthquake locator program, U.S. Geol. Survey Open–File Report 85–749.

Lee, W. H. K., D. Tottingham, and J. Ellis (1988). Seismic data acquistion system based on a personal computer, U.S. Geol. Survey Open–File Report (in preparation).

Valdes, C. M., PCEQ: an interactive earthquake processing program for personal computers, IASPEI Seismological Software Library Volume I, edited by W. H. K. Lee (in press).

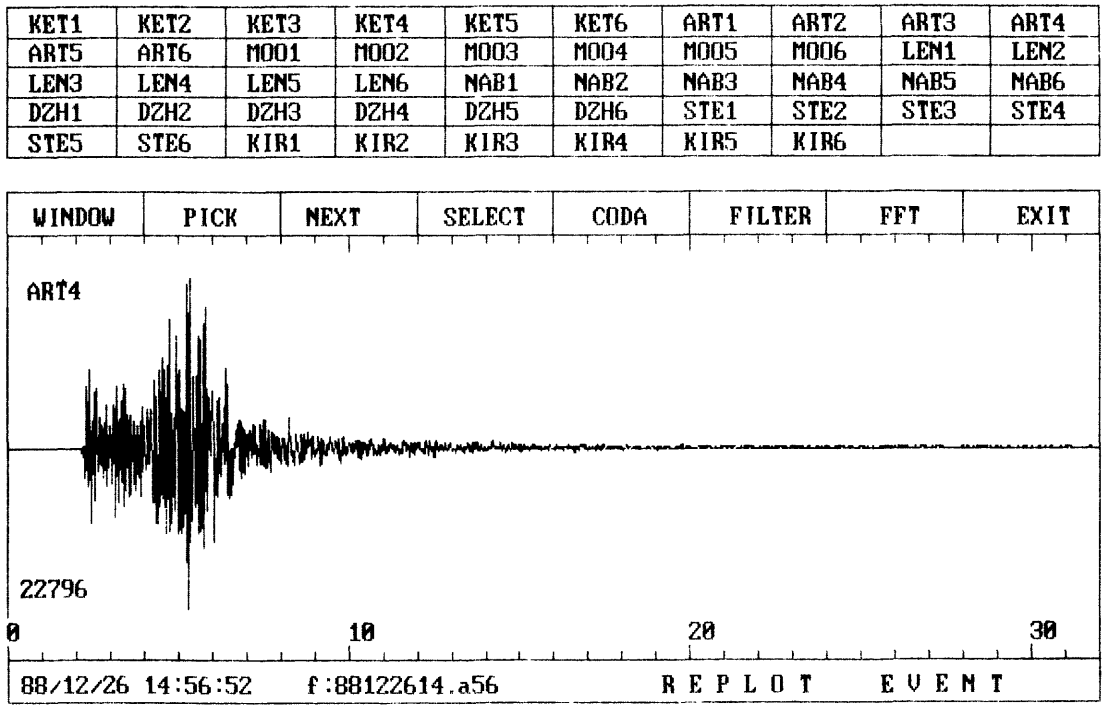

FIGURE 11.1. Example of PCEQ monitor display. The seismogram corresponds to an event on December 26, 1988, at 14:56 recorded by the vertical velocity transducer at station ART. Pressing the SELECT option displays the names of the available stations on the top of the figure. The program interactively allows the user to display different stations, filter the seismic records, select P- and S-wave arrivals, and measure spectral parameters.

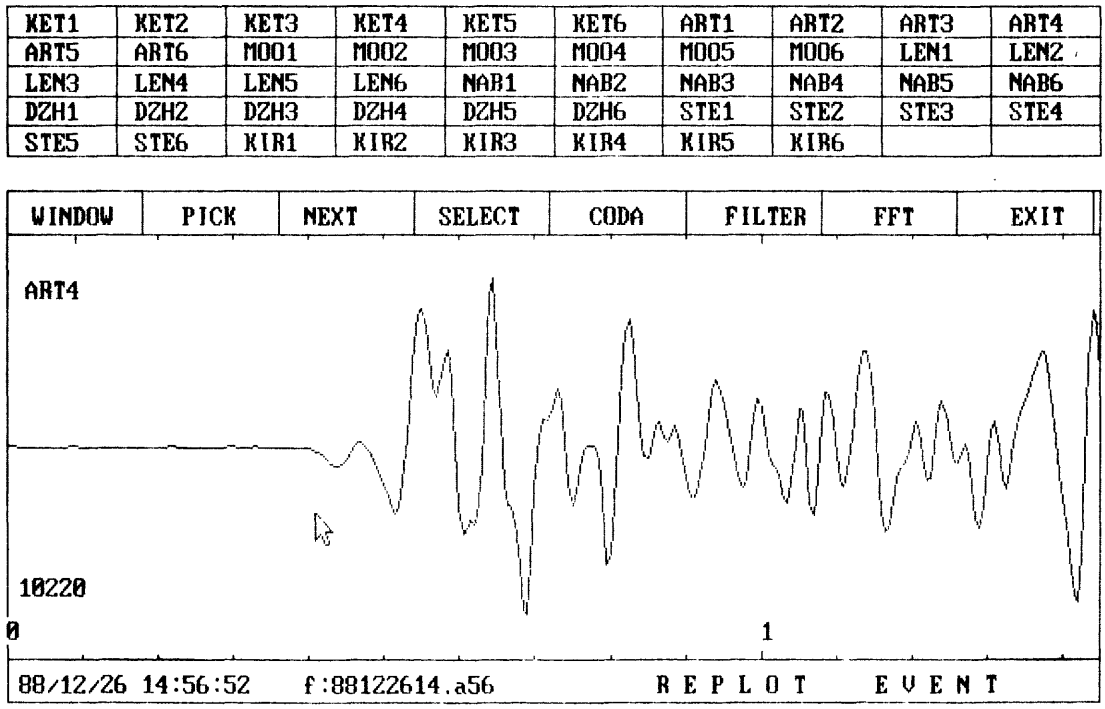

FIGURE 11.2. Enlarged display of 1 1/2 around the P-wave in Figure 1.

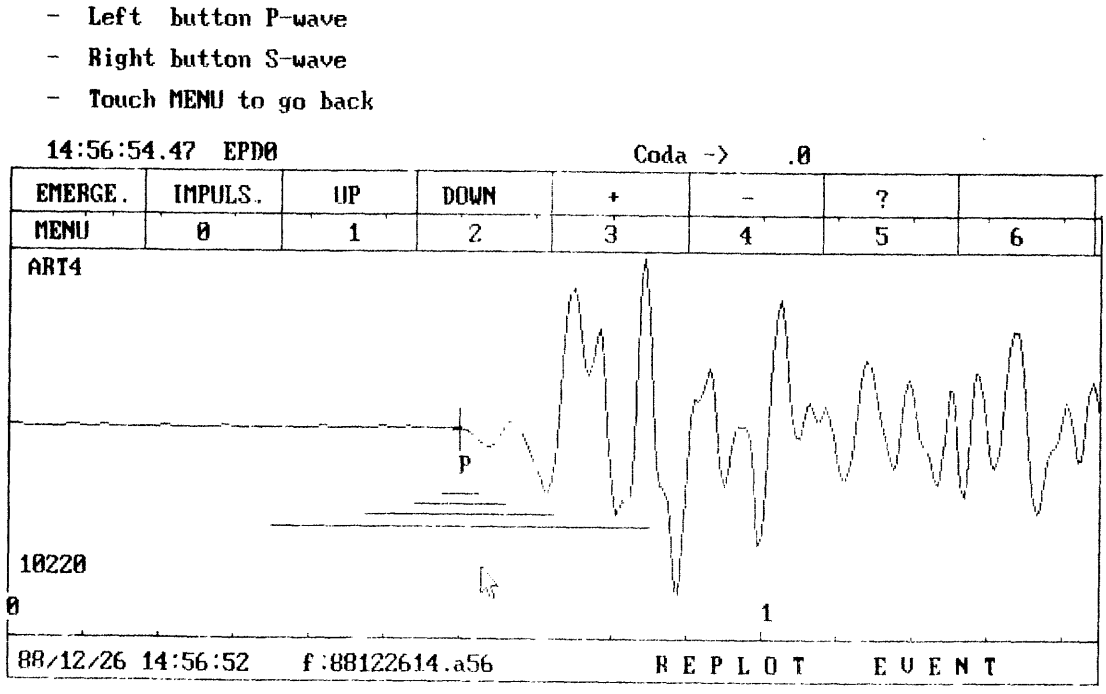

FIGURE 11.3. Same display as in Figure 2, but with the PICK option on. In this mode the P- and S-wave arrivals can be selected.

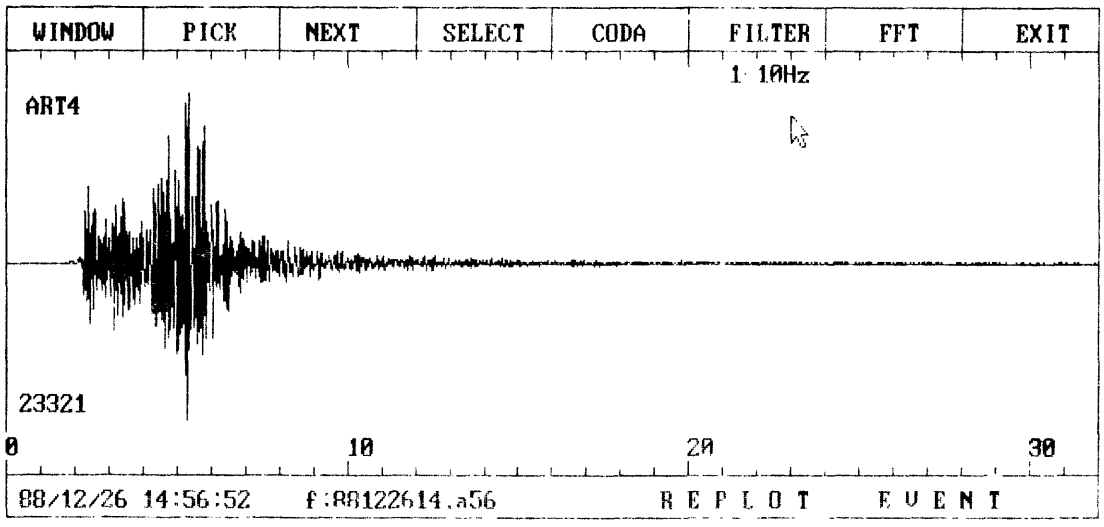

FIGURE 11.4. Seismogram from Figure 1 bandpass filtered between 5 and 10 Hz.

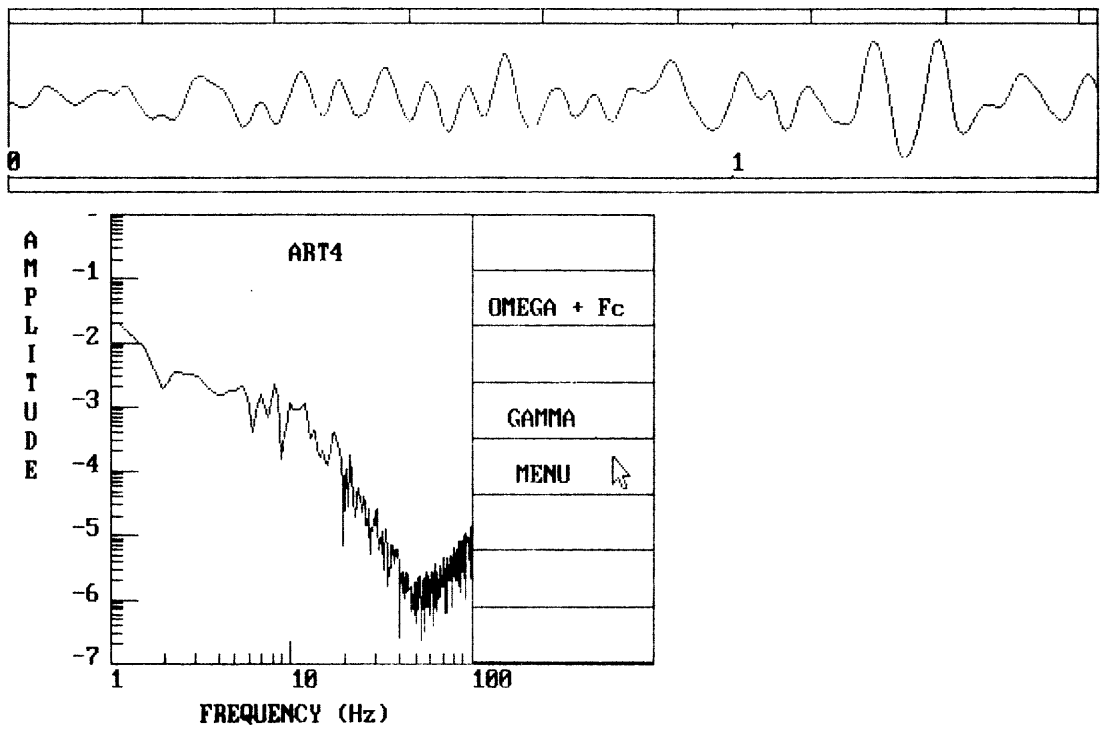

FIGURE 11.4. Spectral displacement of a window of 1 1/2 seconds around the S-wave in Figure 1. The program PCEQ allows the user to select the amplitude at the low frequency, the corner frequency, and the spectral rolloff decay at high frequencies.

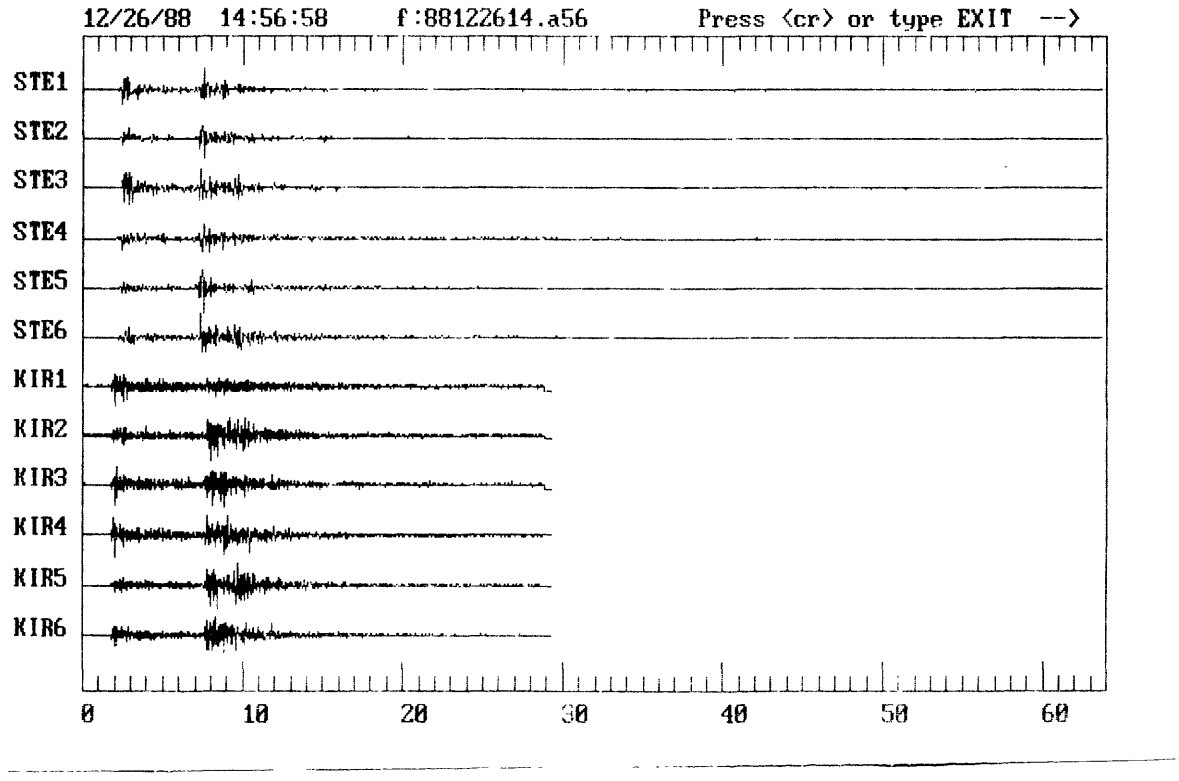

FIGURE 11.6. Example of program PLOTPCEQ display of 12 stations from the December 26, 1988 14:56 event.

ACKNOWLEDGMENTS FOR SEISMOLOGIC STUDIES

R. Borcherdt

The seismologic data set described herein could not have been acquired without the support of numerous individuals both in the Soviet Union and in the United States. The support and assistance of all those mentioned in Chapter 1 of this report is gratefully acknowledged.

In preparing for our departure to the Soviet Union numerous individuals contributed as a team to make our departure possible. In addition, to those in our Reston office, acknowledged in Chapter 1, T. Holzer and J. Van Schaack made every effort to help coordinate activities in Menlo Park. G. Maxwell, E. Cranswick, and M. Kennedy assembled the necessary hardware and software to deploy a self-contained computer system compatible with those of our host. P. Cuneo, A. Huerta, A. Margrave, and C. Ramseyer coordinated logistics. J. Sena, G. Sembera, C. Dietel, and T. Noce prepared recording equipment for shipment. K. Harms and K. Budding handled map acquisitions, W. Lee and C. Valdes assembled PC computer equipment and software, L. Baker and H. Bundock assisted in acquisition of computer hardware, and numerous other individuals helped on a variety of other tasks.

The Institute of Physics of the Earth in Moscow and Yerevan and the Geological Institute in Yerevan made the deployment of instrumentation possible. Without the assistance of numerous individuals from these Institutes and those at the seismic stations in Yerevan and Leninakan our task could not have been accomplished. In particular the efforts of U. I. Keilis–Borok, I. L. Nersesov, N. B. Shabalin, A. V. Nikolaev, S. Lander, and S. S. Arefiev of the Institutes of Physics of the Earth are appreciated. Support provided by members of the Geological Institute in Yerevan and at the seismic station in Yerevan were essential to the deployment of stations and the establishment of the computer center. In particular, those of S. V. Grigorian, E. Geodakian, A. Karpathian, M. Satian, L. Hakhverdian, G. Khachatrian, N. Sarkisian, and numerous others, were particularly helpful and

hospitable. Their support for the seismologists and technicians sent to continue operation of the stations has been invaluable and is appreciated immensely. In spite of difficult times, generous assistance also was provided by all of the people at each of our station locations. The assistance was provided with exceptional hospitality and warmth.

Upon return to the United States numerous people contributed to the maintenance of the stations and the playback and analysis of the data sets. In particular, M. Andrews, T. Noce and C. Mueller in maintaining the stations, G. Glassmoyer, E. Cranswick, G. Maxwell, and H. Bundock in data playback. C. Valdes and E. Cranswick made significant contributions to preparing the data and software for data analyses on a PC. Software developed by C. Mueller proved especially useful in computing spectra and spectral ratios for the analyses presented in Chapter 9. The efforts of all of those that have contributed to the establishment and maintenance of the National Strong Motion Data Center are appreciated, in particular, L. Baker, J. Fletcher, H. Bundock, and J. Vinton. Without the cooperation and assistance of our technical reports unit, in particular, R. Wood, J. Pinkerton, and N. Chapman, the timely publication of this report could not have been accomplished. C. Sullivan spent Saturdays and long hours in applying her excellent talents to the conversion of drafts into text via TEX. R. Eis and L. Hollis applied their conscientous talents to the production of figures on short notice.

APPENDIX A

Site Descriptions

C. Dietel and C. Langer

This Appendix provides a description of the recording sites used for seismological studies of aftershocks of the earthquakes of December 7, 1988 near Spitak, Armenia S.S.R.

GSS MEQ

Station GSS was deployed in an underground seismic vault at the Garni Seismic Station located 20 km east of Yerevan and 5 km north of the town of Garni in mountainous terrain. At the seismic station, a three-story structure is built on the side of a steep slope from which a north-south trending tunnel penetrates approximately 100 m into mountain bedrock. The seismic vault is located near the northern end of the tunnel roughly 20 m below the ground surface. Sensors were placed on a concrete seismic pier about 7 by 2 m in lateral dimension and 1 m above the floor surface. The pier is set in bedrock.

BYR

Station BYR was deployed in the basement of the south end of a two-story apartment building in the town of Byurakan, the site of the Byurakan Astrophysical Observatory, located 25 km northwest of Yerevan in semi-mountainous terrain. The velocity sensor was placed on a seismic pier about 1 by 1 m in lateral dimension and ½ m above the floor surface, and the accelometer was placed on the ground next to the pier.

KIR KIR

Station KIR was deployed beneath a two-story structure located 1–2 km south of Kirovakan in the mountainous terrain that rises from the Kirovakan valley. The two-story structure, used by the Yerevan Geological Institute, is built on the side of a steep slope and was damaged by the earthquake, showing cracks in the walls and stair wells. The GEOS and MEQ instruments and sensors were deployed in the crawl space beneath the structure, and sensors were buried in sandy soil.

KI2

Station KI2 was located in the same structure as KIR; however the GEOS unit and sensors at station KIR were moved. The new station was designated KI2 to indicate that the recorder was moved to the first floor of the building and the sensors were moved about 35 meters south of the KIR location. Station KI2 was equipped with extra batteries and solar panels to record data for an extended duration. The acclerometer was placed near the recorder on the first floor of the building. The velocity sensor was buried in sandy soil beneath the structure.

STE ARM

Station STE was deployed at a residence on the northwest edge of the town of Armanis located 25 km northwest of Kirovakan in mountainous terrain. Armanis lies on a broad basalt flow roughly 300 m higher in elevation than Stepanavan located 7 km to the east. About 100 m west of the station lies a 100-m deep canyon with steep walls of basalt. The GEOS and MEQ instruments were set on the back porch of a small stone and concrete house. The velocity sensors were buried in hard rocky soil about 15 m northwest of the residence, and the accelometer was buried near the porch. Bedrock is estimated to be only 0 to 1 m deep.

SSS

Station SSS was deployed in a seismic vault at the Stepanavan Seismic Station located 20 km northwest of Kirovakan on the southern edge of the Stepanavan valley in mountainous terrain. The seismic vault is built partially below the ground surface approximately 20 m north of the main seismic station structure. The velocity sensor was placed on a concrete seismic pier about 7 by 2 m in lateral dimension and 1 m above the surface floor.

MOO MOS

Station MOO was deployed beneath a two-story cinder-block school building in the small town of Moosailanski located 25 km north of Leninakan in an alluvial valley surrounded by mountainous terrain. The GEOS and HEQ instruments were placed in the crawl space beneath the structure by the northwest wall where the accelerometer was buried in hard sandy soil. The velocity sensor for the MEQ was buried about 10 m away

from the recorder and the GEOS velocity tranducers about 20 m southeast near the opposite wall in hard sandy soil. The school building was supported by several concrete pilings that were visible in the crawl space. The outside structure showed only minor damage, but the inside walls were cracked and severly damaged. The building was later demolished by the Army, necessitating movement of the recorder to site MO2.

MO2 MO2

The GEOS and MEQ instruments and sensors at station MO2 were taken from station MOO. The new station MO2 was deployed inside a 7 by 7 m stone, floorless structure approximately 200 m southwest of station MOO. The sensors were partially buried in hard rocky soil.

KET KET

Station KET was deployed beneath a residence in the town of Keti located 10 km north of Leninakan in lower foothills, possibly on a broad alluvial plane. The GEOS and MEQ instruments and sensors were deployed in a crawl space beneath a single-story wood and cinder-block structure. Surrounding cinder-block structures were heavily damaged. The sensors were placed near the instrument on hard silty soil, and the velocity sensor was partially buried. Depth to rock at this site is probably no more than 1–2 meters.

DZH DZH

Station DZH was deployed at a residence in the town of Dzhrashen located 5 km south of Spitak at the base of a small mountain range. The residence is built on the side of a steep slope, presumably on bedrock, and is relatively higher in elevation than most of Dzhrashen. Cracks were visible on the exterior walls of the house. The GEOS and MEQ instruments and sensors were deployed at the bottom of a garage pit in a cinder-block garage located about 10 m east of the house. Sensors were placed on hard compact soil at the bottom of the 2 by 5 m, 2-m deep pit. GEOS sensors were on concrete floor; MEQ sensor was in soil outside structure.

GOG

Station GOG was deployed at a residence in the town of Gorgaran located 5 km northwest of Spitak in mountainous terrain. The residence is built on the side of a slope,

presumably on bedrock, and was considerably damaged by the earthquake. The GEOS instrument and sensors were deployed in a small floorless storage room between the house and the garage. Sensors were placed on hard compact soil and were not buried.

SPT

Station SPT was deployed in a garage pit in southern Spitak, which is relatively higher in elevation than the rest of the city. Surrounding structures were heavily damaged and collapsed. The GEOS instrument and sensors were deployed in the 2 by 5 m, 2-m deep garage pit. Sensors were placed on the hard compact soil at the bottom of the pit and were not buried.

NAB

Station NAB was deployed at a residence in the town of Nalband located 10 km west of Spitak on the northern edge of a broad, east-west-trending alluvial valley. The small wood and cinder-block structures in Nalband were heavily damaged. The GEOS instrument and sensors were deployed in a small shed roughly 15 m south of the residence. Sensors were buried in clay soil.

ART ART

Station ART was deployed in a stone structure on the western edge of the town of Artagyukh located 15 km east of Leninakan on the western edge of a roughly north-south-trending alluvial valley. The stone structure, an old church now used for storage, is built on the base of a rocky moutain slope and is approximately 20 m above the average elevation of Artagyukh. The accelerometer was placed near the recorder on the stone foundation inside the structure. The velocity sensors were placed on rocky soil $\frac{1}{2}$ m outside the north wall of the structure and was coupled to the outside ground surface with snow and frozen water. GEOS and MEQ instruments were colocated at this site.

LEN

Station LEN was deployed in a seismic laboratory room in the basement of a two-story structure at the Geophysical Institute in the center of Leninakan. The structure was damaged by the earthquake. A north-south trending wall on the first floor of the structure was standing but detached and could easily be moved by gentile pushing. The sensors

were placed on a concrete pier about 7 by 2 m in lateral dimension and about 1 m above the floor surface. The site is probably underlain by a thick sequence of thin layers of clay, sand, and volcanic tuffs.

APP

Station APP was deployed in an underground vault at the Armenian nuclear power plant located southwest of Yerevan. The site is located in an area of flat topography thought to be underlain by interbedded layers of alluvium and volcanic tuff. The underground vault was used to house a wide variety of seismic instrumentation. The sensors were placed on a seismic pier about 2 by 2 m in lateral dimension and about 1 m above the floor surface.

YSS

Station YSS was deployed at the Yerevan Seismic Station located near the top of a hill in the western part of the city. The sensors were placed on a seismic pier about 4 by 4 m in lateral dimension and 1 m above the floor surface. The pier is located in the basement of a three-story cinder-block structure and is either near or in contact with rock.

SEV

Station SEV was deployed in a two-story residence near northwestern Lake Sevan located 60 km northeast of Yerevan. The residence is located on the grounds of a biological gardens 1–2 km west of the lake on relatively flat topography about 1 km from the steeper slopes associated with hills in the area. The site is probably underlain by several meters of alluvium. The sensors were placed on a concrete floor in a vacant room located roughly in the center of the structure near the structure's western wall.

GIB GIB

Station GIB was deployed on the grounds of the Geological Institute base in a small village located approximately 25 km southeast of Kirovakan in mountainous terrain. Sensors were placed on a concrete floor of an empty barn and were not buried. GEOS and MEQ instruments were colocated at this site occupied the evening of December 21, 1988.

SCH

Station SCH was deployed at the site of a collapsed school building in the town of Dzhrashen located 5 km south of Spitak in an alluvial valley surrounded by mountainous terrain. The GEOS instrument and sensors were placed beneath fallen concrete slabs, and the sensors were placed on compact silty soil.

KAT

Station KAT was occupied by an MEQ located in basement of private home in the village of Katnakhpur. Seismometer was located in rocky soil on side of hill next to house.

ALI

Station ALI was occupied by an MEQ located on the dirt floor of an abandoned house in the deserted village of Alivar. The sensor was buried in soil. The site was located near rock near the bottom of a north-south trending canyon.

SIP

Station SIP was occupied by an MEQ located in house under construction in the village of Sipan. The sensor was buried in soil. The site was located near alluvial fan in a broad north-south trending valley.

PIN

Station PIN was occupied by an MEQ located in a shed next to Los Pinos resort for children, south of Stepanavan. Velocity sensor was buried in soil. The site was located on a hill about 200 meters above the valley floor.

BAZ

Station BAZ was occupied by an MEQ located in a root cellar in the basement of an abandoned house in the village of Bazum. Sensor was buried in soil. The site was about 150 meters up the flank of a north-south trending ridge.

ARE

Station ARE was occupied by an MEQ located in a root cellar under a collapsed building in the village of Arevashok. The sensor was buried in soil. The site was located in an alluvial valley about 5 km north of Spitak.

APPENDIX B

Event and Station Listing for Digital Data

G. Glassmoyer

This Appendix contains a listing of GEOS recordings indicated by start-of-record time and recording station.

Table B.1 Complete listing of digital seismograms collected through 7 February 1989.

	APP	ART	BYR	DZH	GIB	GOG	GSS	KET	KIR	KI2	LEN	MOO	MO2	NAB	SCH	SEV	SPT	SSS	STE	YSS
3561354T							T													
3561355P							P													
3561358M							M													
3561417O	O																			
3561418K	K																			
3561423H	H																			
3561424Q	Q																			
3561633P							P													
3561828C							C													
3562045E							E													
3562139R							R													
3562212F							F													
3562308O							O													
3570018H							H													
3570035J							J													
3570123K							K													
3570220H							H													
3570235I							I													
3570501A							A													
3570555D																				D
3570555T																				T
3570557J																				J
3570806F							F													
3571012L							L													
3571025S							S													
3571137S							S													
3571158I							J													I
3571224M							M													
3571253J							J													
3571347H							H													
3571354N							N													
3571514B							B													
3571542B							B													
3571558Q					Q															
3571559M					M															
3571601R					R															
3571604R					E															
3571606T					T															
3571701F					F															
3571708P							P													
3571719L					L															
3571732E					E		H													
3571813E					E		H													
3571815J					J															
3571817R							R													
3571819H					H		K													
3571831M					M		O													
3571848J					J															
3571919R							R													
3571928J					J		K													K
3571932L					L															
3571937Q					Q		S													
3571938G					G															
3571950G					G															
3572007D							D													
3572014S							S													
3572024I					I		M													
3572102C					C		F													
3572112B					B															
3572123S					S		B													
3572256T					T															
3572305D																				D
3572334F					F															
3580013L																				L
3580132G					G															
3580211R					R															
3580349P					P															
3580742Q																				Q
3581037M																			M	
3581038H																			H	
3581042K																			K	
3581046T																			T	

Table B.1 (continued)

	APP	ART	BYR	DZH	GIB	GOG	GSS	KET	KIR	KI2	LEN	MOO	MO2	NAB	SCH	SEV	SPT	SSS	STE	YSS
3581056S																			S	
3581119F																				F
3581129G																			G	
3581134S																	S			
3581135O																	O			
3581139H																	H			
3581141H												H								
3581142D												D								
3581149R												R								
3581153Q																			Q	
3581155R												R							T	
3581212F																			K	
3581217I																			I	
3581222D																			D	
3581228B												B								
3581231E																			E	
3581238D												D								
3581258N																			N	
3581300P																	P		P	
3581309F															F				M	
3581310A															A					
3581311A															A					
3581312P																			P	
3581315D																			D	
3581317D																			D	
3581325T																			T	
3581406B								H											B	
3581407D								D												
3581408P								P												
3581415S																			S	
3581421P																			P	
3581430H																			H	
3581448S														S						
3581449N														O					N	
3581450M																			M	
3581452M														M						
3581453A								B				A							C	
3581459C																			C	
3581501T														T						
3581511C																			C	
3581523N																			N	
3581527S																			S	
3581537G											G									
3581538C											C									
3581541J																			J	
3581542C																			C	
3581546N											N									
3581600Q																			Q	
3581607M																			M	
3581611P								P											P	
3581616K								K				K							L	
3581623F																			F	
3581623T																			T	
3581624L												L								
3581633O																			O	
3581635M																			M	
3581637A																			A	
3581637T																			T	
3581641F																			F	
3581643M								M			N	M					N		N	
3581657S								T				T		S			T		T	
3581714S																			S	
3581716Q																			Q	
3581737J								K				J							K	
3581746A																			A	
3581747N								O				N							P	
3581748C																	C			
3581801L								M				L								
3581803S																			S	
3581808D								D											D	
3581820C																			C	
3581824B																	B		D	
3581903H																			H	

Table B.1 (continued)

	APP	ART	BYR	DZH	GIB	GOG	GSS	KET	KIR	KI2	LEN	MOO	MO2	NAB	SCH	SEV	SPT	SSS	STE	YSS
3581906D																			D	
3581917D																			D	
3581934L																			L	
3581935T																			T	
3581942L																	L			
3581948P									P											
3581949L									L											
3581951T									T											
3581953O																			O	
3581958J								K				J		K					L	
3582000H																	H			
3582033E												E								
3582045G														G						
3582056T												T								
3582129M																	M			
3582134N																				N
3582141I																	I			
3582151K												K								
3582204D																	D			
3582207N														N						
3582211T																	F			
3582216L																	L			
3582218O								P						O						
3582220C																	C			
3582222K																	K			
3582223B																	B			
3582226F																	F			
3582228G																	G			
3582229H																	H			
3582231Q																	Q			
3582232E																	E			
3582232R																	R			
3582234D																	D			
3582235M																	M			
3582236B																	B			
3582242R														R						
3582246A								E				D		D			A			
3582251T																	T			
3582252K																	K			
3582254M												M								
3582257M																	M			
3582259K																	K			
3582305N																	N			
3582309O																	O			
3582311B																				B
3582312B																	B			
3582322R																	R			
3582327E																	E			
3582327M																	M			
3582331L																	L			
3582333G									L								L			
3582333Q																	Q			
3582334O																	O			
3582335I																	I			
3582336G																	G			
3582337A																	A			
3582337Q																	Q			
3582339Q																	Q			
3582341D								G	D											
3582341M																	M			
3582344K																	K			
3582345Q																	Q			
3582349I																	I			
3582352D																	D			
3582355H																	H			
3582357B																	B			
3582359D																	D			
3590000G																	G			
3590002S																	S			
3590008L																	L			
3590027G																	G			
3590028K																	P			
3590029L									N								L			

Table B.1 (continued)

	APP	ART	BYR	DZH	GIB	GOG	GSS	KET	KIR	KI2	LEN	MOO	MO2	NAB	SCH	SEV	SPT	SSS	STE	YSS
3590031P																	P			
3590033Q																				Q
3590034G												G								
3590039M																	M			
3590042E																	E			
3590046S																	S			
3590047T																	T			
3590138O								O				O								
3590147E								F				E								
3590205K												K								
3590222S												S								
3590238D												D								
3590246R									R											
3590341J								J												
3590344B								C				B								
3590527A								C	A											D
3590548L								N	L			M								
3590549S									S											
3590550K								K												
3590552C												C								
3590558A								C				A								
3590642D									D											
3590652D								E				D								
3590659L												L								
3590700F									F											
3590731L												L								
3590836A								A				A								
3590957H									H											
3591012Q									Q											
3591024T								T												
3591033Q									Q											
3591043S								A	S											
3591111B								B												
3591142G								I	G			H								
3591145D												D								
3591156G												G								
3591233C		C																		
3591240F		F																		
3591329C														C						
3591330C														C						
3591331A								A												
3591331K		K																		
3591332K														K						
3591408B									B											
3591411H		I						J				H								
3591411S									S											
3591414Q		Q						R	Q			Q		Q						
3591421E																	E			
3591429L		M						N				L								
3591448E		F												E						
3591457D		D										D								
3591505J									J											
3591544N									N											
3591602R		R						T				S		R						
3591617H									H											
3591625A									A											
3591631C												C								
3591647D		D						F				D								
3591702H												H								
3591708M		M						O	M			N		M						
3591717K		K																		
3591719A		A																		
3591721T									T											
3591732B									B											
3591748F		F																		
3591756A								B				A								
3591812H																	H			
3591835K												K								
3591837S												S								
3591848O												O								
3591856H												H								
3591954R												R								
3592008D		D						E												

Table B.1 (continued)

	APP	ART	BYR	DZH	GIB	GOG	GSS	KET	KIR	KI2	LEN	MOO	MO2	NAB	SCH	SEV	SPT	SSS	STE	YSS
3592012K									K											
3592019F												F								
3592057M									M											
3592059H																				H
3592110I		I						K				I								
3592145F																				F
3592150I									I											
3592229D																	D			
3592300O		O						Q												
3592309A								E	A											
3592346L									L											
3592353G								G												
3592355Q		R						S				Q								
3600012I		I						L												
3600017M		M						O												
3600036C		C						E												
3600107C								C												
3600111P		Q						R				P								
3600118T		A						C									T			
3600122S												S								
3600123Q								Q												
3600139F												F								
3600145F		F																		
3600152I		J															I			
3600221D																	D			
3600250M												M								
3600258F		F										F								
3600315Q		Q																		
3600327G		G																		
3600333S		S																		
3600347O		O																		
3600357B									B											
3600408J		J																		
3600444D									D											
3600452E												E								
3600523A								A												
3600524O		O																		
3600527C		D															C			
3600537H								H												
3600544C		C																		
3600555Q												Q								
3600558T												T								
3600625D									D											
3600631G									G											
3600643F		F																		
3600648C		C						E	E			C								
3600707J									J											
3600748E									E											
3600843I								I												
3600856I									I											
3600918T									T											
3600928F								F												
3600936R																			R	
3601002B								B												
3601023E												E								
3601029H								H												
3601056H												H								
3601101R									R											
3601114A								C				A							C	
3601145K																			K	
3601146E												E								
3601203S																			S	
3601226I								I												
3601249R								T	R			T							A	
3601308E									E											
3601309D									D											
3601319O																				O
3601323E								F				E							G	
3601333R											R									
3601335I																			I	
3601418N				N																
3601419J				J																
3601421P									P											

Table B.1 (continued)

	APP	ART	BYR	DZH	GIB	GOG	GSS	KET	KIR	KI2	LEN	MOO	MO2	NAB	SCH	SEV	SPT	SSS	STE	YSS
3601427B				B																
3601437B									B											
3601442Q				Q																
3601514B																			B	
3601518D									D											
3601539G									G										G	
3601553Q												Q							R	
3601614M												M								
3601623O									O											
3601632C																			C	
3601637T									T											
3601653M																			M	
3601706L												L								
3601748A									A										A	
3601749P												P							P	
3601801B																			B	
3601801P														P						
3601808H									H											
3601819R																			R	
3601829C																				C
3601904F												F								
3601934J								J				J								
3601936G																			G	
3601947G								H				G							H	
3602045B												B								
3602056O																			O	
3602057T				T										T					A	
3602100T																			T	
3602122R				R					R										S	
3602128M									M										N	
3602153J									J										K	
3602155E																			E	
3602156D																				D
3602204O								Q						P					O	
3602207N								N												
3602229F																				F
3602233Q																				Q
3602241J				J															K	
3602307I								K	I										J	
3602348H																			H	
3610144S								S											T	
3610150L								M						L						
3610254D														D						
3610258A								A				A								
3610334T				A					T										B	
3610342B												B								
3610347A												A								
3610356F																			F	
3610407K												K								
3610420Q																			Q	
3610531A								A											A	
3610542F																				F
3610601E																				E
3610619G									G											
3610649I								I											I	
3610725I				I																
3610750K								K												
3610752E				E															E	
3610827M				N					M										N	
3610830H														H						
3610845G																				G
3610908J									J										J	
3610919P									P											
3610924F									F											
3610937D									D											
3611011G		G																		
3611023L		L																		
3611025D									D										F	
3611030Q		Q		R										R						
3611035J		J						J											K	
3611048B									B											
3611059S								S												
3611108T											T									

Table B.1 (continued)

	APP	ART	BYR	DZH	GIB	GOG	GSS	KET	KIR	KI2	LEN	MOO	MO2	NAB	SCH	SEV	SPT	SSS	STE	YSS
3611111I											I									
3611112O											O									
3611117P											C									
3611118N											N									
3611128H									H											
3611134P									P										Q	
3611145R																			R	
3611202T											T									
3611205D		D						D											E	
3611212B																			B	
3611233C											C									
3611237C											C									
3611257F									F					J						
3611300K		K																		
3611307K												K								
3611311B		B		B										B					C	
3611311I		I		I										I					J	
3611326K																			K	
3611412P								P	A					P						
3611437J									J											
3611443B		C		B					C					B					B	
3611445H									H										J	
3611451J		J		J					J					J					J	
3611456R		R		S				R	T		S	R		S					S	
3611501M		M																		
3611504K									K											
3611543M		N		N										M					N	
3611554H									H										I	
3611614D		E												D					E	
3611706B																			B	
3611737L												L								
3611756C		C		C										C					C	
3611817M									M											
3611830C		D		C										C					D	
3611841F		G						F				F		G					H	
3611857A				A										A					A	
3612002P												P							Q	
3612037O																			O	
3612100N														N						
3612129R									R											
3612141I																			I	
3612156D									D											
3612211I				J					I											
3612227T									T											
3612242N		N																		
3612249F														F						
3612302H														H						
3612308S									S											
3612321L														L						
3612350H				H					H					H						
3620004C									C											
3620005L									L											
3620006H														H						
3620015B				C					C					B						
3620018A														A						
3620057I				K				I												
3620104N											O	N								
3620108F														F						
3620149R														R						
3620155G												G								
3620219E											E									
3620223G														G						
3620238P														P						
3620309Q									Q											
3620349O														O						
3620414A				A					A											
3620433T									T											
3620439O												O		O						
3620444G														G						
3620446N												N								
3620504F				F				F			G	F		F						
3620510R				S					R					S						
3620513C									C											

Table B.1 (continued)

	APP	ART	BYR	DZH	GIB	GOG	GSS	KET	KIR	KI2	LEN	MOO	MO2	NAB	SCH	SEV	SPT	SSS	STE	YSS
3620514T												T								
3620516S									S											
3620547D												D								
3620554L				L																
3620556D								D												
3620614T														T						
3620634A				B					A											
3620652E	E																			
3620701J	J																			
3620714D									D											
3620734D									D											
3620742E																				M
3620745F				G				F	H		G	G		F						
3620751K																				R
3620818C														C						
3620847O							O													
3620851B							B													
3620926K				L			O		K											
3621115I				J			O	I			J	J		J						
3621117H				I				H			I	H		H						
3621129T				A							T	T								
3621136T				T																
3621209G				G					G											
3621213F							F													
3621230E				F				E	H		F	F		F						
3621246F									F											
3621312P								P												
3621317B				B					B					B						
3621323E				E																
3621324F									F											
3621330A									A											
3621408A												A								
3621417O				O					O											
3621446Q														Q						
3621619K														K						
3621649E				F							F	E		F						
3621710O									O											
3621720M							M													
3621741M									M											
3621802P				Q			A	P	Q		Q	Q		P						
3621809D									D											
3621836L									L											
3621839O				O																
3621840J														J						
3621849D				D										D						
3621943L												L								
3621948P				P										P						
3621955R				S			D	S						R						
3621956Q				Q										Q						
3622031L								L			M	M		M						
3622044N				P			A	N			O	O		P						
3622116K														K						
3622125H														H						
3622152R														R						
3622157L												L								
3622217G												H		G						
3622235I												I								
3622237E								E				F								
3622240J									J											
3622251F														F						
3622253T												T								
3622301S														S						
3622310A											B	A		B						
3622337E												E								
3630158Q									Q											
3630255E									E											
3630312B				B																
3630330D												D								
3630346A				C			H	A	E		C	B								
3630352F								F				G								
3630353J								J												
3630428P												P								
3630438B												B								

Table B.1 (continued)

	APP	ART	BYR	DZH	GIB	GOG	GSS	KET	KIR	KI2	LEN	MOO	MO2	NAB	SCH	SEV	SPT	SSS	STE	YSS
3630516S									S											
3630554L									L											
3630601N				O			R	O	A											
3630611H												H								
3630624D				F				D				E								
3630637D								D												
3630709F				F																
3630736P									P											
3630848D							G		G											
3630851L									L											
3630855H												H								
3630906J								J												
3630907D							H		D											
3630908H				H																
3630909E		E																		
3630910A		A																		
3630912I				J					I											
3630916J							M		J											
3630923B							B													
3630925I							I													
3630958A				A																
3631014K								K												
3631018T									T											
3631051E		E																		
3631115D								D												
3631115T								T												
3631121Q				Q																
3631141C																			C	
3631200J									J											
3631203Q								B			Q									
3631241S												S								
3631242O												O								
3631255S								D			S									
3631257F									F										G	
3631300N									N											
3631307P				P					P										Q	
3631326H									H											
3631337B									B										C	
3631342J																			J	
3631426B											B									
3631428S												S								
3631436D									D											
3631452E		E																		
3631459H		H																		
3631501F		F																		
3631514O											O									
3631515K											K									
3631517A											A									
3631524P									P											
3631542H				H				I											H	
3631558Q				Q			A	S	Q										R	
3631625G												G								
3631658Q									Q										R	
3631701B									B										C	
3631715Q				Q								R							R	
3631751D																			D	
3631801H												H							I	
3631803T												T								
3631807R				R															S	
3631821P									P										Q	
3631826R												R								
3631859S												S								
3631904L												L								
3631920S												S							T	
3631924H									H											
3631926H								I				H							J	
3631928L							L													
3631953P																			P	
3631955T							D		T										A	
3632026H																			H	
3632049S												S								
3632147E												E								
3632159C																			C	

Table B.1 (continued)

	APP	ART	BYR	DZH	GIB	GOG	GSS	KET	KIR	KI2	LEN	MOO	MO2	NAB	SCH	SEV	SPT	SSS	STE	YSS
3632233Q																			Q	
3632236S												S								
3632240A												A								
3632246T				A			F	T			A	T							A	
3632249M				N				M				M							N	
3632309J				J					J										K	
3632311Q								R				Q								
3632345D																			D	
3632348R								R				R								
3640000R				S				R				R							S	
3640021O												O								
3640023E				E			I	G	E			G							F	
3640031K								K												
3640038K												K								
3640042M									M										N	
3640045L				M				M			M	L							M	
3640054Q																			Q	
3640120L																			L	
3640133G																			G	
3640159P												P								
3640224B																			B	
3640232F												F								
3640243Q									Q											
3640247D							D													
3640249I									I											
3640257R				R			C	S	R			S							R	
3640413D												D								
3640444Q								Q												
3640625E				E																
3640634B									B											
3640658N				N																
3640703O									O											
3640711B												B								
3640803T				T				T												
3640948A												A								
3640949R				R															T	
3640952J				O				J				N								
3641008O				O			T	P	O										O	
3641017H																			H	
3641036P								P				P								
3641053D								D												
3641123B				B															B	
3641128G							G													
3641200G								N			G									
3641242A								A												
3641302M				M															M	
3641312O													O							
3641313K													K							
3641316E													E							
3641319E													E							
3641324C								C												
3641344J				J															J	
3641402B				C				C					B						D	
3641403J													J							
3641407J											J									
3641407R								R												
3641414I													I							
3641425S													S							
3641432D				D			I	E	E				E						E	
3641440L									L										N	
3641448O				O				P	O				P						O	
3641459F									F											
3641525A													A							
3641532K		K																		
3641538C		C																		
3641538N		S																		
3641541N		N																	P	
3641543C		C																		
3641548H				I				J	H										I	
3641718G													G							
3641718R													R							
3641743J				J				K											J	
3641825E																			E	

Table B.1 (continued)

	APP	ART	BYR	DZH	GIB	GOG	GSS	KET	KIR	KI2	LEN	MOO	MO2	NAB	SCH	SEV	SPT	SSS	STE	YSS
3641843Q				R			C	Q	S		R		Q						S	
3641847G													G							
3641851T													T							
3641913E													E							
3641915S				T									S							
3642002M													M							
3642026K													K						K	
3642135H													H							
3642200G													G							
3642203S													S							
3642210A				A																
3642220F													F							
3642252K													K							
3642311E				F				E			F		E						G	
3650004N													N							
3650016L													L						M	
3650022D								D			D		D						D	
3650049C													C							
3650134N													N							
3650139I								J					I						J	
3650146F													F						F	
3650147N													N							
3650154E													E							
3650206H													H							
3650230I				I									J						J	
3650249L				L				L			L								L	
3650253G																			G	
3650320F																			F	
3650338B																			B	
3650342J				J															J	
3650345F																			F	
3650502M				M			Q	N	M											
3650523L				L					L											
3650535D				D																
3650649D									D											
3650741I								P			I									
3650746F	F																			
3650748G	G																			
3650749E	E																			
3650821A								H			A									
3650822M				M																
3650933C		C																		
3650938L								L												
3650954R								E												
3651008Q							Q													
3651020M		M																		
3651053G								G												
3651101O								O												
3651132B								B												
3651135K								K												
3651146G		G																		
3651151H								H												
3651151Q		Q		R																
3651200A						A														
3651200Q						Q														
3651202A						A														
3651205M						M														
3651208Q								Q												
3651215P								P												
3651237K								K												
3651239K							K													
3651244D							D													
3651247R		R		R		R	C	S	S											
3651252G								G												
3651259B		B																		
3651259T								T												
3651307K								K												
3651308B								B												
3651322R		R																		
3651328Q		Q		Q		Q	C	Q	S		Q									
3651330G		H		H		H		G	I		H									
3651331E		E		E		E		E	F		E									
3651339E								E												

Table B.1 (continued)

	APP	ART	BYR	DZH	GIB	GOG	GSS	KET	KIR	KI2	LEN	MOO	MO2	NAB	SCH	SEV	SPT	SSS	STE	YSS
3651400Q			Q																	
3651404B		B		B				B												
3651407D		E						D												
3651423D		D		D																
3651441I		I																		
3651456G											G									
3651507N		N																		
3651535O		O																		
3651538Q				Q																
3651552H		H																		
3651614F		F																		
3651659F				F																
3651907M		M		M		M														
3651917K		K		K		K		L												
3652035T									T											
3652130I		I																		
3652138T		T																		
3652322J									J											
3652330B				C		B		C												
3660221P									P											
3660226I						I														
3660249E				E		E														
3660407D			G	D		D	J	D	F		D									
3660410M				N				M												
3660426S				S		S			A											
3660428D								D												
3660448M						M														
3660459A				A				A												
3660525S				S																
3660535P								P												
3660542E						E														
3660651M				M		M		N												
3660702N									Q											
3660811Q				R		Q		Q												
3660827N						N														
3660829O				O																
3660930S				S																
3661008F													F							
3661008R						R														
3661011P				P																
3661016D				D																
3661027J													J							
3661111Q																			Q	
3661113D																			D	
3661135I											I									
3661136D											D									
3661136T											T									
3661138G											G									
3661148K				K																
3661159N				N															O	
3661220E								E												
3661234M				N									M						O	
3661238A																			A	
3661253T								T												
3661405R				R															R	
3661411L		L																		
3661429Q																			Q	
3661432R		R		S				R					R						S	
3661535G		H		G		G		I											G	
3661546D																			D	
3661548O																			O	
3661554L		M		L		L		M											L	
3661555Q						Q														
3661616O		O																		
3661625J																			J	
3661626H																			H	
3661633G		H		G		G		H											G	
3661710R		S		R		R		T											S	
3661713D		D																		
3661722M		N		M		M		O											N	
3661728S		S																		
3661740I																			I	
3661813J		J																		

Table B.1 (continued)

	APP	ART	BYR	DZH	GIB	GOG	GSS	KET	KIR	KI2	LEN	MOO	MO2	NAB	SCH	SEV	SPT	SSS	STE	YSS
3661910J		K																	J	
3661924A		A						A					A							
3661931D		D											D							
3661945R		S		R																
3662033A																			A	
3662051C													C							
3662055B																			B	
3662142S																			S	
3662144P		Q						P					P						R	
3662154J		J																		
3662218G		G																		
3662223T		T											T						T	
3662233C		C																		
3662239K								K					K							
3662258Q													Q							
3662302M													M							
3662307K																			K	
3662343B								B					B							
0010010I		J		I				J											I	
0010020T																			T	
0010024L								L												
0010054J				J																
0010058P													P							
0010156T						T														
0010158F								G					F						H	
0010202S								T					S							
0010204B								C					B							
0010300F													F							
0010421F																			F	
0010426Q								Q												
0010433R													R							
0010434Q								Q												
0010444T													T							
0010500S				S		S		A											T	
0010514Q													Q							
0010619G						G													H	
0010631K				K															K	
0010635D				D															E	
0010728P								P												
0010901F									F											
0010912J				J					J										K	
0010917P				P																
0010923N						N														
0010924D						D														
0010943G						G														
0010948C													C						D	
0011001A				A																
0011012A								A												
0011030N								N												
0011100J		J																		
0011123D										D										
0011123S										S										
0011200L						L														
0011241H										H									I	
0011251N																			N	
0011301A										A										
0011302D				D						E									E	
0011320P										P									R	
0011322O		O																	O	
0011351M																			M	
0011354Q				Q																
0011439P		P																		
0011546D		D																		
0011647P																			P	
0011707B		C		C		B		D											C	
0011728M		M						N					M						N	
0011730N																			N	
0011802B																			B	
0011802O						O													P	
0011827O		O																		
0011848L		L																		
0011903T		T																	T	
0011916F										F									H	

Table B.1 (continued)

	APP	ART	BYR	DZH	GIB	GOG	GSS	KET	KIR	KI2	LEN	MOO	MO2	NAB	SCH	SEV	SPT	SSS	STE	YSS
0011924C						C														
0011936Q		Q																	R	
0011946K		K																		
0012029K																			K	
0012043N						N													O	
0012149B													B							
0012151B		B																		
0012219J		J																	J	
0012233O		O																		
0012252D				D																
0012255A													A							
0012259M		O		N		N		O		M			O						N	
0012323M		M																		
0012324P				P																
0012331B		C		B				D		B			D						C	
0012335G													G							
0012338S		S																		
0012350R		R																		
0020015T								T					T							
0020024I		I						I											I	
0020027Q																			Q	
0020029K								K												
0020030B																			B	
0020036L						L														
0020042E		E		F				E												
0020142F						F														
0020251T		T																		
0020304C		C		C		C		C												
0020308H		H						H												
0020350E				F						E										
0020444M				O						M										
0020602K						K														
0020712B						B														
0020737H				H																
0020805G				H		G														
0020813F								F												
0020900D						D														
0020910O													O							
0020925A								A												
0020951R													R							
0021012P				Q		P														
0021120E													E							
0021152H				H																
0021217F								F												
0021304L																L				
0021305H																H				
0021315E																E				
0021451H						H														
0021459J				J		J		J					J							
0021517M						M														
0021519A													A							
0021539O				O		O														
0021540R													R							
0021548K								K					K							
0021707D						D														
0021811D				D				D					D							
0021813L				L		L		L					L							
0021815G													G							
0021818H													H							
0021819S													S							
0021824J								K					J							
0021839H													H							
0021857O						O		P												
0021910E													E							
0021912S													S							
0021934E													E							
0021951N													N							
0022023H													H							
0022037O													O							
0022038S				S																
0022113T						T														
0022116T													T							
0022120P													P							

Table B.1 (continued)

	APP	ART	BYR	DZH	GIB	GOG	GSS	KET	KIR	KI2	LEN	MOO	MO2	NAB	SCH	SEV	SPT	SSS	STE	YSS
0022122O													O							
0022234N				N		N														
0022239N													N							
0022251B								C					B							
0022309G				H				G					G							
0022321S													S							
0022346M						M														
0022356A													A							
0030021S								T					S							
0030041K													K							
0030117L																L				
0030120Q						Q														
0030126O													O							
0030201P													P							
0030238R						R														
0030322O													O							
0030334F						F														
0030346O																O				
0030445J								J												
0030452L								L												
0030512F								F												
0030525A						A							A							
0030531M				N		N		N					M							
0030615H										H										
0030616D										D										
0030623A				B						A										
0030629S										S										
0030630M										M										
0030720I				J		J				I										
0030747F				F																
0030809N				N																
0030819S				S		S		T		S			T							
0030821O						O														
0030827I				J									I							
0030836G						G														
0030918R		R																		
0030919G						G														
0030927A		A		B				B												
0030957S																S				
0031009J				J																
0031052S																S				
0031118K																		K		
0031119H																		H		
0031122F																		F		
0031129O																		O		
0031300G																G				
0031328F		G		G		F														
0031335C				E				D					C							
0031348P		Q		P		P		Q		P			Q					P		
0031445C		D		D		C		E												
0031600R						R														
0031653L						L														
0031705M						M														
0031810F						F														
0031852J				J																
0031941J						J														
0032000E				E		E		E		F			E					F		
0032050F										F										
0032133G						G														
0032138J								J												
0032229T				T		T														
0032258P								P												
0032303J				K						J										
0032327I				I		I														
0040127C				C																
0040154A										A										
0040209B				B		B														
0040247A				B				C		A										
0040250I								I												
0040258P				P						P										
0040456Q													Q							
0040601S				S																
0040729N			Q	N		N		O		N			O			Q		N		

Table B.1 (continued)

	APP	ART	BYR	DZH	GIB	GOG	GSS	KET	KIR	KI2	LEN	MOO	MO2	NAB	SCH	SEV	SPT	SSS	STE	YSS
0040735M				M														M		
0040738J			M	J		J		K		J								J		
0040740P				Q		P		R		P								P		
0040809E				E																
0040901T				T																
0040950C				C																
0040954M				M																
0041016H						H														
0041024P						P														
0041029G						G														
0041030J						J												J		
0041033K													K							
0041055D						D														
0041100B								B												
0041101Q								Q												
0041103O						O														
0041122O																		O		
0041228O								O												
0041724H																		H		
0041726D																		D		
0042356F										F								G		
0050815E			H					F		E						G		E		
0051149P							P													
0051150K							K													
0051151N							N													
0051152J							J													
0051319Q							Q													
0051354S																		S		
0051530I										I										
0051627C			C																	
0051851B																		B		
0051917A							E			A								B		
0060322K							P	M		L								K		
0060735T								T												
0060827E																		E		
0061054E			E																	
0061055H			H																	
0061108F			F																	
0061214P			P																	
0061601S										S										
0061718T										T								A		
0061947R																		R		
0062053G								J		G								I		
0062209F								F												
0062303I										I										
0062314N										N										
0070220O										O								O		
0070303I										I								J		
0070328F										F										
0070624R							B											R		
0070753G										G										
0070820Q										Q										
0071504A										A										
0071519D																				D
0071527F										F										
0071757D										D										
0080732A			A																	
0081026P							A	Q		Q								P		
0081201E								E												
0081301M							Q	O		M								M		
0081306J								J										K		
0081309H			J				L	H		I								H		
0081332N																		N		
0081400K								K										L		
0081454O								O										P		
0081557B																		B		
0081653L			O				P	M		L								L		
0081945F								F										G		
0081948J										J										
0090411H								H										I		
0091107H																		H		
0091408O								O										P		
0091518D																		D		

Table B.1 (continued)

	APP	ART	BYR	DZH	GIB	GOG	GSS	KET	KIR	KI2	LEN	MOO	MO2	NAB	SCH	SEV	SPT	SSS	STE	YSS
0091529I										I										
0092001K								K										L		
0092359H								H												
0100004H								H												
0100011M								M												
0100852T			T																	
0101200P			P																	
0110621M										M										
0111223B			B																	
0111410I																		I		
0111516K										K										
0111611A										A										
0111933S			B					S										T		
0112147K								K												
0112230Q								Q										R		
0120242Q																		Q		
0120312O																		O		
0120445K								L		K								L		
0120506D										D										
0120517O										O								P		
0120634P										P										
0121948D										D										
0122244R								R												
0130027M								M												
0130629M								M												
0130756I										I										
0130942N																		N		
0131046N																		N		
0131102S										S										
0131401M																				M
0131420G										G								H		
0131701S										S										
0131749I			I																	
0140405N								N												
0140458P								P										R		
0140957E								E												
0141403A																		A		
0141552S							D	S		A								T		
0141748K			K																	
0142126M			O				Q	N		M						O		M		Q
0142232M																		M		
0151324L										L										
0152029L								L										L		
0160119M										M										
0160737D																		D		
0160821S																S				
0161313I																		I		
0161838J																		J		
0161922C								C												
0162112O								O										O		
0170049H										H										
0171025N			N																	
0171206Q								S		Q								R		
0171926S								T		S								S		
0181156Q																		Q		
0181343J			J																	
0190441N										N								O		
0190448O										O								P		
0190727R								T		R								S		
0190813N							N													
0191404E										E										
0191645P																		P		
0191902E																		E		
0200240G							K	H		G								G		
0200324C								C										C		
0200450B																		B		
0200626J										J										
0200932P																P				
0201054E																E				
0201120E										E										
0201204D								D												
0201833R							B			R								R		
0202026H										H								H		

Table B.1 (continued)

	APP	ART	BYR	DZH	GIB	GOG	GSS	KET	KIR	KI2	LEN	MOO	MO2	NAB	SCH	SEV	SPT	SSS	STE	YSS
0202345J										J										
0210100H							H													
0210151D										D										
0210154M										M										
0210809K																		K		
0210920P								P												
0211518C										C										
0220216Q										Q										
0220222F								F												
0220813E								E		E								E		
0221357E										E										
0221526F										F								G		
0221705E																		E		
0222335Q										Q										
0230141C								C												
0230505M										M								M		
0230744P								P												
0230914L										L										
0231614F										F										
0231729O																		O		
0232043L								L										M		
0232347L								L										N		
0240208C																		C		
0240231C							H	D		D								C		G
0240645B																				B
0241207H																				H
0241249S																				S
0241433Q																		Q		
0250828S																S				
0251206S										S										
0251556T								T												
0252206R								S		R								S		
0260808I																		I		
0261515I																		I		
0261942J										J								K		
0270243I							J	J		I						J		J		J
0270343D																		D		
0270635K										K										
0271034M										M										
0272028F										F										
0272235Q																				Q
0272356D							D													
0280149F										F										
0280937J		J																		
0281408S		S																		
0281507B		B																		
0290209L																				L
0290401S		S																		
0291711G								G										I		
0292123F																				F
0292227B																				B
0292348Q																				Q
0300033M							Q			M										
0300204E								E										F		
0301557O																		O		
0310432J							N			J								J		
0310458M								M												
0311115H							H													
0311116J							J													
0311212S		S																		
0311430G								G												
0311501N		N																		
0311502P								P												
0311956O										O										
0312008J										J										
0312118L										L										
0320346H																		H		
0320407O								O										P		
0321005N																				N
0321105C										C										
0321420Q																		Q		
0330741E		E																		
0330751L		L																		

Table B.1 (continued)

	APP	ART	BYR	DZH	GIB	GOG	GSS	KET	KIR	KI2	LEN	MOO	MO2	NAB	SCH	SEV	SPT	SSS	STE	YSS
0330821L			L																	
0332128B										B										
0340922O								O												
0341035G								G												
0341041L								L												
0341234A			A																	
0342009Q										Q										
0350316T			T																	
0350552L																		L		
0350943C																		C		
0350958C																		C		
0350958S																		S		
0351248K										K										
0351310H										H										
0351320C										C										
0352148L			L				M													
0352327Q							Q													
0370146T							T													
0372040C							C													C
0382236P							P													

APPENDIX C

Record Sections for Events Recorded on Six or More Stations

E. Cranswick

This Appendix provides three-component record sections, for events recorded on six or more GEOS stations. These data are discussed in Chapter 7.2

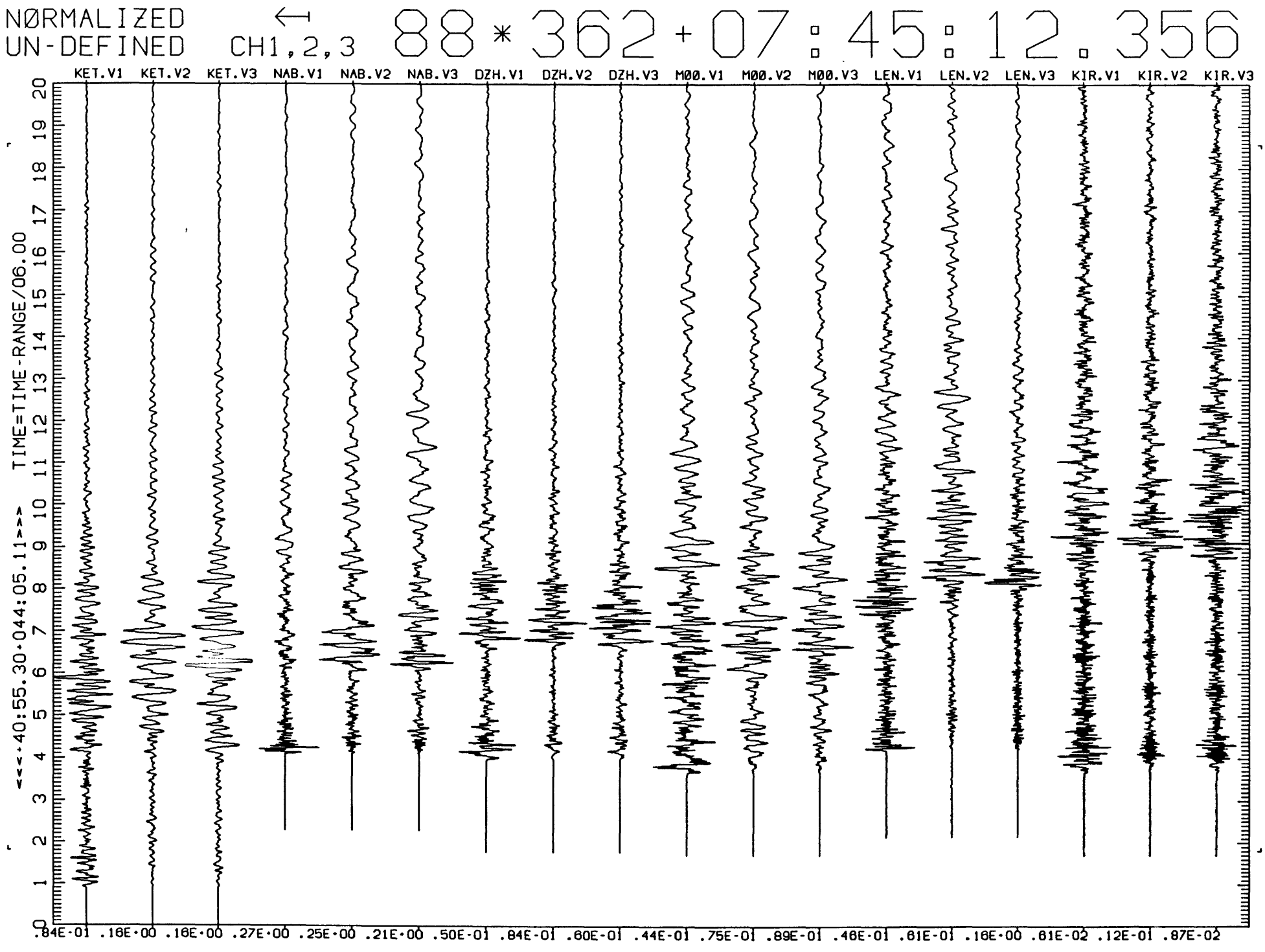
NØRMALIZED
UN-DEFINED
CH1,2,3
88*362+07:45:12.356
KET.V1 KET.V2 KET.V3 NAB.V1 NAB.V2 NAB.V3 DZH.V1 DZH.V2 DZH.V3 M00.V1 M00.V2 M00.V3 LEN.V1 LEN.V2 LEN.V3 KIR.V1 KIR.V2 KIR.V3
<<<+40:55.30+044:05.11>>> TIME=TIME-RANGE/06.00
0 1 2 3 4 5 6 7 8 9 10 11 12 13 14 15 16 17 18 19 20
.84E-01 .18E+00 .16E+00 .27E+00 .25E+00 .21E+00 .50E-01 .84E-01 .60E-01 .44E-01 .75E-01 .89E-01 .46E-01 .61E-01 .16E+00 .61E-02 .12E-01 .87E-02

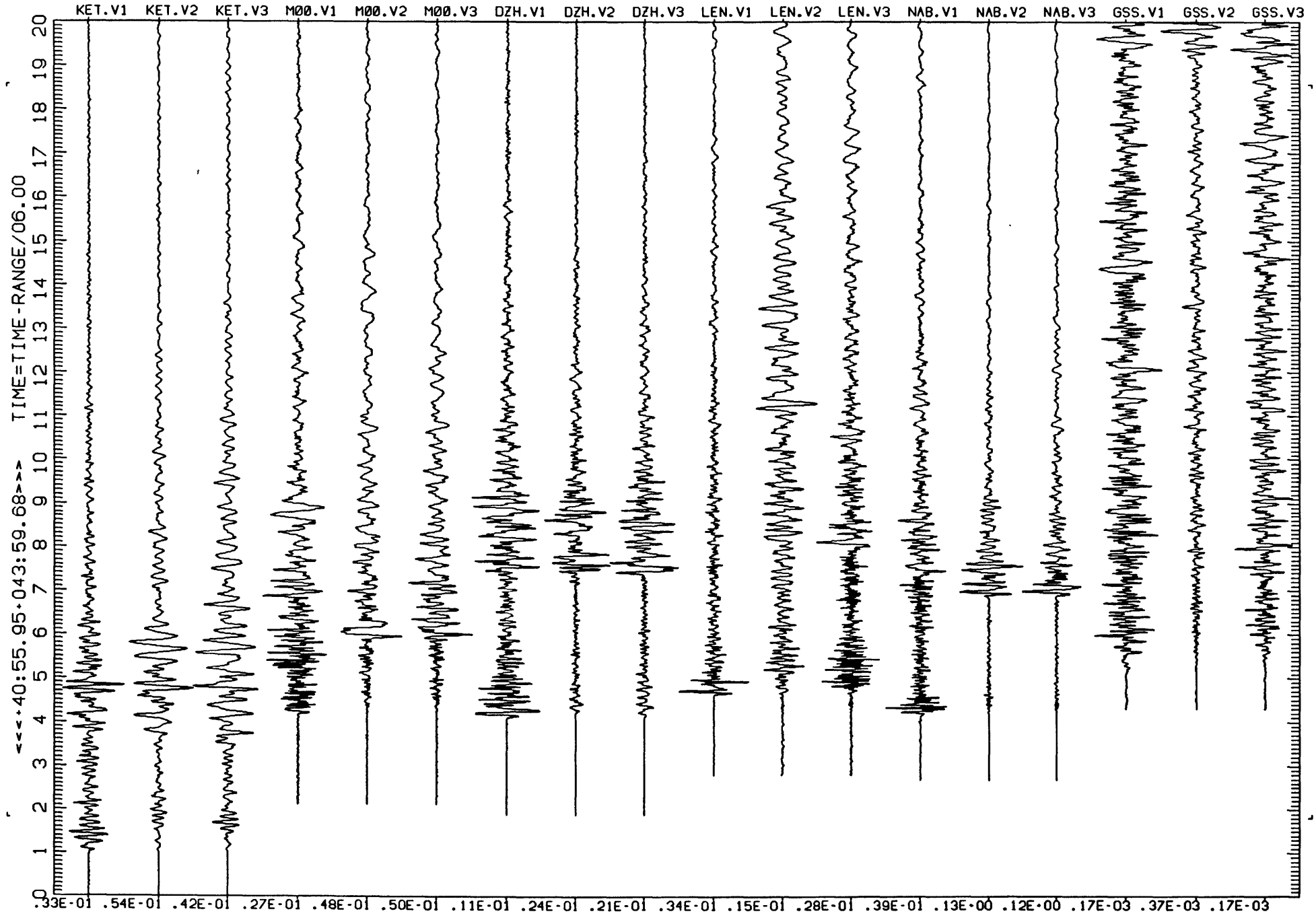
NØRMALIZED
UN-DEFINED
CH1,2,3
88*362+11:15:22.658
KET.V1 KET.V2 KET.V3 MØØ.V1 MØØ.V2 MØØ.V3 DZH.V1 DZH.V2 DZH.V3 LEN.V1 LEN.V2 LEN.V3 NAB.V1 NAB.V2 NAB.V3 GSS.V1 GSS.V2 GSS.V3
TIME=TIME-RANGE/06.00
<<<+40:55.95+043:59.68>>>
0 1 2 3 4 5 6 7 8 9 10 11 12 13 14 15 16 17 18 19 20
.33E-01 .54E-01 .42E-01 .27E-01 .48E-01 .50E-01 .11E-01 .24E-01 .21E-01 .34E-01 .15E-01 .28E-01 .39E-01 .13E+00 .12E+00 .17E-03 .37E-03 .17E-03

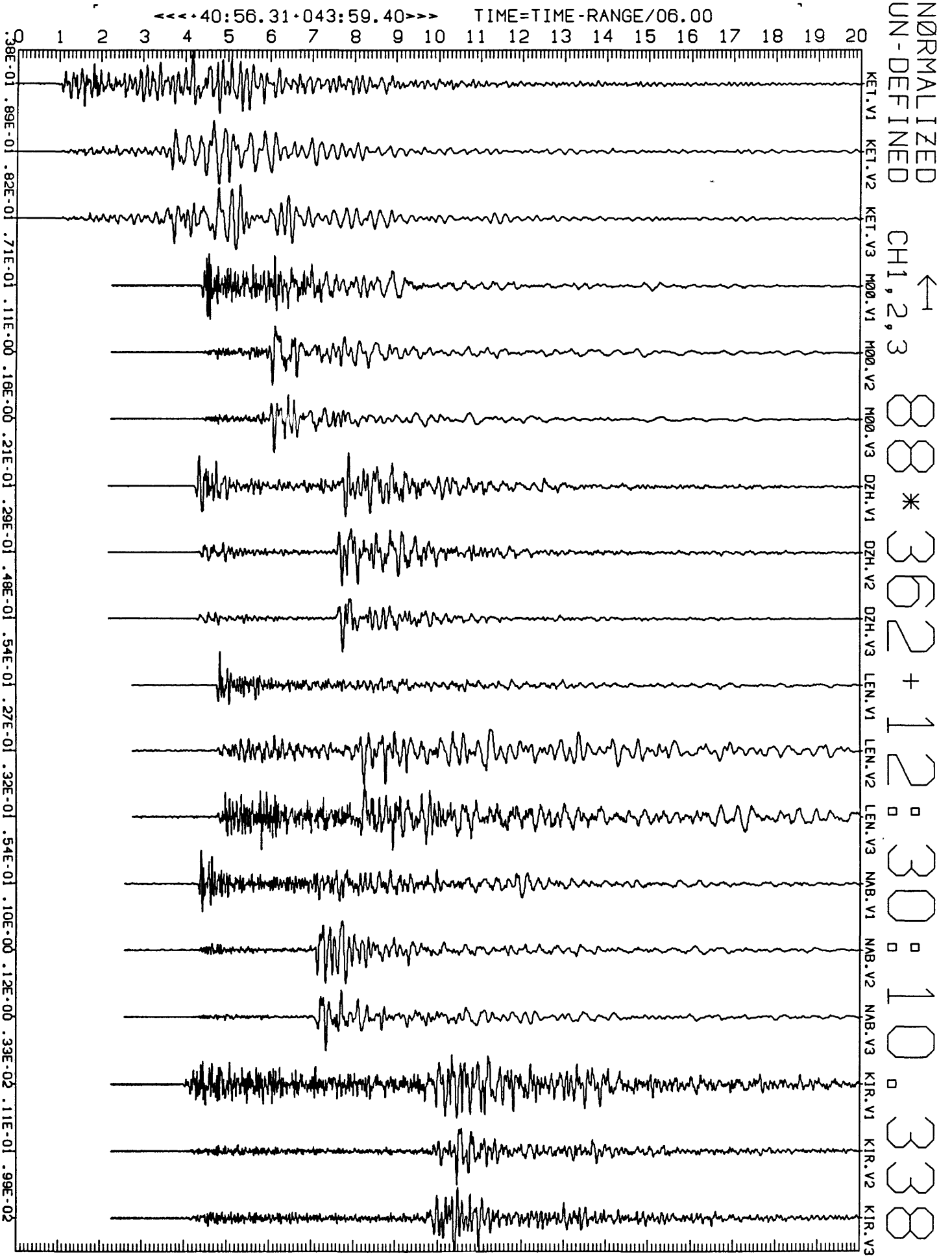
NORMALIZED
UN-DEFINED
CH1, 2, 3
88 * 362 + 12 . 30 . 10 . 38
<<<+40:56.31+043:59.40>>>
TIME=TIME-RANGE/06.00
0 1 2 3 4 5 6 7 8 9 10 11 12 13 14 15 16 17 18 19 20
.38E-01 .89E-01 .82E-01 .71E-01 .11E-00 .10E-00 .21E-01 .29E-01 .48E-01 .54E-01 .27E-01 .32E-01 .54E-01 .10E-00 .12E-00 .33E-02 .11E-01 .99E-02
KET.V1 KET.V2 KET.V3 M00.V1 M00.V2 M00.V3 DZH.V1 DZH.V2 DZH.V3 LEN.V1 LEN.V2 LEN.V3 NAB.V1 NAB.V2 NAB.V3 KIR.V1 KIR.V2 KIR.V3

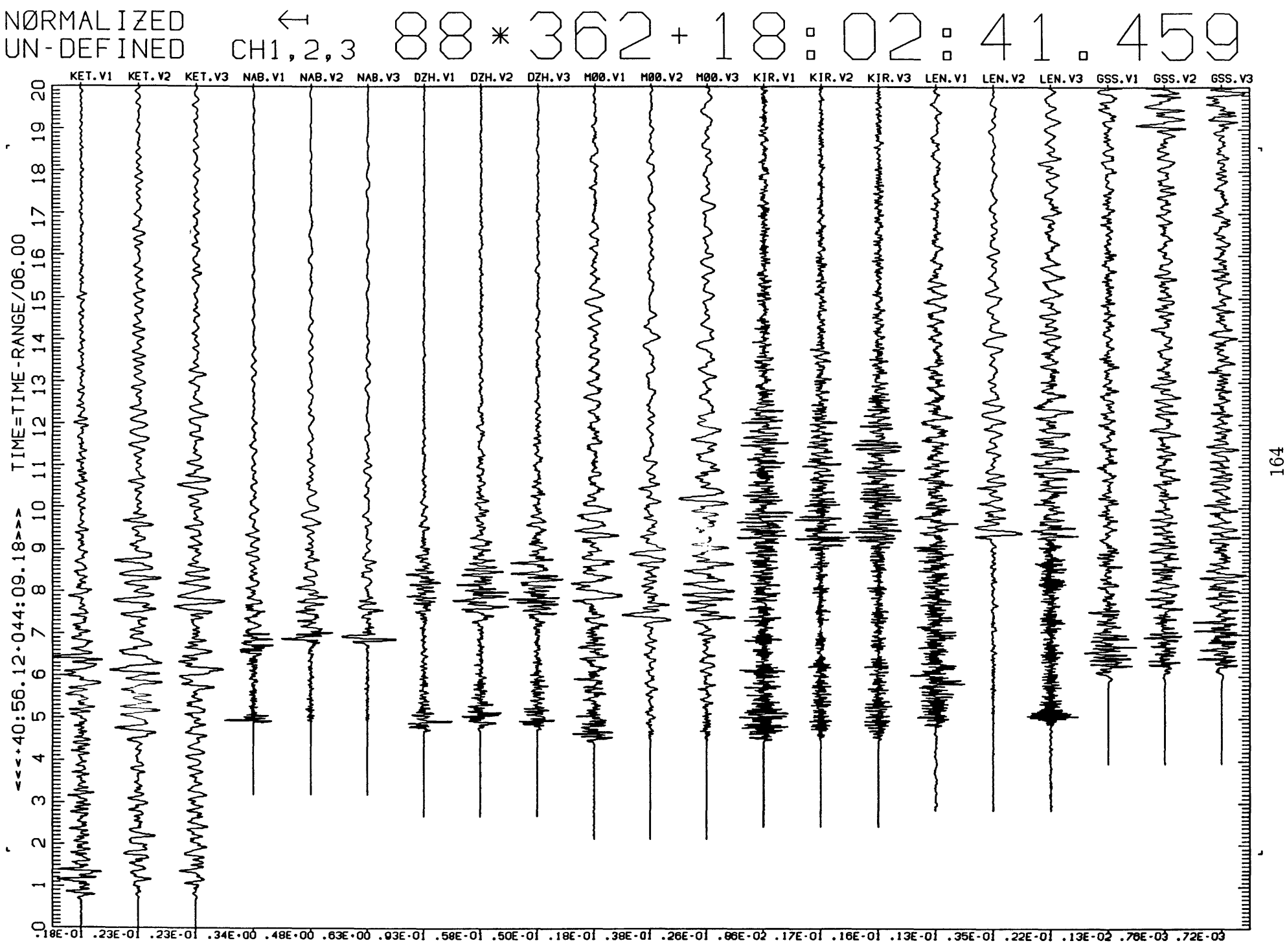
NØRMALIZED
UN-DEFINED
CH1,2,3
88*362+18:02:41.459
KET.V1 KET.V2 KET.V3 NAB.V1 NAB.V2 NAB.V3 DZH.V1 DZH.V2 DZH.V3 M00.V1 M00.V2 M00.V3 KIR.V1 KIR.V2 KIR.V3 LEN.V1 LEN.V2 LEN.V3 GSS.V1 GSS.V2 GSS.V3
TIME=TIME-RANGE/06.00
<<<+40:56.12+044:09.18>>>
0 1 2 3 4 5 6 7 8 9 10 11 12 13 14 15 16 17 18 19 20
.18E-01 .23E-01 .23E-01 .34E+00 .48E+00 .63E+00 .93E-01 .58E-01 .50E-01 .18E-01 .38E-01 .26E-01 .86E-02 .17E-01 .16E-01 .13E-01 .35E-01 .22E-01 .13E-02 .78E-03 .72E-03

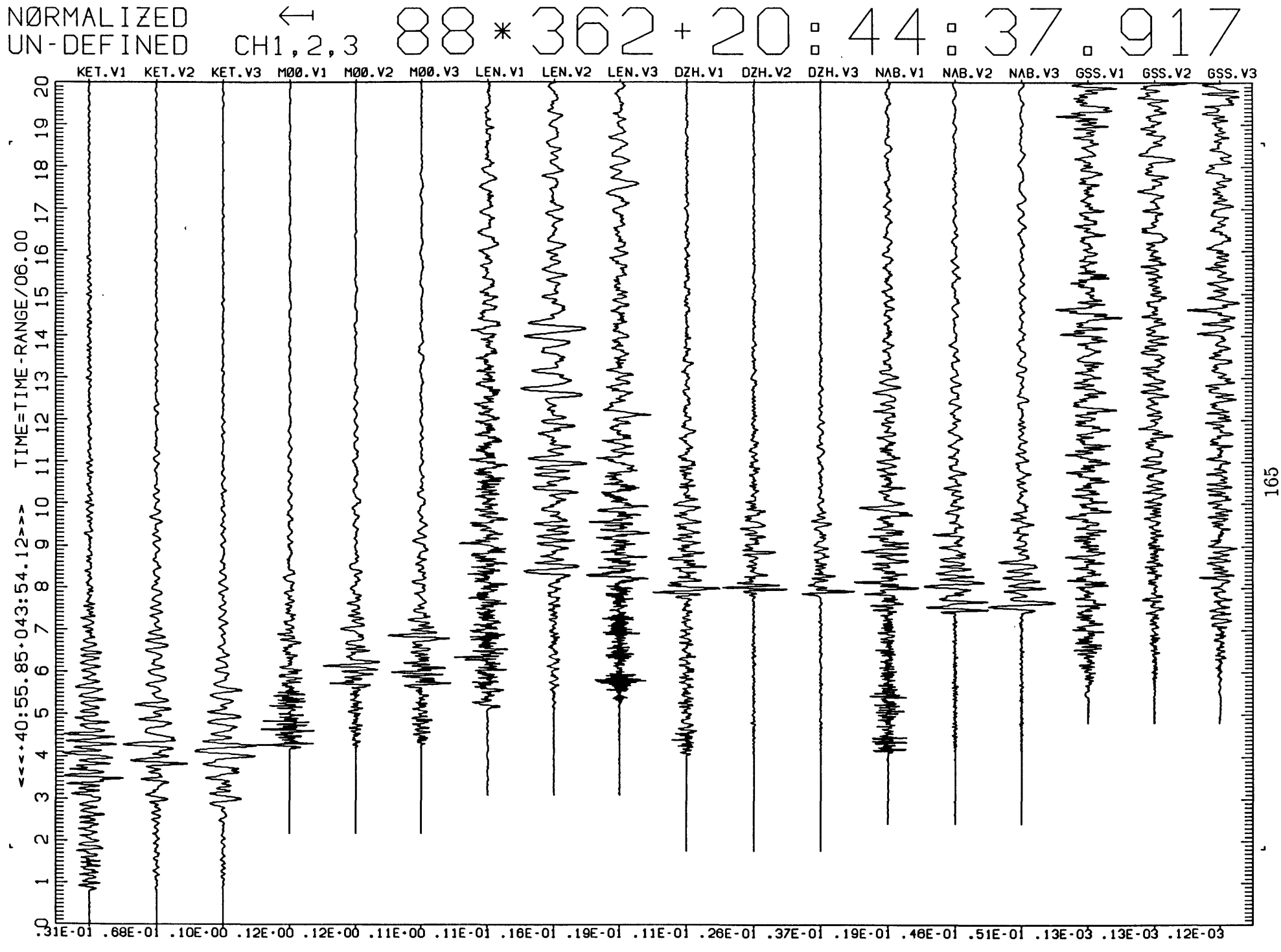
NØRMALIZED
UN-DEFINED
CH1,2,3
88*362+20:44:37.917
KET.V1 KET.V2 KET.V3 MØØ.V1 MØØ.V2 MØØ.V3 LEN.V1 LEN.V2 LEN.V3 DZH.V1 DZH.V2 DZH.V3 NAB.V1 NAB.V2 NAB.V3 GSS.V1 GSS.V2 GSS.V3
<<<+40:55.85+043:54.12>>> TIME=TIME-RANGE/06.00
0 1 2 3 4 5 6 7 8 9 10 11 12 13 14 15 16 17 18 19 20
.31E-01 .68E-01 .10E-00 .12E-00 .12E-00 .11E-00 .11E-01 .16E-01 .19E-01 .11E-01 .26E-01 .37E-01 .19E-01 .46E-01 .51E-01 .13E-03 .13E-03 .12E-03

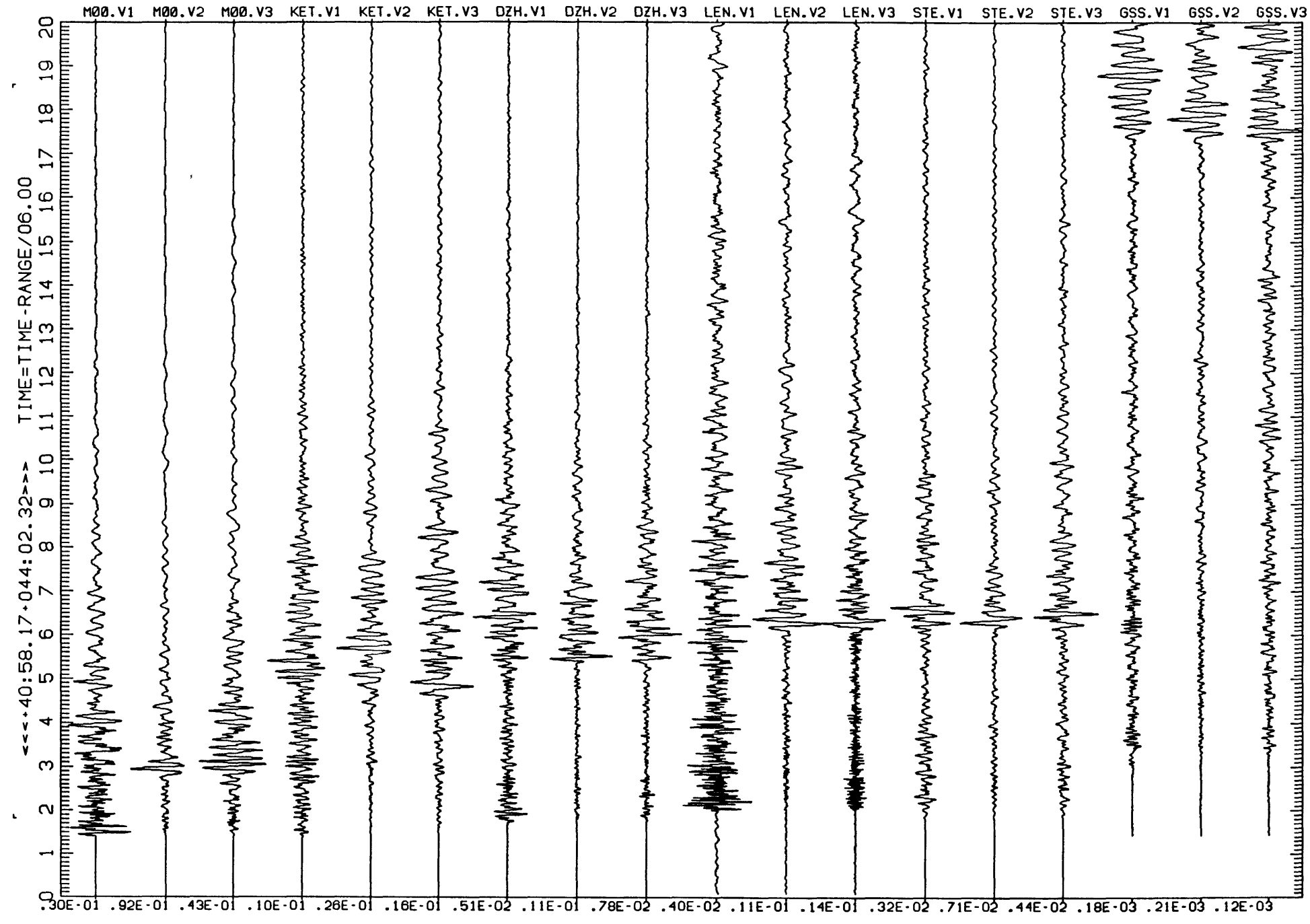
NØRMALIZED
UN-DEFINED
CH1,2,3
88*363+22:46:56.756
M00.V1 M00.V2 M00.V3 KET.V1 KET.V2 KET.V3 DZH.V1 DZH.V2 DZH.V3 LEN.V1 LEN.V2 LEN.V3 STE.V1 STE.V2 STE.V3 GSS.V1 GSS.V2 GSS.V3
<<<+40:58.17+044:02.32>>> TIME=TIME-RANGE/06.00
0 1 2 3 4 5 6 7 8 9 10 11 12 13 14 15 16 17 18 19 20
.30E-01 .92E-01 .43E-01 .10E-01 .26E-01 .16E-01 .51E-02 .11E-01 .78E-02 .40E-02 .11E-01 .14E-01 .32E-02 .71E-02 .44E-02 .18E-03 .21E-03 .12E-03

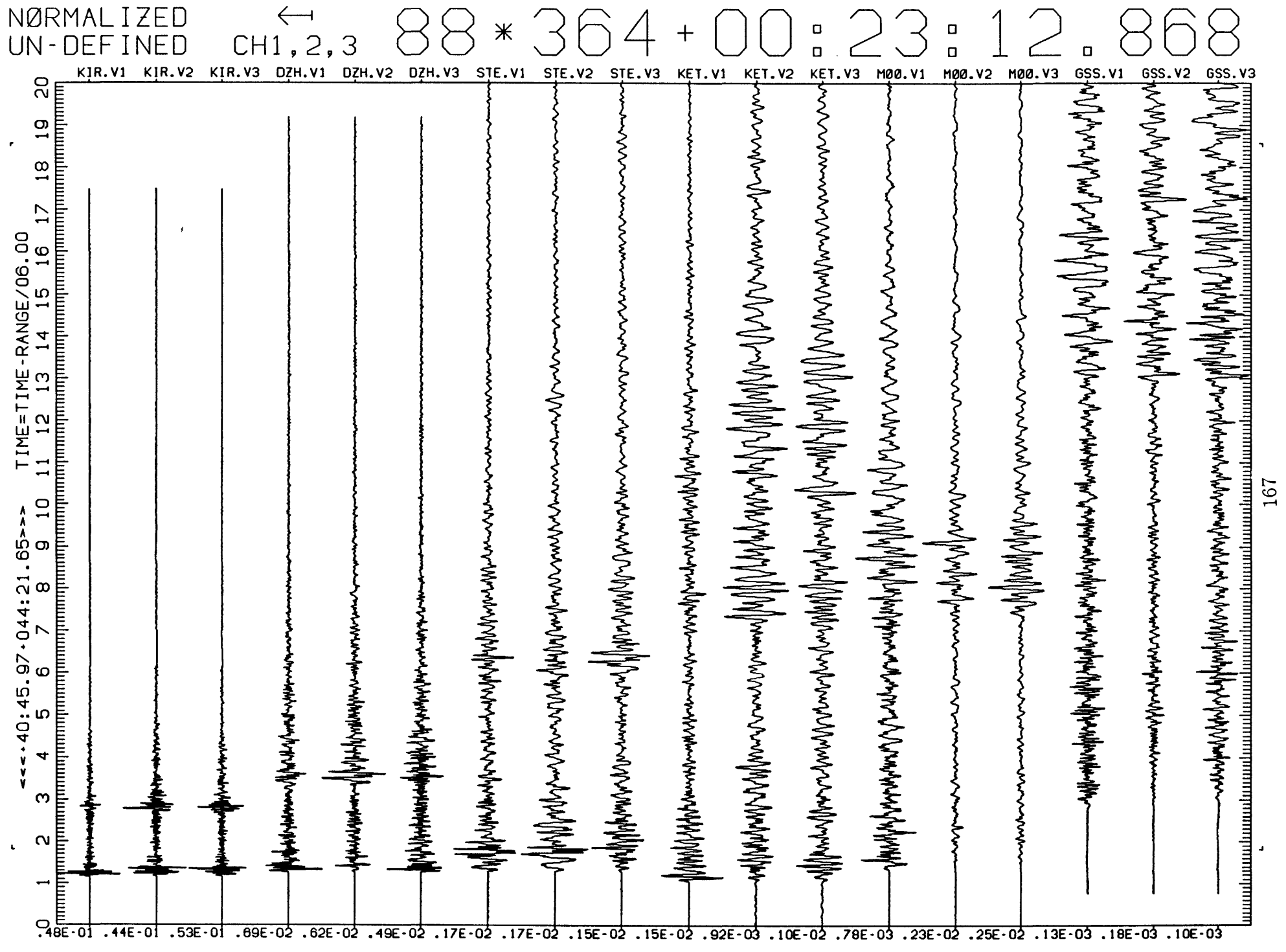
NØRMALIZED
UN-DEFINED
CH1,2,3
88*364+00:23:12.868
KIR.V1 KIR.V2 KIR.V3 DZH.V1 DZH.V2 DZH.V3 STE.V1 STE.V2 STE.V3 KET.V1 KET.V2 KET.V3 MØØ.V1 MØØ.V2 MØØ.V3 GSS.V1 GSS.V2 GSS.V3
<<<+40:45.97+044:21.65>>> TIME=TIME-RANGE/06.00
0 1 2 3 4 5 6 7 8 9 10 11 12 13 14 15 16 17 18 19 20
.48E-01 .44E-01 .53E-01 .69E-02 .62E-02 .49E-02 .17E-02 .17E-02 .15E-02 .15E-02 .92E-03 .10E-02 .78E-03 .23E-02 .25E-02 .13E-03 .18E-03 .10E-03

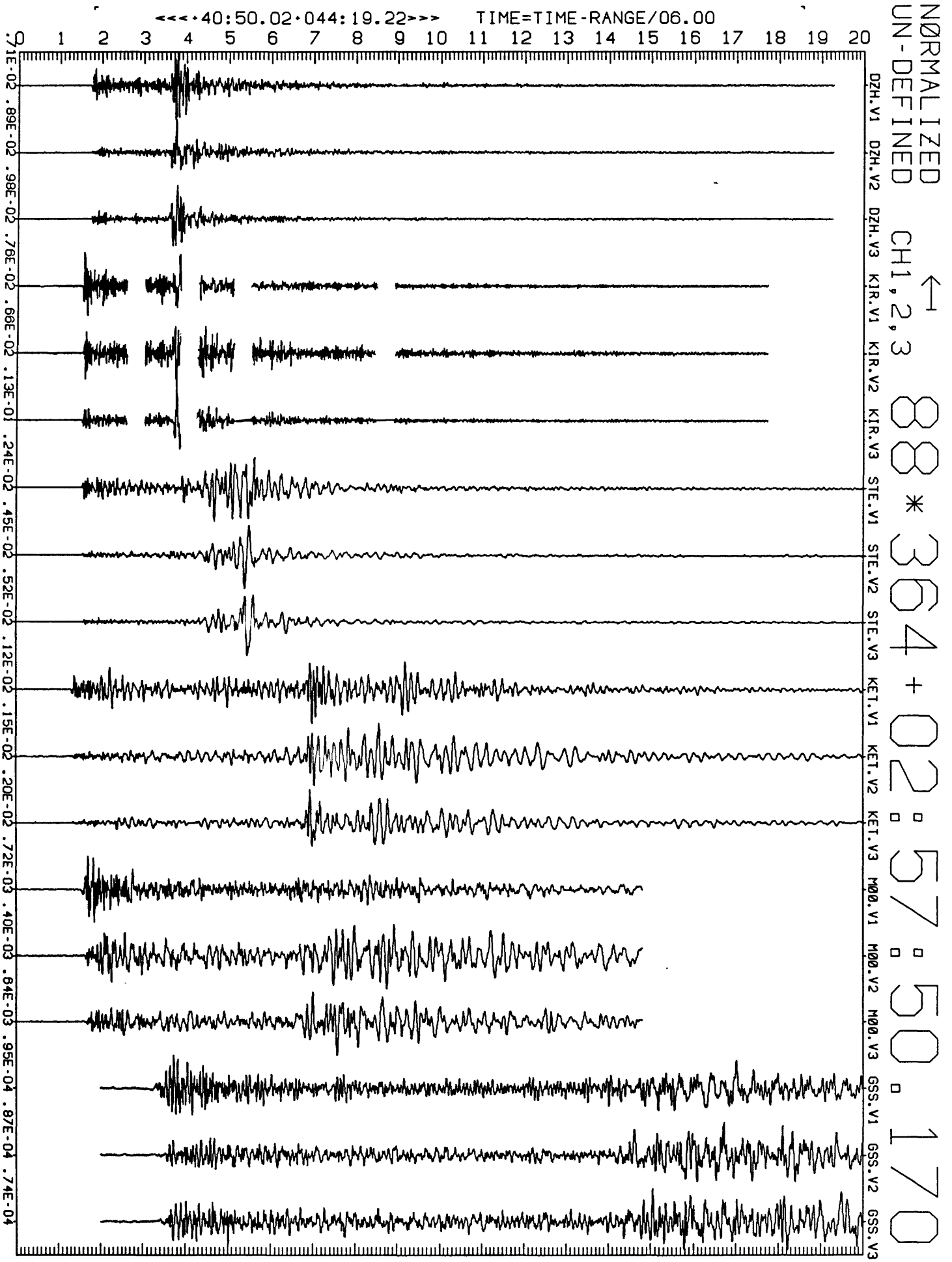
<<<+40:50.02+044:19.22>>> TIME=TIME-RANGE/06.00
0 1 2 3 4 5 6 7 8 9 10 11 12 13 14 15 16 17 18 19 20
.71E-02
.89E-02
.98E-02
.76E-02
.66E-02
.13E-01
.24E-02
.45E-02
.52E-02
.12E-02
.15E-02
.20E-02
.72E-03
.40E-03
.84E-03
.95E-04
.87E-04
.74E-04
DZH.V1
DZH.V2
DZH.V3
KIR.V1
KIR.V2
KIR.V3
STE.V1
STE.V2
STE.V3
KET.V1
KET.V2
KET.V3
M00.V1
M00.V2
M00.V3
GSS.V1
GSS.V2
GSS.V3
NORMALIZED
UN-DEFINED
CH1,2,3
88*364+02:57:50.170

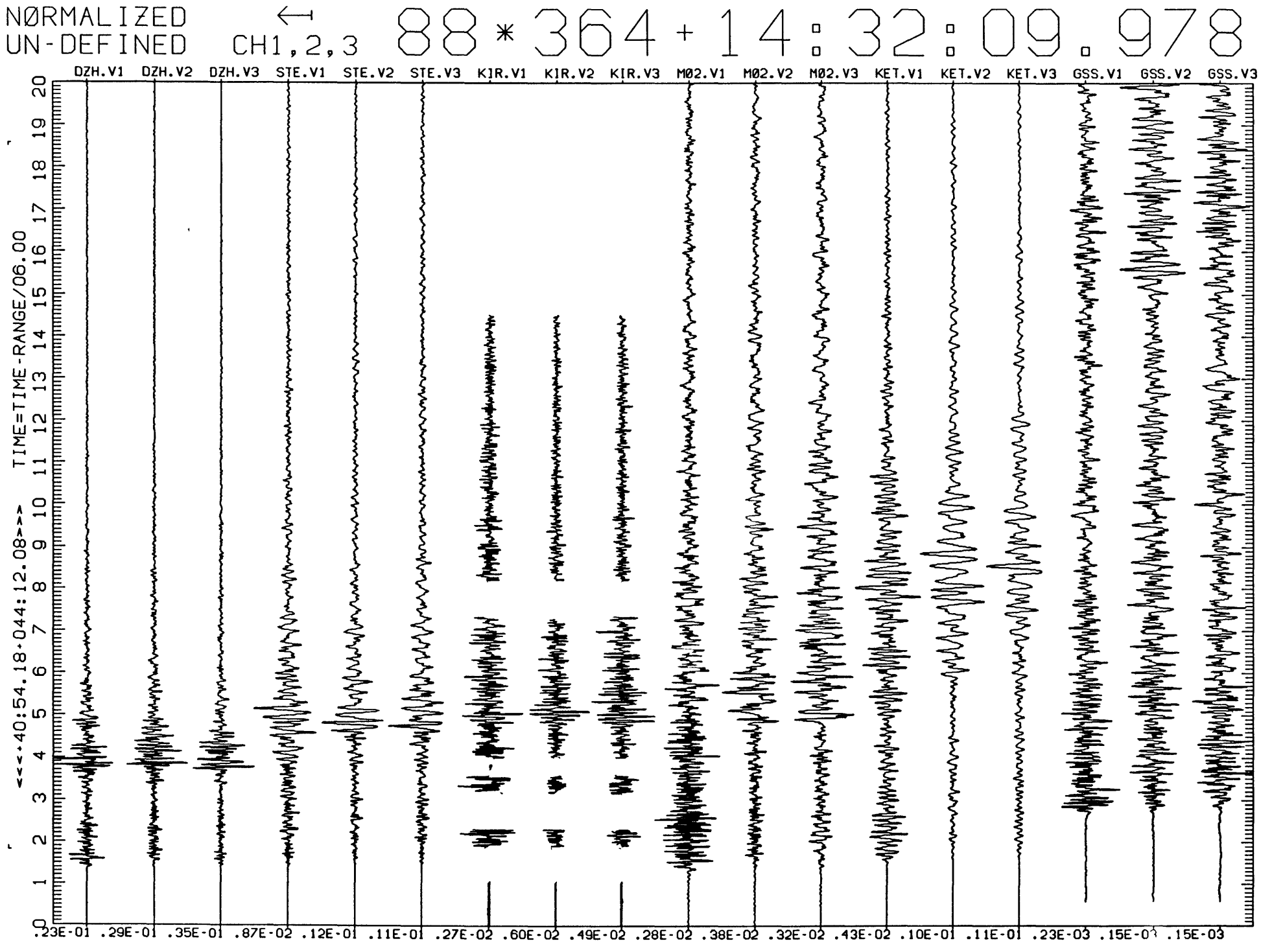
NØRMALIZED
UN-DEFINED
CH1,2,3
88*364+14:32:09.978
DZH.V1 DZH.V2 DZH.V3 STE.V1 STE.V2 STE.V3 KIR.V1 KIR.V2 KIR.V3 MØ2.V1 MØ2.V2 MØ2.V3 KET.V1 KET.V2 KET.V3 GSS.V1 GSS.V2 GSS.V3
<<<-40:54.18-044:12.08>>> TIME=TIME-RANGE/06.00
0 1 2 3 4 5 6 7 8 9 10 11 12 13 14 15 16 17 18 19 20
.23E-01 .29E-01 .35E-01 .87E-02 .12E-01 .11E-01 .27E-02 .60E-02 .49E-02 .28E-02 .38E-02 .32E-02 .43E-02 .10E-01 .11E-01 .23E-03 .15E-03 .15E-03

NØRMALIZED
UN-DEFINED
CH1,2,3
88*364+18.43.48.851
<<<+40:57.45+043:57.51>>>
TIME=TIME-RANGE/06.00
0 1 2 3 4 5 6 7 8 9 10 11 12 13 14 15 16 17 18 19 20
.19E+00
.19E+00
.18E+00
.15E+00
.23E+00
.17E+00
.83E-01
.94E-01
.10E+00
.31E-01
.76E-01
.11E+00
.74E-02
.11E-01
.10E-01
.37E-02
.13E-01
.13E-01
.81E-03
.95E-03
.98E-03
M02.V1
M02.V2
M02.V3
KET.V1
KET.V2
KET.V3
LEN.V1
LEN.V2
LEN.V3
DZH.V1
DZH.V2
DZH.V3
STE.V1
STE.V2
STE.V3
KIR.V1
KIR.V2
KIR.V3
GSS.V1
GSS.V2
GSS.V3

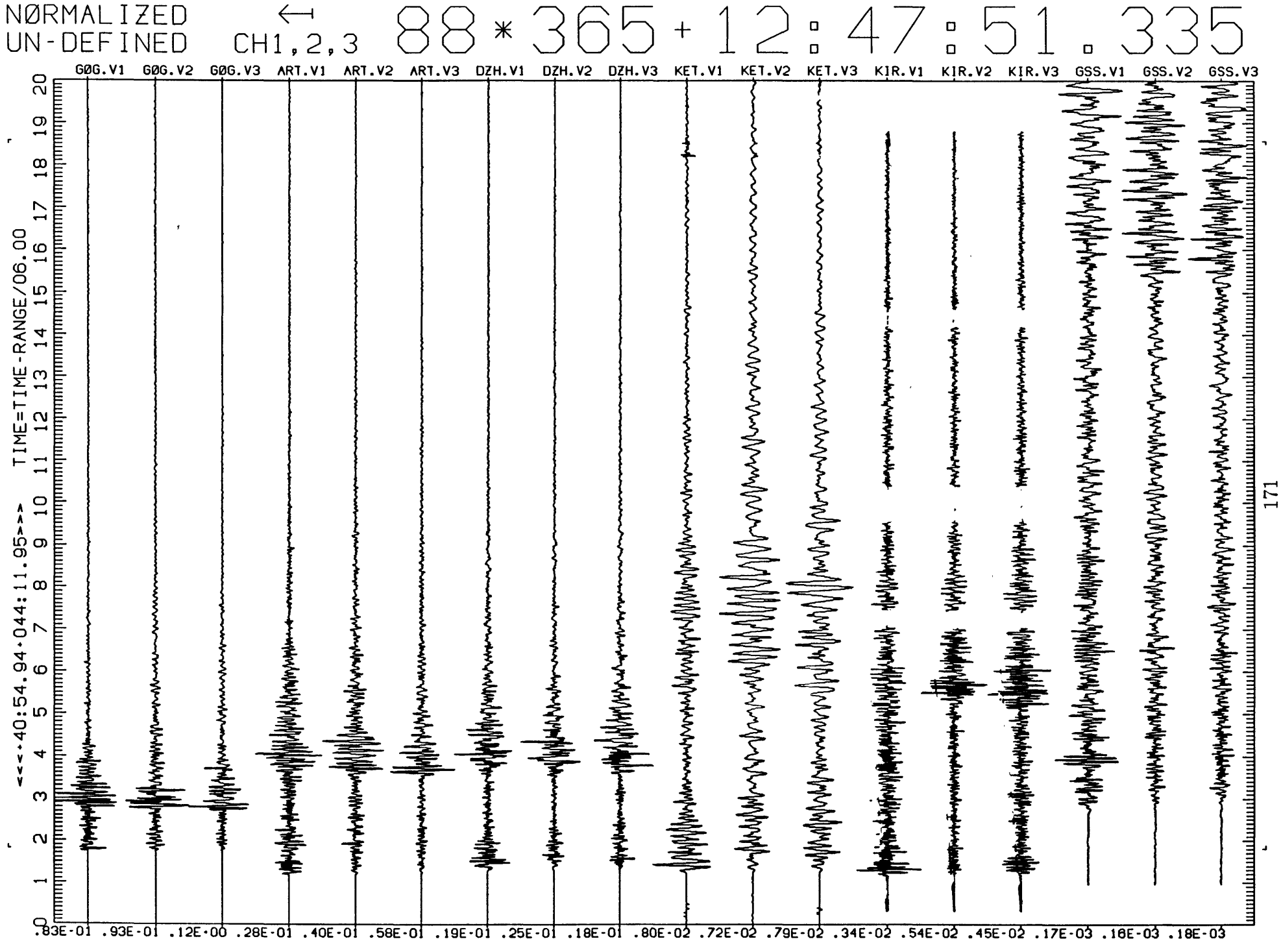
NØRMALIZED
UN-DEFINED
CH1,2,3
88*365+12:47:51.335
GØG.V1
GØG.V2
GØG.V3
ART.V1
ART.V2
ART.V3
DZH.V1
DZH.V2
DZH.V3
KET.V1
KET.V2
KET.V3
KIR.V1
KIR.V2
KIR.V3
GSS.V1
GSS.V2
GSS.V3
<<<+40:54.94+044:11.95>>>
TIME=TIME-RANGE/06.00
0 1 2 3 4 5 6 7 8 9 10 11 12 13 14 15 16 17 18 19 20
.83E-01 .93E-01 .12E+00 .28E-01 .40E-01 .58E-01 .19E-01 .25E-01 .18E-01 .80E-02 .72E-02 .79E-02 .34E-02 .54E-02 .45E-02 .17E-03 .16E-03 .18E-03

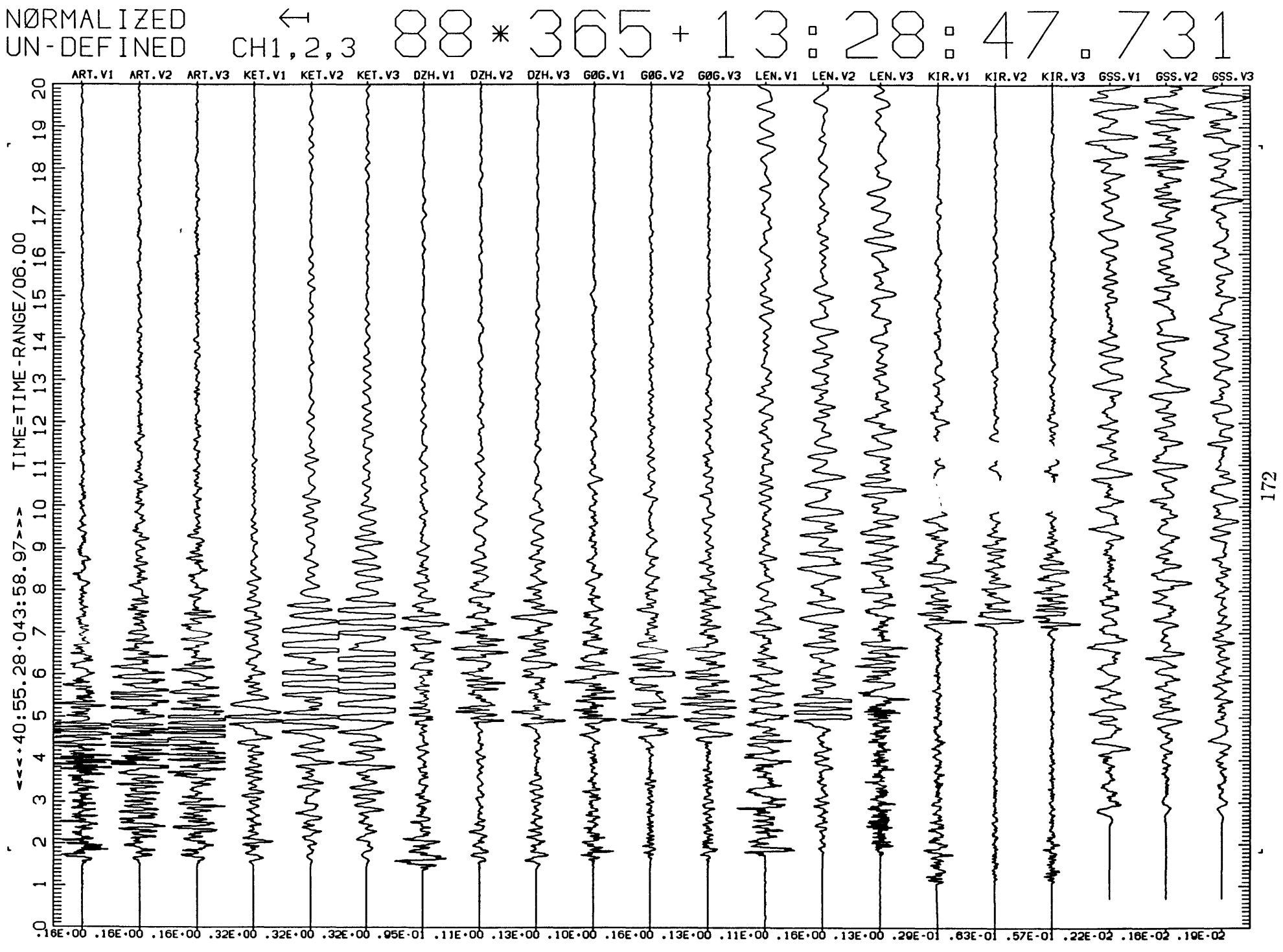
NØRMALIZED
UN-DEFINED
CH1,2,3
88*365+13:28:47.731
ART.V1 ART.V2 ART.V3 KET.V1 KET.V2 KET.V3 DZH.V1 DZH.V2 DZH.V3 GØG.V1 GØG.V2 GØG.V3 LEN.V1 LEN.V2 LEN.V3 KIR.V1 KIR.V2 KIR.V3 GSS.V1 GSS.V2 GSS.V3
<<<-40:55.28-043:58.97>>> TIME=TIME-RANGE/06.00
0 1 2 3 4 5 6 7 8 9 10 11 12 13 14 15 16 17 18 19 20
.16E+00 .16E+00 .16E+00 .32E+00 .32E+00 .32E+00 .95E-01 .11E+00 .13E+00 .10E+00 .16E+00 .13E+00 .11E+00 .16E+00 .13E+00 .29E-01 .63E-01 .57E-01 .22E-02 .16E-02 .19E-02
172

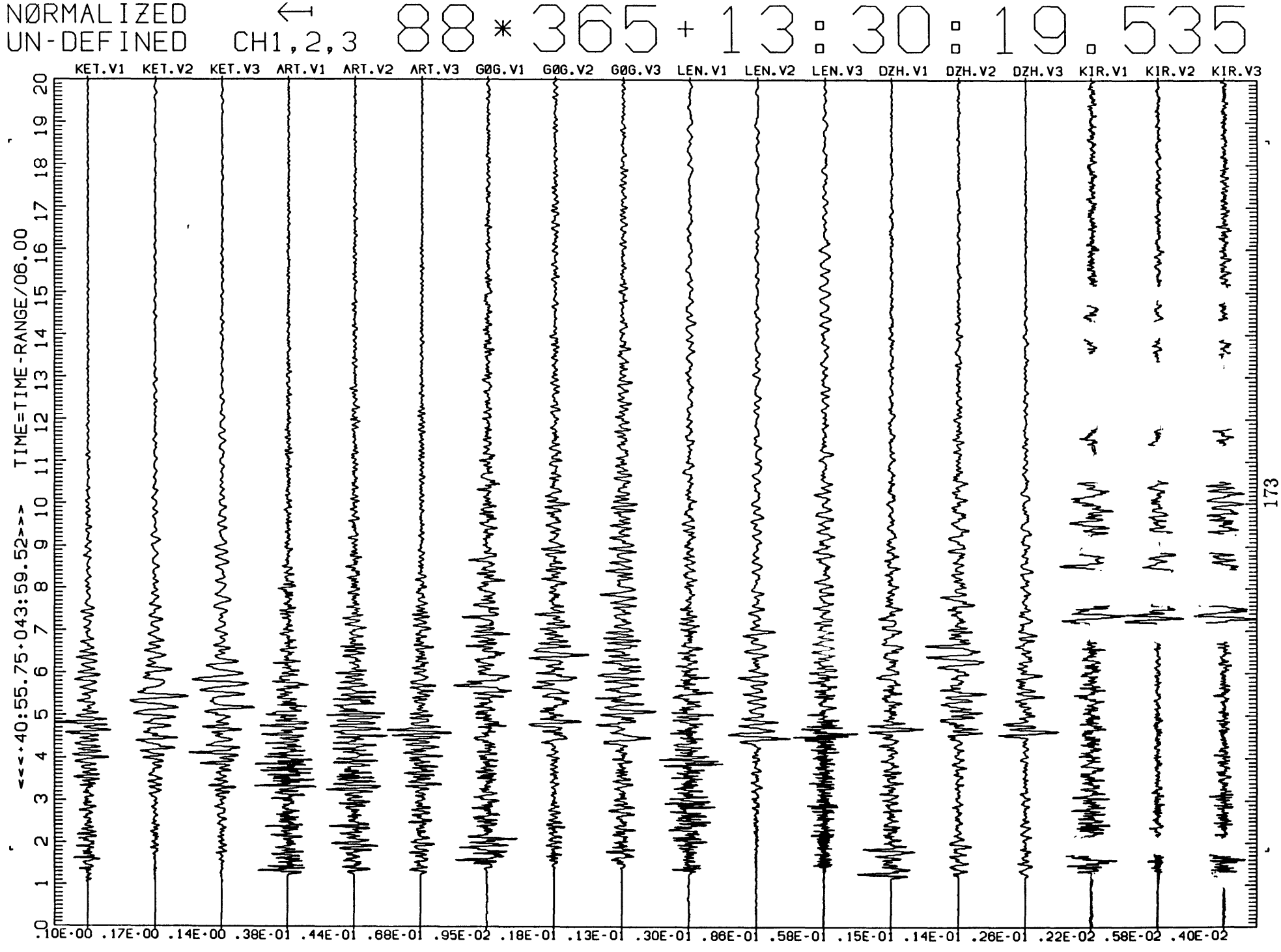
NØRMALIZED
UN-DEFINED
CH1,2,3
88*365+13:30:19.535
KET.V1 KET.V2 KET.V3 ART.V1 ART.V2 ART.V3 GØG.V1 GØG.V2 GØG.V3 LEN.V1 LEN.V2 LEN.V3 DZH.V1 DZH.V2 DZH.V3 KIR.V1 KIR.V2 KIR.V3
<<<<40:55.75+043:59.52>>>> TIME=TIME-RANGE/06.00
0 1 2 3 4 5 6 7 8 9 10 11 12 13 14 15 16 17 18 19 20
.10E+00 .17E+00 .14E+00 .38E-01 .44E-01 .68E-01 .95E-02 .18E-01 .13E-01 .30E-01 .86E-01 .58E-01 .15E-01 .14E-01 .26E-01 .22E-02 .58E-02 .40E-02

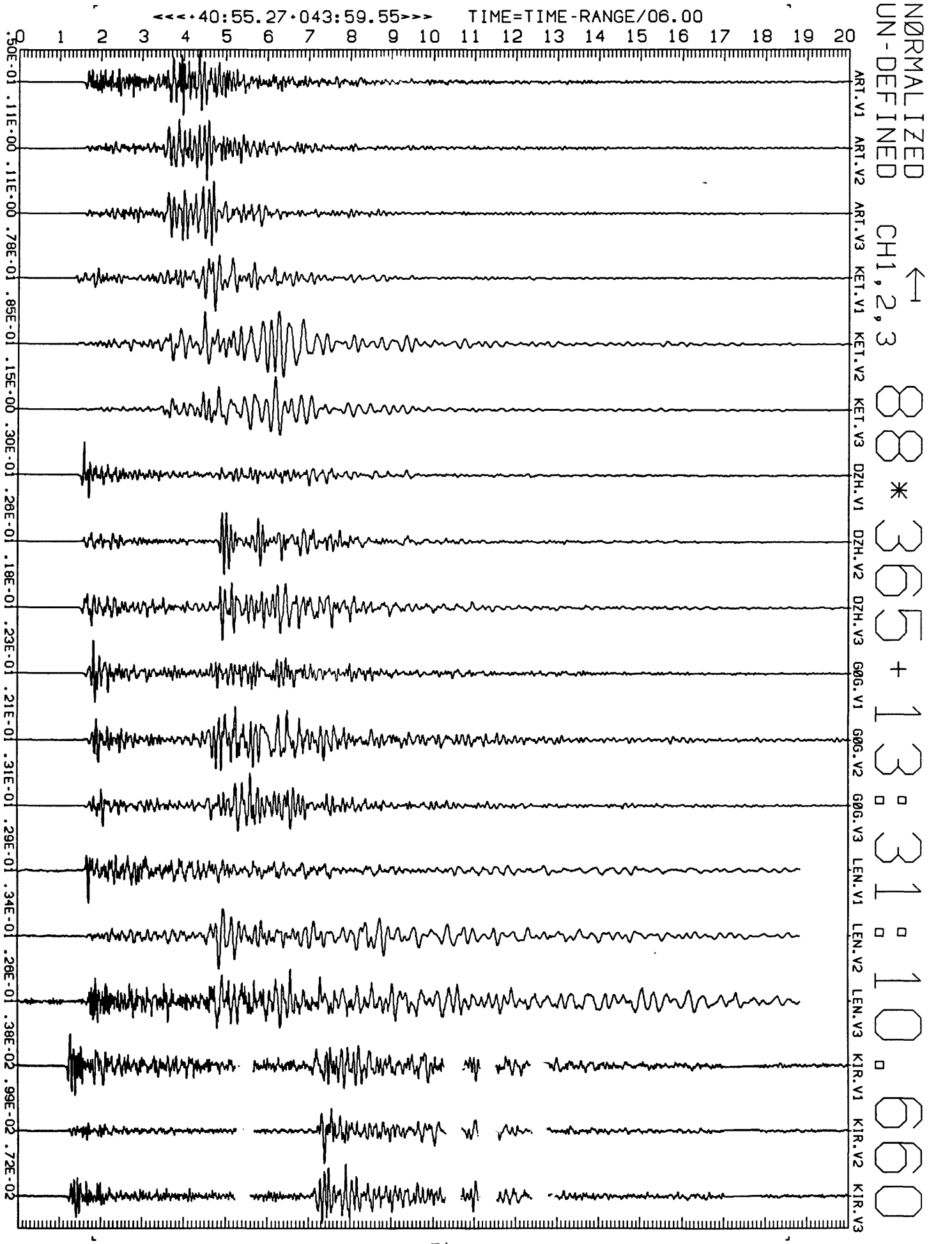
NØRMALIZED
UN-DEFINED
CH1,2,3
88*365+13.31.10.60
<<<+40:55.27+043:59.55>>>
TIME=TIME-RANGE/06.00
0 1 2 3 4 5 6 7 8 9 10 11 12 13 14 15 16 17 18 19 20
.50E-01 .11E+00 .11E+00 .78E-01 .85E-01 .15E+00 .30E-01 .26E-01 .18E-01 .23E-01 .21E-01 .31E-01 .29E-01 .34E-01 .26E-01 .38E-02 .99E-02 .72E-02
ART.V1 ART.V2 ART.V3 KET.V1 KET.V2 KET.V3 DZH.V1 DZH.V2 DZH.V3 GØG.V1 GØG.V2 GØG.V3 LEN.V1 LEN.V2 LEN.V3 KIR.V1 KIR.V2 KIR.V3

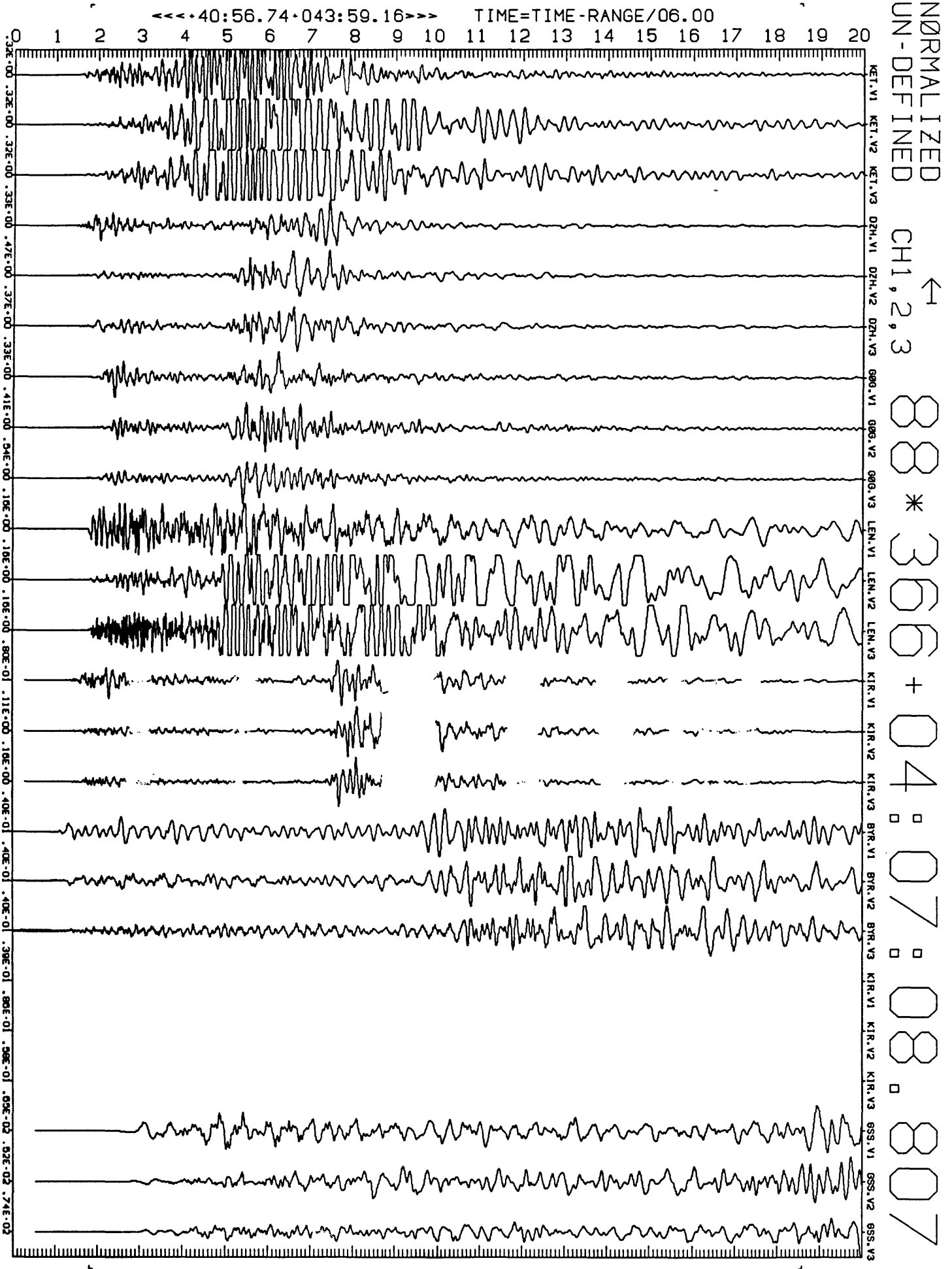
<<<+40:56.74+043:59.16>>> TIME=TIME-RANGE/06.00
0 1 2 3 4 5 6 7 8 9 10 11 12 13 14 15 16 17 18 19 20
NORMALIZED
UN-DEFINED
CH1,2,3
88*366+04.07.08.807
KET.V1
KET.V2
KET.V3
DZH.V1
DZH.V2
DZH.V3
GOG.V1
GOG.V2
GOG.V3
LEN.V1
LEN.V2
LEN.V3
KIR.V1
KIR.V2
KIR.V3
BYR.V1
BYR.V2
BYR.V3
KIR.V1
KIR.V2
KIR.V3
GSS.V1
GSS.V2
GSS.V3

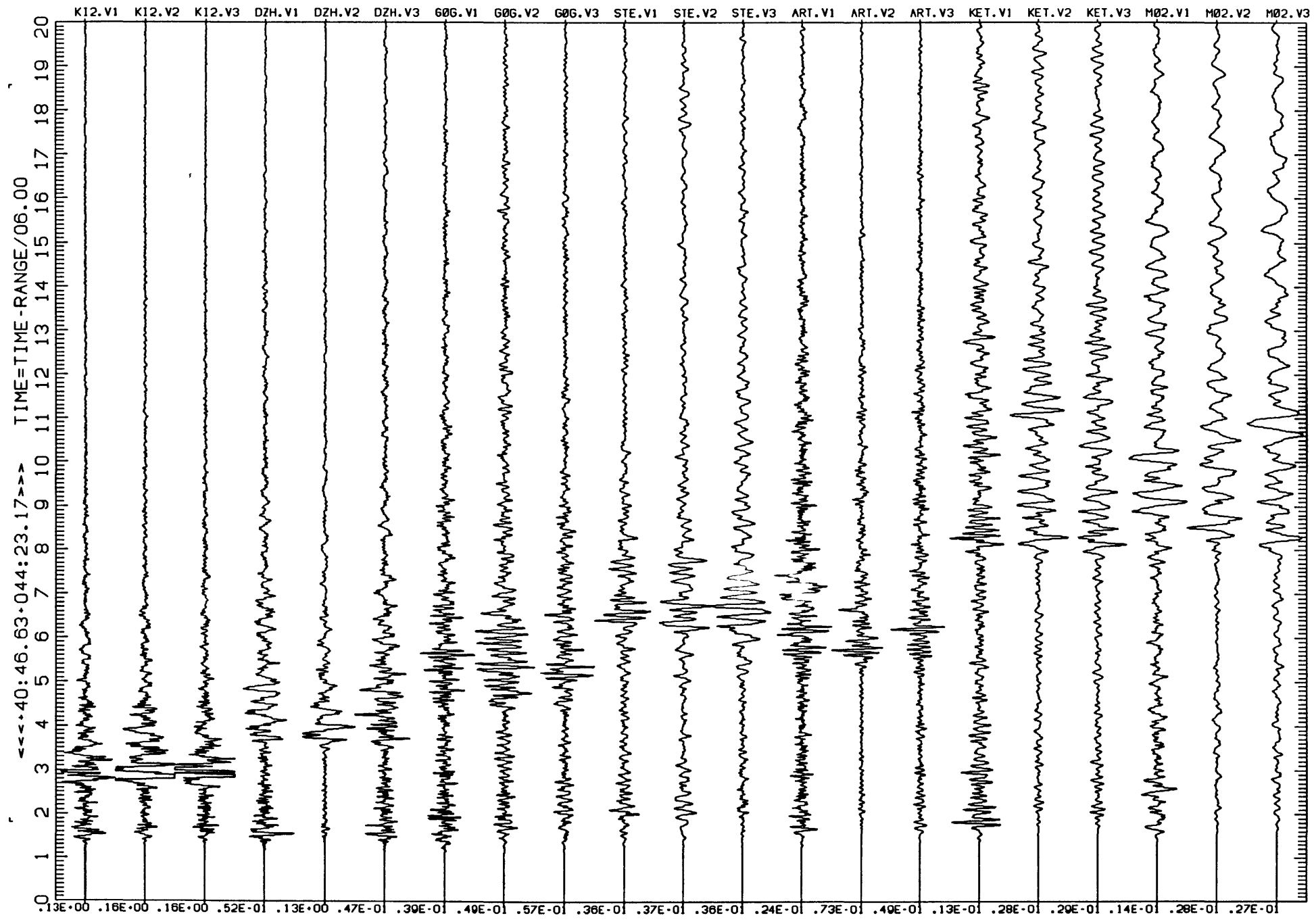
NØRMALIZED
UN-DEFINED
CH1,2,3
89*001+22:59:37.401
K12.V1 K12.V2 K12.V3 DZH.V1 DZH.V2 DZH.V3 GØG.V1 GØG.V2 GØG.V3 STE.V1 STE.V2 STE.V3 ART.V1 ART.V2 ART.V3 KET.V1 KET.V2 KET.V3 MØ2.V1 MØ2.V2 MØ2.V3
<<<+40:46.63+044:23.17>>> TIME=TIME-RANGE/06.00
0 1 2 3 4 5 6 7 8 9 10 11 12 13 14 15 16 17 18 19 20
.13E+00 .16E+00 .16E+00 .52E-01 .13E+00 .47E-01 .39E-01 .49E-01 .57E-01 .36E-01 .37E-01 .36E-01 .24E-01 .73E-01 .49E-01 .13E-01 .28E-01 .20E-01 .14E-01 .28E-01 .27E-01

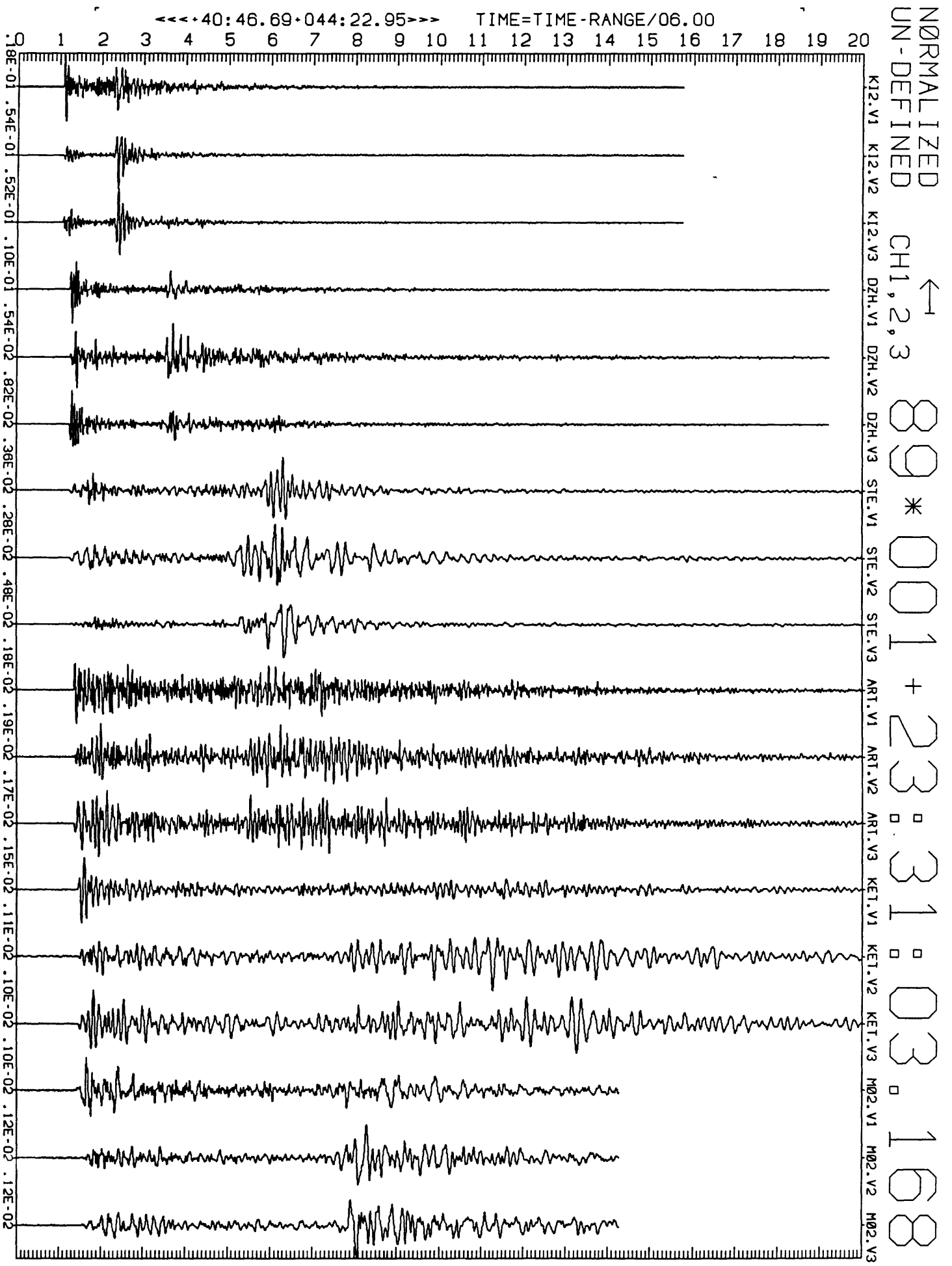
NORMALIZED
UN-DEFINED
CH1,2,3
89*001+23:31:03.168
<<<+40:46.69+044:22.95>>>
TIME=TIME-RANGE/06.00
0 1 2 3 4 5 6 7 8 9 10 11 12 13 14 15 16 17 18 19 20
.18E-01
.54E-01
.52E-01
.10E-01
.54E-02
.82E-02
.36E-02
.28E-02
.48E-02
.18E-02
.19E-02
.17E-02
.15E-02
.11E-02
.10E-02
.10E-02
.12E-02
.13E-02
K12.V1
K12.V2
K12.V3
DZH.V1
DZH.V2
DZH.V3
STE.V1
STE.V2
STE.V3
ART.V1
ART.V2
ART.V3
KET.V1
KET.V2
KET.V3
M02.V1
M02.V2
M02.V3

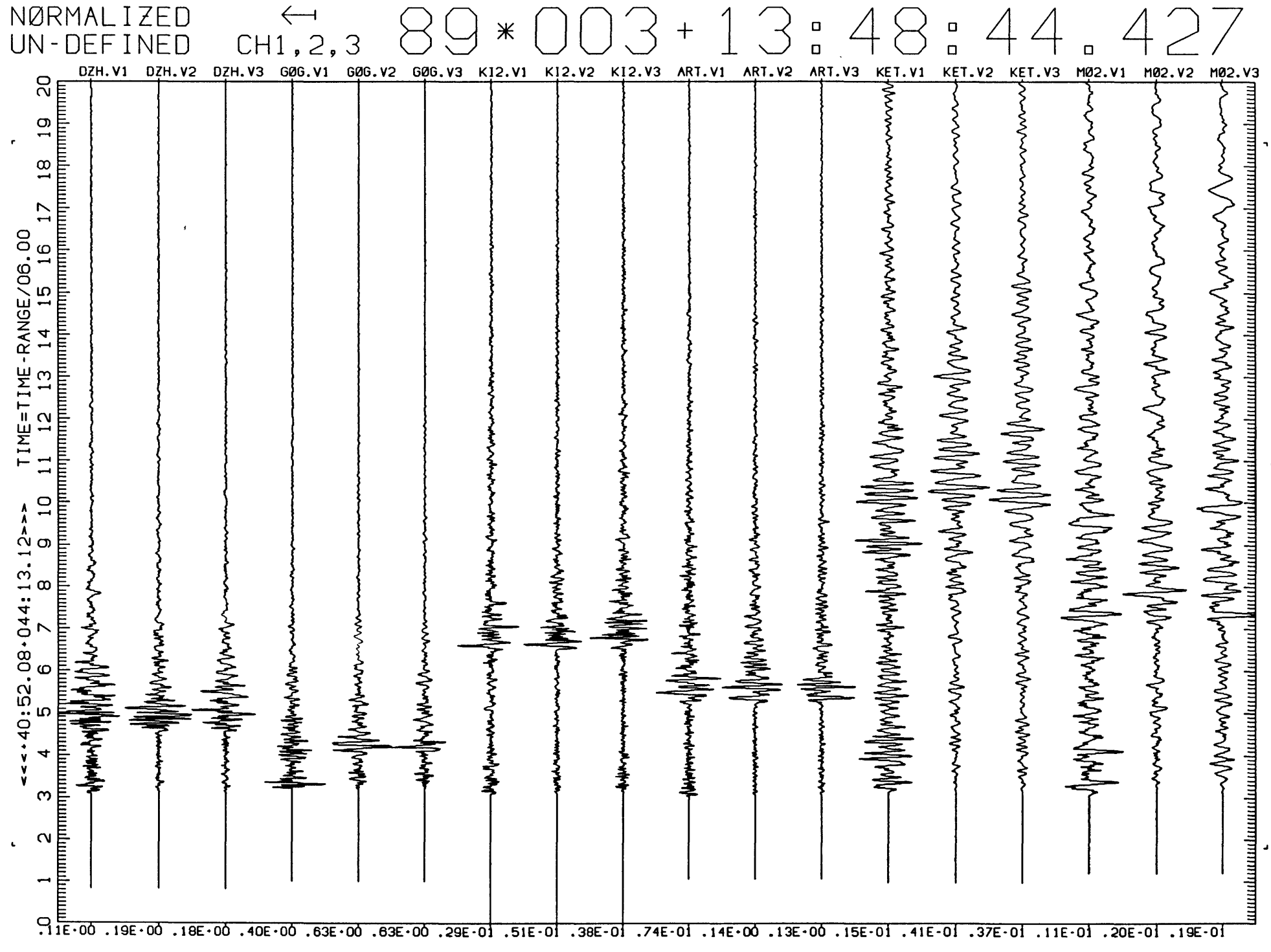
NØRMALIZED
UN-DEFINED
CH1,2,3
89*003+13:48:44.427
DZH.V1 DZH.V2 DZH.V3 GØG.V1 GØG.V2 GØG.V3 KI2.V1 KI2.V2 KI2.V3 ART.V1 ART.V2 ART.V3 KET.V1 KET.V2 KET.V3 MØ2.V1 MØ2.V2 MØ2.V3
<<<·40:52.08·044:13.12>>> TIME=TIME-RANGE/06.00
0 1 2 3 4 5 6 7 8 9 10 11 12 13 14 15 16 17 18 19 20
.11E·00 .19E·00 .18E·00 .40E·00 .63E·00 .63E·00 .29E·01 .51E·01 .38E·01 .74E·01 .14E·00 .13E·00 .15E·01 .41E·01 .37E·01 .11E·01 .20E·01 .19E·01

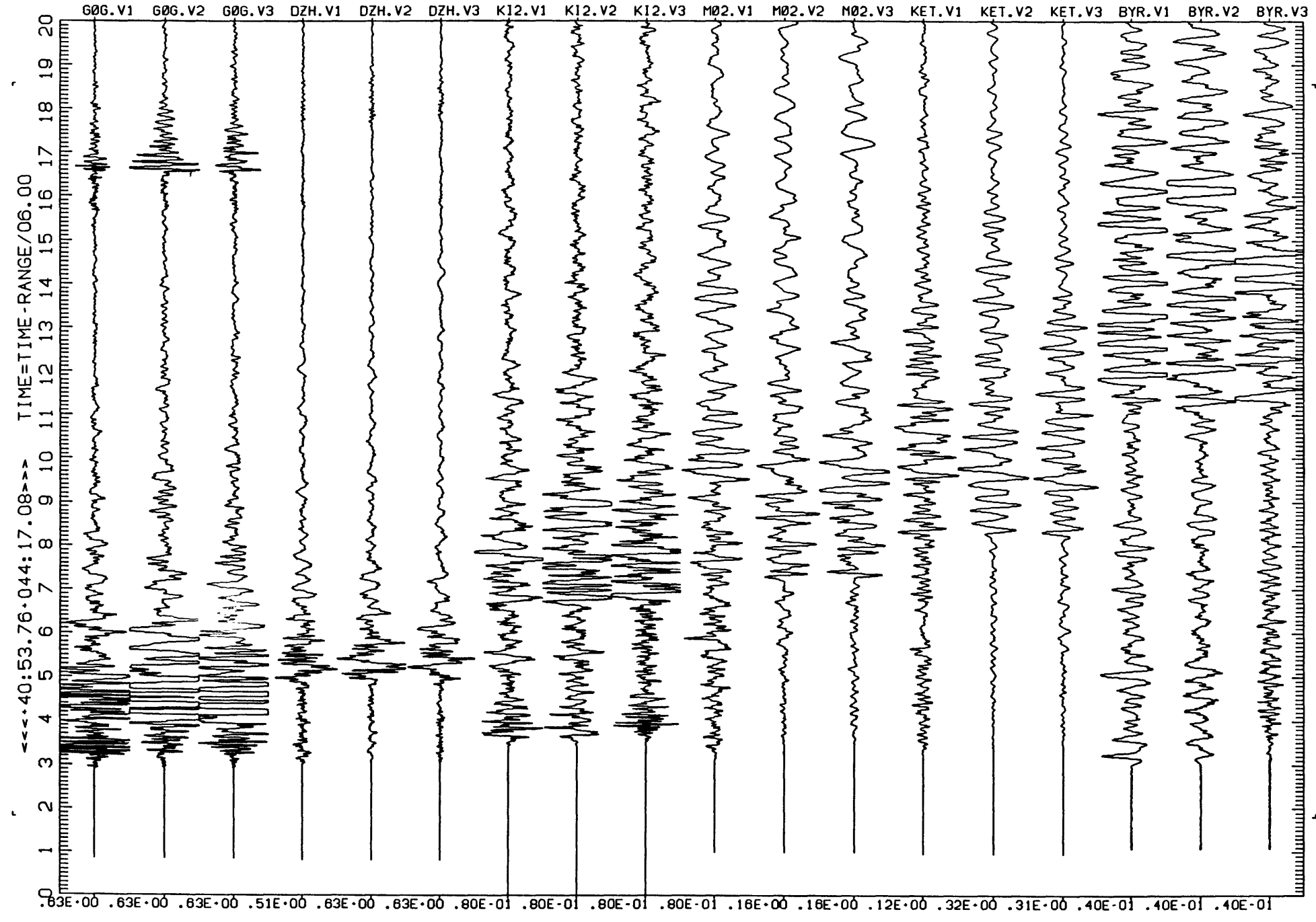
NØRMALIZED
UN-DEFINED
CH1,2,3
89*004+07:29:37.580
GØG.V1 GØG.V2 GØG.V3 DZH.V1 DZH.V2 DZH.V3 KI2.V1 KI2.V2 KI2.V3 MØ2.V1 MØ2.V2 MØ2.V3 KET.V1 KET.V2 KET.V3 BYR.V1 BYR.V2 BYR.V3
<<<·40:53.76·044:17.08>>> TIME=TIME-RANGE/06.00
0 1 2 3 4 5 6 7 8 9 10 11 12 13 14 15 16 17 18 19 20
.63E·00 .63E·00 .63E·00 .51E·00 .63E·00 .63E·00 .80E-01 .80E-01 .80E-01 .80E-01 .16E·00 .16E·00 .12E·00 .32E·00 .31E·00 .40E-01 .40E-01 .40E-01

APPENDIX D

Site Map and Geotechnical Logs in Leninakan, Armenia S.S.R.

T. O'Rourke

This Appendix contains the geotechnical logs from shallow borings at seven sites indicated on the site location map for Leninakan, Armenia S.S.R. The logs and map were acquired and drafted by T. O'Rourke during the initial investigations of the U.S. team.

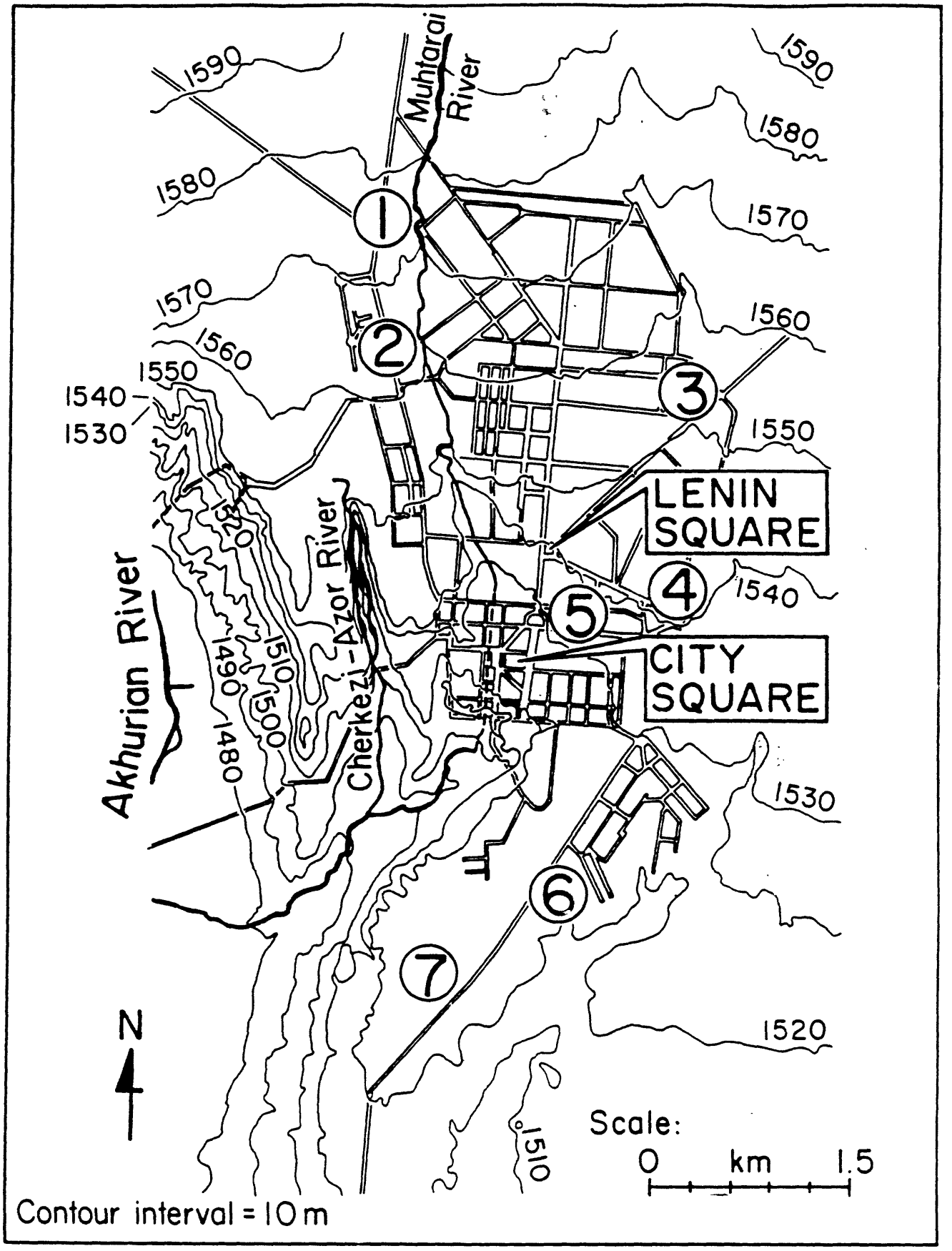
Muhtarai River
1590
1580
1570
1560
1550
1540
1530
1520
1510
1500
1490
1480
LENIN SQUARE
CITY SQUARE
Akhurian River
Cherkezi-Azor River
1
2
3
4
5
6
7
N
Scale:
0 km 1.5
Contour interval = 10 m

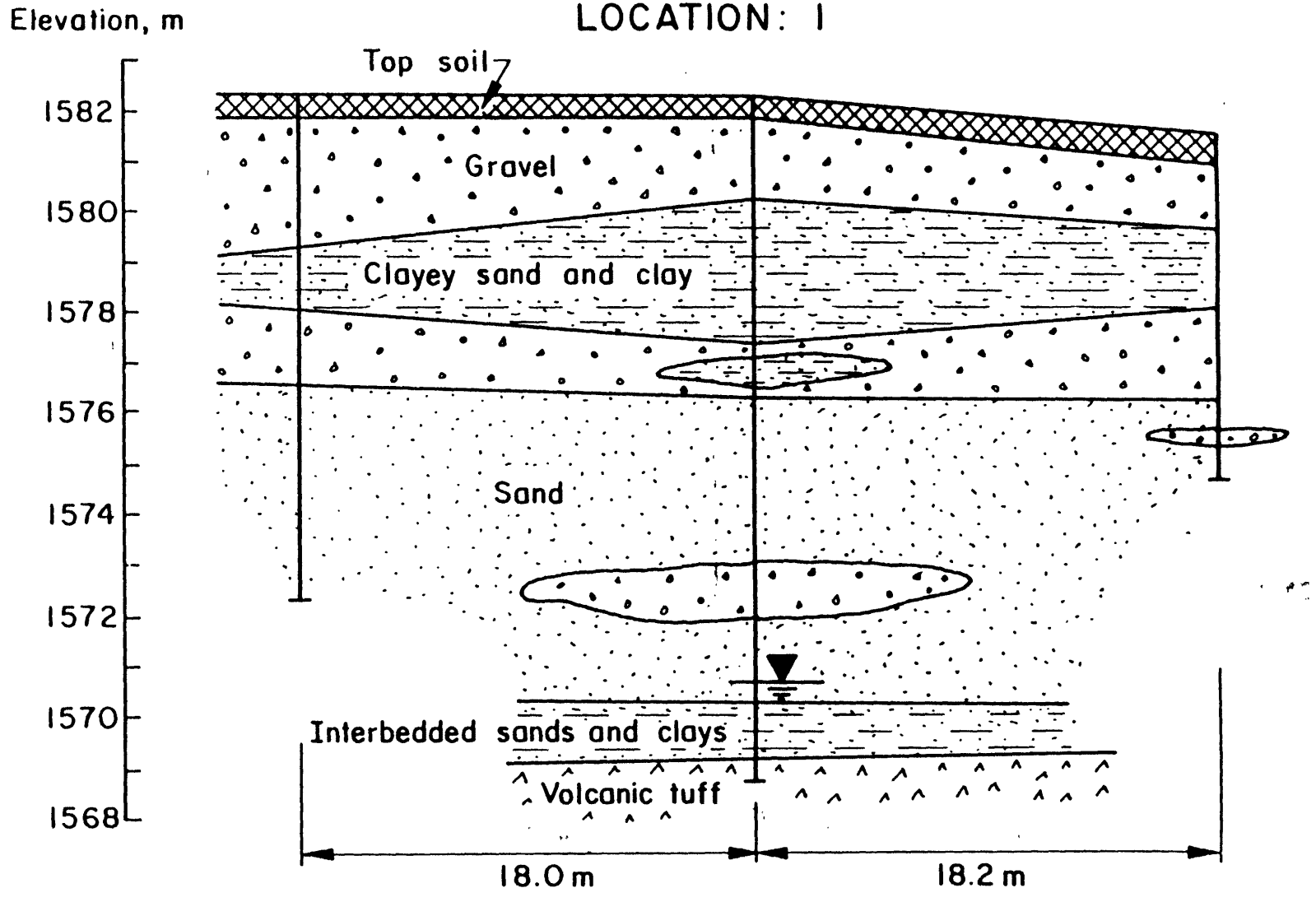
Elevation, m
LOCATION: I
Top soil
1582
1580
1578
1576
1574
1572
1570
1568
Gravel
Clayey sand and clay
Sand
Interbedded sands and clays
Volcanic tuff
18.0 m
18.2 m

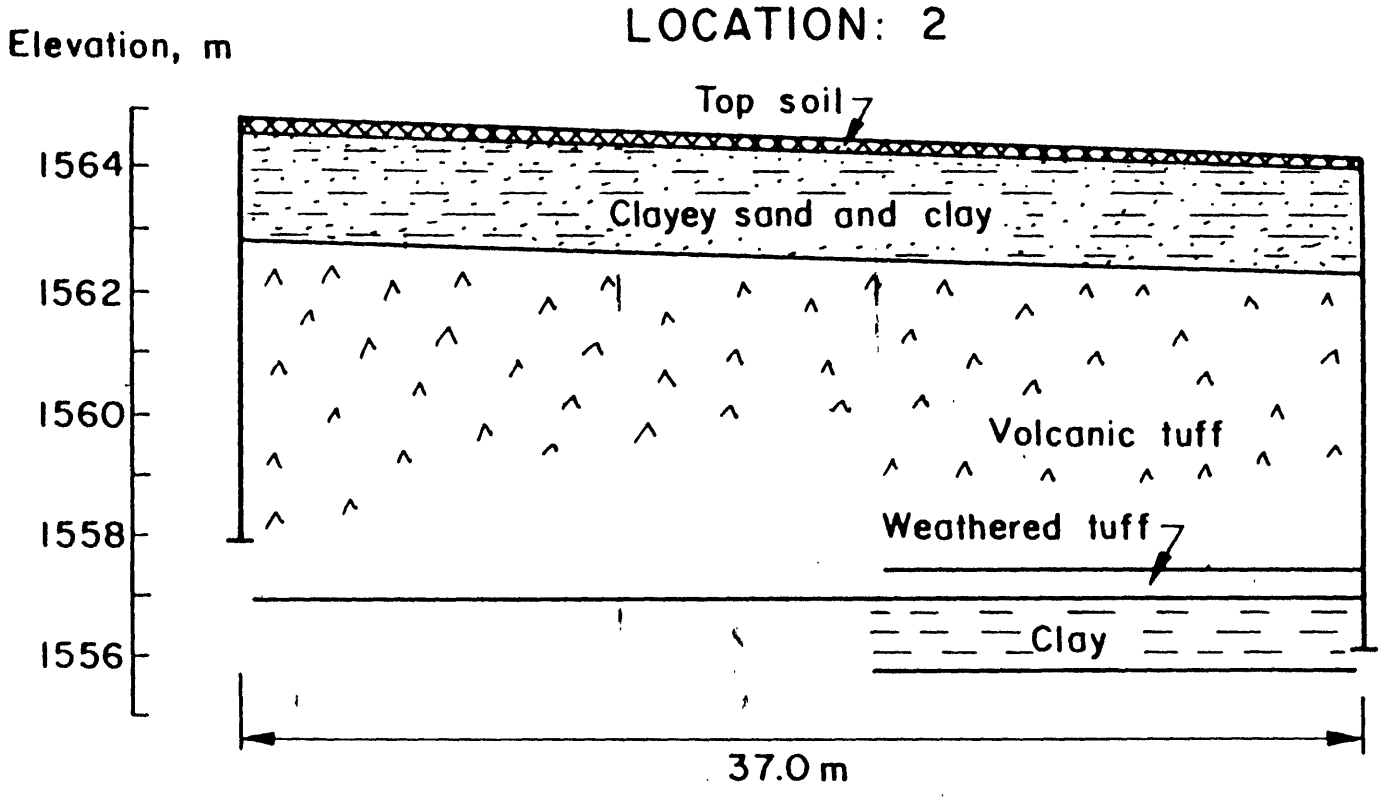
LOCATION: 2
Elevation, m
1564
1562
1560
1558
1556
Top soil
Clayey sand and clay
Volcanic tuff
Weathered tuff
Clay
37.0 m

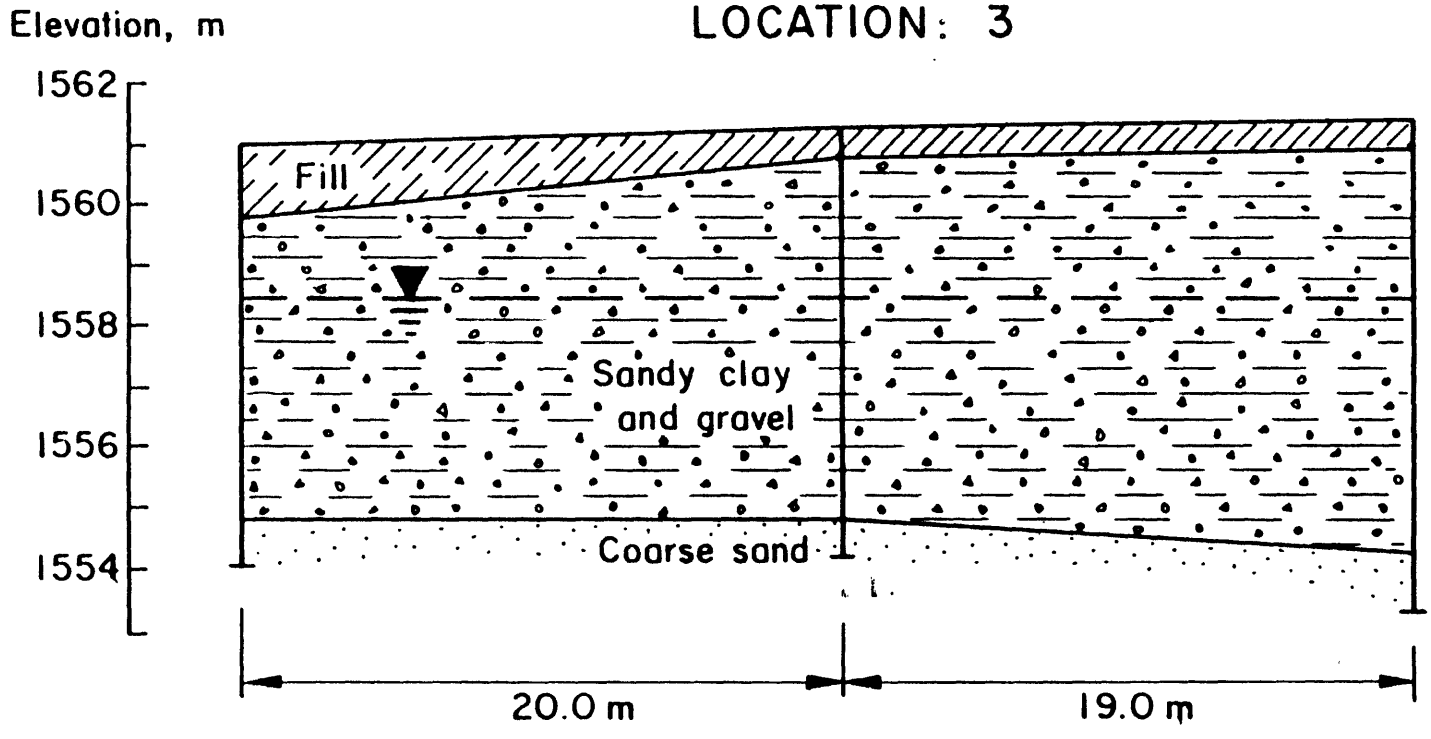
Elevation, m
LOCATION: 3
1562
1560
1558
1556
1554
Fill
Sandy clay
and gravel
Coarse sand
20.0 m
19.0 m

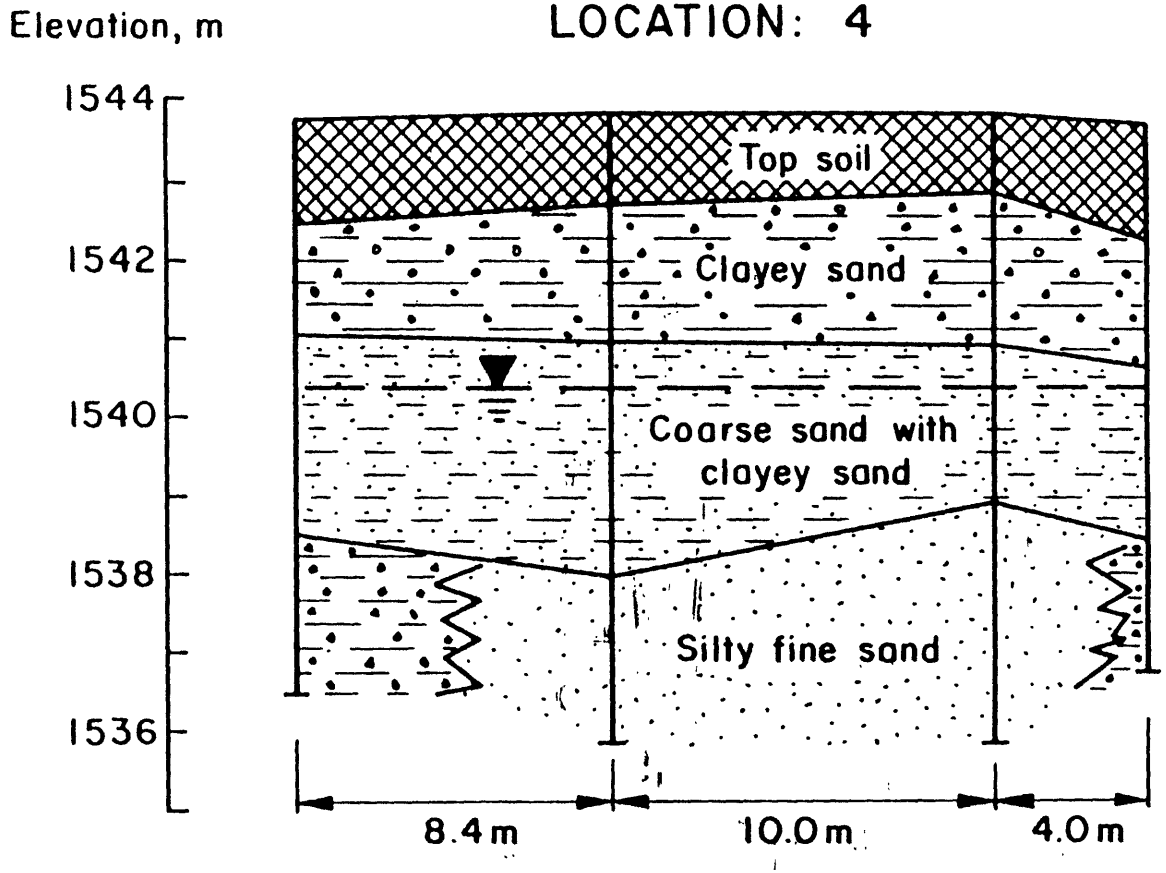
LOCATION: 4
Elevation, m
1544
1542
1540
1538
1536
Top soil
Clayey sand
Coarse sand with clayey sand
Silty fine sand
8.4m
10.0m
4.0m

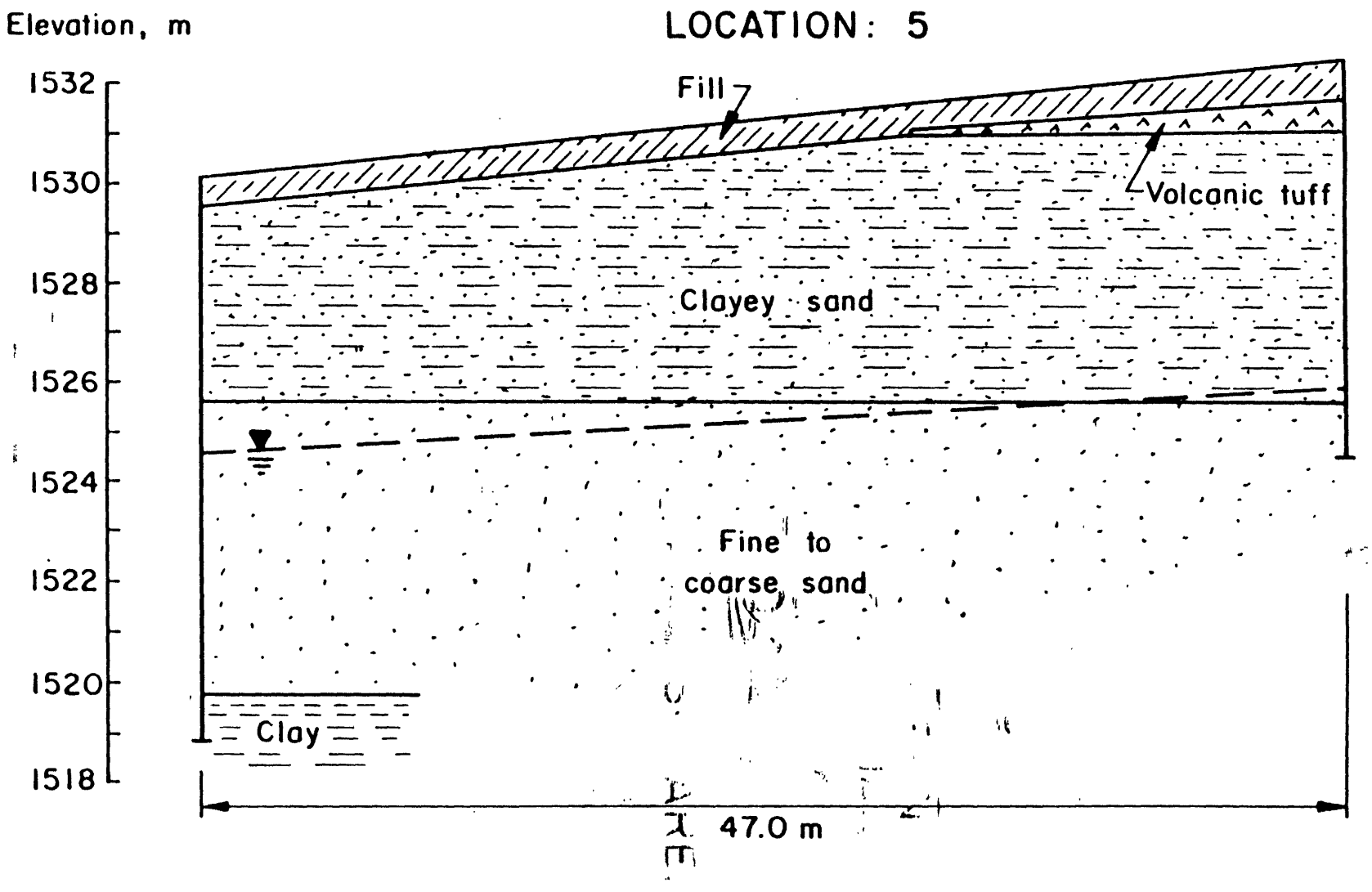
Elevation, m
LOCATION: 5
1532
1530
1528
1526
1524
1522
1520
1518
Fill
Volcanic tuff
Clayey sand
Fine to
coarse sand
Clay
47.0 m

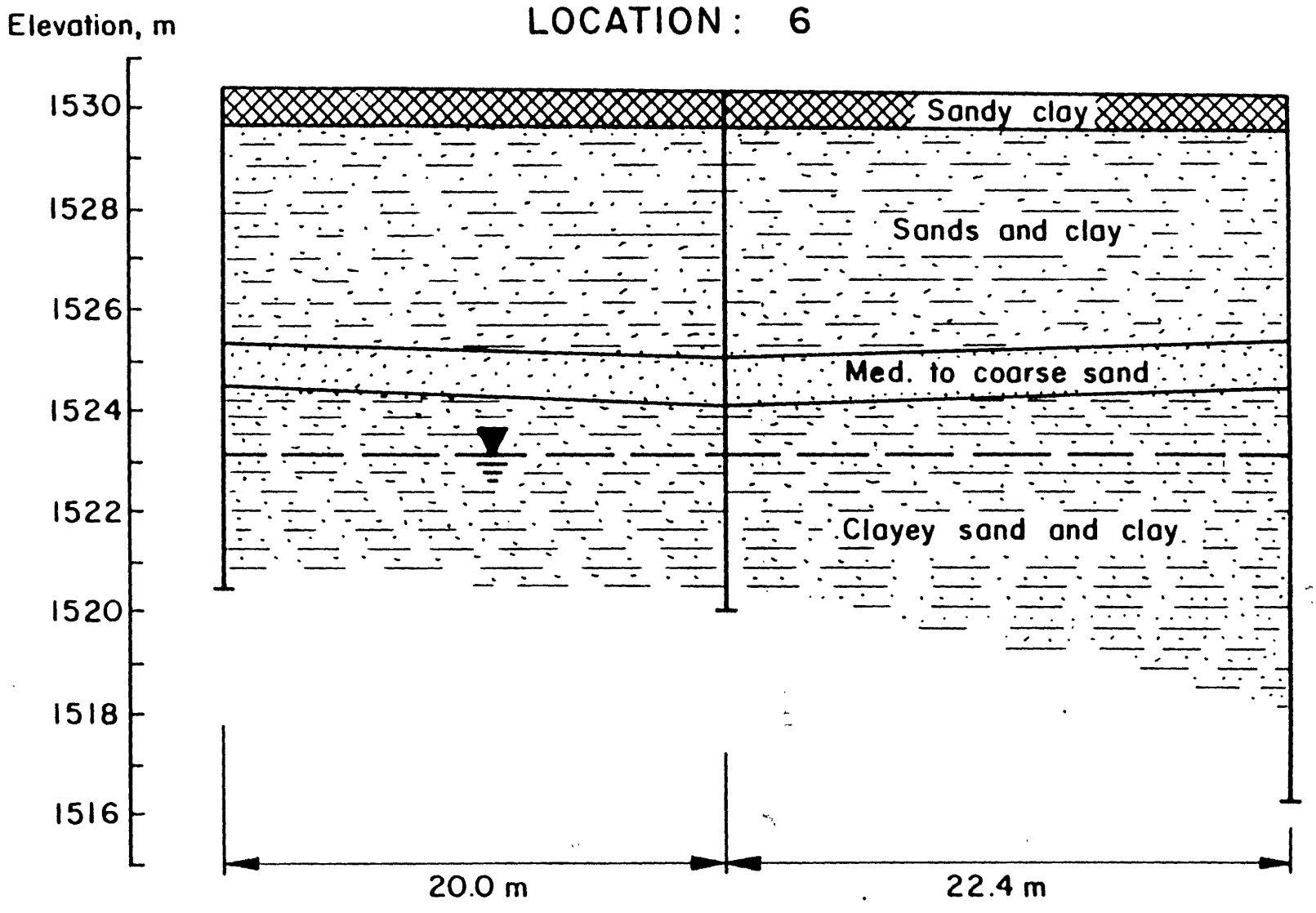
LOCATION: 6
Elevation, m
1530
1528
1526
1524
1522
1520
1518
1516
Sandy clay
Sands and clay
Med. to coarse sand
Clayey sand and clay
20.0 m
22.4 m

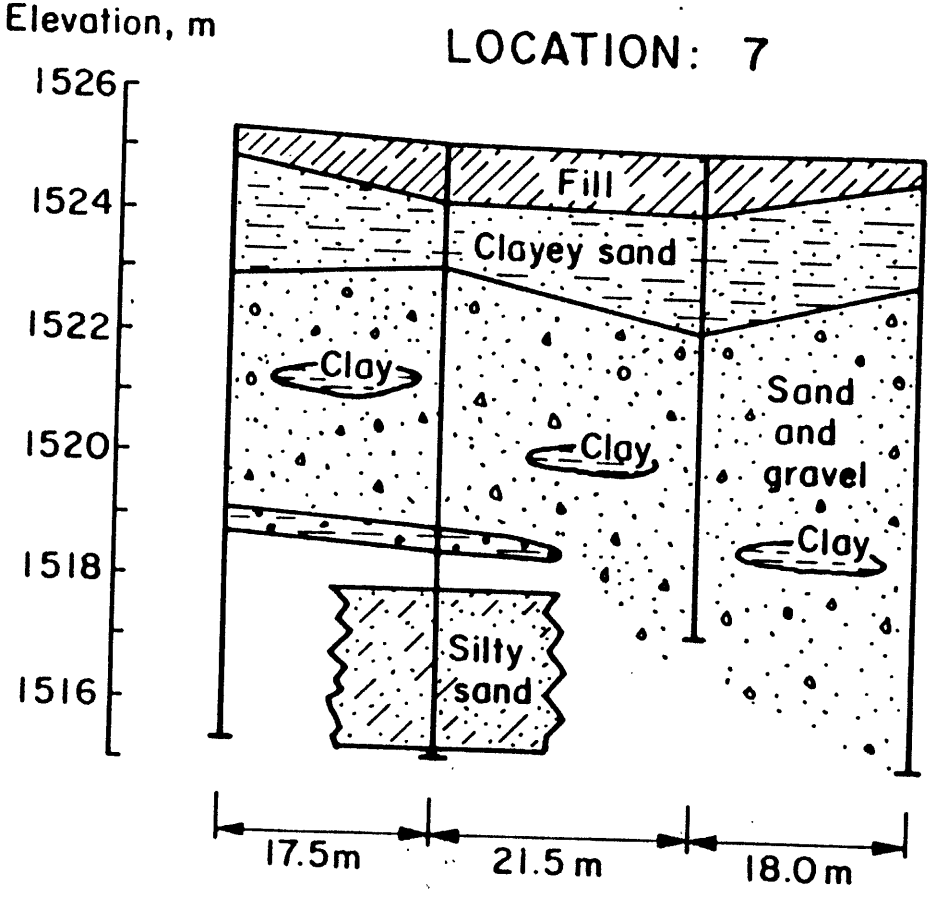
Elevation, m
LOCATION: 7
1526
1524
1522
1520
1518
1516
Fill
Clayey sand
Clay
Clay
Sand and gravel
Clay
Silty sand
17.5m
21.5 m
18.0 m